LUND UNIVERSITY

The HCCI Fuel Number - Measuring and Describing Auto-ignition for HCCI Combustion Engines

Truedsson, Ida

2014

The HCCI Fuel Number

Measuring and Describing Auto-ignition for HCCI Combustion Engines

Ida Truedsson

LUND
UNIVERSITY

DOCTORAL DISSERTATION
by due permission of the Faculty of Engineering, Lund University, Sweden.
To be defended at M-building, LTH, room M:A. 25/4 2014, 10.00.

Faculty opponent
Christopher L. Hagen, Oregon State University

Organization	Document name
LUND UNIVERSITY	DOCTORAL DISSERTATION
	Date of issue
Author	Sponsoring organization
Ida Truedsson	Chevron Inc.

Title and subtitle

The HCCI Fuel Number - Measuring and Describing Auto-ignition for HCCI Combustion Engines

Abstract

HCCI is an advanced combustion concept, using premixed fuel and air with a diluted charge. This is thermodynamically favorable, leading to high efficiency and therefore lower CO_2 emissions. The well-premixed and diluted fuel charge gives lower cylinder temperatures than conventional diesel compression ignition and spark ignited gasoline combustion, resulting in low engine out emissions of both nitrogen oxides and soot.

To be able to optimize and use the advanced combustion concepts in commercial engines, knowledge of fuel behavior is needed, and a way to describe it. This thesis work provides detailed information about HCCI auto-ignition by studying parameters such as low temperature heat release and auto-ignition temperatures.

An HCCI Fuel Number is then presented, developed with the purpose to describe fuel performance. By comparing fuels such as full distillate gasolines or biofuels to the required compression ratio for reference fuels, a measure on HCCI fuel performance is gained. This fuel number was shown to correlate well with pre-reactions in the fuels.

The thesis work is based on CFR engine experiments, studying over 40 different reference fuels consisting of blends of n-heptane, iso-octane, toluene, and ethanol, which are model surrogates for gasoline. In addition, 21 different full distillate gasoline fuels prepared from refinery feedstocks, some with addition of single components, were tested as well. Five different inlet air temperatures ranging from 50°C to 150°C were used to achieve different temperature-pressure histories, and the compression ratio was changed accordingly to keep a constant combustion phasing, CA50, of 3±1° after TDC. The main parts of the experiments were carried out in lean operation with a constant equivalence ratio of 0.33 and with an engine speed of 600 rpm. Additional experiments were performed at higher engine speeds.

Studied fuel effects include low temperature heat release quenching effects, were ethanol was found to quench low temperature heat release at all conditions, and toluene had an in comparison very weak effect on these pre-reactions.

All conditions and fuels with extensive low temperature heat release showed similar auto-ignition temperatures. When LTHR diminished, either due to fuel quenching from ethanol or toluene, or when the inlet air temperature was increased, the auto-ignition temperature was increased.

Key words

HCCI, Fuel Classification, Reference Fuels, Gasoline, Low Temperature Heat Release

Classification system and/or index terms (if any)

Supplementary bibliographical information	Language
	English

ISSN and key title	ISBN
0282-1990	978-91-7473-949-7

Recipient's notes	Number of pages 186	Price
	Security classification	

Signature _____ Date _____

The HCCI Fuel Number

Measuring and Describing Auto-ignition for HCCI Combustion Engines

Ida Truedsson

LUND
UNIVERSITY

Faculty of engineering
Department of energy sciences
Division of combustion engines
ISBN 978-91-7473-949-7 (Printed)
ISBN 978-91-7473-950-3 (Electronic version)
ISRN LUTMDN/TMHP-14/1101-SE
ISSN 0282-1990

Lund University
Lund 2014

List of Publications

Paper I

Pressure Sensitivity of HCCI Auto Ignition Temperatures for Primary Reference Fuels

Truedsson, I., Johansson, B., Tuner, M., Cannella, W.

SAE Int. J. Engines 5(3):1089-1108, 2012, doi:10.4271/2012-01-1128

Paper II

Pressure Sensitivity of HCCI Auto-ignition Temperatures for Oxygenated Reference Fuels

Truedsson, I., Johansson, B., Tuner, M., Cannella, W.

J. Eng. Gas Turbines Power 135 (7), 13, doi:10.1115/1.4023614

Paper III

Pressure Sensitivity of HCCI Auto-Ignition Temperature for Gasoline Surrogate Fuels

Truedsson, I., Tuner, M., Johansson, B., and Cannella, W.

SAE Technical Paper 2013-01-1669, 2013, doi:10.4271/2013-01-1669

Paper IV

Emission Formation Study of HCCI Combustion with Gasoline Surrogate Fuels

Truedsson, I., Tuner, M., Johansson, B., and Cannella, W.

SAE Technical Paper 2013-01-2626, 2013, doi:10.4271/2013-01-2626

Paper V

Submitted to SAE 2014 International Powertrain, Fuels and Lubricants meeting

Engine Speed Effect on Auto-Ignition Temperature and Low Temperature Reactions in HCCI Combustion

Truedsson, I., Johansson, B., Tuner, M., Cannella, W.,

Paper VI

Submitted to SAE 2014 International Powertrain, Fuels and Lubricants meeting

Development of New Test Method for Evaluating HCCI Fuel Rerformance

Truedsson, I., Johansson, B., Tuner, M., Cannella, W.

Abstract

HCCI is an advanced combustion concept, using premixed fuel and air with a diluted charge. This is thermodynamically favorable, leading to high efficiency and therefore lower CO_2 emissions. The well-premixed and diluted fuel charge gives lower cylinder temperatures than conventional diesel compression ignition and spark ignited gasoline combustion, resulting in low engine out emissions of both nitrogen oxides and soot.

To be able to optimize and use the advanced combustion concepts in commercial engines, knowledge of fuel behavior is needed, and a way to describe it. This thesis work provides detailed information about HCCI auto-ignition by studying parameters such as low temperature heat release and auto-ignition temperatures.

An HCCI Fuel Number is presented, developed with the purpose to describe fuel performance. By comparing fuels such as full distillate gasolines or biofuels to the required compression ratio for auto-ignition for reference fuels, a measure on HCCI fuel performance is gained. This fuel number was shown to correlate well with pre-reactions in the fuels.

The thesis work is based on CFR engine experiments, studying over 40 different reference fuels consisting of blends of n-heptane, iso-octane, toluene, and ethanol, which are model surrogates for gasoline. In addition, 21 different full distillate gasoline fuels prepared from refinery feedstocks, some with addition of single components, were tested as well. Five different inlet air temperatures ranging from 50°C to 150°C were used to achieve different temperature-pressure histories, and the compression ratio was changed accordingly to keep a constant combustion phasing, CA50, of 3±1° after TDC. The main parts of the experiments were carried out in lean operation with a constant equivalence ratio of 0.33 and with an engine speed of 600 rpm. Additional experiments were performed at higher engine speeds.

Studied fuel effects include low temperature heat release quenching effects, were ethanol was found to quench low temperature heat release at all conditions, and toluene had an in comparison very weak effect on these pre-reactions.

All conditions and fuels with extensive low temperature heat release showed similar auto-ignition temperatures. When LTHR diminished, either due to fuel quenching from ethanol or toluene, or when the inlet air temperature was increased, the auto-ignition temperature was increased.

Popular Summary in Swedish

Att mäta och beskriva självantändning vid förblandad kompressionsantändning (HCCI)

HCCI-förbränning går ut på att luft och bränsle blandas, och komprimeras i en kolvmotor tills blandningen självantänder. På grund av den snabba förbränningen med det här konceptet förloras mindre värmeenergi, och verkningsgraden blir därför högre än för vanliga bensin- och dieselmotorer.

Genom att öka verkningsgraden kan vi resa en viss sträcka, eller transportera en viss mängd gods, med lägre bränsleförbrukning. Detta leder till lägre koldioxidutsläpp och därför en mindre påverkan på den globala uppvärmningen. Nya typer av förbränningsmotorer kan också underlätta vid användning av biobränslen, vilket både kan leda till vidare minskning av koldioxidutsläpp och till att minska vårt oljeberoende.

I det här arbetet presenteras en nyutvecklad metod för att mäta hur lätt ett bränsle självantänder vid denna typ av kompressionsantändning.

Arbetet gick ut på att köra en motor med variabelt kompressionsförhållande, vilket betyder att motorn under arbete kan ändras genom att cylinderhuvud och kolv förskjuts relativt varandra. Detta gör att bränslen som självantänder olika lätt kan användas och studeras. Så kallade referensbränslen testades först. Dessa består av två olika typer av kolväten, ett som självantänder enkelt och ett som har högre motstånd mot självantändning. Andra typer av bränslen jämfördes senare med dessa referensbränslen. Det kompressionsförhållande som krävdes för att förbränningen skulle ske vid övre dödläget (när trycket är som högst i cylindern) noterades, och detta värde översattes till ett HCCI-tal för varje bränsle. För att förstå den vetenskapliga bakgrunden studerades även förreaktioner i förbränningen, och vi beräknade även temperaturerna vid vilka de olika bränslena antändes.

För att kunna praktiskt använda moderna koncept för lågtemperaturförbränning måste vi veta hur ett bränsle beter sig. Denna nyutvecklade metod mäter detta på ett enkelt vis.

Acknowledgements

Firstly, I would like to thank my supervisors. Bengt Johansson has helped a lot to improve my work and presentation skills, and so has Martin Tunér. I would also like to thank you for giving me this opportunity. I would like to thank Bill Cannella from Chevron, for numerous helpful discussions, paper- and thesis corrections, for supplying fuel, and for letting me visit Chevron in 2013. I would also like to thank Chevron for financing my project.

I have really enjoyed the working environment in the combustion engine group, and during my time here I've met so many fun and interesting PhD students. Hadeel, a special thanks to you for making the work days a little brighter.

I'm also very grateful to the technicians for keeping the lab and my engine running at all times. Without you there would be no thesis.

Lastly, I would like to thank my family and friends. Mum, thanks for always being there. Dad, thanks for inspiring me to work with engines. Thanks to my brother, Ulf, for taking care of the cats when I travel. It's good to know they are safe.

And Magnus; Thanks for distracting me throughout this thesis work.

Nomenclature

AIT	auto-ignition temperature
ATDC	after top dead center
BTDC	before top dead center
CA 50	crank angle for 50 % of total heat release
CAD	crank angle degree
CI	compression ignition
CFR	cooperative fuel research
CO	carbon monoxide
CO_2	carbon dioxide
CR	compression ratio
CR_{AI}	required compression ratio for CA50 3° after TDC
EGR	exhaust gas recirculation
ERF	ethanol reference fuel
HC	hydrocarbon
HCCI	homogenous charge compression ignition
IVC	inlet valve closing
LTR	low temperature reactions
LTHR	low temperature heat release
MON	motor octane number
NO_x	nitrogen oxides, NO and NO_2 combined
OI	octane index, developed by G. Kalghatgi
ON	octane number
p	pressure
PRF	primary reference fuel
RON	research octane number
RPM	revolutions per minute
S	fuel sensitivity, S = RON-MON
SI	spark ignition
SOC	start of combustion
TDC	top dead center
T_{in}	temperature of fuel air mixture, measured
T_{IVC}	temperature in the cylinder at inlet valve closing, calculated from T_{in}
TERF	toluene ethanol reference fuel
TRF	toluene reference fuel
V	volume
λ	relative air fuel ratio
ϕ	equivalence ratio
γ	specific heat ratio (Cp/Cv)

Contents

1 Introduction

1.1 Background

Today, a significant part of worldwide transportation is met by vehicles propelled by an internal combustion engine. The transportation sector is dominated by diesel compression ignition (CI) engines, and spark ignition (SI) engines. The latter are coupled with a three-way emissions catalyst and give practically zero tailpipe-out emissions of carbon monoxide (CO), nitrogen oxides (NO and NO_2, here combined as NO_x), hydrocarbon (HC), and soot, but have lower efficiency and therefore give an increase in CO_2 emissions in comparison to diesel engines. Diesel engines in turn have higher engine-out particulate emissions, which today is handled by a particulate filter, and NO_x emissions which are reduced by applying exhaust gas recirculation (EGR) coupled with a selective catalytic reduction (SCR) catalyst or a lean NO_x trap in the exhaust system. A diesel oxidation catalyst (DOC) is used to completely oxidize partially combusted hydrocarbons to CO_2 and H_2O.

Emissions legislation continually promotes stricter regulations to ensure a healthier environment for all of us by regulating local emissions such as NO_x and particulates, and to reduce the impact of green house gases (GHG) such as CO_2. The result is development of more efficient engines and vehicles, having the possibility to decrease CO_2 emissions for a certain amount of work output or distance travelled.

Over the past 30-40 years, a significant amount of research and development has been devoted to advanced internal combustion engines that have higher efficiencies and lower engine-out emissions. One broad category that encompasses a number of different approaches is low temperature combustion (LTC). The goal in LTC is to control the combustion process and temperature so that NO_x production is limited, but still achieve high efficiency. One approach in LTC is homogeneous charge compression ignition (HCCI), which is the focus of this thesis.

Another approach to reducing tailpipe emissions that is being pursued is the use of electric vehicles. Relative to advanced internal combustion vehicles, electric vehicles have zero tailpipe emissions, but face the challenges of higher vehicle costs, more limited driving range, GHG emissions at the power plant where the electricity is generated, and limited number of vehicle recharging stations. Electric vehicle development and sales are on the rise, but the combustion engine is still most effective and therefore dominant in

the heavy duty (trucks) sector and for cars going at higher speeds and longer distances than city driving, for many years still. Electrification is not an "either-or" question, but can be applied in the right amount for each vehicle, from simple start-stop techniques in combination with a more powerful engine in some cases, to more battery driven vehicles with the combustion engine as a range extender in other applications, leading to an increased vehicle efficiency. Hybrid vehicles with both an electric motor and an internal combustion engine exist today. HCCI is a combustion concept that could profit from hybrid technology.

1.2 Objective

Previous results by other researchers have demonstrated that for many fuels, conditions can be found where HCCI combustion can be initiated. However; to be able to change fuel in an engine that is designed for a certain operating range, there is need for a way to describe fuel performance. The question is how to evaluate a fuel, to see if it is suitable for a certain application.

The challenge is to determine which fuel properties and composition lead to desired HCCI performance over the wide range of operating conditions that are encountered during driving. Thus there is a need for a fundamental understanding of how fuel properties and composition impact auto-ignition and engine performance (efficiency and emissions) in HCCI combustion. One key objective of this thesis is therefore to study the impact of the properties and composition of gasoline range components on auto-ignitability in HCCI combustion.

For conventional spark ignition engines, the key parameters that are used to describe ignition properties are Research Octane Number (RON) and Motor Octane Number (MON). These indices measure knock in a cooperative fuels research (CFR) engine. Fuel performance for compression ignition engines are measured by the cetane number (CN), in a direct injected version of the CFR engine. For HCCI combustion, there is of yet no standard measure for fuel performance. It is therefore suggested that fuels are tested, in a standard CFR engine, under HCCI conditions, to measure fuel ignition properties.

In previous work, researchers [1] have proposed that knowledge of the fuel properties RON and MON is sufficient to develop an index that relates engine HCCI auto-ignition performance to fuel properties. A second key objective of this thesis study is determine whether the fuel properties RON and MON are sufficient to characterize the HCCI performance of gasoline-type fuels, and if not to propose a new way to characterize fuels in terms of an HCCI number.

1.3 Method

This thesis work is based on experimental measurements performed in a single cylinder engine operated in HCCI mode. The engine chosen for the work is a standardized CFR engine, normally used to perform octane rating of gasoline fuels. The main source of combustion information is the pressure sensor mounted in the cylinder, from which the in-cylinder pressure and temperature evolution was calculated. By adjusting the compression ratio and intake temperature, different operating conditions were achieved. Many fuels, both reference fuels consisting of blends of different single components, as well as full distillate gasoline fuels, were tested and compared. Since the RON and MON tests utilises inlet air temperatures of 50ºC and 600 rpm, and 150ºC and 900 rpm, respectively, these two operating conditions are in focus. Since HCCI combustion with complex fuels often results in two-step combustion (low temperature heat release before the main combustion event), another research question was to see how these affects the fuel performance.

1.4 Contribution

This thesis contains a systematic study of low temperature reactions, auto-ignition temperatures, and other characteristics to define HCCI fuel performance, for more than 40 different gasoline-type surrogate fuels. This extensive database was used to develop a way to describe HCCI fuel auto-ignition more accurately than was previously possible. It could also be of use for modeling purposes, using temperatures and low temperature reactions to develop chemical kinetic models, or to use the combustion rate or general behavior for CFD simulations.

The Lund-Chevron HCCI number that was developed compares reference fuels and full distillate fuels to the behavior of primary reference fuels (blends of n-heptane and iso-octane), and thus provides additional information of auto-ignitability.

2 Engines and Fuels

The two dominating combustion concepts used in the automotive industry today are the spark ignition (SI) and compression ignition (CI) engines. For SI engines, fuel performance, described by knock tendency, is characterized by the research octane number (RON) and motor octane number (MON). For compression ignition engines the fuel auto-ignition properties are measured by ignition delay, using the cetane number (CN).

The regulated emissions for automotive engines are nitrogen oxides (NO_x), hydrocarbons (HC), particulate matter (PM), and carbon monoxide (CO). NO_x emissions lead to acid rain, which has a harmful effect on the environment, such as aquatic animals and plants. Both CO, NO_x, and HC emissions causes smog, which is toxic to humans. Particulates have both environmental effects as well as adverse effects on our health. CO_2 is at low concentrations not harmful to humans, but is a source for global warming. [2]

2.1 Spark Ignited (SI) Gasoline Engines

The port fuel injected spark ignited engine uses a premixed charge of fuel and air, and a spark ignites the charge before top dead center. A turbulent flame front develops and travels through the combustion chamber [3]. The compression ratio is limited to avoid knock, which means spontaneous auto-ignition of the end gas, which at stoichiometric conditions is harmful to the engine. This lower compression ratio limits engine efficiency. Since the air-fuel mixture is stoichiometric, the air flow has to be restricted at lower engine loads, using a throttle in the intake. This gives a pressure drop and reduces engine efficiency at low loads. Very high temperatures in the stoichiometric flame front lead to large amounts of nitrogen oxides (NO_x), which however are reduced to almost zero tailpipe emissions by a three way catalyst. The three way catalyst not only reduces NO_x, but also oxidizes hydrocarbons and carbon monoxides that might have passed through the engine.

2.2 Compression Ignition (CI) Diesel Engines

Compression ignition (CI) engines, often called diesel engines, use direct injection of fuel into the cylinder. Air is introduced in the engine and compressed, and the fuel is injected around top dead center, when the in-cylinder pressure and temperature is high, leading to spontaneous ignition and combustion around the fuel spray [4]. CI engines have high efficiency, due to the high compression ratio that can be used, and due to the thermodynamically favorable use of lean combustion (excess air). The rich combustion in the spray leads to soot formation. In the spray periphery, a stoichiometric flame exists, leading to high temperatures and formation of NO_x. Nowadays, a particulate filter is used for diesel engines to reduce the amount of particulate matter. New diesel engines are also often equipped with a selective catalytic reduction catalyst, where urea is injected to reduce the NO_x to N_2 and O_2.

2.3 Gasoline Direct Injection (GDI) Engines

A slightly newer engine concept is the gasoline direct injection engine. Fuel is injected either early in the compression stroke (giving a more SI engine like combustion), or close to top dead center, and is ignited by a spark. The possibility to use lean combustion leads to an increase in efficiency compared to spark ignited gasoline engines, however it faces the same problems as the diesel engine, where locally rich combustion results in soot emissions.

2.4 Homogenous Charge Compression Ignition (HCCI) Engines

Combining the premixed charge from the SI engine with compression ignition, the homogenous charged compression ignition is the result. HCCI as a concept was developed in the 1970's [5]. By fully premixing fuel and air and then compressing the charge until ignition occurs, simultaneous combustion throughout all parts of the combustion chamber is ideally achieved. Due to the otherwise rapid combustion, excess air or exhaust gas recirculation (EGR) is used to keep pressure rise rates and noise at reasonable levels. The rapid combustion and low combustion temperature due to dilution are what makes the combustion concept thermodynamically favorable, reducing the heat losses and therefore giving an increased engine efficiency. The reduced combustion

temperature avoids hot zones where nitrogen oxides are formed, and the premixed charge avoids fuel rich zones that result in soot emissions.

Along with better hardware and less expensive equipment for monitoring and controlling the combustion, it is today closer to reality than an imaginative concept. However, there are still some challenges to be tackled.

2.4.1 HCCI Reaction Chemistry

The hydrocarbon oxidation can be divided into low, intermediate, and high temperature regions. Combustion of fuel that contains a significant amount of n-paraffins, such as n-heptane, exhibits a characteristic bump in the rate of heat release trace before the main heat release, see Figure 1. This is referred to as low temperature heat release (LTHR), which is caused by the low temperature reactions (LTR) - the exothermic pre-reactions that occur before the main combustion event and generate free radicals [6]. Low temperature chemistry is usually dominant at temperatures from 600 to 800 K [7]. LTR are usually more prominent at lower temperatures but diminish as the temperature increases. The reason is that the precursors for this chain branching (the LTR) are decomposed back to the reactants at higher temperatures [2]. This is called the negative temperature coefficient (NTC) zone. This NTC zone has been shown to be more pronounced at higher temperature, lower pressure, conditions. No NTC zone has been seen for olefins or aromatics. [8] The amount of LTHR also decreases with higher engine speed because there is less time for the pre-reactions to occur [9]. Exhaust gas recirculation (EGR) can advance the start of LTR, probably because they contain reactive species such as H_2O_2 [10,11]. A higher cylinder pressure induced by super- or turbocharging is also known to increase the reaction rate and amount of LTHR [8,12].

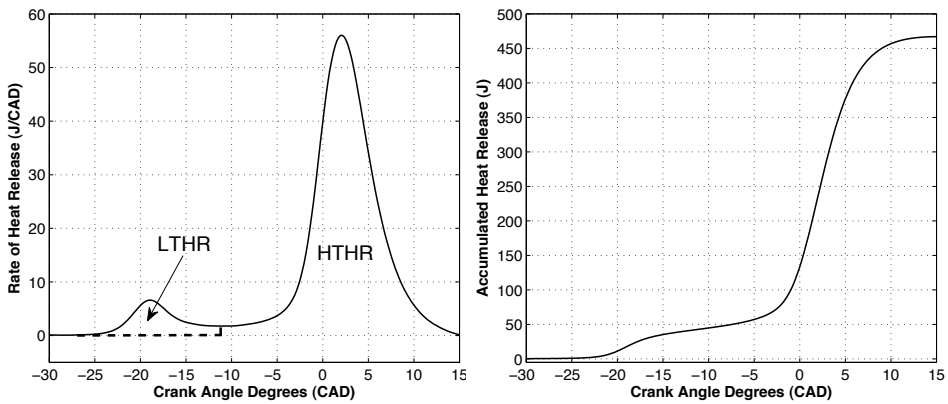

Figure 1. Representative heat release rate (left) and accumulated heat release (right) for a fuel in HCCI operation.

Andrae et al. [13] showed that fuel components such as ethanol, act as radical scavengers and therefore decrease the low temperature reactions. Lü et al. [14] also studied the effect of different inhibitors on LTHR, including ethanol.

The intermediate temperature heat release (ITHR) as a concept was introduced when discussing auto-ignition and pre-reactions, when pre-reactions could be seen, but no peak of the LTHR-rate. ITHR was first described in [15,16] and explained further in [17,18], where it is seen for fuels with no apparent LTHR. Optical experiments [17] showed that this phase was dominated by formaldehyde chemiluminescence, just as for the LTHR phase, even though the temperature was higher than for LTHR. Chemical kinetic models presented in [19] reproduced these findings, and showed that different mechanisms govern the ITHR, compared to LTHR.

The difference between the definitions of and transition between LTHR and ITHR may be a little arbitrary, numbers used are that temperatures from 850 to 1000 K could be considered ITHR [19], temperatures where the low temperature processes should no longer be dominant. In [20], methods of quantifying ITHR are discussed. It is concluded that the temperature definition of 850 to 1000 K is a good indicator for ITHR, but that it is not possible to use to precisely determine the amount of ITHR. The shift in the 850-1000 K temperature range with an increase in engine speed is shown in Figure 2, showing primary reference fuel (PRF) 70. This fuel consists of 70 vol.% iso-octane and 30 vol.% n-heptane. The dashed bold lines for each engine speed highlight the temperature range of 850 to 1000 K. At the lowest engine speed, the ITHR is well within the high temperature reaction phase, and at the highest engine speed the temperature range has shifted earlier, now coinciding with the LTHR and the negative temperature coefficient.

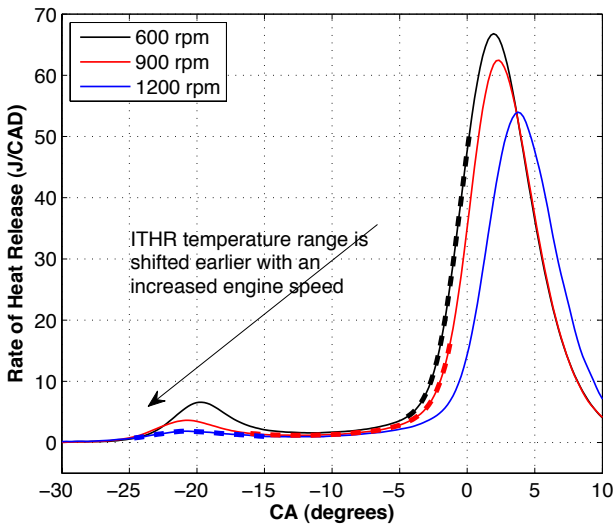

Figure 2. The intermediate temperature heat release temperature range (showed by the dashed line) of 850 to 1000 K is shifted earlier at higher engine speeds, here PRF 70 as an example.

High temperature heat release is usually defined as combustion above a 1000 K. At these temperatures, H_2O_2 decomposition occurs, which leads to an almost explosion-like speed of the combustion event.

2.4.2 HCCI Emissions Formation

As mentioned, no fuel-rich zones should exist in HCCI combustion, and therefore the soot emissions should be low. This theory is supported by reference [21], where soot measurements for HCCI combustion is discussed, both measured particulate matter (PM) and with a Bosch Smoke Number (BSN). They found that when the engine was operated in HCCI mode the soot emissions were always near zero.

NO_x emissions are generally very low for HCCI combustion due to the low combustion temperature. NO_x formation is generally governed by the very temperature sensitive Zeldovich mechanism, which implies that the NO_x formation has a very high activation energy, and is only sufficiently fast at higher temperatures (above 1700 K) [2]. Except for this thermal NO_x pathway, NO_x can also stem from the fuel or from more complex reaction pathways that are not as temperature sensitive.

One of the drawbacks for HCCI combustion are the HC and CO emissions, which are relatively high compared to SI and CI engines, due to the low combustion temperature. The low combustion temperature also leads to lower exhaust gas temperatures, which makes the use of an oxidation catalyst for removing HC and CO more difficult.

2.5 Research Octane Number (RON) and Motor Octane Number (MON) - Fuel Indices for Spark Ignition

The two standards for quantifying auto-ignition properties, or knock tendency, for SI engines are the research octane number (RON), and the motor octane number (MON). ASTM methods D2699 and D2700 are used to measure RON and MON, respectively. In these test methods, a fuel is tested with spark ignition combustion in a Waukesha cooperative fuels research (CFR) engine, and the compression ratio is adjusted to achieve a knocking intensity level of 50. A fuel with a high ignition resistance will require a higher compression ratio and therefore get a higher octane rating, and vice versa. The knocking behavior of the fuel is compared with that of so called primary reference fuels (PRF). These are binary reference fuels, consisting of n-heptane and iso-octane, where the number (for example PRF80) represents the volume % of iso-octane. PRF 0 is pure n-heptane, and PRF 100 is pure iso-octane. In RON and MON testing, all fuels are compared with PRFs and are assigned the RON value as that of the PRF blend which gives the same knocking behavior.

There are three main differences between the RON and MON test conditions, see Table 1. Firstly the inlet temperatures are different, 52°C for RON and 149°C for MON. In the RON test this temperature is the air temperature before fuel introduction while in the MON test the temperature is measured as the fuel-air mixture temperature. This difference will account for difference in heat of vaporization, and a fuel with a high heat of vaporization will for this reason have a higher difference between RON and MON. Secondly, the spark timing is changed between these methods. The third difference is the engine speed: 600 rpm for the RON test and 900 rpm for the MON test, see summary in Table 1.

The sensitivity of a fuel or fuel component, S, is a measure of the difference in knock tendency for a fuel at different operating conditions. S is defined as the difference between the RON and MON value (i.e. S=RON-MON). The sensitivity equals 0 for fuels/components whose RON=MON, for example, iso-octane, n-heptane, and their PRF blends.

Fuels with a higher octane rating than 100 (e.g. a higher knock resistance than iso-octane), are instead compared to iso-octane with small amounts of tetraethyl lead (TEL). The octane number is then extrapolated from the original 0-100 scale, and is calculated from the amount of TEL needed to match the fuel anti-knock properties [22].

Table 1. Operating conditions of the RON and MON standards. [3,22]

	RON	MON
Engine speed (rpm)	600 ± 6	900 ± 9
Intake air temperature (°C)	52	38 ± 2.8
Intake charge temperature (°C)	not stated	149 ± 1.1
Spark advance (CA°)	13	Variable (19 to 26)
Mixture equivalence ratio	Adjusted to achieve maximum knock intensity	
Venturi diameter (mm)	14.3	
Coolant temperature (°C)	100 ± 1.5	
Oil temperature (°C)	57.0 ± 8.5	

2.5.1 Difficulties with the Current Octane Rating Methods

Leppard [8] concluded that the compression ratio needed for auto-ignition of different paraffins did not rank with octane number. The experiments were performed in a CFR engine without the use of the spark. Their method was to compress fuel and air and measure reactivity by studying CO emissions at different compression ratios, but avoiding complete combustion. They attribute the differences mainly to fuel chemistry, not accounted for by the RON and MON methods. Differences between this motored method and the RON and MON methods included partially reacted residuals (since they had no combustion), different from the residuals of a fired RON or MON cycle.

Problems with using RON and MON as indicators of auto-ignition behavior are further discussed in [23,24,25]. They conclude that the ASTM knock detection system does not describe pressure fluctuations from auto-ignition in the end gas, but that it rather describes the rate of change of pressure prior to knocking. Despite these issues, RON and MON measurements in a CFR engine are the basis for commercial gasoline octane standards and sales around the world. These studies however show that RON and MON are not true indicators of auto-ignition, and should not be used for determining fuel performance for HCCI combustion.

In the current thesis work, a CFR engine was selected to study HCCI auto-ignition and combustion because this instrument is so widely used in the fuels industry. To operate in HCCI mode, the spark plug was not used. Instead ignition was initiated via compression of the fuel mixture alone.

2.6 Fuel Metrics for HCCI Combustion

A key objective of this thesis project was to determine a suitable metric for characterizing fuel combustion behavior under HCCI conditions, analogous to the RON and MON fuel metrics for spark ignition engines. Several metrics that can be used for HCCI combustion have been proposed by other researchers. Two of these are discussed below.

2.6.1 Kalghatgi's Octane Index

The octane index, originally developed for SI engines by Kalghatgi [26], was extended to HCCI combustion [1,27,28,29]. As shown in Equation 2.1, the only two fuel parameters used in this index are RON and MON. The index includes an engine parameter, K, whose value depends upon the specific engine and the specific engine operating conditions.

$$OI=(1-K)\ RON+K\ MON = RON-KS \qquad (2.1)$$

OI: Octane index

K: Engine parameter that varies with engine and operating conditions

S: Fuel Sensitivity = RON - MON

At each engine operating condition, the value of K is determined by using a regression technique to determine the value of K that gives the best linear fit to a plot of CA50 (the engine crank angle where 50% of the combustion has occurred) vs. OI (= RON – KS) for a set of different fuels. For the engine used in those studies, Kalghatgi found that K could be related to $T_{comp,15}$, the temperature in the cylinder when pressure is equal to 15 bar during the compression stroke, through Equations 2.2 and 2.3.

$$K=0.0426(T_{comp,15})-35.2 \text{ if } T_{comp,15} \text{ is above 825 K} \quad (2.2a)$$

or

$$K=0.0056(T_{comp,15})-4.68 \text{ if } T_{comp,15} \text{ is below 825 K} \quad (2.2b)$$

Or with lambda dependence;

$$K=0.00497*T_{comp,15}-0.135*\lambda-3.67 \quad (2.3)$$

The applicability of the above equations for calculating K values from $T_{comp,15}$ in engines other than the ones used by Kalghatgi is not known. It may be necessary to use the original regression analysis discussed above.

The value of K is dependent on the in cylinder temperature and changes for engine-type and operating conditions such as inlet air temperature, compression ratio, inlet air pressure, and engine speed.

Liu et al. [30] showed that Kalghatgi's index does not work well for reference fuels containing ethanol. This is unfortunate since most commercial gasolines contain ethanol to meet government regulatory requirements.

2.6.2 Shibata and Urushihara Index

Shibata and Urushihara [31,32,33] found that Kalghatgi's Octane Index which only relies on RON and MON for fuel properties was insufficient to describe HCCI combustion. They developed an HCCI index based on MON, and amounts of five components (n-paraffin, iso-paraffin, olefin, aromatic, and oxygenates). They initially prepared and tested a set of 23 surrogate fuels composed of 11 pure compounds. For their fuels, they found a linear relationship between the HCCI Index and HTHRCA20, the crank angle timing where 20% of the HTHR has occurred. The Shibata-Urushihara absolute HCCI Index is shown in Equation 2.4.

$$\text{S-U HCCI Index (abs)} = m \cdot MON + a \cdot (nP) + b \cdot (iP) + c \cdot (O) + d \cdot (A) + e \cdot (OX) + Y \quad (2.4)$$

where (nP) is the percent n-paraffins by volume, (iP) is the percent iso-paraffins by volume, (O) is the percent olefins by volume, (A) is the percent aromatics by volume, (OX) is the percent oxygenates by volume, and m, a, b, c, d, e, and Y are temperature dependent constants shown in Table 2. Furthermore, the value of coefficient e depends upon the specific oxygenate in the fuel formulation (ethanol, MTBE, or ETBE). Only operating points in the same temperature range can be compared with each other.

Table 2. Coefficients of parameters for Equation 2.6, from reference [31].

		Area 1	Area 2	Area 3	Area 4	Area 5	Area 6
Temp. at 15bar		- 670K	670-700K	700-730K	730-790K	790-820 K	820 K -
MON	m	1.17	1.197	1.168	0.763	0.342	0.271
n-Paraffin	a	-0.383	-0.434	-0.489	-0.356	-0.153	-0.088
iso-Paraffin	b	-0.378	-0.45	-0.513	-0.315	-0.085	-0.043
Olefin	c	-0.13	-0.19	-0.257	-0.185	-0.081	-0.056
Aromatic	d	-0.131	-0.228	-0.324	-0.193	-0.04	-0.016
ETBE	e	-0.131	-0.174	-0.23	-0.173	-0.069	-0.034
Et-OH	e	0.388	0.31	0.183	0.062	-0.009	-0.008
MTBE	e	-0.116	-0.114	-0.122	-0.102	-0.047	-0.022
y-intersept	Y	-63.47	-60.59	-53.95	-36.43	-22.48	-22.29

Since they felt that RON was more widely used than MON, they also developed an HCCI Index expression that was based on RON, see Equation 2.5, using a separate set of coefficients that can be found in [31].

$$\text{S-U HCCI Index (abs)} = r'\text{RON} + a''(\text{n-p}) + b''(\text{i-p}) + c''(\text{O}) + d''(\text{A}) + e''(\text{OX}) + Y' \qquad (2.5)$$

The Kalghatgi and Shibata-Urushihara HCCI indices will be compared to the HCCI number proposed by the author in the results chapter.

2.7 Fuels

Currently, transportation fuels are predominantly produced in refineries that process crude oil, although there is a growing amount of biofuels used (mostly as blend components), including ethanol and fatty acid methyl ester (FAME)-based biodiesel. Refineries process the crude oil into three main categories; light distillates (liquefied petroleum gas (LPG), gasoline, naphtha), middle distillates (kerosene, diesel), and heavy distillates and residuum (heavy fuel oil, lubricating oils, wax, asphalt).

The fraction of each product produced is dependent on factors such as: the properties of the crude oil, the capacity and types of processing units in the refinery, the conversion catalysts used, and the unit operating conditions. The quantity of each product produced must balance the market demands since all of the products must be used. If there is an imbalance, a decrease in refinery capacity utilization and a decrease in production of desired products would occur. An existing refinery can only vary the relative amounts of each product over a narrow range. In many countries in Europe, the demand for diesel fuel is significantly higher than the demand for gasoline. This has led to concerns over a shortage of diesel fuel in Europe.

Thus, the use of lighter fractions such as gasoline or naphtha in advanced combustion engines can help the refinery imbalance. A key goal of the present thesis study is to

determine the impact of the properties of fuels in the gasoline and naphtha range can have on HCCI combustion.

2.7.1 Gasoline

Gasoline consists of hundreds of different hydrocarbon species [22]. These species can be grouped into several hydrocarbon classes based on chemical structure. The hydrocarbon classes include: "normal"- or n-alkanes (also known as n-paraffins), iso-alkanes (or iso-paraffins), naphthenes (or cycloalkanes and cycloparaffins), olefins (or alkenes), aromatics, and oxygenates (which contain at least one oxygen atom). These hydrocarbon classes and their chemical structures are shown in Figure 3.

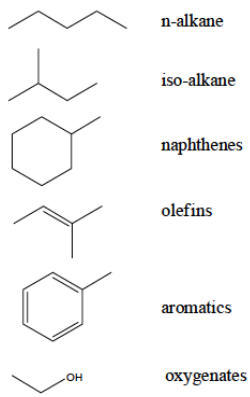

Figure 3. Representative molar structures of components found in gasoline.

With regards to the alkanes, n-alkanes are straight chains, iso-alkanes have at least one "branch" and cycloalkanes have a saturated ring. N-paraffins are very reactive towards formation of a free radical via H atom abstraction and are a primary origin of low temperature reactions.

Olefins (alkenes) are unsaturated, meaning they contain at least one C-C double bond (shown by two parallel lines in the structure). They are not naturally present in crude oil, but can be produced in some refinery processes and added to gasoline to increase octane rating.

Aromatics are unsaturated rings and are depicted as having 3 C-C double bonds. Both aromatics and olefins act as radical scavengers, which reduce the number of free radicals [19].

Oxygenates are hydrocarbons that contain at least one oxygen atom. Examples of oxygenates are alcohols (such as ethanol) and ethers (such as methyl-tertiary-buthyl-ether

(MTBE) and ethyl-tertiary-buthyl-ether (ETBE)). Ethanol is produced from biofeedstocks and it is commonly added to the gasoline as a renewable fuel, and to increase the fuel octane rating.

A representative graph showing the typical distribution of the different hydrocarbon groups in commercial gasolines is shown in Figure 4. The compositions of commercial gasolines vary widely.

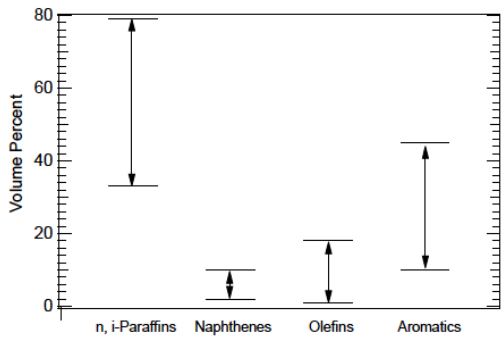

Figure 4. Approximate ranges of paraffins, naphtenes, olefins, and aromatics in U.S. gasoline, from reference [34].

2.7.2 Surrogate Fuels

The complex composition of commercial fuels has led to the use of surrogate fuels, or model fuels, which are simplified fuels used for experimental and modeling work. They are designed to have similar properties to for example gasoline (e.g. ignition quality, molar H/C ratio, viscosity), and since they contain only a certain set of chemical constituents they can be modeled more accurately than full distillate fuels. The primary reference fuels (PRF), blends of n-heptane and iso-octane, are the simplest, and they are often used as a surrogate fuel for gasoline or diesel. By adding for example an aromatic (often represented by toluene, since this is the most common aromatic in gasoline) to the primary reference fuel, the gasoline surrogate behavior can more accurately mimic that of gasoline, although its distillation characteristics will still be different from a full boiling range fuel such as gasoline [34]. In reference [35], it is concluded that high-octane oxygenated gasolines can be represented by four-component surrogate fuels consisting of n-heptane, iso-octane, toluene, and ethanol. These four components make up the surrogate fuels used in this thesis work.

3 Combustion Engine Analysis

3.1 Combustion Stoichiometry

Oxidation of a hydrocarbon is dependent on the mixture with air. In combustion engines the air/fuel ratio is often used to describe the mixing proportions, relating the amount of air used to the stoichiometric proportions. Stoichiometric combustion is when a hydrocarbon is fully oxidized with all hydrocarbon and oxygen completely consumed, forming only water and carbon dioxide. With more excess air the combustion is called lean, with excess of fuel the combustion is called rich.

3.2 Heat Release Analysis

The main part of the information used in this thesis is extracted from the pressure trace, measured by a piezoelectric pressure transducer mounted in the cylinder. With knowledge of the temperature in the cylinder when the intake valve closes, and by calculation of the heat transfer to the cooled walls, this pressure trace will provide information about the released heat. From the pressure in the cylinder a non-dimensional global temperature, assuming complete mixing, can also be calculated. The heat release calculations were made for each individual cycle of the pressure trace, and all figures in this work were based on the mean value of 300 cycles. The heat release calculation is according to Heywood [3]. Equation 3.1 gives the rate of heat release as a function of crank angle degree (CAD, θ). Crevice flow losses are assumed negligible.

$$\frac{\partial Q}{\partial \theta} = \frac{\gamma}{\gamma-1} p \frac{\partial V}{\partial \theta} + \frac{\gamma}{\gamma-1} V \frac{\partial P}{\partial \theta} + \frac{\partial Q_{HT}}{\partial \theta} + \frac{\partial Q_{crevice}}{\partial \theta} \qquad (3.1)$$

Where V and p are the cylinder volume and pressure, respectively, and γ is the ratio of specific heats, C_p/C_v. This is a single zone heat release model, assuming that the temperature and the gas composition are the same in the whole bulk, which is quite a good assumption for HCCI combustion. Gamma, γ, is approximated by Equation 3.2 and is temperature dependent. The temperature of the cylinder wall, T_{cyl}, is assumed to be the same temperature as the engine coolant, 373 K. The heat transfer model was tuned by changing the γ_0 and k with respect to the shape of the heat release curves, and the applied

values are presented in Table 3. The heat release was tuned for the motored pressure trace to be as close to zero as possible and that the burned pressure trace at the same time fit fuel flow measurement data. The same parameters were used for all fuels and cases.

$$\gamma = \gamma_0 - \frac{T_{cyl}-300}{1000} \cdot k \tag{3.2}$$

Table 3. Parameters for gamma calculation.

	γ_0	k
Motored	1.40	0.07
Combustion	1.37	0.05

The heat loss term is calculated with Equation 3.3 and 3.4 according to Woschni. B is the engine bore, p and T are the in-cylinder temperature and pressure, and w is a characteristic gas velocity, which is defined according to Equation 3.4. C_1 and C_2 are coefficients that must be tuned to the specific engine. In this work, parameters are modified to better suit HCCI combustion [36]. S_p is the mean piston speed, V_d is the displacement volume, and V_{IVC}, T_{IVC}, and p_{IVC}, are reference volume, temperature, and pressure, respectively, representing conditions in the cylinder when the inlet valve closes (IVC). p_f and p_m are the calculated pressure in the fired and motored cycle, respectively. Examples of accumulated heat release for a motored and a fired cycle are shown in Figure 5.

$$h = C \cdot B^{-0.2} \cdot p^{0.8} \cdot T^{-0.55} \cdot w^{0.8} \tag{3.3}$$

$$w = C_1 \cdot S_p + C_2 \cdot \left(\frac{V_d}{V_{IVC}}\right)\left(\frac{p_f - p_m}{p_{IVC}}\right) \cdot T_{IVC} \tag{3.4}$$

To calculate the temperature in the cylinder when the inlet valve closes (IVC), the heat transfer between the fuel air mixture and the walls in the intake was calculated. The Woschni heat transfer model was used with the same parameters as in the cylinder, and with an assumed wall temperature of 373 K. Equation 3.5 gives an effect of ±5°C. The effect of heat transfer to the fuel mass was assumed to be negligible.

$$\Delta T_{inlet} = \frac{hc_{inlet} \cdot A_{inlet} \cdot (T_{wall,inlet} - T_{in})}{m_{air} \cdot c_{p,air}} \tag{3.5}$$

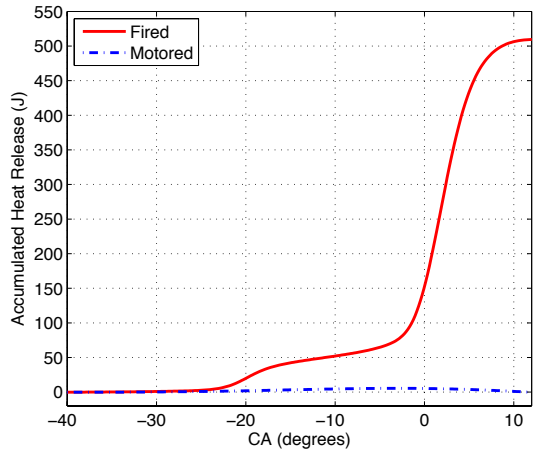

Figure 5. Example of fired and motored heat release calculated from pressure trace.

The amount of residuals was used to calculate the temperature in the cylinder when the inlet valve closed. The amounts of residuals in the cylinder were approximated using Equation 3.6 [3]. The cylinder pressure 10 CAD before exhaust valve opens was used as p_4 and the measured pressure in the exhaust was used for p_e. This gives about 3% residuals at high compression ratios (CR=15.5) and up to 10% at lower compression ratios (CR=5.5), which gives a heating effect of +5° to +35°.

$$x_r = \frac{\left(p_e/p_4\right)^{1/\gamma}}{r_c} \tag{3.6}$$

T_{IVC} is then calculated with Equation 3.7. The residuals were assumed to have the same temperature as the measured exhaust gas temperature.

$$T_{IVC} = T_{air,cyl} \cdot (1 - x_{res}) + T_{exhaust} \cdot x_{res} + \Delta T_{inlet} \tag{3.7}$$

3.3 Combustion Chemistry

3.3.1 Low Temperature Heat Release and Pre-reactions

In this work, two methods were used for determining the amount of pre-reactions. The first method was used for low temperature heat release (LTHR), which is shown in Figure 6. The period of LTHR is defined as the time between the start of combustion and the minimum value between the LTHR and high temperature heat release (HTHR, main combustion) peak.

The second method to quantify pre-reactions included both LTHR and what is also called intermediate temperature heat release. Since the rate of heat release for the main peak has a curve often resembling a normal distribution, a gaussian curve was fit to the main heat release. The area before this was called early heat release (eHR), see Figure 7. Sometimes ITHR pre-reactions are present even when LTHR is not, see Section 2.3.1. With this method, fuels showing the least low temperature reactivity (here represented by PRF 100), at conditions having a high inlet air temperature and high engine speed (known to reduce LTHR), show some early heat release by this definition, see Figure 8. For both methods, pre-reactions were normalized by dividing with the total amount of heat released to account for the different fuel amounts at the different inlet air temperatures, giving a LTHR or eHR fraction.

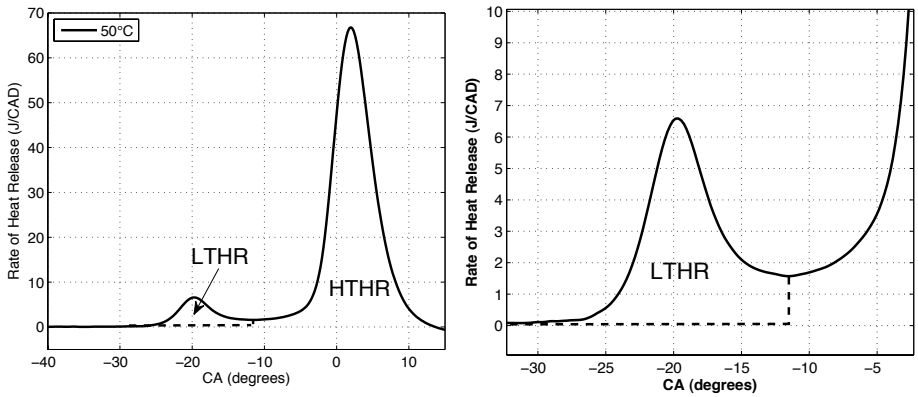

Figure 6. Rate of heat release trace and definition of low temperature heat release.

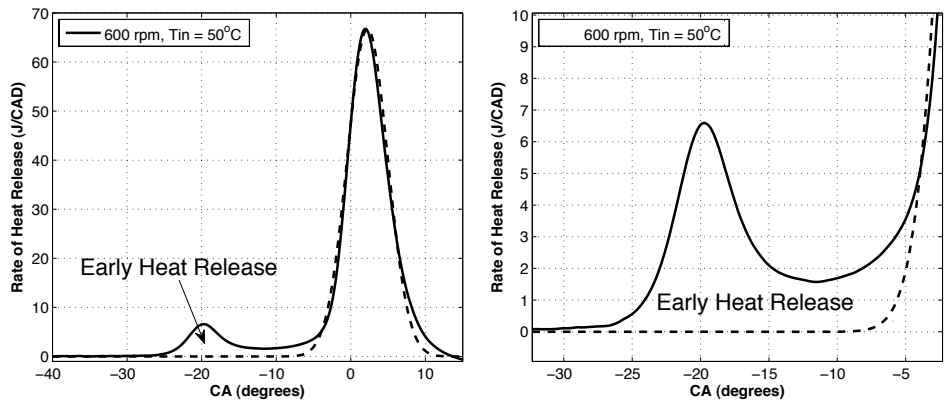

Figure 7. Rate of heat release trace and early heat release, gaussian definition.

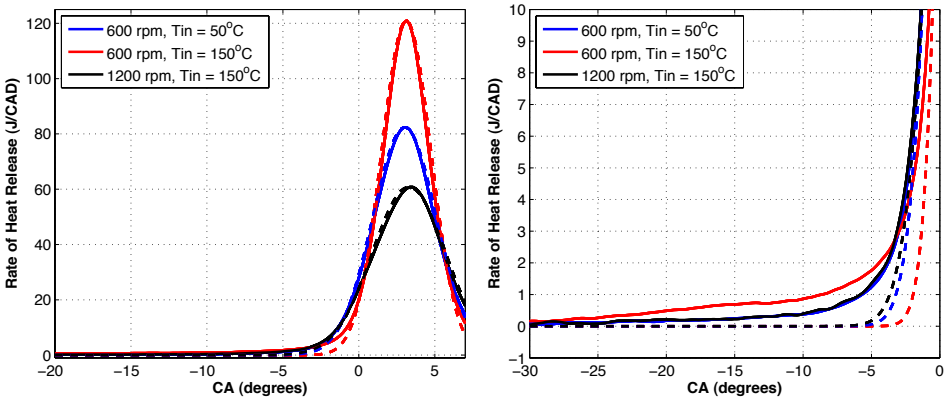

Figure 8. Rate of heat release trace and early heat release, gaussian definition, PRF 100.

3.4 Auto-ignition Temperature

Start of combustion was defined as when the rate of heat release had reached 0.2 J/CAD, shown by the black circles in the left hand portion of Figure 9. This low value was chosen to be able to detect the point where very small amounts of heat start to be released. A discussion about how this affects the results is included in [37]. The auto-ignition temperature was extracted from the start of combustion event described above. Corresponding auto-ignition temperatures for PRF90 are shown by black circles in the right hand portion of Figure 9. The blue diamonds mark the maximum rate of heat release for the LTHR and the red squares mark the minimum rate of heat release between LTHR and the main combustion.

Other definitions used to some extent in this thesis and in the literature are CA1, CA10, and CA20; where CA*x* means the event where *x* percent of the fuel charge has been consumed, see Figure 10. It can be seen that these measures, maybe with an exception for CA1, does not mark the start of combustion, but a point well within the main heat release, and are not suitable for use in this study for detection of auto-ignition.

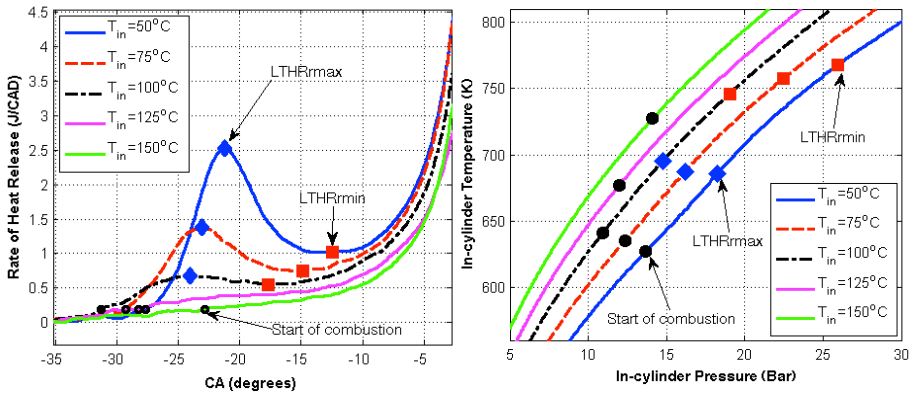

Figure 9. Auto-ignition temperatures for PRF 90. On the left, rate of heat release curve from which each point is extracted. On the right, resulting temperatures and pressures at corresponding events. Start of combustion is defined as 0.2 J/CAD.

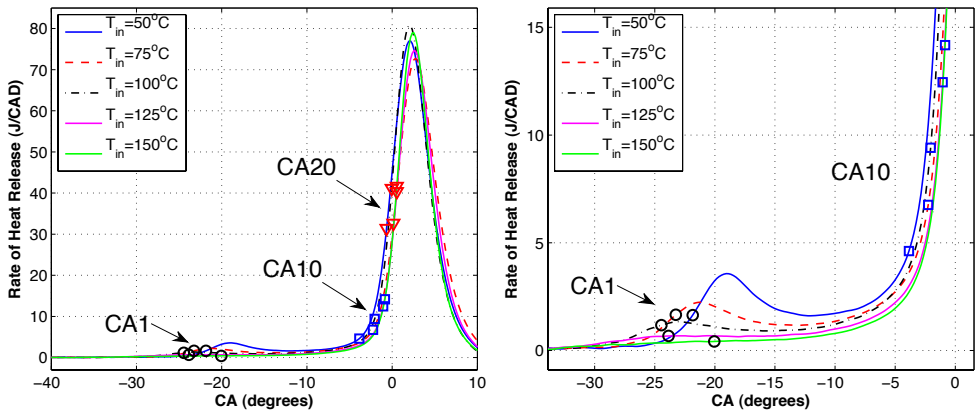

Figure 10. Three alternatives for detection of start of combustion; CA1, CA10, and CA20 marked for five different operating conditions for toluene ethanol reference fuel T9.

4 Experimental

4.1 Experimental Setup

A Waukesha variable compression ratio cooperative fuels research (CFR) engine was used for the experiments. The engine setup was modified to fit HCCI experiments. The original carburetor was replaced with port injection of the fuel. The setup included an air-fuel mixture heater mounted after the fuel port injector. Temperature of the fuel-air mixture (inlet air temperature, T_{in}) was measured by a thermocouple placed in the inlet, close to the inlet valve. A scale was used for measuring the fuel flow. The heat release was calculated from the pressure trace measured with a water-cooled Kistler piezoelectric pressure transducer mounted in the cylinder. An intake air refrigerator was included in the setup to ensure a constant water content of 0.0036 to 0.0072 kg H_2O/kg dry air throughout the experiments, fulfilling the standards in the ASTM methods for RON and MON testing. The spark ignition was switched off to enable combustion to be initiated by compression ignition. The original convectively driven water-cooling system of the CFR engine was kept. It provided a water temperature of 100ºC, relying on a condenser condensing the produced steam. The water temperature was measured during engine warm-up, and the engine was fired until the water temperature had reached at least 97ºC before the measurements were performed. An orifice plate with a diameter of 14 mm was mounted in the intake in the original carburetor of the CFR engine, and this was kept in the modified setup, placed just before the fuel injectors, 50 cm upstream from the intake valve. The orifice plate caused a pressure drop at higher engine speeds, which is also discussed in reference [8]. The engine specifications are listed in Table 4. HC, CO, CO_2, and NO_x emissions were measured with a Horiba Mexa 7500 analyzer system. Oxygen emissions are not measured but calculated. Equivalence ratio was calculated from the measured emissions.

Table 4. CFR engine specifications.

Displacement volume	612 cm^3
Number of cylinders	1
Bore	83 mm
Stroke	114 mm
CR	Variable (4:1 to 18:1)
Number of valves	2
Length of connecting rod	254 mm
Intake valve opens	10°ATDC±2.5°
Intake valve closes	146°BTDC±2.5°
Exhaust valve opens	140°ATDC±2.5°
Exhaust valve closes	15°ATDC±2.5°
Valve lifts	6.25 mm
Fuel supply	Port injection

4.2 Fuels

The fuels tested consisted of reference fuel blends of pure components and "real" fuels blended from refinery streams, all in the gasoline volatility range.

4.2.1 Reference Fuels

Four sets of reference fuels were used in the studies. Since a higher octane rating has been shown to be essential to reach higher loads in HCCI combustion [38], most surrogate fuels were designed to have a RON above 70. The first set of fuels consisted of Primary Reference Fuel (PRF) blends of n-heptane and iso-octane: PRF 0, 20, 40, 60, 80, 90, 95, and 100, where the number represents the volume % of iso-octane and corresponds to the RON and MON values.

The second set of test fuels consisted of blends of n-heptane, iso-octane and toluene (referred to as toluene reference fuels (TRFs). Table 5 shows octane ratings for these pure components and ethanol. The compositions and measured octane numbers for the TRFs are listed in Table 6. Fuels designated as HxTy contain x vol.% n-heptane, y vol.% toluene, and the balance (100-x-y) vol.% iso-octane. For this fuel set, the n-heptane content was kept constant at 20 vol.% while the toluene content was varied from 10 to 60 vol.%. These fuels were tested to study the effects of adding toluene to replace various amounts of iso-octane in blends of n-heptane and iso-octane.

The third set of test fuels, referred to as ethanol reference fuels (ERFs), were blends of n-heptane, iso-octane and ethanol. The compositions and measured octane numbers for these fuels are listed in Table 7. Fuels designated as HxEy contain x vol.% n-heptane, y vol.% ethanol, and (100-x-y) vol.% iso-octane.

The fourth test matrix, referred to as toluene-ethanol reference fuels (TERFs), consisted of blends of n-heptane, iso-octane, toluene and ethanol according to Table 8. This matrix was designed as a central composite face-centered (CCF) mixture design, in three levels and with three centerpoint runs. Three components (n-heptane, toluene, and ethanol) are varied, and the rest of the fuel consists of iso-octane (so-called filler). RONs and MONs were measured for these fuels, and the results are presented in Table 8. They were not measured for toluene reference fuel #17, but rather assumed to be the same as for the other centerpoint fuels #7 and #11, since it is not a separate fuel but a re-run.

Table 5. Properties of pure components used to blend the reference fuels. Ethanol data from [39, 40], toluene data from [3].

Pure component	RON	MON	S (RON-MON)	Boiling point
n-Heptane	0	0	0	98.42 °C [22]
iso-Octane	100	100	0	99.23 °C [22]
Ethanol	109	90	19	78.4 °C
Toluene	120	109/103.5[22]	11	110.65 °C [22]

Table 6. Composition and octane measurements for toluene reference fuels (TRF)

Fuel	n-Heptane (vol.%)	Toluene (vol.%)	iso-Octane (vol.%)	RON	MON	S
H20T10	20	10	70	82.8	80.7	2.1
H20T20	20	20	60	84.9	81.8	3.1
H20T40	20	40	40	89.8	82.9	6.9
H20T60	20	60	20	93.9	83.9	10

Table 7. Composition and octane measurements for ethanol reference fuels (ERF)

Fuel	n-Heptane (vol.%)	iso-Octane (vol.%)	Ethanol (vol.%)	RON	MON	S
PRF80	20	80	0	80	80	0
H20E1	20	79	1	80.5	80.4	0.1
H20E5	20	75	5	84.4	83.2	1.2
H20E10	20	70	10	87.9	85.6	2.3
H20E20	20	60	20	94.1	88.2	5.9
PRF70	30	70	0	70	70	0
H30E1	30	69	1	70.6	70.2	0.4
H30E5	30	65	5	73.2	73.1	0.1
H30E10	30	60	10	78.7	76.7	2
H30E20	30	50	20	85.1	81.2	3.9
H60E40	60	0	40	71.4	65	6.4
H55E45	55	0	45	78	71.6	6.4
H50E50	50	0	50	84.7	76.8	7.9
H45E55	45	0	55	89.7	80.4	9.3
H40E60	40	0	60	94.4	82.8	11.6

Table 8. Composition and octane measurements for toluene ethanol reference fuels (TERF)

Fuel	n-Hept (vol.%)	Toluene (vol.%)	Ethanol (vol.%)	iso-Oct (vol.%)	RON	MON	S
T1	40	10	5	45	67.1	63.7	3.4
T2	20	10	20	50	94.7	88.5	6.2
T3	20	30	20	30	97	87.6	9.4
T4	40	30	20	10	80.8	73	7.8
T5	30	20	5	45	79.6	74.5	5.1
T6	30	30	12.5	27.5	85.3	78.6	6.7
T7	30	20	12.5	37.5	83.8	78.1	5.7
T8	40	30	5	25	71.8	65.8	6
T9	30	10	12.5	47.5	81.6	77.9	3.7
T10	20	30	5	45	90.2	84.1	6.1
T11	30	20	12.5	37.5	83.8	78.2	5.6
T12	40	10	20	30	78.3	74.3	4
T13	20	10	5	65	86.1	83.6	2.5
T14	40	20	12.5	27.5	74.8	68.9	5.9
T15	20	20	12.5	47.5	92.3	86.4	5.9
T16	30	20	20	30	87.9	81.4	6.5
T17	30	20	12.5	37.5	-	-	-

4.2.2 Refinery Gasoline Fuels

Fuels prepared primarily from blends of refinery components were provided by Chevron and are listed in Table 9.

Table 9. Main properties of gasoline fuels.

Gasoline fuel set #1				Gasoline fuel set #2			
Fuel label	RON	MON	S	Fuel label	RON	MON	S
G0	87.1	80.5	6.6	G82	83.5	79.9	3.6
G1	92.9	84.7	8.2	G83	91.4	83.9	7.5
G2	97.7	87.5	10.2	G84	87.7	80.9	6.8
G3	78.2	73.4	4.8	G85	86.7	79.7	7
G4	69.4	66.1	3.3	G86	91.6	84.0	7.6
G5	99	96.9	2.1	G87	90.1	83.4	6.7
G6	70.3	65.9	4.4	G88	92.5	83.5	9
G7	96.5	86.1	10.4	G89	92.4	84.5	7.9
G8	88.6	79.5	9.1	G90	88.6	81.4	7.2
				G91	89.9	82.2	7.7
				G92	86.2	79.4	6.8
				G93	91.6	82.2	9.4

5 Results and Discussion

First, the auto-ignition properties of the reference fuels are summarized, focusing on the effects of intake air temperature (Tin), engine speed, and fuel composition, on the resulting auto-ignition temperatures and the amount of low temperature heat release. Next, analysis of emissions formation in HCCI and effects from fuel components are presented. Different metrics and indices are evaluated for the use of determining HCCI fuel-engine performance, and the need of a new fuel number is expressed. Finally, an HCCI number, used to quantify fuel behavior in HCCI combustion, is described. This Lund-Chevron HCCI number is then explained in terms of agreement with auto-ignition properties.

5.1 Auto-ignition Properties (Papers I,II,III, and V)

The auto-ignition properties such as the auto-ignition temperature and the amount of low temperature reactions for reference fuels were studied in detail and were presented in four publications [37,41,42], on which this chapter is based. Auto-ignition temperature and low temperature reactions were believed to be closely coupled with the auto-ignition qualities of a fuel. This chapter provides a summary of these properties; first the low temperature heat release, then the auto-ignition temperatures. Data on repetition runs and error analysis are presented in Appendix.

5.1.1 Changing Pressure-Temperature History

The experimental method consisted of varying the inlet air temperature to achieve different pressure-temperature combinations for each fuel. Compression ratio was then adjusted to keep CA50 at 3° after TDC. Resulting pressure-temperature traces for Fuel T1 are presented in Figure 11. A certain combination of compression ratio and inlet air temperature will create the same pressure-temperature history, see fuel tests T13, T16, and T17, for which the pressure-temperature is overlapping on the left hand side of Figure 11. All these fuels were run with a compression ratio of about 10.8 at the inlet air temperature of 150°C. As seen in this figure, a similar effect could have been achieved for a constant compression ratio, instead changing the inlet air temperature. A lower inlet air

temperature will require a higher compression ratio, and the in-cylinder pressure will be higher for a given temperature. For the motored cycle, changing inlet air temperature will only change the temperature (and not pressure) at TDC, whereas the compression ratio will change both pressure and temperature. The pressure-temperature effect can be represented by a temperature pressure ratio, here done by using the in-cylinder temperature at 15 Bar pressure during the compression stroke, see Figure 12.

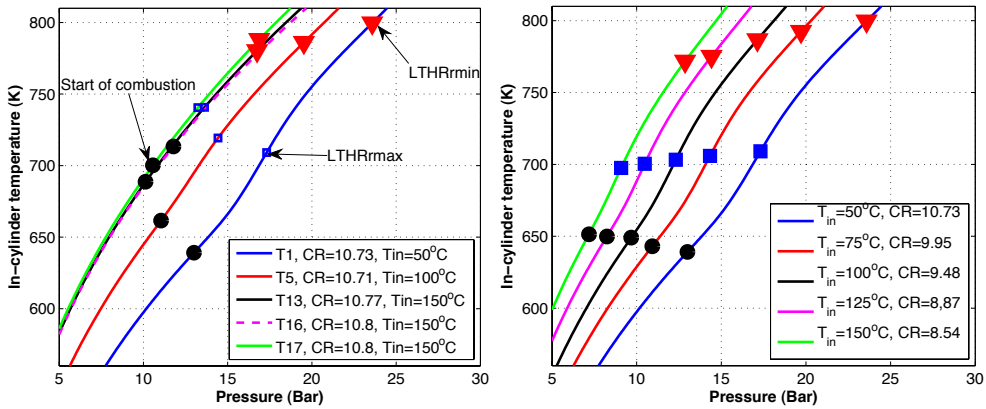

Figure 11. Pressure-temperature histories for various toluene ethanol reference fuels (left) and toluene ethanol reference fuel test T1 (right).

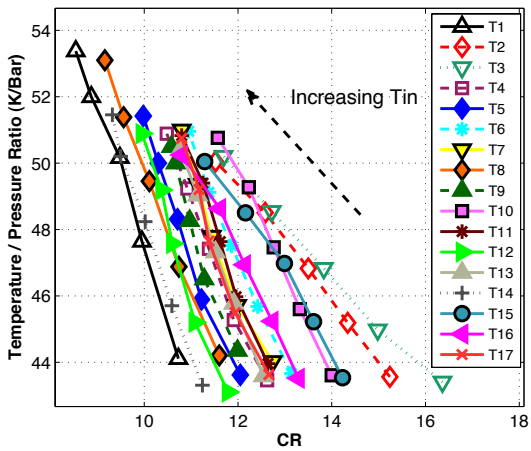

Figure 12. Temperature / pressure ratio, calculated at 15 bars pressure during compression, for all toluene ethanol reference fuels. T/P ratio is increased with increased inlet air temperature. The five marks for each fuel are the five inlet air temperatures.

5.1.2 Low Temperature Heat Release

The amount of low temperature heat release (LTHR) was studied for all fuels at 600 rpm and at an equivalence ratio of 0.33, with a change in inlet air temperature in five steps from 50 to 150°C to achieve different pressure-temperature histories. Additionally, experiments were made at higher engine speeds for four primary reference fuels, and these will be discussed in the last part of this section. The low temperature reactions are scaled with the total heat relased, and are therefore expressed in fractions (%).

5.1.2.1 Inlet Air Temperature and Fuel Effects on LTHR

The amount of LTHR was determined by the method presented in Section 3.3.1. The values are presented in Tables 17, 18, 19, and 20 in Appendix, for the PRFs, TRFs, ERFs, and TERFs, respectively. The amount of LTHR decreased with inlet air temperature, as shown in Figure 13 for fuel PRF 70, for inlet air temperatures from 50 to 150°C. The reason for this is that the precursors for this chain branching (the LTR) are decomposed back to the reactants at higher temperatures [2]. This can be explained by looking at the right hand side in Figure 13. By the different temperature/pressure histories created by the change in inlet air temperature, we can see that at the lowest inlet air temperature, the cylinder pressure is the highest during the temperature range when LTR is dominating, speeding up these reactions, resulting in a larger amount of LTHR. When temperature reaches about 700 K, the radicals are starting to decompose and the low temperature heat release reaches a minimum rate, corresponding to an in-cylinder temperature of 800 K, before the main combustion starts.

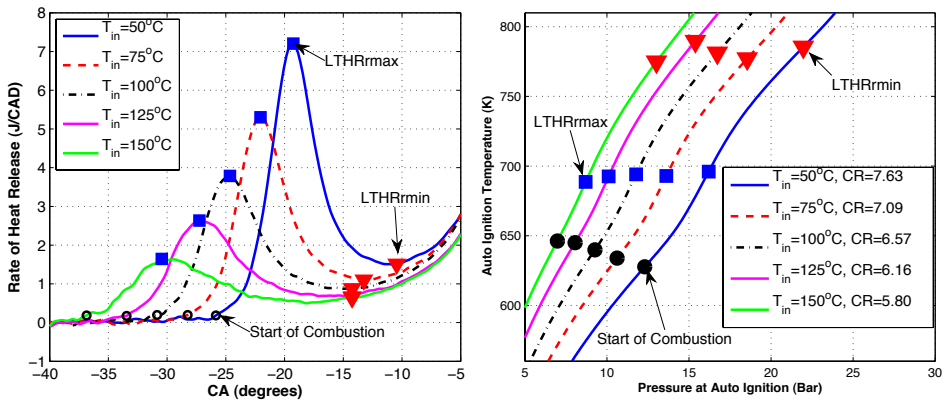

Figure 13. Low temperature reactions (left) and temperature-pressure history (right) for PRF 70.

For primary reference fuels, the LTHR was seen to decrease almost linearly with increased amount of iso-octane, e.g. fuel RON, see Figure 14. Figure 15 shows that for more complex reference fuels, here containing ethanol, the amount of LTHR is no longer

linearly dependent on the RON, as was the case for the PRFs. The low temperature heat release is shown at two levels, corresponding to inlet air temperatures of 50° and 150°C, for each fuel. For example, the two-component ERFs (H40E60, H50E50, etc.) show less LTHR than expected from their RON.

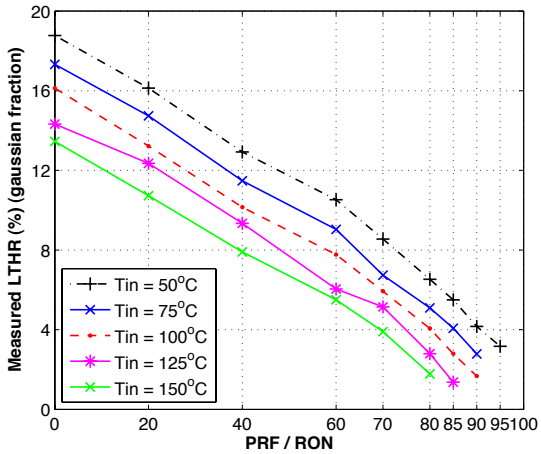

Figure 14. Amount of LTHR for primary reference fuels.

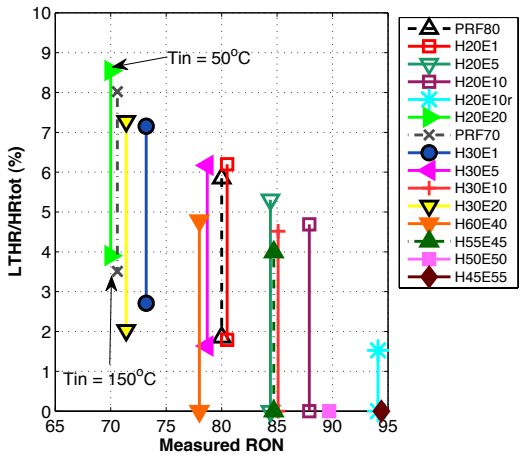

Figure 15. LTHR quenching effect of ethanol. The two different markers for each fuel denotes the different inlet air temperatures, 50°C above and 150°C below. Zero means no LTHR at one or more temperatures.

Both ethanol and toluene are known to reduce low temperature reactions by acting as radical scavengers [13, 19], and both components were seen to reduce low temperature reactions in the experiments. This ethanol quenching effect was studied in detail, and is originally presented in [41]. Please note that the study of the ethanol reference fuels did not originally include measured RON and MON, instead calculated values based on

blending by volume method are reported in the paper. Some octane values are therefore different when presenting these results in this thesis.

On the left hand side in Figure 16, the fraction of LTHR is shown as a function of the ethanol fraction, and it is apparent that not only ethanol affects the LTHR. Also fuels with high concentrations of ethanol (H60E40, H55E45, H50E50, containing 40-50 vol. % ethanol) showed significant LTHR. Since it is known that n-heptane induces LTHR, this fraction was also considered. The LTHR fraction was shown to be proportional to the difference between the n-heptane and ethanol volume fractions, see Figure 16. For example, at the medium inlet air temperature of 100°C, n-heptane induced as much LTHR as the same volume of ethanol quenched [41]. The lines are the best fits at the different inlet air temperatures. A higher temperature again gives more LTHR. No fuel with higher volume fractions of ethanol than n-heptane showed significant LTHR.

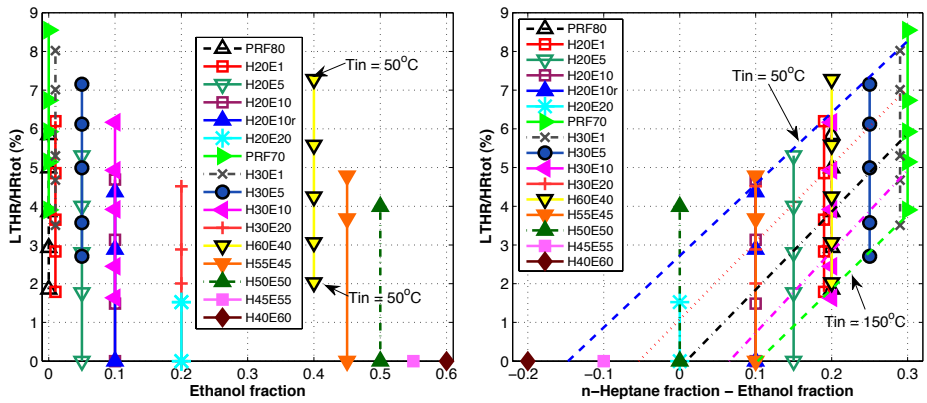

Figure 16. Low temperature heat release quenching by ethanol. The amount of LTHR is a result of LTHR producing component (n-heptane) and LTHR quenching component (ethanol). Lines in the figure to the right are best fits at each inlet air temperature.

By comparing the amount of low temperature heat release for three fuels with a constant amount of n-heptane (30 vol.%), and toluene (20 vol.%) but varying amounts of ethanol (5, 12.5, 20 vol.%) and iso-octane (45, 37.5, 30 vol.%), the quenching effect of ethanol could be seen, see Figure 17. This is based on the assumption that iso-octane (whose concentrations are also changing) has a much smaller effect on LTHR that ethanol. A similar example of toluene quenching effect is presented in Figure 18. The two fuels have a constant amount of n-heptane (40 vol.%), and ethanol (5 vol.%) but varying amounts of toluene (10, 30 vol.%) and iso-octane (45, 25 vol.%). The quenching effect of toluene can be seen by the lower LTHR for the fuel with a higher toluene concentration. Despite the higher RON of toluene than ethanol (120 compared to 109), toluene has the weaker LTHR quenching effect.

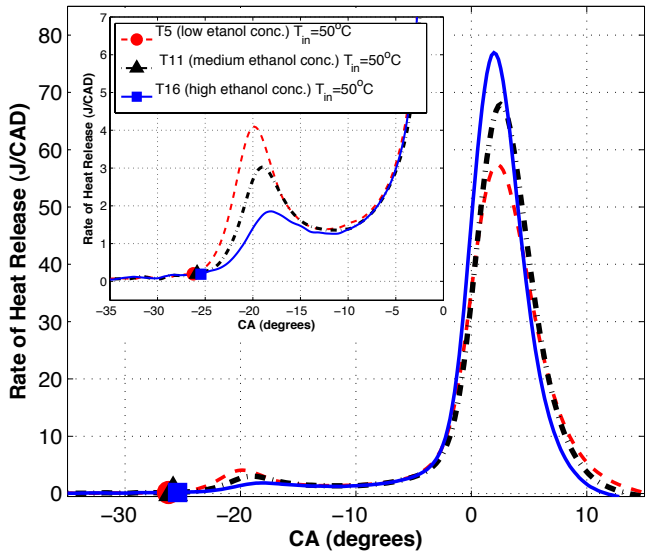

Figure 17. Low temperature reaction quenching effect from ethanol.

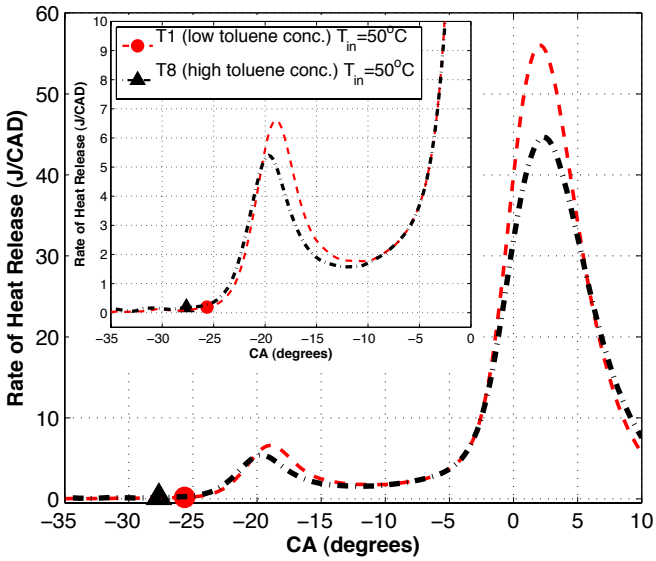

Figure 18. Quenching effect of toluene on low temperature heat release.

A linear model for low temperature heat release, based on all data for reference fuels (PRF, TRF, ERF, TERF) is shown in Equation 5.1, with cofficients in Table 10. Operating points showing no heat release were not included, leaving 154 data points with LTHR at the five different inlet air temperatures for the model. Only 600 rpm data were used. For the model of all fuels, a positive effect on LTHR was seen for toluene addition, indicating that toluene induced LTHR, if not by much. A second model based on only TERF data (48 operating conditions with LTHR) shows similar results as the previous model, however in this range the toluene addition quenched LTHR.

A linear model based on early heat release data for all reference fuels is shown in Equation 5.2, including concentrations of n-heptane, toluene, and ethanol (in volume percentage, vol.%), and inlet air temperature (in K). The constants shown in Table 10 indicate that n-heptane induces early heat release, while toluene quenches it, and ethanol has an even stronger quenching effect. As mentioned earlier, it is again seen that n-heptane has about as strong of an effect on pre-reactions as ethanol has, although opposite.

$$LTHR = a + b*x_{n\text{-}heptane} + c*x_{toluene} + d*x_{ethanol} + e*Tin \quad (5.1)$$

$$Early\ heat\ release = a' + b'*x_{n\text{-}heptane} + c'*x_{toluene} + d'*x_{ethanol} + e'*Tin \quad (5.2)$$

Table 10. Values of coefficients for Equations 5.1 and 5.2, where x is volume percentage of component, and Tin is in K.

Low temperature heat release, Equation 5.1			
Coefficient		All reference fuels	TERF
a	-	16.30	18.65
b	n-Heptane	0.1496	0.2252
c	Toluene	0.01829	-0.0424
d	Ethanol	-0.1793	-0.1997
e	Tin	-0.04008	-0.0522
Model R^2		0.86	0.98
Early heat release, Equation 5.2			
Coefficient		All reference fuels	TERF
a'	-	17.704	15.971
b'	n-Heptane	0.146	0.185
c'	Toluene	-0.036	-0.015
d'	Ethanol	-0.14	-0.166
e'	Tin	-0.034	-0.033
Model R^2		0.96	0.98

5.1.2.2 Speed Effects on LTHR

The amount of early heat release decreased as engine speed increased, as shown in Figure 19 for gasoline fuel G3. Among other things, engine speed effects the available time for the low temperature heat release, which is explained in [12]. Higher engine speeds lead to less time available for the LTHR reactions to develop before the HTHR reactions occur. Using the LTHR definition, many of the fuels did not show any LTHR. By instead using the definition of early heat release, see Section 3.3.1, pre-reactions could

still be studied. Low temperature and early heat release data for the primary reference fuels in the speed sweep, are presented in Tables 24 and 25 in Appendix.

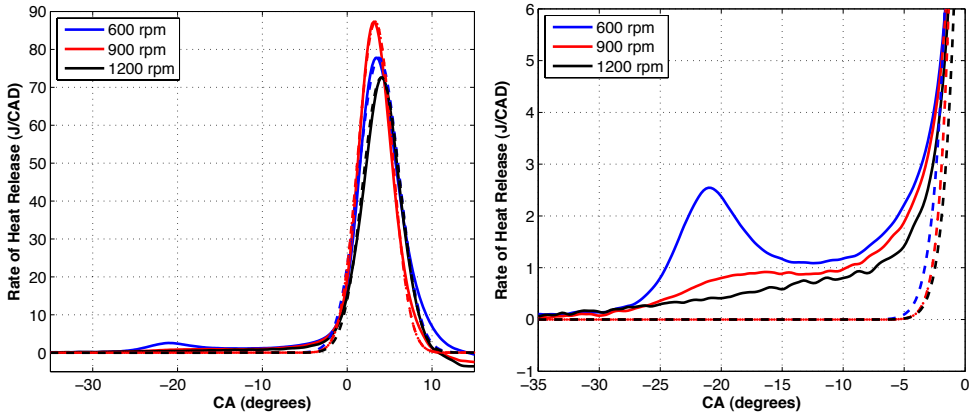

Figure 19. Speed effect on pre-reactions for gasoline fuel PRF90. The gaussian fit used for determining the baseline for early heat release is also shown for each engine speed by dashed lines.

One fuel showing LTHR at all engine speeds was PRF70, see Figure 20. Even though it appears at the same crank angle, the temperature range of the negative temperature coefficient zone is changed when increasing the engine speed. The temperature range is from 700-800 K at the lowest engine speed, up to 900-1000 K at the highest engine speed. This shift is also seen in Figure 21, when the temperature range of 850-1000 K, sometimes referred to as the intermediate temperature area, are shown to shift with higher engine speeds. This therefore shows that this temperature interval does not always correlate with intermediate temperature heat release.

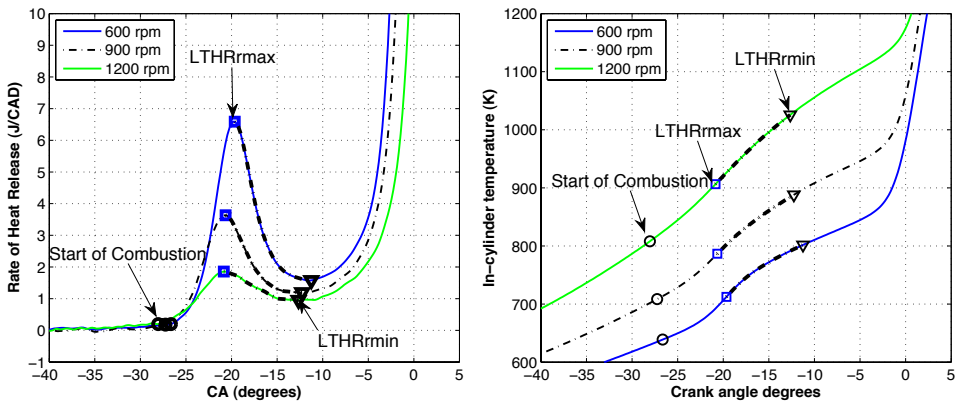

Figure 20. Low temperature heat release for PRF 70 and corresponding temperature evolution during speed sweep with Tin = 50°C.

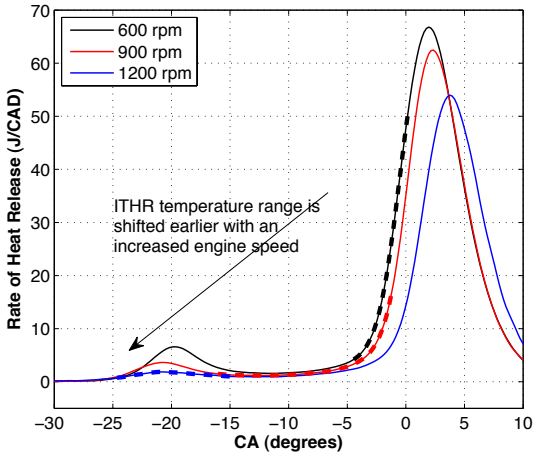

Figure 21. The intermediate temperature heat release temperature range of 850 to 1000 K is shifted earlier at higher engine speeds, here PRF 70 as an example.

5.1.3 Auto-ignition Temperatures

The procedure to determine the auto-ignition temperature is explained in Chapter 3.4. The calculated auto-ignition temperatures for PRFs are shown in Figure 22, where five pressure levels where achieved by adjusting the inlet air temperature in five steps from 50 to 150°C, and compression ratio was adjusted for achieving a constant CA50 3° after TDC. Temperature range for low temperature reactions are shown in Figure 24, and are seen to range from 650 to 800 K for TERFs. A similar range is seen in [37], about 600 to 800 K for primary reference fuels. This agrees with previous research [7]. These temperatures should be kept in mind when looking at the auto-ignition temperatures. For the primary reference fuels, the auto-ignition temperature was seen to be nearly constant for fuels with extensive low temperature reactions, such as PRF0 to PRF60. The auto-ignition temperature for these fuels was around 600 K and it was constant even as the cylinder pressure was changed by adjusting the inlet air temperature. For PRFs with less n-heptane, the auto-ignition temperature started to significantly increase when the low temperature reactions disappeared, see for example PRF 90 in Figure 25. At the inlet air temperature of 125°C, the LTHR has diminished to the point where there is no longer a rate of reaction peak, and over this transition the auto-ignition temperature has risen about 50°. The increase in auto-ignition temperature was seen both as n-heptane concentration was decreased and as the inlet air temperature was increased. A fuel that only shows less low temperature reactivity, and therefore higher auto-ignition temperatures, are presented in Figure 23.

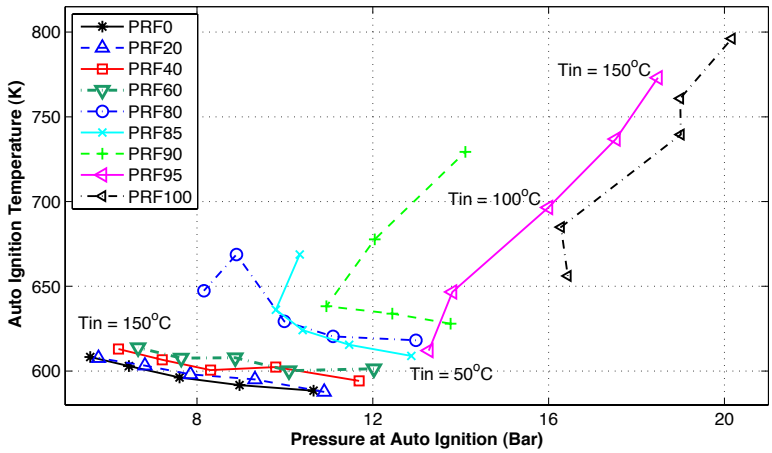

Figure 22. Auto-ignition temperatures for primary reference fuels.

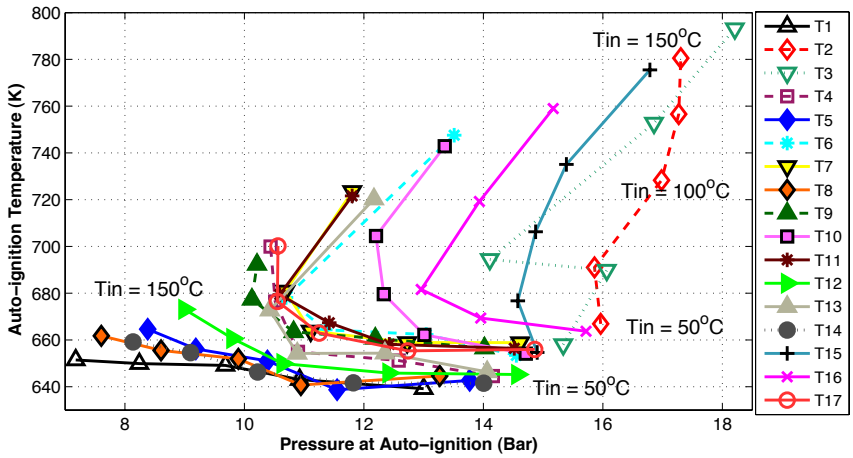

Figure 23. Auto-ignition temperatures of TERFs.

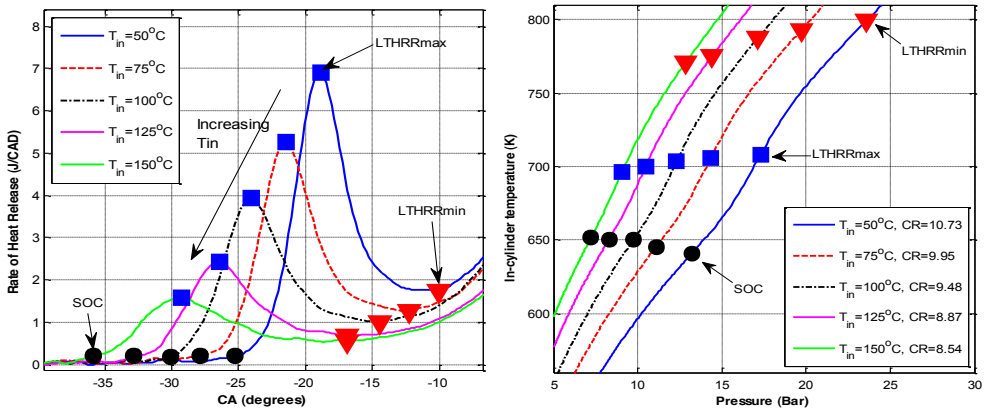

Figure 24. Low temperature reactions and corresponding temperatures for toluene ethanol reference fuel T1.

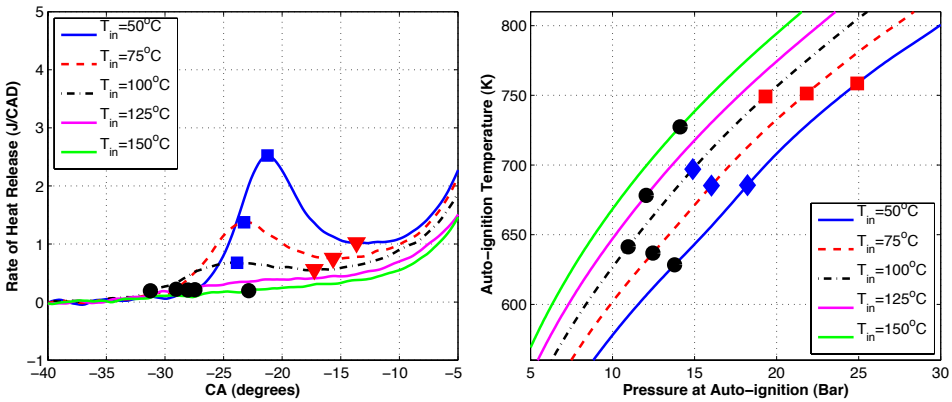

Figure 25. Auto-ignition temperatures (right) and low temperature heat release (left) for PRF90.

Auto-ignition temperatures for all reference fuels (PRF, TRF, ERF, and TERF) were modeled as a linear function of the inlet air temperature (in K) in combination with the concentrations (in vol.%) of n-heptane, toluene, and ethanol. Although this was not a true linear function (linear equation, $r^2 = 0.48$), Equation 5.3 gives some perspective on the auto-ignition, with coefficients shown in Table 11.

$$AIT = a + b*x_{n\text{-}heptane} + c*x_{toluene} + d*x_{ethanol} + e*Tin. \quad (5.3)$$

Table 11. Coefficients for Equation 5.3.

Coefficient		All reference fuels	Only TERF
a	-	448.19	482.71
b	n-Heptane	-0.88	-2.8
c	Toluene	0.5	0.29
d	Ethanol	1.09	2.7
e	T_{in}	0.62	0.64
R^2	-	0.48	0.80

Conclusions that can be drawn from this model is that n-heptane decreases the auto-ignition temperature, and ethanol increases it. The effect of toluene is to increase AIT, but the magnitude is only a tenth of the effects of n-heptane or ethanol (at least in the TERF-based model). As seen previously, temperature increases the auto-ignition temperature. From Figure 22 and 23, we know that this effect is not linear, but only true after a certain threshold, when the LTHR disappears.

The negative temperature coefficient regions are marked in Figure 26. It can be seen that it starts at about 700 K for the three inlet air temperatures leading to low temperature heat release. For the two highest inlet air temperatures, the auto-ignition coincides with the NTC area, why combustion starts slowly and no pre-reactions can be seen.

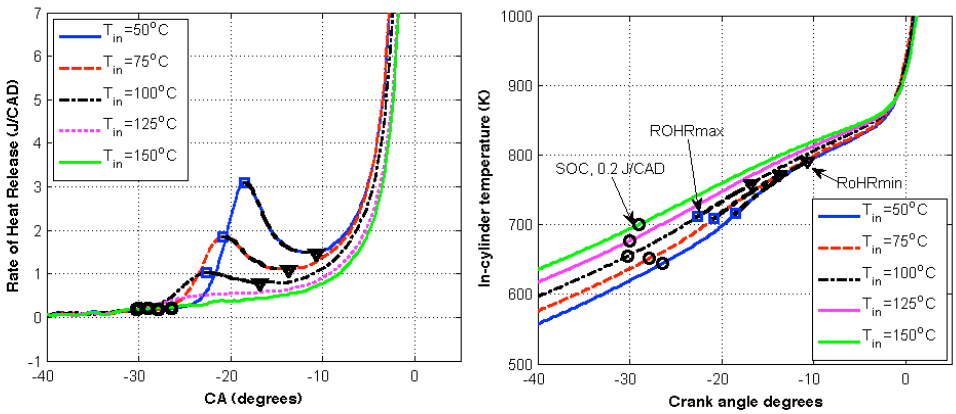

Figure 26. On the left, low temperature reactions and on the right, in-cylinder temperature evolution. The negative temperature coefficient (NTC) region is marked in both figures, defined as the decreasing rate of heat release in the left figure. Toluene ethanol reference fuel T1 is shown (see Chapter 4.2.1 for specifications).

Increasing inlet air temperature, decreasing inlet air pressure, and increasing engine speed, are all shown to give a more pronounced NTC region [8], as shown in Figure 27 for PRF 70, where the NTC zone is the duration between the squares and triangles in this figure. All these changes are performed together when changing from RON to MON conditions,

and are connected with the effect on auto-ignition temperatures. Leppard [8] concludes that NTC behavior is more prominent at MON conditions (higher speed and intake temperature) than at RON conditions.

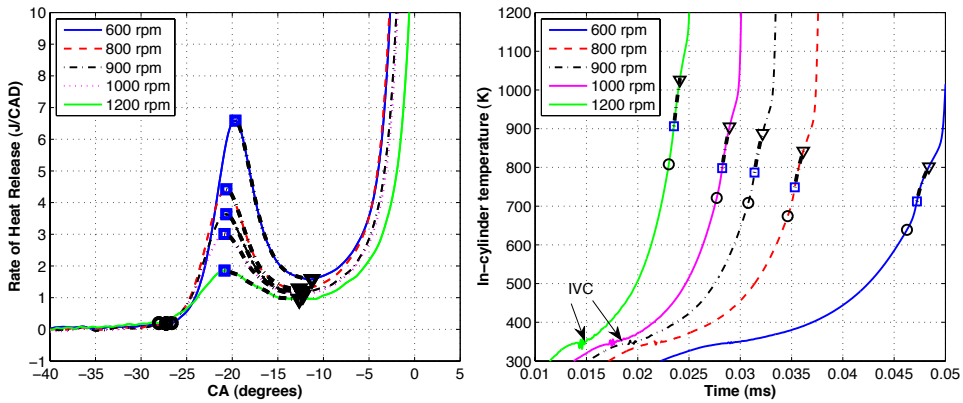

Figure 27. Low temperature reactions as a function of engine speed (left) and speed effect on temperature history (right) for PRF 70.

5.2 Emissions in HCCI Combustion (Paper IV)

To give a full description of the fuel effects on combustion, detailed analysis was performed on emissions for all reference fuels. The emission measurements are described in Chapter 4.1. Unburned hydrocarbons (HC), carbon monoxide (CO), and nitrogen oxides, NO and NO_2, (here measured together as NO_x) were studied, and the effects from fuel versus in-cylinder conditions were analyzed. The detailed results and analyses were published in [43].

The net CO emissions were a balance of the initial formation from HC oxidation and subsequent oxidation to CO_2. The CO emissions were related to the in-cylinder temperature. As shown in Figure 28, at maximum cylinder temperatures below 1710K, as temperature increased, the amount of CO increased because the rate of CO oxidation to CO_2 is very low. This was confirmed by the high HC emissions at these low cylinder temperatures. At temperatures above 1710K, the amount of CO decreases with temperature because the oxidation of CO to CO_2 is very active. Beyond the effects of fuel composition on maximum cylinder temperatures, there were no other obvious trends with fuel composition.

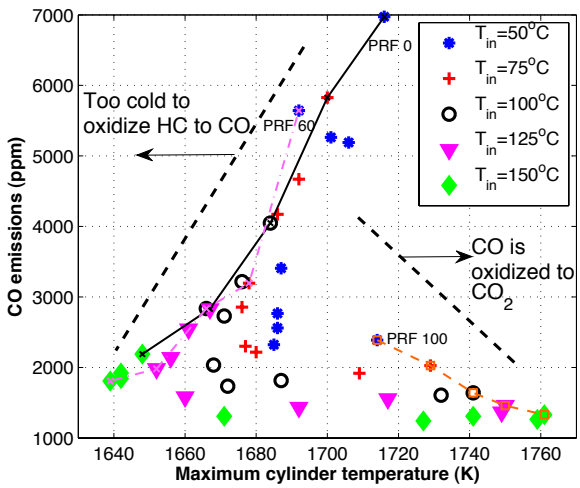

Figure 28. CO emissions for primary reference fuels, shown at different maximum values of the calculated global in-cylinder temperature. The trends were similar for all reference fuels.

HC emissions were found to be mainly dependent on the compression ratio used in each case, and were therefore attributed mainly to crevice losses. As to fuel effects, ethanol addition was shown to reduce HC emissions for combustion at a given compression ratio. Toluene addition was found to increase HC emissions at a given CR when high concentrations (40-60 vol.%) were added. Low concentrations of toluene showed a small decrease of or no effect on HC emissions. NO_x emissions were low for all operating points, but both ethanol and toluene addition were found to further decrease NO_x emissions for higher octane fuels, see Figure 29.

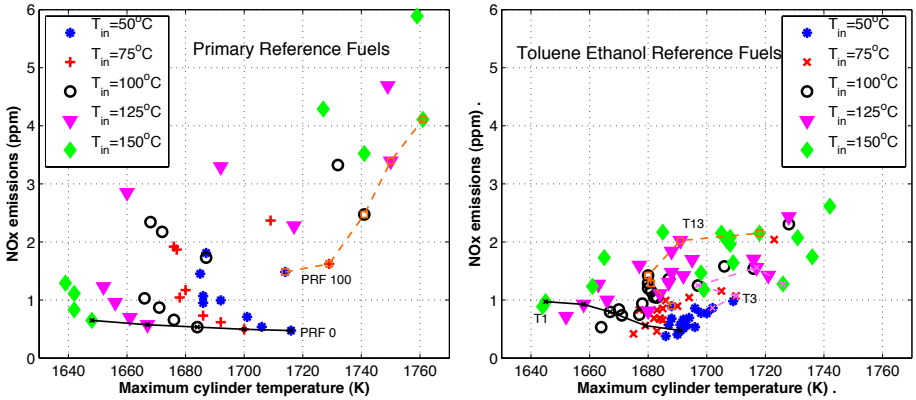

Figure 29. NO_x emissions for PRFs (left) and TERFs (right).

5.3 Fuel Metrics for HCCI Combustion

The fuel combustion properties can be quantified in several ways. The RON and MON ratings use comparison with reference fuels (PRFs), Kalghatgi's octane index [26] combines the RON and MON with a parameter dependent on the engine and operating conditions, whereas Shibata [31] calculates an HCCI index based on the fuel composition, created from engine experiments of an extensive fuel matrix. In this chapter, these indices are compared with respect to performance for the author's datasets. Finally, the Lund-Chevron HCCI number is presented and explained.

5.3.1 Research Octane Number (RON) and Motor Octane Number (MON)

Figure 30 shows that four fuels having very similar RON numbers can exhibit very different combustion behavior in an HCCI engine. Correlation between research octane number and the required compression ratio for a CA50 3° after TDC (CR_{AI}) at Tin=50°C, and Tin=150°C, respectively, are shown in Figures 31 and 32. For a given RON, the required compression ratio varies with up to almost two units. Alternatively, for a given CR, the octane number varies by up to 10 units. This large amount of scatter indicates that neither RON nor MON are sufficient fuel parameters to characterize the auto-ignition behavior of the fuels.

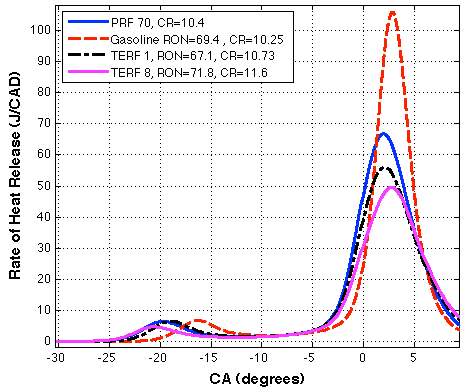

Figure 30. Four fuels of similar RON values that behave differently in an HCCI engine.

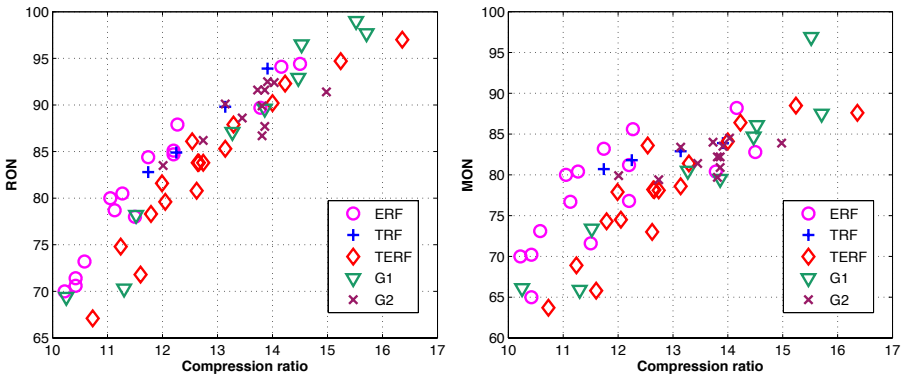

Figure 31. Agreement between RON and MON vs. required compression ratio for combustion 3° after TDC. All fuels run with an inlet air temperature of 50°C and an engine speed of 600 rpm. G1 and G2 are gasoline fuel datasets, see Table 9.

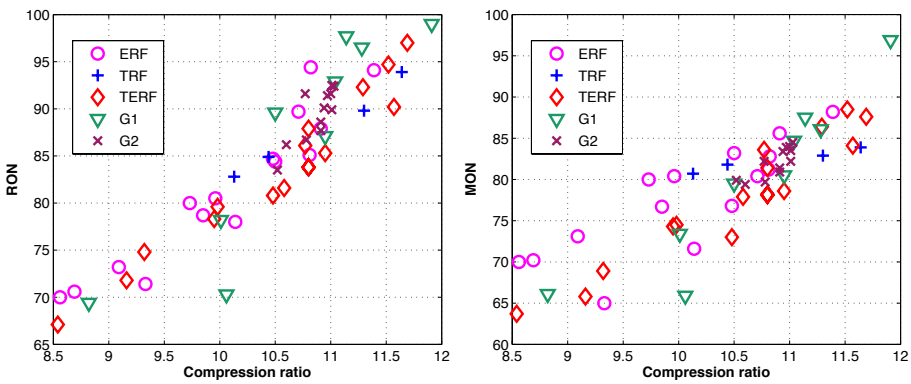

Figure 32. Agreement between RON and MON vs. required compression ratio for combustion 3° after TDC. All fuels run with an inlet air temperature of 150°C and an engine speed of 600 rpm. G1 and G2 are gasoline fuel datasets, see Table 9.

5.3.1.1 Composition Based Octane Modeling

As started by [44,45] and continued by Solaka [46], the RON and MON values for reference fuels can be estimated from fuel composition. For this model, see Equation 5.4, TRF, ERF, and TERF data, were used. Coefficients can be found in Table 12. By looking at these coefficients, it can be seen that n-heptane and ethanol had the strongest effects on the RON value, but that toluene had a significant effect as well. However, for MON, toluene had a much smaller effect. This does not correlate with the RON and MON values of the pure components, see Table 5, where toluene has both greater RON and MON than ethanol.

$$RON_{surrogate\ fuel} = a + b * x_{n\text{-}heptane} + c * x_{toluene} + d * x_{ethanol} \qquad (5.4)$$

Table 12. Coefficients for Equation 5.4. Concentrations are in vol.% and temperature in K.

Coefficient		All reference fuels	
		RON	MON
a	-	97.72	96.32
b	n-Heptane	-0.8558	-0.8089
c	Toluene	0.2137	0.0514
d	Ethanol	0.5755	0.3875
R^2	-	0.98	0.95

This effect could be why MON is not indicative of HCCI behavior in this study, see Figure 33, where fuels with the highest amount of toluene (from left; T8, T4, T6, T10, and T3) are indicated with dashed arrows. These fuels needed a greater compression ratio than indicated by their RON, and especially be their MON, meaning that toluene might have a larger effect on HCCI combustion than on knock measurements for RON and MON.

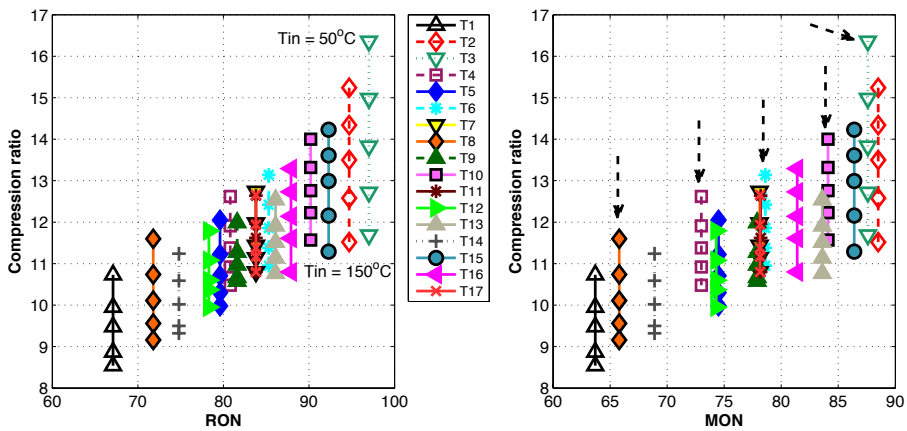

Figure 33. Measured RON and MON, respectively, and corresponding compression ratios. The five marks for each fuel correspond to the five different inlet air temperatures, with 50°C from above.

5.3.2 Kalghatgi's Octane Index

As mentioned in Section 2.4.1, Kalghatgi has proposed an octane index for HCCI that is dependent only on the fuel parameters RON and MON (or S=RON-MON) and an engine parameter K, see Equation 5.5.

$$OI=(1-K)*RON + K*MON = RON - K*S \quad (5.5)$$

Combustion phasing (CA50) is proposed to be a linear function of OI, see Equation 5.6.

$$CA50 = c + (a+b)*OI = c + (a+b)*(RON-K*S) \quad (5.6)$$

At each operating condition, the CA50 values for fuels having various RON and MON values are measured and the value of K is determined through regression analysis by finding the value that provides the best linear fit in the plot of CA50 vs. OI. The K values are reported as being truly a property of the specific engine and operating conditions and independent of fuel properties. In this thesis study, CA50 was held constant for all fuels and conditions while the compression ratio at onset of auto-ignition (CR_{AI}) was measured. So direct use of Kalghatgi's correlation was not possible. Instead the applicability of Equation 5.7 was tested.

$$CR_{AI} = c' + (a'+b')*OI' = c' + (a'+b')*(RON - K'*S) \quad (5.7)$$

For each fuel set, the values of K' at each T_{in} were determined by finding the values that gave the best linear fit to the plot of CR vs OI' (=RON-K*S).

Plots of the compression ratio and octane index data at Tin=50°C are shown in Figures 34 and 35 for the all reference fuels, TERFs, ERFs, and gasolines, respectively. The K' values for all fuel sets at the 5 intake air temperatures are listed in Table 13. The very different values of K' for each fuel set suggest that the linear OI approach does not apply here. The K-value calculated from regression analysis was found to differ significantly from the empiric correlations in Equations 2.2 and 2.3.

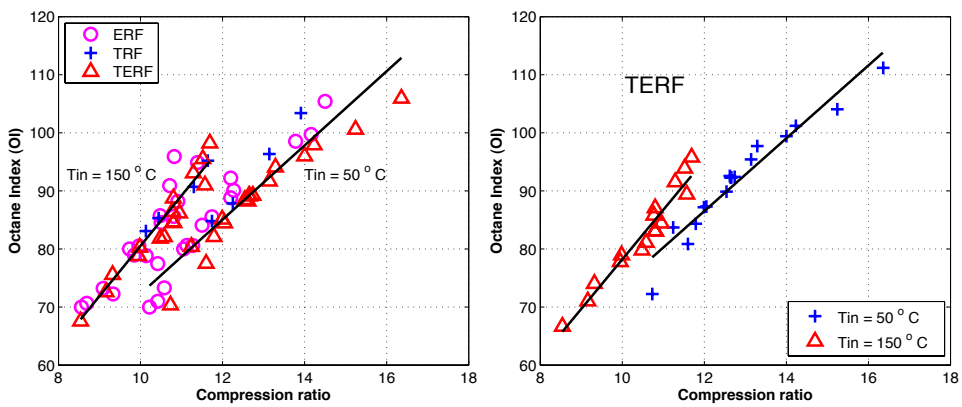

Figure 34. Agreement between the octane index (OI) and compression ratio for all reference fuels (left) and only TERFs (right).

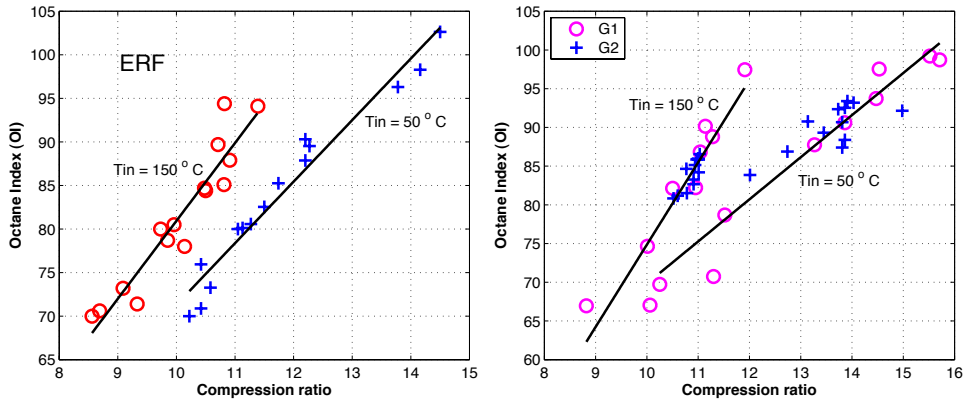

Figure 35. Agreement between the octane index (OI) and compression ratio for ethanol reference fuels (left) and gasolines (right). G1 and G2 are gasoline fuel datasets, see Table 9.

Table 13. K values from linear regression at the different inlet air temperatures.

K-values (R^2)				
Tin	ERF	TERF	All reference fuels	Gasolines
50 °C	-0.71 (0.96)	-1.51 (0.93)	-0.95 (0.89)	-0.1 (0.89)
75 °C	-0.58 (0.97)	-1.13 (0.94)	-0.76 (0.94)	0.09 (0.92)
100 °C	-0.43 (0.96)	-0.65 (0.97)	-0.54 (0.95)	0.25 (0.91)
125 °C	-0.29 (0.94)	-0.24 (0.98)	-0.34 (0.95)	0.41 (0.88)
150 °C	0 (0.90)	0.13 (0.94)	-0.13 (0.91)	0.74 (0.86)

5.3.3 Shibata and Urushihara Index

Shibata and Urishihara's HCCI index [31] uses the detailed fuel composition data to predict fuel performance, as described in Chapter 2.4.2. Their index was developed to predict the crank angle where 20% of the HTHR occurs, i.e. HTHR CA20. Since combustion phasing was held constant in this thesis study, an attempt was made to apply their index equation to the CR_{AI} values obtained. The index was calculated for all reference fuels used in this thesis project. This HCCI index can only be compared at similar operating conditions, and data was divided in regard to the T_{comp15}, the temperature at 15 bar's pressure in the cylinder. The values are plotted in Figure 30. For all fuels in this figure, extracted from the operating condition of Tin=50°C, T_{comp15} was below 670 K, (i.e. all fuels were in group 1, see Chapter 2.4.2). At many CR_{AI} values, there is a significant spread in index values, suggesting that a better approach is needed. The five ERFs that do not align with the other fuels are two component fuels consisting of n-heptane and ethanol alone. Even if those are not considered, there is a spread of 1-2 compression ratio units for a certain index value.

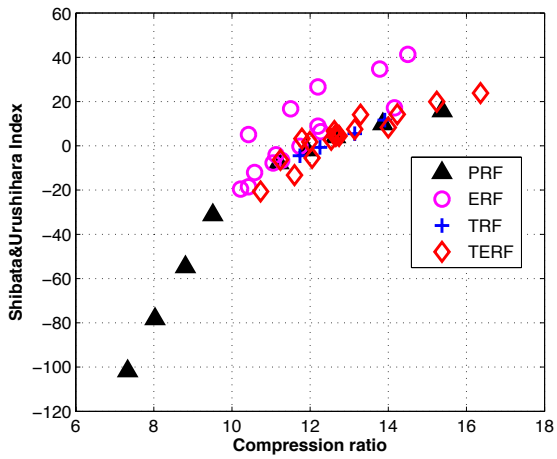

Figure 36. Shibata HCCI index calculated for all reference fuels at operating conditions with Tin=50°C.

5.3.4 Lund-Chevron HCCI Number (Paper VI)

The results discussed above indicate that a need exists for an HCCI number analogous to that of RON and MON for SI engines. For this purpose the Lund-Chevron HCCI number was developed.

The first step for determining the Lund-Chevron HCCI number of a fuel consists of determining the compression ratio required to obtain auto-ignition with a CA50 of 3˚ after TDC for various PRFs, the combustion phasing chosen to ensure stable combustion for all fuels. These data are plotted in Figure 37 for intake temperatures of 50, 75, 100, 125, and 150˚C. A quadratic equation was fit to the PRF data in the gasoline range (PRF 60 to 100 was chosen) for each intake temperature Coefficients for the quadratic equations are listed in Table 14.

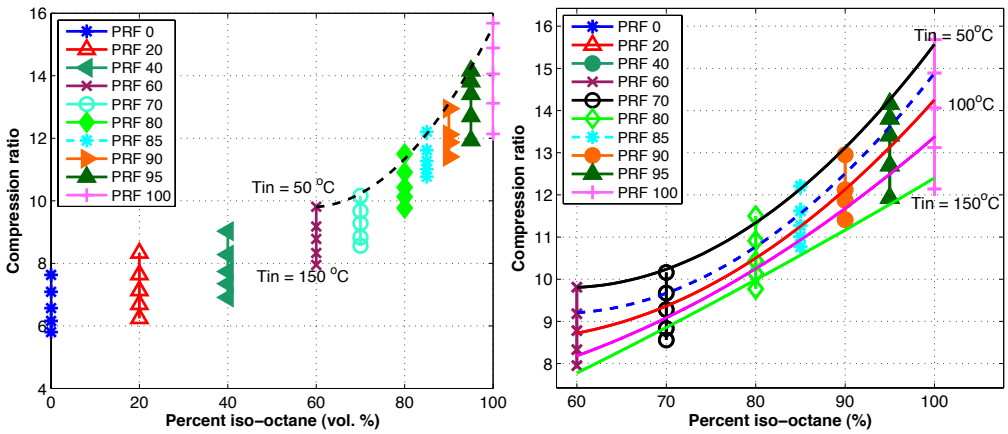

Figure 37. A quadratic approximation is done at each operating condition, relating the iso-octane percentage (for PRFs, this is the same as the RON and MON) to required compression ratio. The five different curve fits in the right figure are for inlet air temperatures of 50, 75, 100, 125, and 150°C.

For each fuel of interest, the next step is to measure the compression ratio required to achieve auto-ignition with a CA50 of 3˚ after TDC. The Lund-Chevron HCCI number is then set equal to the percentage iso-octane in the PRF fuel that has the same compression ratio (e.g. PRF 80 contains 80 vol.% iso-octane). For example, as shown in Figure 38, for fuel T1, the compression ratio is 10.8, which is the same value as for PRF 75, and so the HCCI number is set equal to 75. The HCCI numbers are then all a function of the fuel's compression ratio required for auto-ignition, see Figure 39.

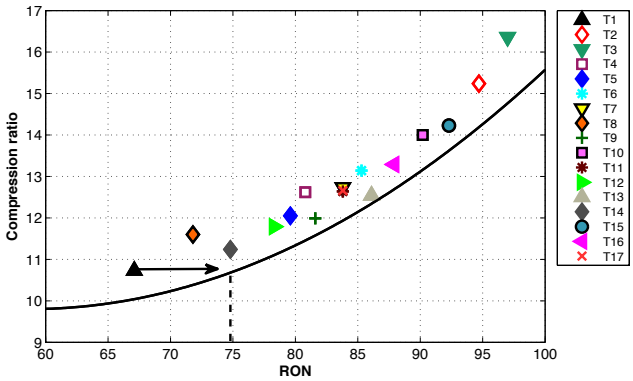

Figure 38. The required compression ratio for a fuel gives a corresponding % iso-octane, and therefore also HCCI number. As an example, fuel T1, requiring a compression ratio of 10.8, receives an HCCI number of 75.

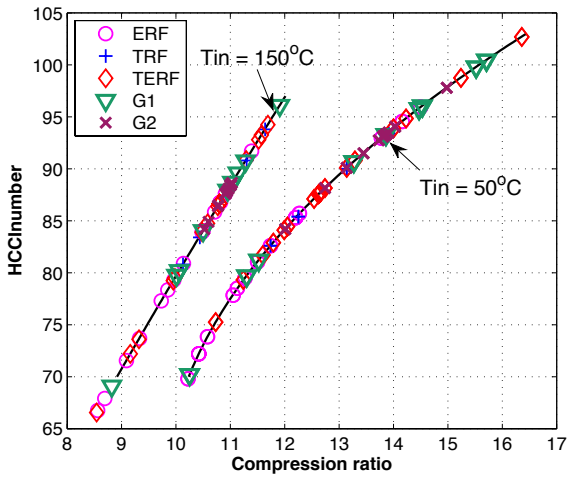

Figure 39. The Lund-Chevron HCCI number is a function of the compression ratio needed to achieve auto-ignition with CA50 at 3° after TDC. The curve used to obtain the HCCI number is also shown. Shown in this plot are the HCCI numbers at Tin = 50°C and Tin = 150°C, both at 600 rpm. G1 and G2 are gasoline fuel datasets #1 and #2, see Table 9.

5.3.4.1 Inlet Air Temperature Effect on HCCI Number

The effect of inlet air temperature on the HCCI number was studied for each fuel. A constant engine speed of 600 rpm was used, and equivalence ratio was kept at 0.33. For each inlet air temperature, the behavior of the PRFs and therefore the fuel baselines change. A fuel that behaves like the PRFs will not see a change in HCCI number. The values for the Lund-Chevron HCCI numbers for all of the fuels tested at all 5 intake temperatures are listed in Tables 21 to 23 in Appendix. Coefficients for the polynomials are presented in Table 14. In Equation 5.8, x is the volume % of iso-octane in the primary reference fuels used to develop the correlation. The quadratic Equation 5.8 can

be re-written for calculating HCCI number from compression ratio, see Equation 5.9, using the same coefficients as in Equation 5.8.

$$CR = a \cdot x^2 + b \cdot x + c \tag{5.8}$$

$$HCCI\ number = -\frac{b}{2 \cdot a} + \sqrt{\left(\frac{b}{2 \cdot a}\right)^2 - \left(\frac{c - CR}{a}\right)} \tag{5.9}$$

Table 14. Parameters for the equation; $CR_{AI} = a^*x^2+b^*x+c$.

$CR_{AI} = a^*x^2+b^*x+c$, x is vol. % iso-octane in primary reference fuel used					
Tin	50°C	75°C	100°C	125°C	150°C
a	$3.377*10^{-3}$	$3.192*10^{-3}$	$2.471*10^{-3}$	$1.323*10^{-3}$	$2.557*10^{-4}$
b	-0.3962	-0.3687	-0.2571	-0.08202	0.07468
c	21.42	19.84	15.25	8.341	2.374

The temperature effect on the HCCI number for the toluene ethanol reference fuels are shown in Figure 40. Some fuels (e.g. T1, T2, and T8) have a larger change in HCCI number, whereas other fuels (T6, T9, T10) have practically constant HCCI number over the whole temperature range.

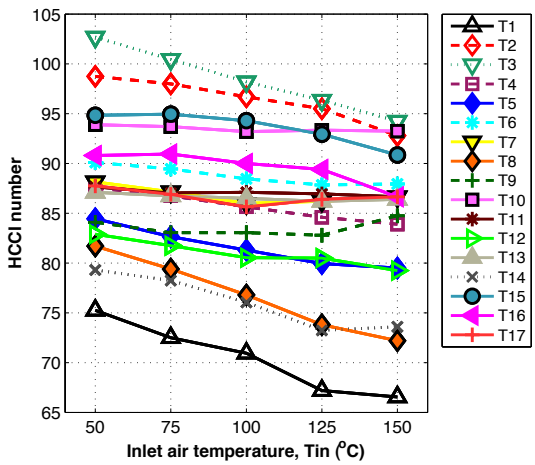

Figure 40. Effect of inlet air temperature on HCCI number for toluene ethanol reference fuels.

5.3.4.2 Effect from Engine Speed on HCCI Number

The effect of engine speed was studied by changing engine speed from 600 to 1200 rpm at intake temperatures of 50, 100, and 150°C. As discussed previously, conditions with both increased inlet air temperature and higher engine speed will decrease the low temperature chemistry. At each speed and inlet air temperature, the required compression

ratio data for PRF 70, 80, 90, and 100 was used to develop reference functions as shown in Figure 41, and equations and parameters are shown in Table 15. At the lowest inlet air temperature, the required compression ratio increased exponentially with engine speed, making auto-ignition unattainable at high engine speeds for fuels with an octane rating over about 105 (for the compression ratio span in this engine). However, at the highest inlet air temperature, the curve flattened out, and at high engine speeds there was small difference in required compression ratio for higher octane fuels, PRF 90 and PRF 100 for example, having almost the same compression ratios.

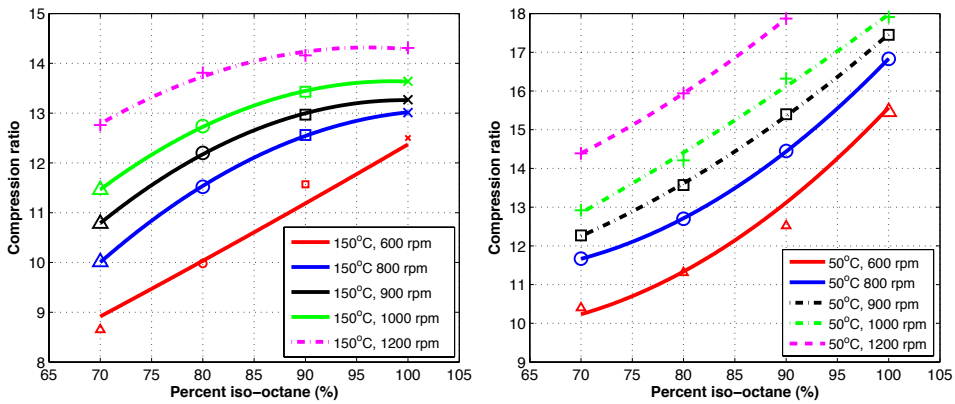

Figure 41. Compression ratio as a function of iso-octane concentration (equivalent to RON and MON) and engine speed for primary reference fuels.

Table 15. Equations and parameters for PRF correlations at higher engine speeds. x is the vol. % of iso-octane in the reference fuels used to obtain the correlation.

Engine speed (rpm)					
	600	800	900	1000	1200
Tin = 50°C, $CR_{AI} = a*x^2+b*x+c$					
a	$3.377*10^{-3}$	$3.375*10^{-3}$	$1.875*10^{-3}$	$7.500*10^{-4}$	$1.900*10^{-3}$
b	-0.3962	-0.4015	-0.1451	0.0433	-0.1300
c	21.42	23.23	13.22	6.147	14.18
Tin = 100°C, $CR_{AI} = a*x^2+b*x+c$					
a	$2.429*10^{-3}$	$5.00*10^{-5}$	$-6.00*10^{-4}$	$-1.775*10^{-3}$	$-2.65*10^{-3}$
b	-0.2513	0.1367	0.234	0.4207	0.5387
c	15.08	0.698	-2.08	-8.617	-10.95
Tin = 150°C, $CR_{AI} = a*x^2+b*x+c$					
a	$1.660 * 10^{-4}$	$-2.65*10^{-3}$	$-2.80*10^{-3}$	$-2.675*10^{-3}$	$-2.25*10^{-3}$
b	0.08698	0.5509	0.5584	0.5271	0.4325
c	2.014	-15.57	-14.58	-12.32	-6.465

5.3.4.3 Pre-reactions and HCCI Number

Early heat release (eHR) was determined as discussed in Section 3.3.1. Plots of early heat release vs. RON and the Lund-Chevron HCCI number are presented in Figure 42 for the refinery gasoline blends. For these refinery fuels, the HCCI number is more closely correlated than RON to the amount of early heat release (R^2 for HCCI number vs. eHR = 0.93, R^2 for RON vs. eHR = 0.77). The same is seen for correlation between early heat release vs. MON and the HCCI number at Tin = 150°C, see Figure 43. This was also true when looking at the low temperature heat release, see Figure 44.

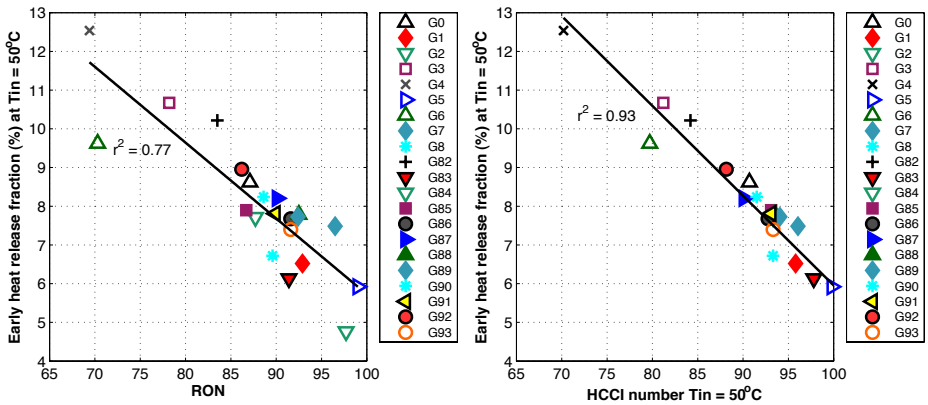

Figure 42. Correlation between early heat release for gasoline fuels vs. HCCI number and RON, respectively. HCCI number at 600 rpm and Tin= 50°C are used.

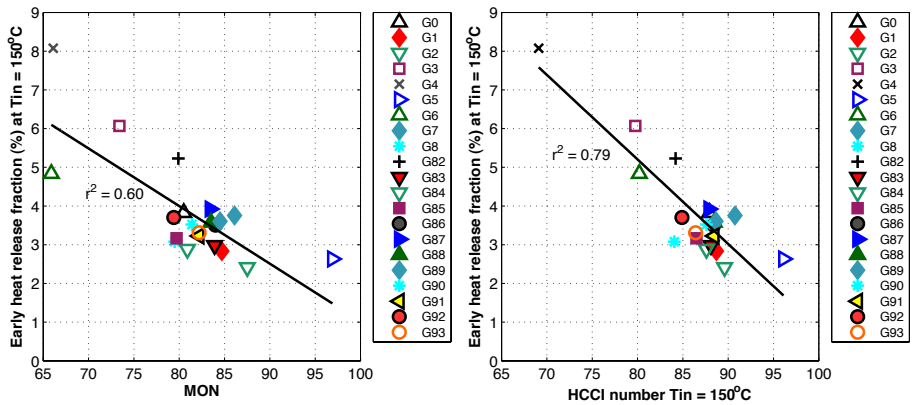

Figure 43. Correlation between early heat release for gasoline fuels vs. HCCI number and MON, respectively. HCCI number at 600 rpm and Tin= 150°C are used.

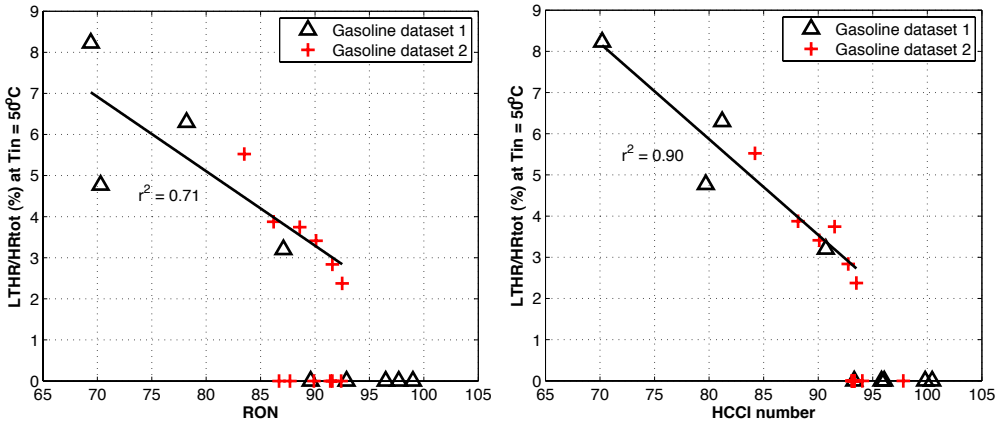

Figure 44. Correlation between low temperature heat release for gasoline fuels vs. HCCI number and RON, respectively. HCCI number at 600 rpm and Tin= 50°C are used. Only data point with LTHR were used for the correlation.

A linear model for HCCI number, based on compositions and inlet air temperatures of the reference fuels (TRF, ERF, and TERF) is presented in Equation 5.10, with coefficients in Table 16. Ethanol gave a higher value of the HCCI number, and so did toluene, but only with about half the effect. n-Heptane decreased the HCCI number. In contrast to the fuel effect on MON, described in Section 5.3.1.1, where practically no effect is seen from toluene, the HCCI number has a similar effect from toluene both at low (Tin=50°C) and high (Tin=150°C) inlet air temperatures.

$$HCCIn = a + b*x_{n\text{-}heptane} + c*x_{toluene} + d*x_{ethanol} + e*Tin \qquad (5.10)$$

Table 16. Coefficients for Equation 5.10, where concentrations are in vol. % and temperature in K. Two additional models were done for constant inlet air temperatures of 50°C and 150°C.

Coefficient		All reference fuels		
		With T dependence	Tin=50°C	Tin=150°C
a	-	104.5	95.34	94.51
b	n-Heptane	-0.7405	-0.7253	-0.7304
c	Toluene	0.2719	0.2997	0.2541
d	Ethanol	0.5479	0.5544	0.4967
e	T_{in}	-0.0253	-	-
R^2		0.90	0.92	0.85

By definition, the HCCI number is directly correlating to the compression ratio needed to phase combustion 3° after TDC, which the RON is not, see Figure 45.

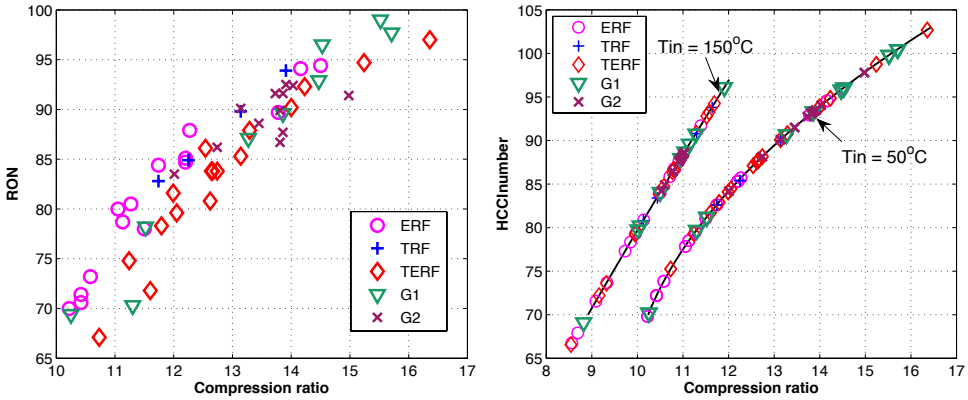

Figure 45. RON and compression ratio needed at Tin=50°C (left) and HCCI number as a function of compression ratio (right). G1 and G2 are gasoline fuel datasets, see Table 9.

The HCCI number is compared to RON and MON in Figure 46. It is shown that the ethanol reference fuels, for example, receives similar values at RON and HCCI number at low inlet air temperature conditions, but that many of these fuels show a greater difference between MON and HCCI number at high inlet air temperatures. The toluene ethanol reference fuels shows an offset, and show higher HCCI numbers than their RONs and MONs at both high and low inlet air temperatures. Most fuels have a higher HCCI number that RON and MON, which means that they require a higher compression ratio in HCCI operation, than the PRF correlating to their RON.

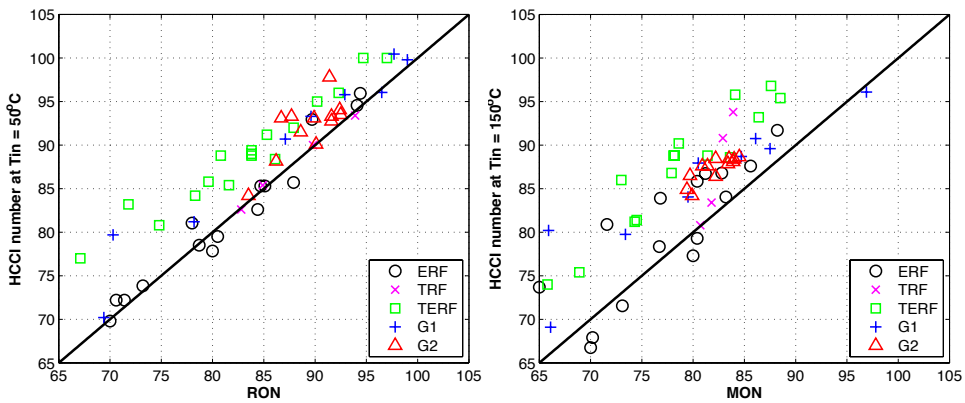

Figure 46. Correlation between HCCI number at low inlet air temperatures and RON, and HCCI number at high inlet air temperatures and MON, respectively. The black line is 1:1 correlation, and G1 and G2 are gasoline fuel datasets #1 and #2.

6 Conclusions

Previous methods for measuring HCCI fuel performance, were found not to be able to predict required CR for HCCI auto-ignition. The Lund-Chevron HCCI number was instead proposed, using fuel testing in a CFR engine just as for the indices for spark ignition (research octane number and motor octane number, RON and MON) and compression ignition (cetane number, CN). By running the engine in HCCI mode, the required compression ratio for achieving a combustion phasing of CA50 3º after TDC was noted for each fuel, and this value was compared to a primary reference fuel at the same operating condition.

The Lund-Chevron HCCI number was seen to be closely coupled with the amount of pre-reactions.

Fuel properties such as amount of low temperature heat release (LTHR) and auto-ignition temperature were systematically studied, and thereafter modeled as a function of inlet air temperature and fuel composition.

Ethanol had a strong quenching effect on LTHR, corresponding to the magnitude of which n-heptane induced LTHR. Toluene on the other hand showed almost no effect on low temperature reactions.

Auto-ignition temperatures were lower for fuels with more n-heptane. All fuels with extensive low temperature heat release showed similar auto-ignition temperatures, indicating that the LTHR started at a certain temperature (around 600-650 K) for all fuels. When LTHR diminished, either due to fuel quenching from ethanol or toluene, or when the inlet air temperature was increased, the auto-ignition temperature was increased. Maximum auto-ignition temperatures found, leading directly to high temperature heat release, reached 800 K.

Ethanol addition was found to increase auto-ignition temperatures. Toluene also increased auto-ignition temperatures, but not to the same extent.

Emission studies were performed, with a focus on fuel effects. CO emissions were found to be independent of fuel chemistry, beyond it's effect on cylinder temperature. HC emissions were found to mainly stem from crevice losses, making it proportional to the compression ratio in the CFR engine. Ethanol was also shown to decrease HC emissions for combustion at a certain compression ratio. NO_x emissions were low for all operating points studied, but the NO_x emission levels were further decreased for high octane fuels when adding ethanol.

7 Future Work

To fully understand the fuel effects on HCCI combustion, more detailed analysis with different components has to be performed. Other operating conditions, such as effect of EGR or supercharging has to be further studied. Also further experiments for full distillate gasoline fuels could contribute with useful information.

The Lund-Chevron HCCI number should be further refined, by experiments of more primary reference fuels in the interval. A method for determining HCCI numbers outside of the 0-100 interval should also be considered.

The Lund-Chevron HCCI Fuel Number should be evaluated for predicting fuel performance for HCCI operation in other engines.

By applying chemical kinetic modeling to these data, the reasons for the fuel differences might be better explained. Chemical kinetic models of low temperature chemistry could also gain from looking at the low temperature reaction data provided in this thesis.

8 References

1. Kalghatgi, G.T., 2005, ”Auto-Ignition Quality of Practical Fuels and Implications for Fuel Requirements of Future SI and HCCI Engines”, SAE 2005-01-0239

2. Warnatz, J., Maas, U., Dibble, R.W., 2006, “Combustion Physical and Chemical Fundamentals, Modeling and Simulation, Experiments, Pollutant Formation”, Springer, Berlin

3. Heywood, J. B., 1988, “Internal Combustion Engine Fundamentals”, McGraw Hill

4. Dec, J., "A Conceptual Model of DI Diesel Combustion Based on Laser-Sheet Imaging*," SAE Technical Paper 970873, 1997, doi:10.4271/970873

5. Onishi, S., Jo, S., Shoda, K., Jo, P. et al., "Active Thermo-Atmosphere Combustion (ATAC) - A New Combustion Process for Internal Combustion Engines", SAE Technical Paper 790501, 1979, doi:10.4271/790501

6. Tanaka, S., Ayala, F., Keck, J.C, Heywood, J.B., 2003, ”Two-stage ignition in HCCI combustion and HCCI control by fuels and additives”, Combustion and Flame, 132, pp. 219-239

7. Westbrook, CK., Pitz, WJ., and Curran, H.J., “Autoignition and chemical kinetic mechanisms of HCCI combustion”, In: HCCI and CAI engines for the automotive industry, Zhao H., editor, Boca Raton: Woodhead Publishing; 2007, p. 433-445.

8. Leppard, W., "The Chemical Origin of Fuel Octane Sensitivity", SAE Technical Paper 902137, 1990, doi:10.4271/902137

9. Hosseini, V., Neill, W.S., Chippior, W.L., 2009, ”Influence of Engine Speed on HCCI Combustion Characteristics using Dual-Stage Autoignition Fuels”, SAE 2009-01-1107

10. Silke, E.J., Pitz, W.J., Westbrook, C.K., Sjöberg, M., Dec, J.E., 2008, ”Understanding the Chemical Effects of Increased Boost Pressure under HCCI Conditions”, SAE 2008-01-0019

11. Sjöberg, M., Dec, J.E., 2011, ”Effects of EGR and its constituents on HCCI autoignition of ethanol”, Proceedings of the Combustion Institute 33, pp. 3031-3038

12. Sjöberg, M., Dec, J.E., 2007, ”EGR and Intake Boost for Managing HCCI Low-Temperature Heat Release over Wide Ranges of Engine Speed”, SAE 2007-01-0051

13. Andrae, J.C.G., Head, R.A., 2009, “HCCI experiments with gasoline surrogate fuels modeled by a semidetailed chemical kinetic model”, Combustion and Flame, 156, pp. 842-851

14. Lü, X., Ji, L., Zu, L., Hou, Y., Huang, C., Huang, Z., 2007, “Experimental study and chemical analysis of n-heptane homogeneous charge compression ignition combustion with port injection of reaction inhibitors”, Combustion and Flame, 149, pp. 261-270

15. Zheng, J., Yang, W., Miller, D., and Cernansky, N., "Prediction of Pre-ignition Reactivity and Ignition Delay for HCCI Using a Reduced Chemical Kinetic Model", SAE Technical Paper 2001-01-1025, 2001, doi:10.4271/2001-01-1025.

16. Chen J.-S., Litzinger, T.A, Curran H.J, ”The Lean Oxidation of Iso-Octane in the Intermediate Temperature Regime at Elevated Pressures”, Combustion Science and Technology, 156:1, 49-79, (2000) DOI:10.1080/00102200008947296

17. W. Hwang, Dec. J., Sjöberg, M., ” Spectroscopic and chemical-kinetic analysis of the phases of HCCI autoignition and combustion for single- and two-stage ignition fuels”, Combustion and Flame 154 (2008) 387–409, doi:10.1016/j.combustflame.2008.03.019

18. Vuilleumier, D., Kozarac, D., Mehl, M., Pitz, W.J., et al., “ Intermediate temperature heat release in an HCCI engine fueled by ethanol/n-heptane mixtures: An experimental and modeling study” Combustion and Flame Volume 161, Issue 3, 680-695 (2013): http://dx.doi.org/10.1016/j.combustflame.2013.10.008

19. Mehl, M., Pitz, W., Sarathy, M., Yang, Y. et al., "Detailed Kinetic Modeling of Conventional Gasoline at Highly Boosted Conditions and the Associated Intermediate Temperature Heat Release", SAE Technical Paper 2012-01-1109, 2012, doi:10.4271/2012-01-1109.

20. Vuilleumier, D., Kozarac, D., Mehl, M., Saxena, S., Pitz, W.J., Dibble, R.W., Chen, J., Sarathy, M., ” Intermediate temperature heat release in an HCCI engine fueled by ethanol/n-heptane mixtures: An experimental and modeling study ”, Combustion and Flame. DOI: 10.1016/j.combustflame.2013.10.008

21. Ryan, T., Callahan, T., and Mehta, D., "HCCI in a Variable Compression Ratio Engine-Effects of Engine Variables", SAE Technical Paper 2004-01-1971, 2004, doi:10.4271/2004-01-1971.

22. "Fuels and Engines - Technology, energy, environment", J.C. Guibet, Éditions Technip, Paris, 1999

23. Yates, A., Swarts, A., and Viljoen, C., "An Investigation Of Anomalies Identified Within The ASTM Research And Motor Octane Scales", SAE Technical Paper 2003-01-1772, 2003, doi:10.4271/2003-01-1772.

24. Perumal, M. and Floweday, G., "An Investigation of Cascading Autoignition and Octane Number using a Multi-zone Model of the CFR Engine", SAE Int. J. Engines 4(1):976-997, 2011, doi:10.4271/2011-01-0850.

25. Swarts, A., Yates, A., Viljoen, C., and Coetzer, R., "A Further Study of Inconsistencies between Autoignition and Knock Intensity in the CFR Octane Rating Engine", SAE Technical Paper 2005-01-2081, 2005, doi:10.4271/2005-01-2081.

26. Kalghatgi, G., "Fuel Anti-Knock Quality - Part I. Engine Studies", SAE Technical Paper 2001-01-3584, 2001, doi:10.4271/2001-01-3584.

27. Risberg, P., Kalghatgi, G., and Ångstrom, H., "Auto-ignition Quality of Gasoline-Like Fuels in HCCI Engines", SAE Technical Paper 2003-01-3215, 2003, doi:10.4271/2003-01-3215.

28. Kalghatgi, G. and Head, R., "The Available and Required Autoignition Quality of Gasoline - Like Fuels in HCCI Engines at High Temperatures", SAE Technical Paper 2004-01-1969, 2004, doi:10.4271/2004-01-1969.

29. Aroonsrisopon, T., Sohm, V., Werner, P., Foster, D.E., Morikawa, T., Iida, M., 2002, “An Investigaton Into the Effect of Fuel Composition on HCCI Combustion Characteristics”, SAE 2002-01-2830

30. Liu, H., Yao, M., Zhang, B., Zheng, Z., 2009, “Influence of Fuel and Operating Conditions on Combustion Characteristics of a Homogenous Charge Compression Ignition Engine”, Energy & Fuels, 23, pp. 1422-1430

31. Shibata, G., Urushihara, T., 2007, ”Auto-Ignition Characteristics of Hydrocarbons and Development of HCCI Fuel Index”, SAE 2007-01-0220

32. Shibata, G., Oyama, K., 2005, ”Correlation of Low Temperature Heat Release With Fuel Composition and HCCI Engine Combustion”, SAE 2005-01-0138

33. Shibata, G., Oyama, K., Urushihara, T., and Nakano, T., "The Effect of Fuel Properties on Low and High Temperature Heat Release and Resulting Performance of an HCCI Engine", SAE Technical Paper 2004-01-0553, 2004, doi:10.4271/2004-01-0553.

34. Pitz, W.J., Cernansky, N.P., Dryer, F.L., Egolfopoulos, F.N., Farrell, J.T., Friend, D.G., Pitsch, H., 2007, “Development of an experimental Database and Chemical Kinetic Models for Surrogate Gasoline Fuels”, SAE 2007-01-0175

35. Machado, G.B., Barros, J.E.M., Braga, S.L., Braga, C.V.M., Oliviera, E.J., Silva, A.H.M.F.T., Carvalho, L.O., 2011, “Investigation on surrogate fuels for high-octane oxygenated gasolines”, Fuel, 90, pp. 640-646

36. H.S. Soyhan, H. Yasar, H. Walmsley, B. Head, G.T. Kalghatgi, C. Sorusbay, "Evaluation of heat transfer correlations for HCCI engine modeling", Applied Thermal Engineering, Volume 29, Issues 2–3, February 2009, Pages 541-549, ISSN 1359-4311, http://dx.doi.org/10.1016/j.applthermaleng.2008.03.014.

37. Truedsson, I., Johansson, B., Tuner, M., Cannella, W., 2012, “Pressure sensitivity of HCCI auto ignition temperatures for primary reference fuels”, SAE Int. J. Engines 5 (3): doi:10.4271/2012-01-1128

38. Ryan, T. and Matheaus, A., "Fuel Requirements for HCCI Engine Operation", SAE Technical Paper 2003-01-1813, 2003, doi:10.4271/2003-01-1813.

39. Yates, A., Bell, A., Swarts, A., 2010, “Insights relating to the autoignition characteristics of alcohol fuels”, Fuel, 89, pp. 83-93

40. Hunwartzen I. "Modification of CFR test engine unit to determine octane numbers of pure alcohols and gasoline–alcohol blends", SAE Technical paper 820002, 1982, doi:10.4271/820002

41. Truedsson, I., Johansson, B., Tuner, M., Cannella, W., 2012, “Pressure sensitivity of HCCI auto-ignition temperatures for oxygenated reference fuels”, J. Eng. Gas Turbines Power 135(7), doi:10.1115/1.4023614

42. Truedsson, I., Johansson, B., Tuner, M., Cannella, W., 2012, “Pressure sensitivity of HCCI auto ignition temperatures for gasoline surrogate fuels”, SAE 2013-01-1669, doi:10.4271/2013-01-1669

43. Truedsson, I., Tuner, M., Johansson, B., and Cannella, W., "Emission Formation Study of HCCI Combustion with Gasoline Surrogate Fuels", SAE Technical Paper 2013-01-2626, 2013, doi:10.4271/2013-01-2626.

44. Morgan, N., Smallbone, A., Bhave, A., Kraft, M., Cracknell, R., Kalghatgi, G., 2010, “Mapping surrogate gasoline compositions into RON/MON space”, Combustion and Flame, 157, pp.1122-1131

45. Anderson, J., Leone, T., Shelby, M., Wallington, T. et al., "Octane Numbers of Ethanol-Gasoline Blends: Measurements and Novel Estimation Method from Molar Composition", SAE Technical Paper 2012-01-1274, 2012, doi:10.4271/2012-01-1274.

46. Solaka Aronsson, H., Tuner, M., Johansson, B., "Using Oxygenated Gasoline Surrogate Compositions to Map RON and MON" SAE Technical Paper 2014-01-1303, 2014

9 Summary of Papers

Paper I

Pressure sensitivity of HCCI auto ignition temperatures for primary reference fuels

Truedsson, I., Johansson, B., Tuner, M., Cannella, W.,

2012, SAE Int. J. Engines 5 (3): doi:10.4271/2012-01-1128. Presented by the author at SAE World congress 2012, in Detroit, Michigan.

A study of auto-ignition of primary reference fuels in a CFR engine run in HCCI mode. The amount of low temperature reactions are quantified and the auto-ignition temperatures of each blend is calculated, and the effects on these by the pressure-temperature evolution in the cylinder is studied.

Experiments and post-processing of data were performed by the author. The paper was written by the author in close cooperation with Bengt Johansson, Martin Tunér, and William Cannella.

Paper II

Pressure sensitivity of HCCI auto-ignition temperatures for oxygenated reference fuels

Truedsson, I., Johansson, B., Tuner, M., Cannella, W.,

2013, J. Eng. Gas Turbines Power 135(7), doi:10.1115/1.4023614. Presented by the author at the ASME 2012 International Combustion Engine Division Fall Technical Conference in Vancouver, Canada.

Auto-ignition temperatures and amount of low temperature heat release are quantified for reference fuels consisting of n-heptane, iso-octane, and ethanol. The quenching effect of ethanol on low temperature reactions are evaluated, and octane rating based on blending RON are discussed and a modification of octane rating are done to match HCCI results.

Experiments and post-processing of data were performed by the author. The paper was written by the author in close cooperation with Bengt Johansson, Martin Tunér, and William Cannella.

Paper III

Pressure Sensitivity of HCCI Auto-Ignition Temperature for Gasoline Surrogate Fuels

Truedsson, I., Tuner, M., Johansson, B., and Cannella, W.

SAE Technical Paper 2013-01-1669, 2013, doi:10.4271/2013-01-1669. Presented by the author at SAE World congress 2013, in Detroit, Michigan.

Four component gasoline surrogate fuels consisting of n-heptane, iso-octane, toluene, and ethanol are studied and compared with previous reference fuel studies. Effects of ethanol and toluene addition on auto-ignition temperatures and low temperature reactions are shown.

Experiments and post-processing of data were performed by the author. The paper was written by the author in close cooperation with Bengt Johansson, Martin Tunér, and William Cannella.

Paper IV

Emission Formation Study of HCCI Combustion with Gasoline Surrogate Fuels

Truedsson, I., Tuner, M., Johansson, B., and Cannella, W.,

SAE Technical Paper 2013-01-2626, 2013, doi:10.4271/2013-01-2626. Presented by the author at SAE 2013 International Powertrains, Fuels and Lubricants Meeting, Seoul, South Korea.

Emission formation of unburnt hydrocarbon, carbon monoxide, and nitrogen oxides (combined to NO_x), in HCCI combustion are related to single zone temperature calculations. Hydrocarbon emissions were proportional to the required compression ratio, why most was assumed to be fuel trapped in crevices. A reduction of HC emissions was seen when adding ethanol to the fuel. No fuel effect was seen for CO emissions, which only seemed to be affected by the cylinder temperature.

Experiments and post-processing of data were performed by the author. The paper was written by the author in close cooperation with Bengt Johansson, Martin Tunér, and William Cannella.

Paper V

Manuscript submitted to SAE 2014 International Powertrain, Fuels and Lubricants meeting

Engine Speed Effect on Auto-Ignition Temperature and Low Temperature Reactions in HCCI Combustion

Truedsson, I., Johansson, B., Tuner, M., Cannella, W.,

Engine speed was varied from 600 rpm up to 1200 rpm, and the speed sensitivity of the fuels was studied. This was performed for four primary reference fuels (PRF 70, 80, 90, and 100) and compared with the responses of 7 gasoline fuels. Speed effects on low temperature reactions and auto-ignition temperatures were quantified and discussed.

Experiments and post-processing of data were performed by the author. The paper was written by the author in close cooperation with Bengt Johansson, Martin Tunér, and William Cannella.

Paper VI

Manuscript submitted to SAE 2014 International Powertrain, Fuels and Lubricants meeting

Development of new test method for evaluating HCCI fuel performance

Truedsson, I., Johansson, B., Tuner, M., Cannella, W.,

A test method for evaluating HCCI fuel performance were introduced, where real fuels are compared with the required compression ratio of primary reference fuels for keeping a constant combustion phasing of 3 degrees after TDC. This HCCI number is compared to previous indices for measuring auto-ignition quality.

Experiments and post-processing of data were performed by the author. The paper was written by the author in close cooperation with Bengt Johansson, Martin Tunér, and William Cannella.

10 Appendix

10.1 Error Analysis

To see the repeatability of the experiments, one of the toluene ethanol reference fuels was repeated two times, resulting in test runs T7, T11, and T17, see rate of heat release traces in Figure 45. Repetitions were made also for primary reference fuels and gasolines, with similar results. For this repetition, maximum variations of auto-ignition temperatures was 22º, see Figure 46. Maximum variation of pressure at auto-ignition was about 1 Bar. Highest variation in required compression ratio for combustion 3º after TDC was less that 0.3 units, see Figure 47, and variation of percentage of low temperature heat release was up to 0.76 %.

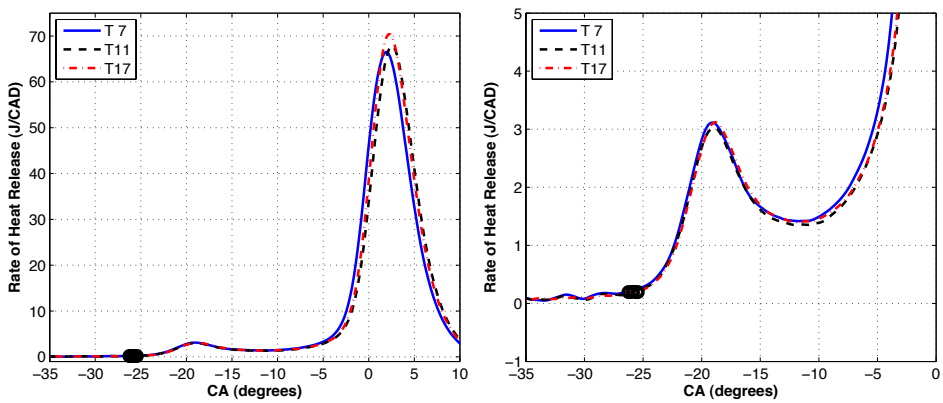

Figure 47. Rate of heat release curves for toluene ethanol reference fuel repetitions, with start of combustion marked, defined as 0.2 J/CAD.

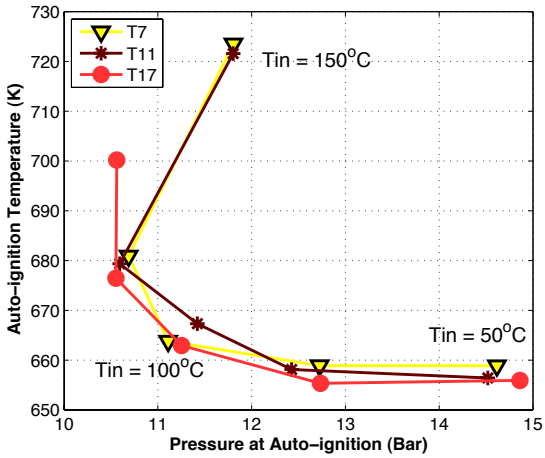

Figure 48. Auto-ignition temperatures for repetitions of toluene ethanol reference fuel, tests T7, T11, and T17. Start of combustion is defined as a rate of heat release of 0.2 J/CAD.

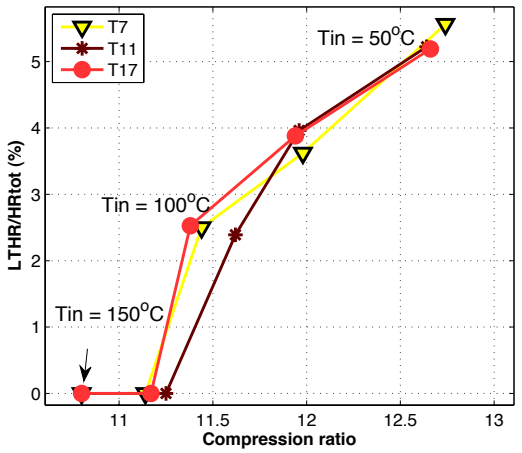

Figure 49. Low temperature heat release and compression ratios required for auto-ignition 3° after TDC for repetitions of toluene ethanol reference fuels.

10.2 Experimental Data

Table 17. Percentage of low temperature heat release and early heat release for primary reference fuels.

Fuel	Tin=50°C	Tin=75°C	Tin=100°C	Tin=125°C	Tin=150°C
Low temperature heat release (Standard definition)					
PRF 0	18.8	17.3	16.1	14.3	13.5
PRF 20	16.1	14.7	13.2	12.4	10.7
PRF 40	12.9	11.5	10.1	9.3	7.9
PRF 60	10.5	9	7.8	6	5.5
PRF 70	8.5	6.7	5.9	5.1	3.9
PRF 80	6.5	5.1	4.1	2.8	1.8
PRF 85	5.5	4.1	2.8	1.4	0
PRF 90	4.2	2.8	1.7	0	0
PRF 95	3.2	0	0	0	0
PRF100	0	0	0	0	0
Early heat release (Gaussian definition)					
PRF 0	19.8	19	18.6	17.5	16.5
PRF 20	18.2	17.4	16.7	15.7	14.3
PRF 40	15.5	14.9	14	13.6	12.5
PRF 60	13.3	12.7	11.8	10.8	10.2
PRF 70	11.9	11.2	10.4	9.7	8.9
PRF 80	10.5	9.4	8.7	8.3	6.7
PRF 85	9.2	8.7	7.5	6.3	5.4
PRF 90	8.1	7.2	6.2	5.3	4.4
PRF 95	6.6	5.7	4.9	4.1	3.5
PRF100	5.4	4.6	4	3.5	3.2

Table 18. Percentage of low temperature heat release and early heat release for toluene reference fuels (TRF).

Fuel	Tin=50°C	Tin=75°C	Tin=100°C	Tin=125°C	Tin=150°C
Low temperature heat release (Standard definition)					
H20T10	6.2	4.8	3.5	2.6	1.7
H20T20	5.5	4.4	3.3	2.5	0
H20T40	4.3	3.5	1.9	0	0
H20T60	3	2.2	0	0	0
Early heat release (Gaussian definition)					
H20T10	9.8	8.9	8.1	7.2	6.4
H20T20	9.6	9	8	7.2	6.3
H20T40	8	7.2	6.4	5.6	4.8
H20T60	7.4	6.8	5.8	5.4	4.7

Table 19. Percentage of low temperature heat release and early heat release for ethanol reference fuels (ERF).

Fuel	Tin=50°C	Tin=75°C	Tin=100°C	Tin=125°C	Tin=150°C
Low temperature heat release (Standard definition)					
PRF80	5.8	5	3.9	2.9	1.9
H20E1	6.2	4.9	3.7	2.8	1.8
H20E5	5.3	4	2.8	1.8	0
H20E10	4.4	2.9	0	0	0
H20E20	1.5	0	0	0	0
PRF70	8.5	6.7	5.9	5.1	3.9
H30E1	8	7	5.3	4.7	3.5
H30E5	7.2	6.1	5	3.6	2.7
H30E10	6.2	4.9	3.9	2.5	1.6
H30E20	4.5	2.9	2	0	0
H60E40	7.3	5.6	4.2	3.1	2
H55E45	4.8	3.7	0	0	0
H50E50	4	0	0	0	0
H45E55	0	0	0	0	0
H40E60	0	0	0	0	0
Early heat release (Gaussian definition)					
PRF80	9.9	9.4	8.4	7.4	6.4
H20E1	10	9	8.2	7.3	6.3
H20E5	9.3	7.5	6.7	5.8	5.3
H20E10	8.2	6.8	5.2	4.5	4.1
H20E20	5.8	5.4	4.3	3.6	3.1
PRF70	11.9	11.2	10.4	9.7	8.9
H30E1	11.6	10.7	9.8	9.2	8.2
H30E5	10.6	10	8.7	8	7.1
H30E10	9.8	8.9	7.9	6.7	6.1
H30E20	8.3	7.4	6.5	5.1	4.2
H60E40	11.2	10	8.8	7.5	5.7
H55E45	8.5	7	5.8	5.2	4.4
H50E50	7.8	6.2	5.5	4.4	3.7
H45E55	5.1	4.4	3.9	2.9	2.6
H40E60	5.1	4.4	3.6	3.1	2.6

Table 20. Percentage of low temperature heat release and early heat release for toluene ethanol reference fuels (TERF).

Fuel	Tin=50°C	Tin=75°C	Tin=100°C	Tin=125°C	Tin=150°C
Low temperature heat release (Standard definition)					
T1	9.6	8	6.7	4.7	4
T2	0	0	0	0	0
T3	0	0	0	0	0
T4	6	4.1	2.6	0	0
T5	6.7	5.4	4.2	2.7	2.1
T6	4.5	3.2	0	0	0
T7	5.6	3.6	2.5	0	0
T8	8.7	7	5.9	4.7	3.6
T9	6	4.6	3.1	0	0
T10	3.8	2.8	0	0	0
T11	5.2	4	2.4	0	0
T12	6.6	4.7	3.7	2.6	0
T13	4.9	3.6	2.1	0	0
T14	7.3	6.2	4.9	3.5	2.4
T15	2.6	0	0	0	0
T16	3.9	0	0	0	0
T17	5.2	3.9	2.5	0	0
Early heat release (Gaussian definition)					
T1	11.9	10.9	10	8.6	8.3
T2	5.1	4.4	3.7	3.1	2.7
T3	4.8	3.7	3.5	3.1	2.8
T4	9.3	8.5	7.5	6.4	5.8
T5	9.7	9.2	7.9	7.1	6.2
T6	8.1	7.3	6.5	5.7	4.7
T7	8.6	7.8	6.9	5.9	5.2
T8	11.2	9.9	9.7	8.9	8.1
T9	9.6	8.5	7.5	6.3	5.6
T10	7.8	7	6.2	5.5	4.6
T11	8.7	8.2	7.3	6.3	5.3
T12	9.4	7.9	7.5	6.2	5.6
T13	8	7.3	5.9	5.5	4.7
T14	10.3	9.9	8.8	7.8	6.5
T15	6.2	5.3	4.6	3.9	3.2
T16	7	6.2	5.1	4.7	3.9
T17	8.5	7.4	6.7	5.6	5

Table 21. HCCI numbers for five different inlet air temperatures for toluene reference fuels (TRF) and ethanol reference fuels (ERF) with compositions presented in Table 6 and 7. All for an engine speed of 600 rpm and an equivalence ratio of 0.33, calculated from Equation 5.8 and Table 14.

Fuel	Tin=50°C	Tin=75°C	Tin=100°C	Tin=125°C	Tin=150°C
H20T10	83	82	82	81	81
H20T20	85	85	84	83	83
H20T40	90	91	89	89	91
H20T60	93	94	93	93	94
H20E1	80	79	79	79	79
H20E5	83	83	83	83	84
H20E10	86	86	88	88	88
H20E20	95	95	95	93	92
H30E1	72	70	69	69	68
H30E5	74	74	73	73	72
H30E10	79	78	78	78	78
H30E20	85	87	87	88	87
H60E40	72	73	72	74	74
H55E45	81	81	83	82	81
H50E50	85	87	87	86	84
H45E55	93	92	91	89	86
H40E60	96	95	92	90	87

Table 22. HCCI numbers for five different inlet air temperatures for toluene ethanol reference fuels (TERF) with composition shown in Table 5. All for an engine speed of 600 rpm and an equivalence ratio of 0.33, calculated from Equation 5.8 and Table 14.

Fuel	Tin=50°C	Tin=75°C	Tin=100°C	Tin=125°C	Tin=150°C
T1	75	72	71	67	66
T2	99	98	97	95	93
T3	103	100	98	96	94
T4	87	87	86	85	84
T5	84	83	81	80	79
T6	90	89	88	88	88
T7	88	87	86	86	87
T8	82	79	77	74	72
T9	84	83	83	83	85
T10	94	94	93	93	93
T11	88	87	87	87	87
T12	83	82	80	80	79
T13	87	87	86	86	86
T14	79	78	76	73	74
T15	95	95	94	93	91
T16	91	91	90	89	87
T17	88	87	86	86	87

Table 23. HCCI numbers for five different inlet air temperatures for gasoline fuels. All for an engine speed of 600 rpm and an equivalence ratio of 0.33, calculated from Equation 5.8 and Table 14.

Fuel	Tin=50°C	Tin=75°C	Tin=100°C	Tin=125°C	Tin=150°C
G82	84	85	86	85	84
G83	98	96	94	91	88
G84	93	94	92	91	88
G85	93	94	92	90	87
G86	93	93	93	91	88
G87	90	91	90	90	88
G88	94	94	93	91	88
G89	94	95	93	91	89
G90	92	92	92	90	88
G91	93	94	92	90	88
G92	88	89	89	87	85
G93	93	93	92	89	86
G0	91	92	91	90	88
G1	96	96	94	92	89
G2	100	98	95	94	90
G3	81	81	81	81	80
G4	70	70	70	69	69
G5	100	100	99	97	96
G6	80	80	81	82	80
G7	96	96	95	93	91
G8	93	93	91	88	84

Table 24. Speed effect on LTHR.

Fuel	600 rpm	800 rpm	900 rpm	1000 rpm	1200 rpm
Tin=50°C					
PRF70	8.9	6.7	6.3	5.6	4.8
PRF80	6.6	4.8	3.3	3.1	2.3
PRF90	4.7	2.6	0	0	0
PRF100	0	0	0	0	0
Tin=100°C					
PRF70	6.1	4.3	3.7	3	0
PRF80	3.8	2.2	1.1	0	0
PRF90	1.6	0	0	0	0
PRF100	0	0	0	0	0
Tin=150°C					
PRF70	3.7	2.4	0	0	0
PRF80	2.3	0	0	0	0
PRF90	0	0	0	0	0
PRF100	0	0	0	0	0

Table 25. Speed effect on early heat release.

Fuel	600 rpm	800 rpm	900 rpm	1000 rpm	1200 rpm
Tin=50°C					
PRF70	11.4	10.1	9.5	9.1	8.7
PRF80	10.9	9.3	8.5	7.8	6.7
PRF90	7.9	6.4	6.1	5.8	6.1
PRF100	5.8	5.2	4.5	4.3	0
Tin=100°C					
PRF70	9.4	8.3	8	7.4	6.5
PRF80	8.9	7.4	6.4	5.9	5.6
PRF90	5.9	5.1	4.4	4.7	4.7
PRF100	4.4	3.6	3.2	3.3	4.2
Tin=150°C					
PRF70	7.9	7.1	6.3	5.9	5.1
PRF80	7.4	5.6	5	4.7	3.8
PRF90	4.1	3.7	3.4	3.5	3.5
PRF100	2.9	3	2.7	2.8	3.2

Paper I

SAE International

2012-01-1128
Published 04/16/2012
doi:10.4271/2012-01-1128
saeeng.saejournals.org

Pressure Sensitivity of HCCI Auto-Ignition Temperature for Primary Reference Fuels

Ida Truedsson, Martin Tuner and Bengt Johansson
Lund University

William Cannella
Chevron USA Inc

ABSTRACT

Some fuels with the same research octane number (RON) have different HCCI engine performance. Therefore RON alone cannot be used for determining auto ignition in HCCI combustion. The current research focuses on creating an HCCI fuel index suitable for comparing different fuels for HCCI operation. More thorough studies are needed to map the fuel effects. One way to characterize a fuel is by using the Auto Ignition Temperature (AIT). The AIT and the amount of Low Temperature Heat Release (LTHR) together describe the auto ignition properties of the fuel. Both can be extracted from the pressure trace. The assumption is that the pressure and temperature are known at inlet valve closing (IVC) and that the mass in the cylinder does not change after IVC.

The purpose of this study was to map the AIT of different Primary Reference Fuels (PRF) for HCCI combustion at different cylinder pressures. Different pressure levels were achieved by changing inlet air temperatures in 5 steps from 50°C to 150°C. A Cooperative Fuel Research (CFR) engine with variable compression ratio was used. The compression ratio was varied from 5.5 to 15.5 to keep combustion phasing, defined as 50% of total heat released, constant at 3±1° after TDC. The experiments were carried out in lean operation with a constant equivalence ratio of 0.33 and with a constant engine speed of 600 rpm.

The results showed that the AITs of the PRFs ranged from around 580 K for PRF 0 to up to 800 K for PRF 100. Auto ignition was defined as the point where the rate of heat released had reached 0.2 J/CAD. At the lowest inlet air temperatures all fuels except PRF 100 showed Low Temperature Heat Release (LTHR) from about 3% LTHR/Total Heat Release for PRF 95 with up to 19% for PRF 0. Amount of LTHR was found to decrease linearly with increasing octane rating.

The low octane PRFs ignited at almost the same temperature independent of the cylinder pressure. The high octane number PRFs (PRF 95 - 100) displayed a wide range of auto ignition temperatures resulting from the different inlet air temperatures. PRF 80, PRF 85 and PRF 90 showed an intermediate behavior. A constant auto ignition temperature was seen at the low inlet air temperature but at higher inlet air temperatures the IAT quicky rised when the LTHR disappeared.

CITATION: Truedsson, I., Tuner, M., Johansson, B. and Cannella, W., "Pressure Sensitivity of HCCI Auto-Ignition Temperature for Primary Reference Fuels," *SAE Int. J. Engines* 5(3):2012, doi:10.4271/2012-01-1128.

INTRODUCTION

HCCI is a combustion mode used to reduce emissions to the level of traditional spark ignition engines combined with maintaining efficiency as high as for diesel combustion. The main challenge for HCCI is to control the ignition timing and combustion rate, since they are not controlled by a spark (SI combustion) or by fuel injection (CI combustion) but are controlled by chemical kinetics.

The aim of this work was to map the auto ignition temperatures of different Primary Reference Fuels (PRF) at different cylinder pressures. This study tries to establish whether it is possible to determine the temperature at Start of Combustion and relate this to the HCCI engine fuel performance. The auto ignition is dependent on temperature, pressure and fuel air ratio, but also on the residence time of the fuel air mixture. Much work has been reported in the literature on auto ignition of PRFs, but only a small amount of it was conducted in combustion engines.

RON and MON are known to be insufficient to explain the fuel behavior in an HCCI engine [1,2,3]. More knowledge of the combustion process is needed to create a useful HCCI

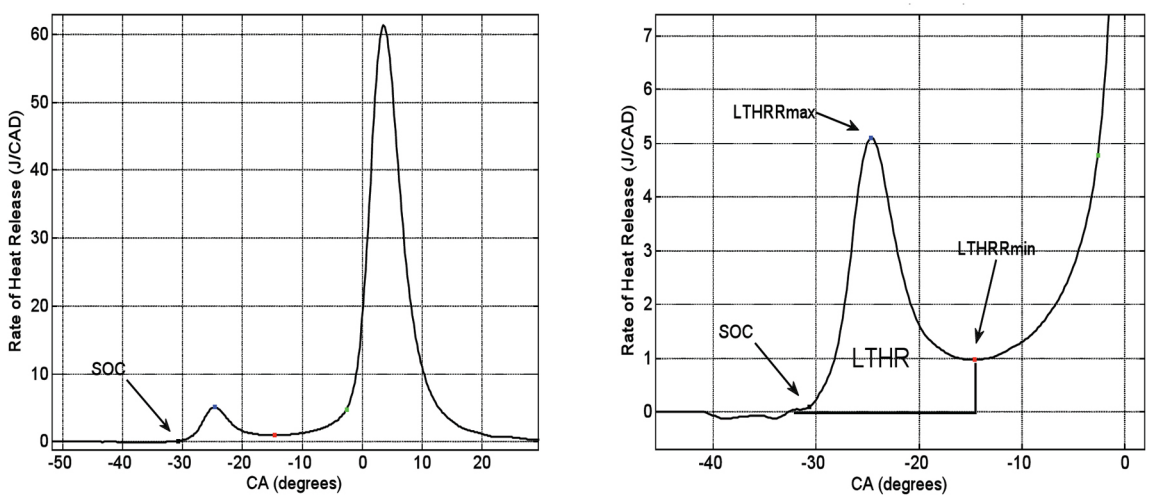

Figure 1. Definition of Heat Release Data.

fuel index, which is why a standardized method for determining the HCCI fuel performance was desired. The idea is that the fuel auto ignition temperature in combination with the amount of Low Temperature Heat Release (LTHR) can be related to the fuel performance in an HCCI engine. It was decided to use a standardized engine for the experiments, which is why the Cooperative Fuel Research (CFR) engine was chosen. This engine is normally used in SI mode to measure RON and MON values for fuels. This engine is suitable because it can be used for many types of fuels since it has a variable compression ratio. It is equipped with a spark plug and can therefore be used for both HCCI and SI combustion.

When burning fuels that contain a significant amount of n-paraffins, such as n-heptane, a characteristic bump is usually seen before the main heat release. This is called the Low Temperature Reactions (LTR) or the Low Temperature Heat Release (LTHR), referring to the exothermic pre-reactions that occur before the main combustion event (see Figure 1). At lower inlet air temperatures, depending on the fuel, there can be extensive LTHR, but this decays with higher temperature because of the higher amount of available energy and therefore earlier main combustion. The amount of LTHR also decreases with higher engine speed because there is less time for reactions [4]. A higher cylinder pressure induced by super- or turbocharging is also known to increase the amount of LTHR [5]. When LTHR is present the auto ignition temperature is substantially lower.

The oxidation mechanism of hydrocarbons is shown in Figure 2. Reactions are initiated by the abstraction of H from a fuel molecule (RH) by O_2, where an alkyl radical (R) and HO_2 are formed. At low temperatures the alkyl radical then reacts with oxygen to produce RO_2. This then gives H_2O and an alkyl peroxide (O=ROOH). This is a highly exothermic reaction. This continues until the temperature is high enough for the alkyl radical and oxygen to instead form olefins and HO_2, which terminates the first reaction step. After this the high temperature reaction starts producing olefins and H_2O_2. This is the stage between LTHR and HTHR. Here the rate of temperature rise decreases sharply, called the Negative Temperature Coefficient (NTC) zone. After this the temperature slowly rises until the H_2O_2 decomposes leading to a branched thermal explosion. At this stage the O=ROOH and olefin decompose irreversibly to H_2O and CO. Then CO is converted to CO_2 in the reaction $CO+OH=CO_2+H$ [6,7].

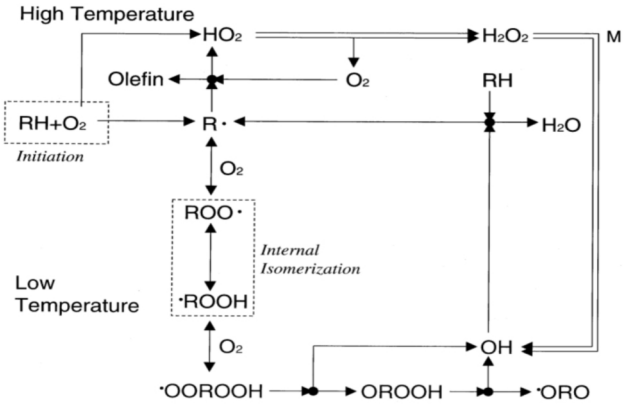

Figure 2. Oxidation scheme for heavy hydrocarbons at low and high temperatures. Reprinted from 6, copyright (2003), with permission from Elsevier.

The LTHR of the n-paraffins can be explained by the possibility for n-heptane to form a transitional ring with low ring strain for internal H atom transfer, the so called internal isomerization (Figure 2). This reaction has a much higher energy barrier for a more compact molecule as for example iso-octane [12].

Studies of auto ignition properties of different fuels have been done before, for example by Shibata and Kalghatgi [2,3,6]. Shibata et al. [2] studied surrogate fuels and created an HCCI index calculated by using the fuel RON and amounts of the different fuel components. Kalghatgi [6]

developed the Octane Index using the RON and MON for the fuel in combination with an engine specific parameter K. Studies on auto ignition temperatures in engines divided into pre-reactions and main reactions for HCCI combustion were made by Christenssen [8]. Modeling of LTHR for PRFs was made by Silke et al. [9] and for similar fuel surrogates by Mehl et al. [10].

Machrafi and Cavadiasa [7] also studied the combustion of PRFs in a CFR engine. They did an experimental and modeling study. They varied inlet air temperature, equivalence ratio and compression ratio, and looked at the ignition delay for PRF 0 and 40. The effect of different amounts of residuals were also discussed.

EXPERIMENTAL

A Waukesha Variable Compression Ratio CFR engine was used for the experiments. The setup included an air heater mounted after the port injection. A scale was used for measuring the fuel flow. A Kistler pressure transducer was mounted in the cylinder. An intake air conditioner is included in the setup to ensure constant air humidity throughout the experiments. The engine specifications are listed in Table 1.

Table 1. Engine Specifications.

Displacement volume	612 cm^3
Number of cylinders	1
Bore	83 mm
Stroke	114 mm
CR	Variable (4:1 to 18:1)
Number of valves	2
Length of connecting rod	254 mm
Intake valve opens	10°ATDC±2.5°
Intake valve closes	146°BTDC±2.5°
Exhaust valve opens	140°ATDC±2.5°
Exhaust valve closes	15°ATDC±2.5°
Valve lifts	6.25 mm
Valve diameters	9.53 mm
Engine speed	600 rpm
Fuel supply	Port injection

FUELS

The test fuels were 9 different blends of n-heptane and iso-octane. The mixing accuracy is ±1vol%. The fuels used were PRF 0, 20, 40, 60, 80, 85, 90, 95 and 100. PRF 0 is pure n-heptane, PRF 100 is pure iso-octane and the other fuels are a mix of the two, where the number indicates not only the amount of iso-octane but also the octane rating.

METHOD

A fuel matrix consisting of the nine different Primary Reference Fuels (PRFs) were run. All fuels were run with a change in inlet air temperature from 50° to 150°C. For each temperature a combustion phasing with CA50 at 3±1° after TDC was achieved by varying the compression ratio. Motored pressure traces were extracted for all data points for validation. The engine was run naturally aspirated at 1 bar inlet air pressure. The fuel amount was adjusted for each case to achieve an equivalence ratio of 0.33. All experiments were run at 600 rpm. No EGR was used.

HEAT RELEASE CALCULATION

The heat release calculations were made for each individual cycle of the pressure trace and all figures were based on the mean value of 300 cycles. The heat release calculation is according to Heywood [11]. Equation 1 gives the rate of heat release as a function of CAD, θ. Crevice flow was assumed negligible.

$$\frac{\partial Q}{\partial \theta} = \frac{\gamma}{\gamma - 1} p \frac{\partial V}{\partial \theta} + \frac{\gamma}{\gamma - 1} V \frac{\partial P}{\partial \theta} + \frac{\partial Q_{HT}}{\partial \theta} + \frac{\partial Q_{crevice}}{\partial \theta} \quad (1)$$

A single zone heat release model was used, assuming that the temperature and the gas composition are the same in the whole bulk. This is quite a good assumption for HCCI combustion. Gamma is approximated by Equation 2 and is temperature dependent. The heat transfer model was tuned by changing the γ_0 and k with respect to the shape of the heat release curves. The heat release was tuned for the motored pressure trace to be as close to zero as possible and that the burned pressure trace at the same time fit fuel measurement data. The same parameters were used for all fuels and cases.

$$\gamma = \gamma_0 - \frac{T_{cyl} - 300}{1000} \cdot k \quad (2)$$

	γ_0	k
Motored	1.40	0.07
Combustion	1.37	0.05

The heat loss term is calculated in Equation 3 according to Woschni with constants recalculated to fit the SI-unit system.

$$h = 131 \cdot B^{-0.2} \cdot p^{0.8} \cdot T^{-0.55} \cdot w^{0.8} \quad (3)$$

Where:

$$w = 2.28 \cdot S_p + 3.24 \cdot 10^{-3} \cdot \left(\frac{V_d}{V_{IVC}} \right) \left(\frac{p_f - p_m}{p_{IVC}} \right) \cdot T_{IVC} \quad (4)$$

To calculate the temperature in the cylinder when the Inlet Valve Closes (IVC), the heat transfer between the fuel air mixture and the walls in the intake was calculated. The Woschni heat transfer model was used with the same parameters as in the cylinder, and with an assumed wall temperature of 100°C. Equation 5 gives an effect of ±5°C.

The effect of heat transfer to the fuel mass was assumed to be negligible.

$$\Delta T_{inlet} = \frac{hc_{inlet} \cdot A_{inlet} \cdot (T_{wall,inlet} - T_{in})}{m_{air} \cdot c_{p,air}} \quad (5)$$

The amount of residuals was used to calculate the temperature in the cylinder when the inlet valve closed. The amounts of residuals in the cylinder were approximated using Equation 6 [11]. The cylinder pressure 10 CAD before exhaust valve opens was used as p_4 and the measured pressure in the exhaust was used for p_e. This gives about 3% residuals at high compression ratios (CR=15.5) and up to 10% at lower compression ratios (CR=5.5). This gives a heating effect of +5° to +35°.

$$x_r = \frac{\left(\frac{p_e}{p_4}\right)^{1/\gamma}}{r_c} \quad (6)$$

T_{IVC} is then calculated with Equation 7. The residuals were assumed to have the same temperature as the measured exhaust gas temperature.

$$T_{IVC} = T_{air,cyl} \cdot (1 - x_{res}) + T_{exhaust} \cdot x_{res} + \Delta T_{inlet} \quad (7)$$

RESULTS AND ANALYSIS

CALCULATED T_{IVC}

The temperature in the inlet was held constant at five different temperatures from 50°C to 150°C. Due to heat transfer in the inlet and mixing of air and residual gas, the temperature changes before the inlet valve closes. The temperature change, ΔT, calculated from the models (See section above on Heat Release Calculations) is shown in Figure 3. The higher ΔT for the low octane number PRFs is a result of the lower compression ratios needed which leads to a higher amount of hot residual gas.

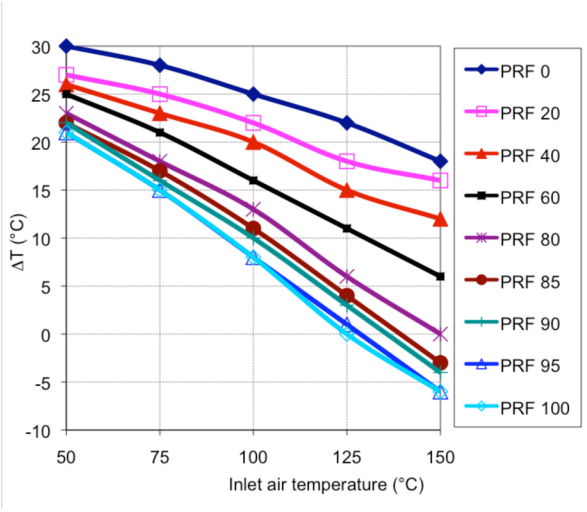

Figure 3. Calculated T_{IVC} for the different fuels and inlet air temperatures.

CA 50 PRESSURE SENSITIVITY

Since the CA50 is kept constant by changing the compression ratio, a high compression ratio corresponds to a higher ignition resistance. Figure 4 shows the different compression ratios required for a constant CA50 at 3±1° after TDC for the PRFs as a function of inlet air temperature.

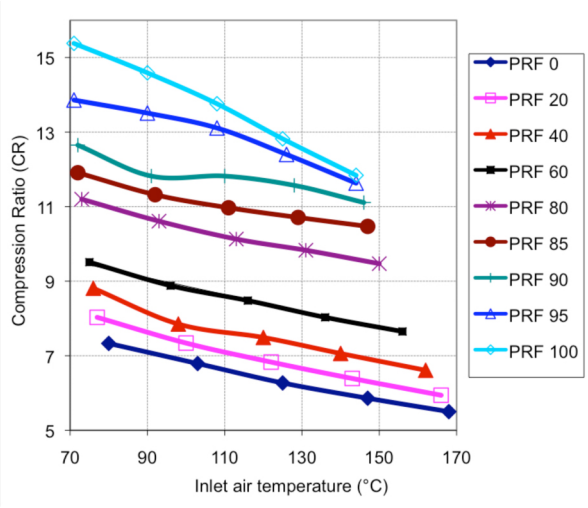

Figure 4. Compression ratios - pressure sensitivity for the different fuels.

Linear fit approximations were made for all fuels and these are presented in Table 2. The largest pressure difference is for PRF 95 and PRF 100, the fuels with little or no LTHR. A much smaller change in compression ratio is needed for the low octane number PRFs.

Table 2. Correlation between Inlet Air Temperature(x) and Compression Ratio(y)

Fuel	Equation	R^2
PRF 0	y=-0.0209x+8.95	0.995
PRF 20	y=-0.023x+9.73	0.992
PRF 40	y=-0.024x+10.46	0.964
PRF 60	y=-0.023x+11.13	0.993
PRF 80	y=-0.022x+12.73	0.987
PRF 85	y=-0.019x+13.14	0.969
PRF 90	y=-0.018x+13.77	0.888
PRF 95	y=-0.031x+16.20	0.966
PRF 100	y=-0.049x+18.94	0.997

LOW TEMPERATURE HEAT RELEASE

The LTHR and start of combustion for the PRFs are shown in Figure 5, Figure 6, Figure 7, Figure 8, Figure 9, Figure 10, Figure 11, Figure 12, Figure 13, Figure 14. The five curves for each PRF represent the 5 different inlet air temperatures, with more extensive LTHR at the lower inlet air temperatures. One possible explanation for the higher amount of LTHR at the lower inlet air temperatures is the higher compression ratio used to achieve a constant CA50, since high pressure is known to increase LTHR. The black dots mark the start of combustion, defined as 0.2 J/CAD (See section below on Start of Combustion for further discussion). For PRF 0-80 LTHR is seen for all inlet air temperatures.

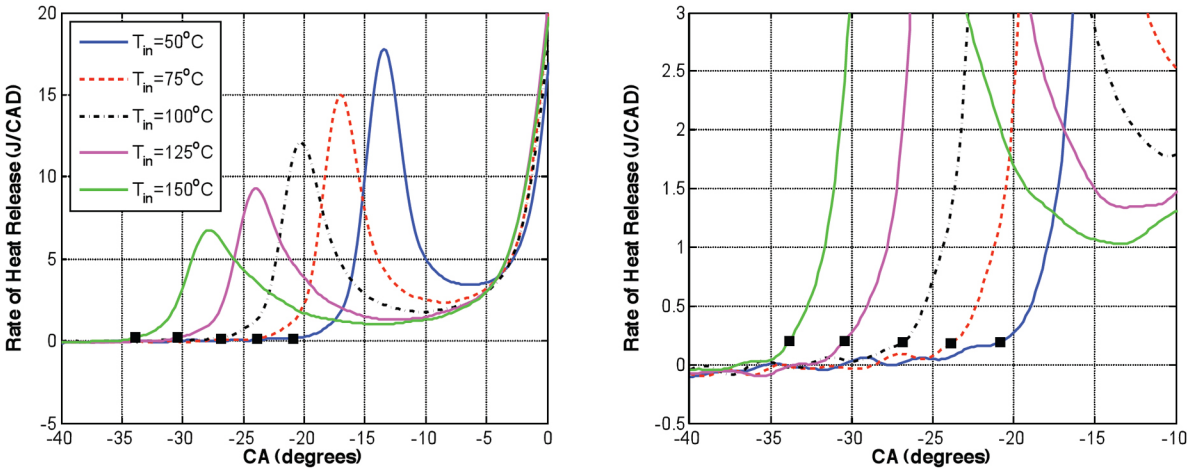

Figure 5. Low Temperature Heat Release and Auto Ignition for PRF 0. The dots mark start of combustion defined as 0.2 J/CAD. The picture to the right is a zoom of the picture to the left.

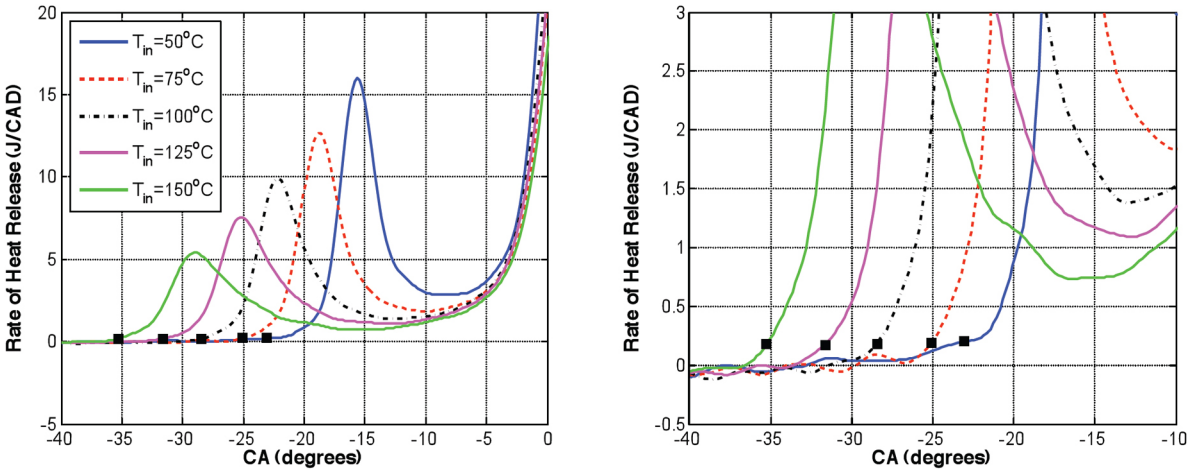

Figure 6. Low Temperature Heat Release and Auto Ignition for PRF 20. The dots mark start of combustion defined as 0.2 J/CAD.

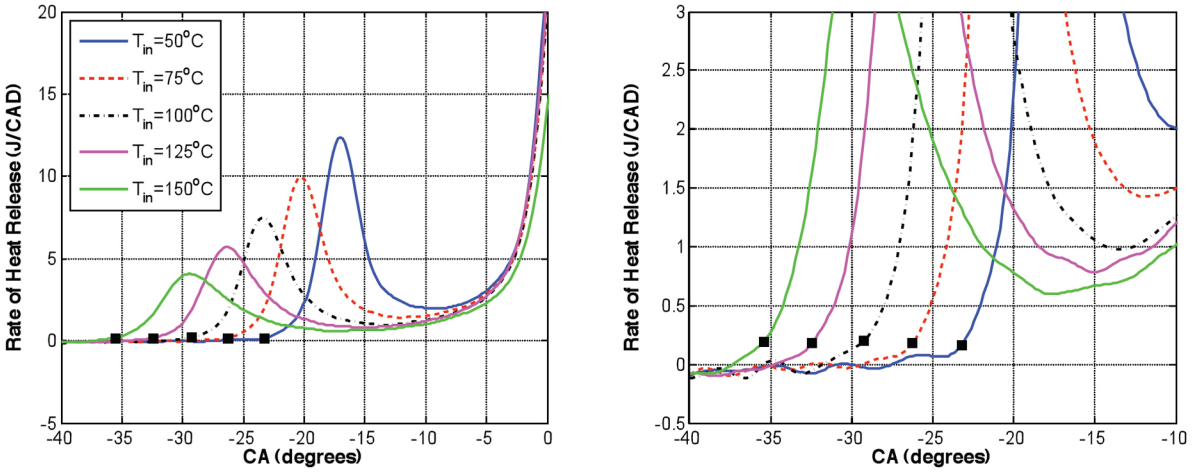

Figure 7. Low Temperature Heat Release and Auto Ignition for PRF 40. The dots mark start of combustion defined as 0.2 J/CAD.

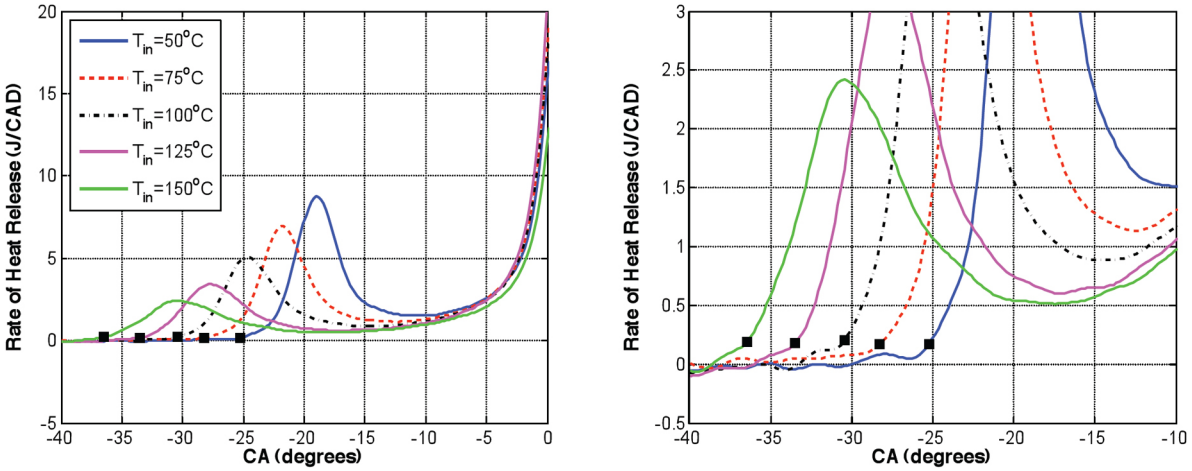

Figure 8. Low Temperature Heat Release and Auto Ignition for PRF 60. The dots mark start of combustion defined as 0.2 J/CAD.

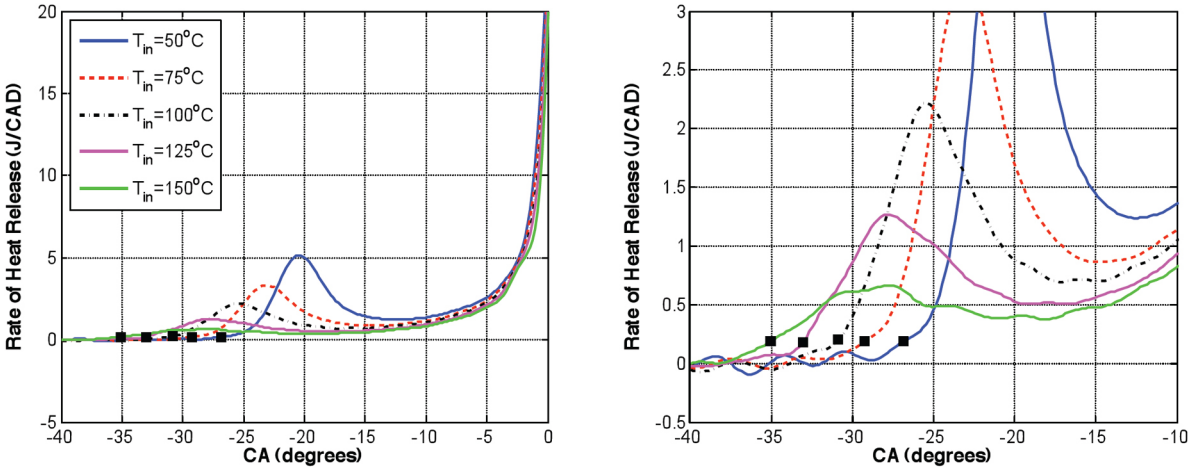

Figure 9. Low Temperature Heat Release and Auto Ignition for PRF 80. The dots mark start of combustion defined as 0.2 J/CAD.

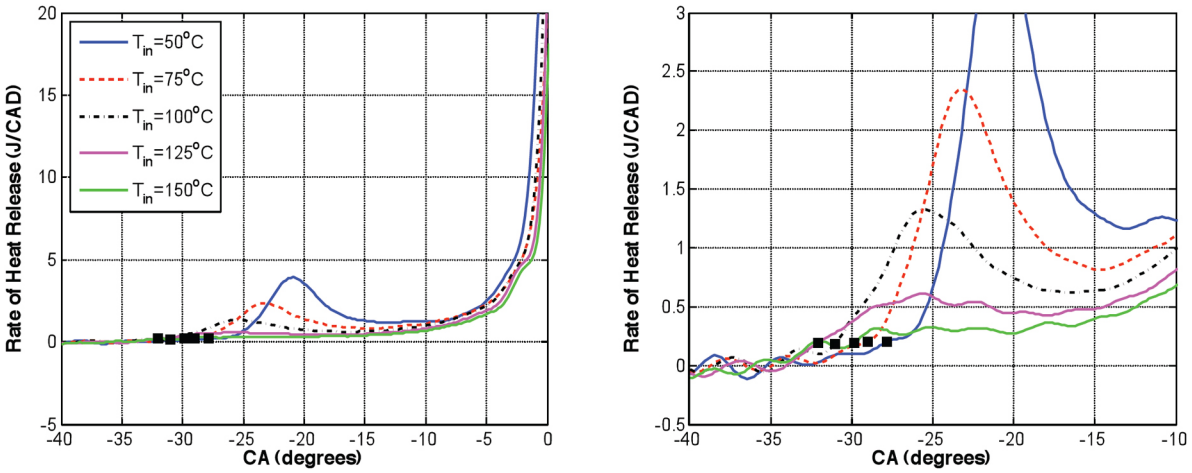

Figure 10. Low Temperature Heat Release and Auto Ignition for PRF 85. The dots mark start of combustion defined as 0.2 J/CAD.

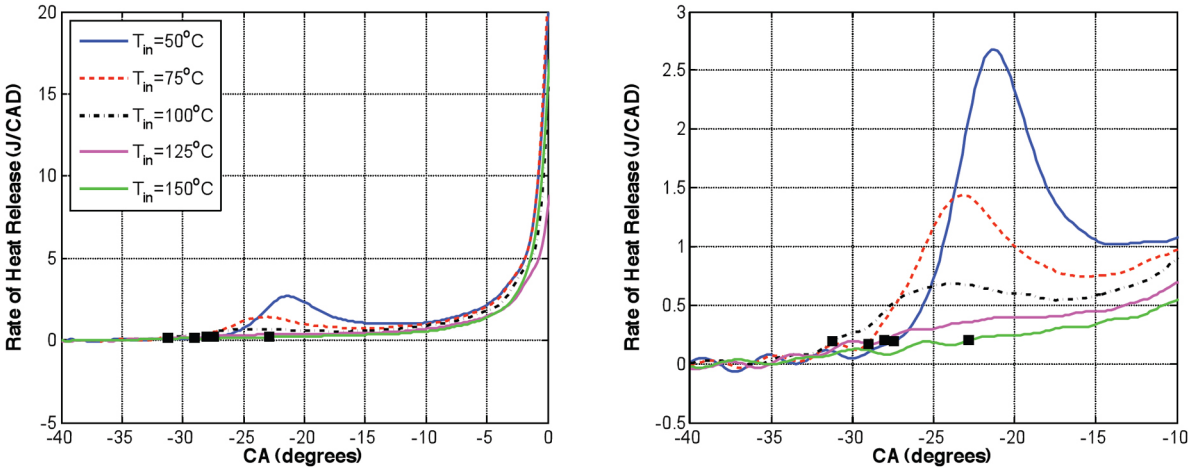

Figure 11. Low Temperature Heat Release and Auto Ignition for PRF 90. The dots mark start of combustion defined as 0.2 J/CAD.

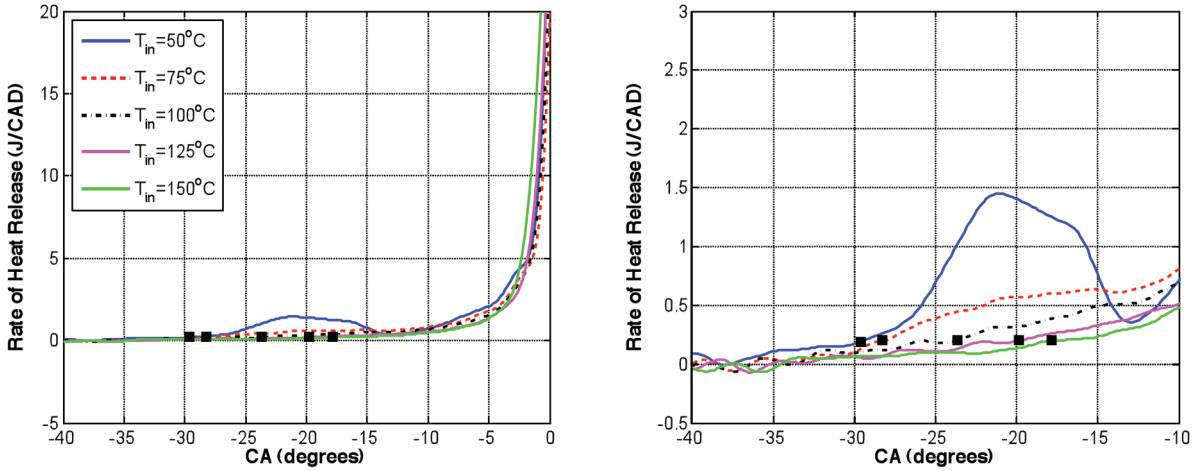

Figure 12. Low Temperature Heat Release and Auto Ignition for PRF 95. The dots mark start of combustion defined as 0.2 J/CAD.

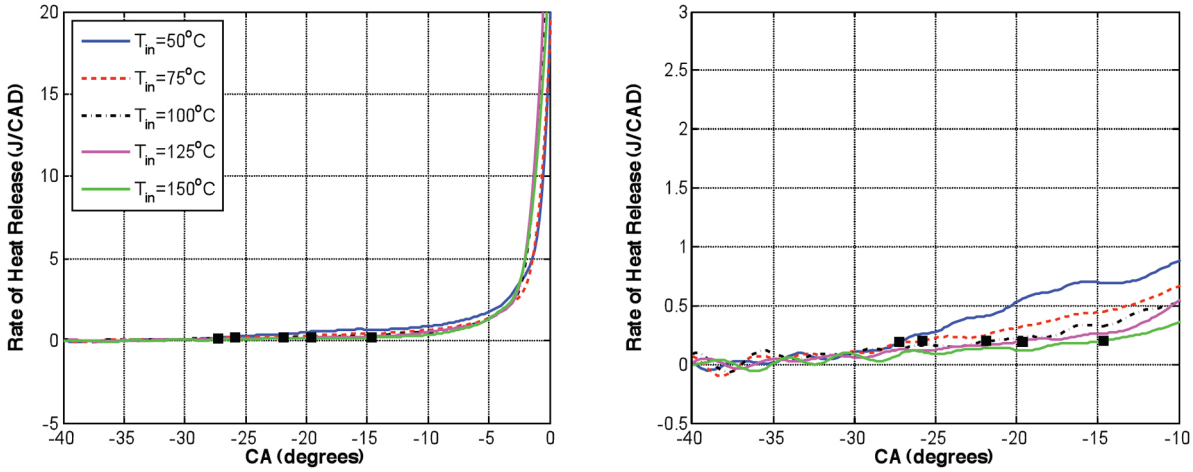

Figure 13. Low Temperature Heat Release and Auto Ignition for PRF 100. The dots mark start of combustion defined as 0.2 J/CAD.

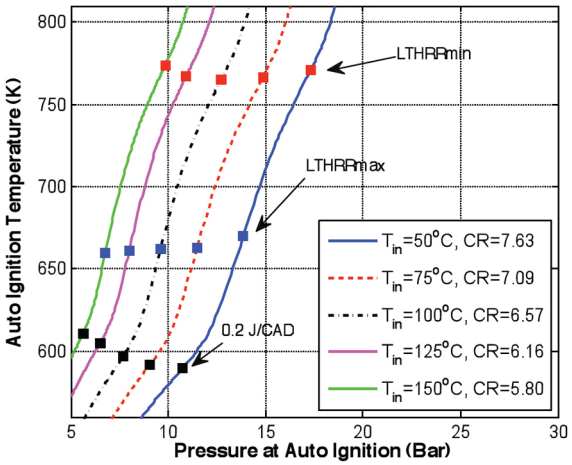

Figure 14. Auto ignition pressures and temperatures for PRF 0.

For PRF 85 the LTHR has diminished to the point where there is no longer a rate of reaction peak at the highest inlet air temperature. According to the definition above, this means there is no longer any LTHR, see Figure 10.

For PRF 90 the LTHR disappears at 125°C. This leads to a later start of combustion for the 125°C case and an even later start at 150°C.

PRESSURE SENSITIVITY

Figure 14 shows the pressure and temperature in the cylinder around and at start of combustion. The black dots at the bottom mark start of combustion defined as 0.2 J/CAD. The blue dots near the middle mark the maximum rate of LTHR and the red dots near the top the minimum value between LTHR and the main heat release as seen in Figure 1. In Figure 14 it can be seen that combustion starts at almost the same temperature independent of cylinder pressure. It also seems like the peak of LTHRR where the reaction rate decreases appears at the same temperature. The same is true for the red dots marking the minimum rate of heat release between LTHR and HTHR, indicating the start of the main heat release. The same behavior is seen also for PRF 20-60 (Figures 15, 16, 17). The Start of Combustion appears at around 600 K for these four fuels, the LTHRRmax around 660 K. The LTHRRmin appears around 750 K for all fuels, including the high octane number fuels.

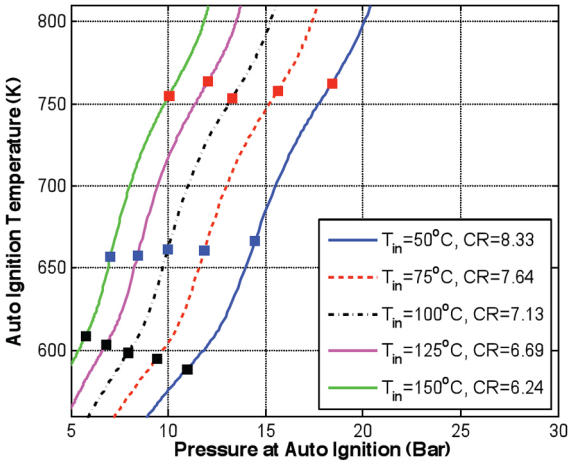

Figure 15. Auto ignition pressures and temperatures for PRF 20.

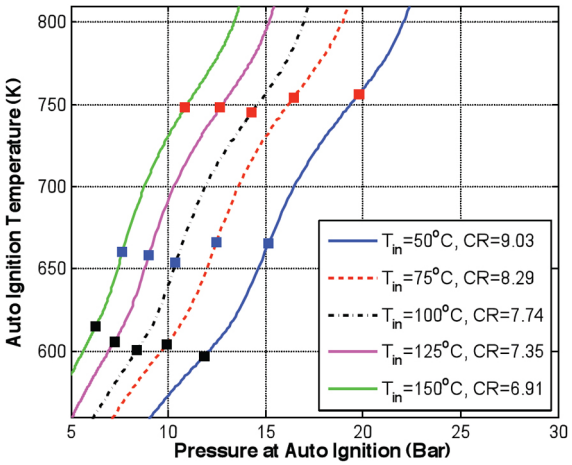

Figure 16. Auto ignition pressures and temperatures for PRF 40.

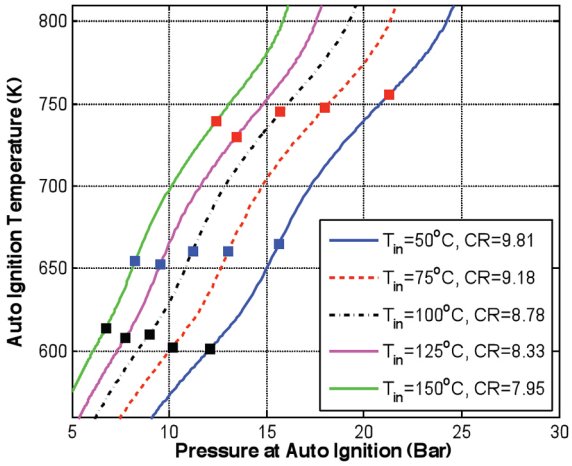

Figure 17. Auto ignition pressures and temperatures for PRF 60.

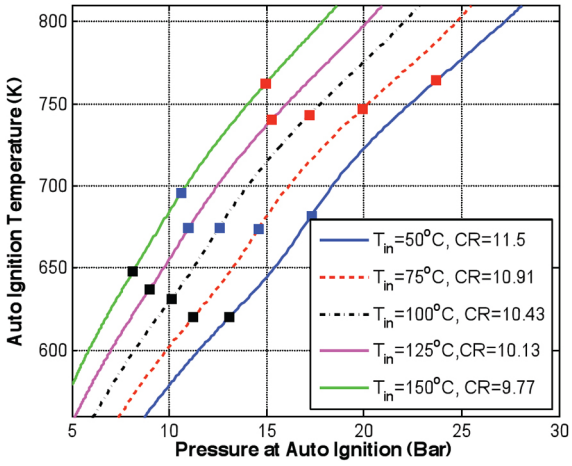

Figure 18. Auto ignition pressures and temperatures for PRF 80.

The disappearance of the LTHR is seen for the 150°C inlet air temperature and therefore lowest compression ratio case in Figure 19. An increase in AIT is seen at the same time. Comparing the rate of heat release in Figure 11 with the rate of heat release of for example PRF 100 in Figure 13 it can be argued that there are still some LTHR even for this case at the lower inlet air temperatures.

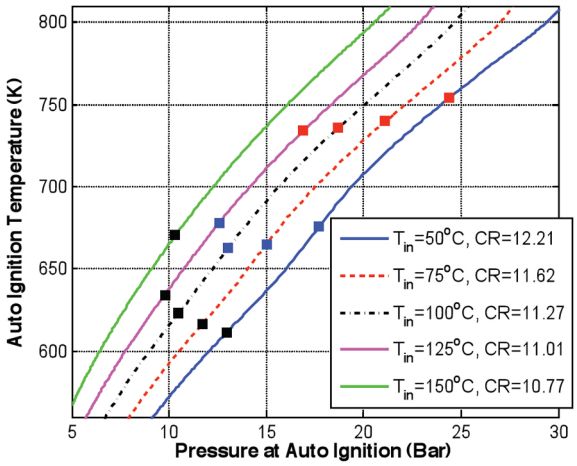

Figure 19. Auto ignition pressures and temperatures for PRF 85.

For PRF 90 the LTHR disappear already at 125°C inlet air temperature with a steep increase in AIT, see the black dots in Figure 20.

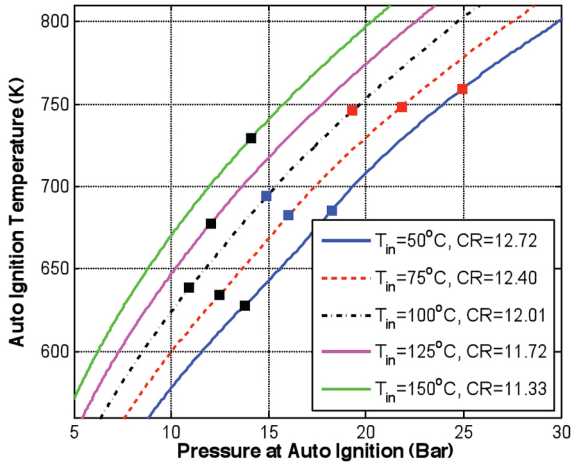

Figure 20. Auto ignition pressures and temperatures for PRF 90.

For PRF 100 no LTHR is detected and the AIT increases quickly when decreasing the compression ratio.

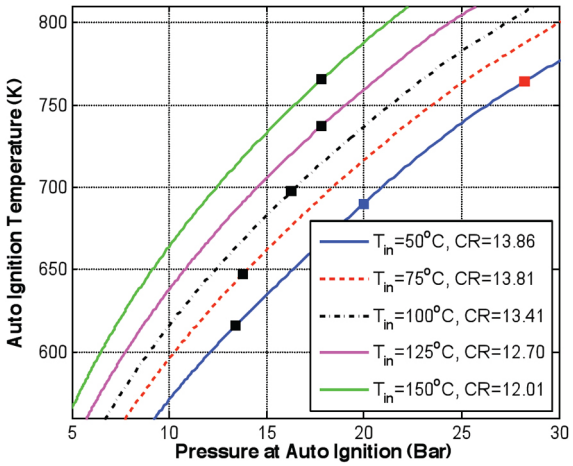

Figure 21. Auto ignition pressures and temperatures for PRF 95.

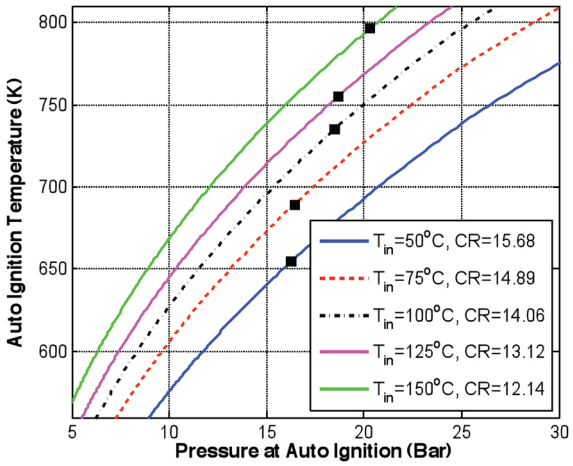

Figure 22. Auto ignition pressures and temperatures for PRF 100.

LOW TEMPERATURE HEAT RELEASE QUANTIFICATION

End of LTHR was set as the minimum value between $LTHRR_{max}$ and $HTHRR_{max}$, shown in Figure 1. An almost linear response between amount of n-heptane in the PRFs and percentage of LTHR was found, especially up to PRF 80 (see Figure 23).

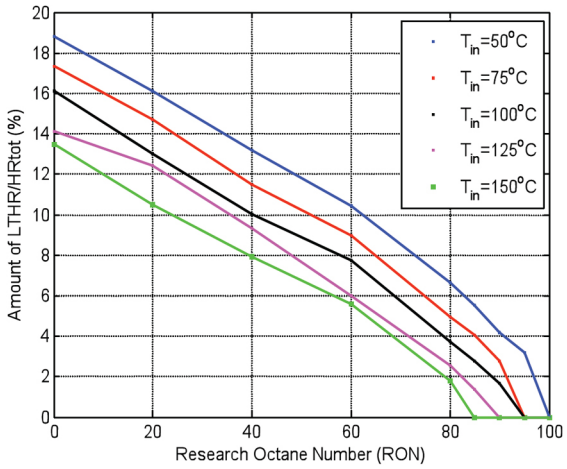

Figure 23. Amount of LTHR for the PRFs.

Linear correlations were found at all 5 temperatures, see example in Figure 24 for 50°C inlet air temperatures. Equations for the linear approximations are presented in Table 3. The amount of LTHR is decreasing with increasing inlet air temperature and with higher RON. Only cases having more than 1% LTHR are presented. By definition above, only cases with a LTHR peak are represented, but it could be argued that LTHR is present in more cases.

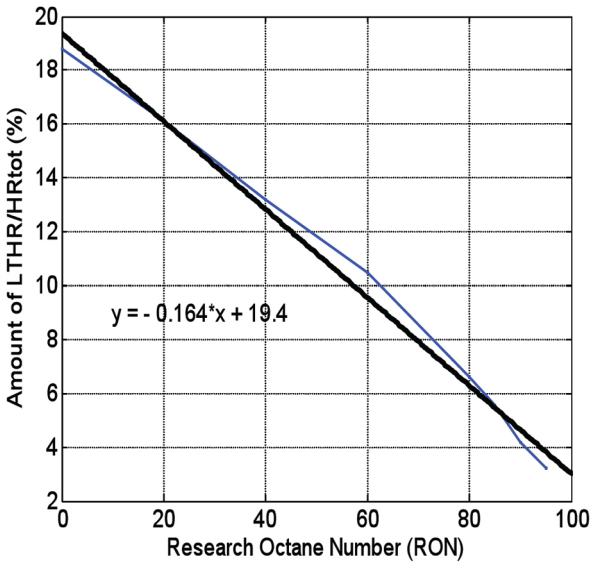

Figure 24. Amount of LTHR for the 50°C inlet air temperature.

Table 3. Correlation between RON(x) and LTHR/ HRtot(y).

Inlet air temperature	Equation	R^2
50°C	y=-0.164x+19.4	0.991
75°C	y=-0.160x+17.8	0.993
100°C	y=-0.158x+16.3	0.994
125°C	y=-0.154x+14.9	0.988
150°C	y=-0.141x+13.5	0.994

START OF COMBUSTION

Start of Combustion (SOC) was defined as when the rate of heat release had reached a certain value. This value was chosen to be 0.2 J/CAD, corresponding to a rate of heat release when early combustion can be seen but still not too close to the noise level. Examples are shown in Figure 25, Figure 26, Figure 27, Figure 28. The five curves in each Figure represent the 5 different inlet air temperatures. Plots for all PRFs with SOC are shown in the previous Section on Low Temperature Heat Release. A definition with a physical explanation was desired, and therefore start of combustion (here denoted as 0.2 J/CAD) was preferred before the more common unit of 1% burnt. For comparison both methods are presented below. To demonstrate the differences between the start of combustion for the PRFs with and without extensive LTHR, both PRF 100 and PRF 80 are presented below.

Also 0.2 % burnt is shown, since this is close to the previously discussed definitions of 0.2 J/CAD. By looking at the cumulative heat release instead of the derivative, noise is suppressed. This is an advantage for the 0.2 % definition. However, looking at Figure 26 and Figure 28 showing rate of heat release, these points represent different stages in the combustion process. At some inlet air temperatures 0.2 % burnt catches the very beginning, but in other cases the combustion has taken off.

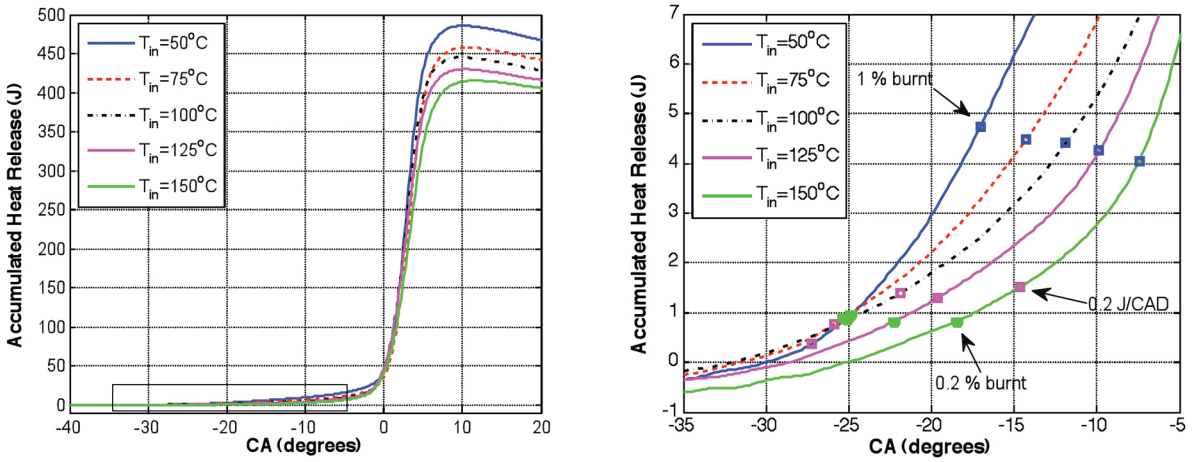

Figure 25. The different definitions of start of combustion, PRF 100. The box in the left figure marks the zoom area.

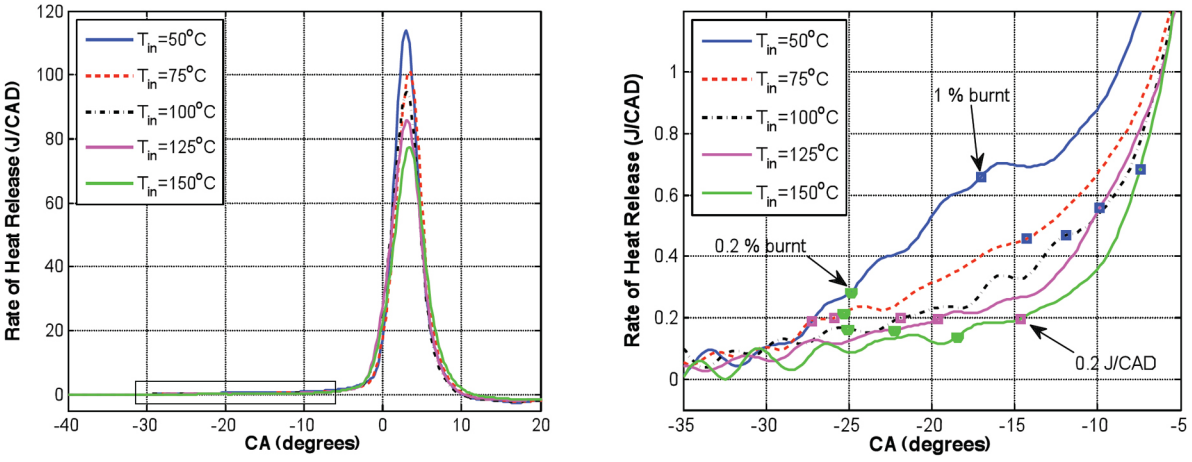

Figure 26. The different definitions of start of combustion, PRF 100. The box in the left figure marks the zoom area.

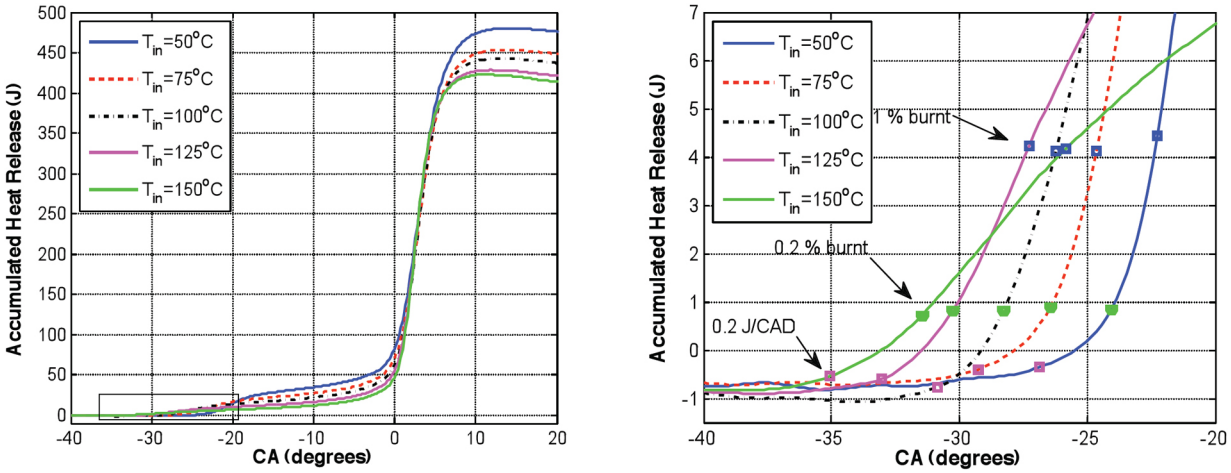

Figure 27. The different definitions of start of combustion, PRF 80. The box in the left figure marks the zoom area.

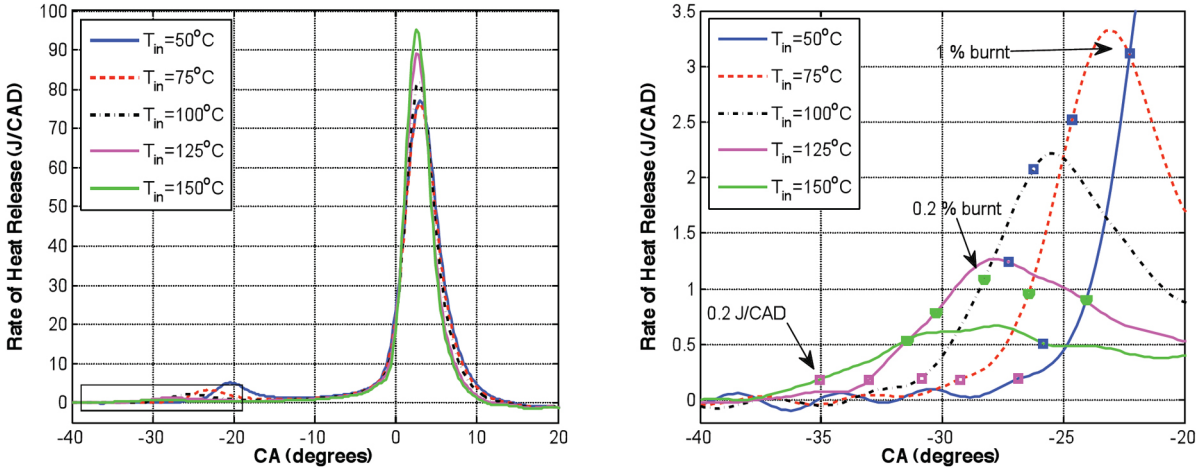

Figure 28. The different definitions of start of combustion, PRF 80. The box in the left figure marks the zoom area.

IGNITION TEMPERATURES

Ignition temperatures resulting from the different cylinder pressures were determined. The ignition temperatures are presented in Figures 29, 30, 31, with 5 different points for each fuel, corresponding to the 5 different inlet air temperatures. This is the same data as presented in Figures 14, 15, 16, 17, 18, 19, 20, 21, 22. To the right for the low octane number fuels (PRF0-90) is the lowest inlet air temperature of 50°C, and to the left is the highest intake temperature, 150°C. The high octane fuels (PRF 95-100) exhibit different behavior. For the high octane fuels (PRF95-100) the lowest inlet air temperature is at the lowest AIT of each curve and the higher intake temperature is at the highest AIT of each curve. In Figure 29 and Figure 30 it can be seen that the PRFs with extensive LTHR, PRF 0-60, behave in the same way, with the auto ignition starting at about the same temperature regardless of the cylinder pressure. The PRF 0 ignites at around 570 K, with a weak trend that a lower cylinder pressure requires a higher temperature for auto ignition. However it seems like the temperature is the crucial parameter for start of combustion for these fuels. The high octane number fuels, PRF 90-PRF 100 on the other hand, shows a different behavior. At low inlet air temperatures and therefore lower cylinder pressures, a small amount of LTHR can be detected, which is why ignition temperature is much lower than at higher cylinder pressures. As the intake temperature and therefore also the cylinder pressure increases and LTHR disappears, auto ignition temperature quickly rises. When the LTHR disappears a much higher temperature is needed for auto ignition to occur.

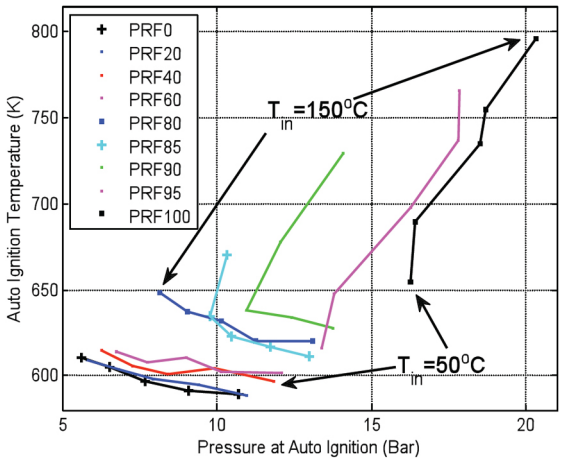

Figure 29. Auto Ignition temperatures and pressures for the PRFs (0.2 J/CAD).

The PRF 85 and PRF 90 curves capture both behaviors. At the lower inlet air temperatures the trend is similar to the lower octane number fuels, however, this changes with an inlet air temperature of 100-125°C. At this temperature the LTHR is gone and ignition therefore starts at a much higher temperature and pressure.

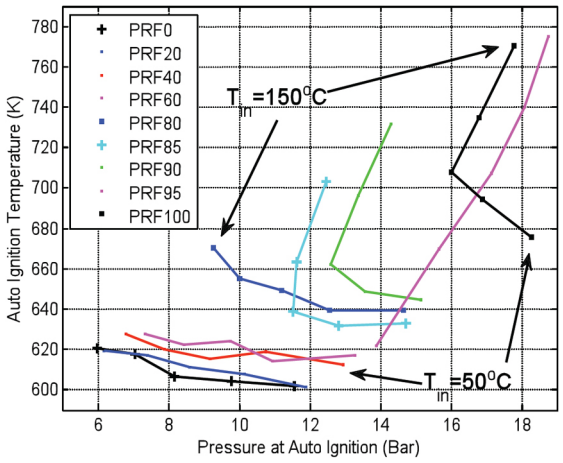

Figure 30. Auto Ignition temperatures and pressures for the PRFs (0.2 % burnt).

When using the 1 % burnt definition, see Figure 31, small amounts of LTHR are not captured, resulting in seemingly much higher auto ignition temperatures and pressures. A distinct difference is seen between the low octane PRFs (PRF 0-PRF 60) and the PRFs with an octane rating of 80 and higher, where for the first 1 % burnt is still well within the LTHR region. Also this definition indicates that the low octane PRFs (PRF 0-PRF 60) ignites at a constant temperature regardless of the cylinder pressure.

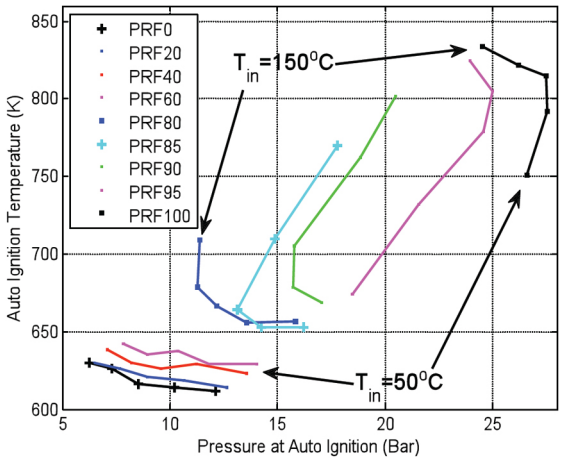

Figure 31. Auto Ignition temperatures and pressures for the PRFs, 1% burnt definition.

Figure 32 shows the temperature and pressure at start of High Temperature Heat Release (HTHR), defined as the point with minimum rate of heat release between LTHRR peak and the main peak of HTHRR. (See section below on LTHR Quantification). With this definition HTHR starts at around 750 K. Note that the temperature at start of main heat release is the highest for PRF 0.

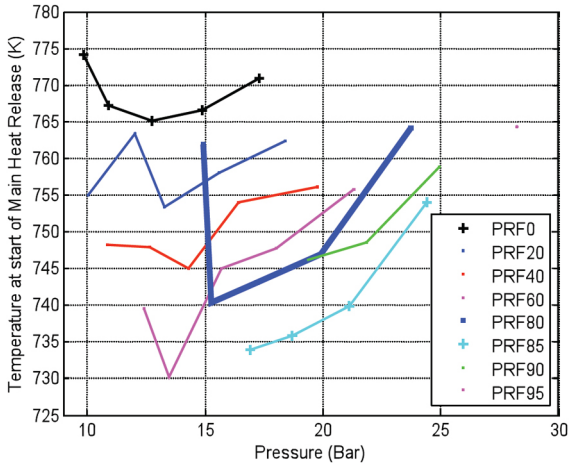

Figure 32. Temperatures and pressures at start of main HR.

Previous work [6] shows that high temperature heat release starts at 1000 K. The difference from these results is the definitions, where they used 20 % burnt as start of HTHR.

Figure 33 shows the crank angle for start of combustion. Since all experiments were made with a combustion phasing, CA50, at 3±1° after TDC, an early start of combustion is the same as a long combustion duration. PRF 0-60 shows the same trend, that an increase in inlet air temperature initiates the LTHR earlier. This could be due to the higher pressure-temperature history. A lower magnitude but longer duration LTHR zone is seen when the octane rating increases. For

PRF 85, the LTHR begins to disappear at the highest inlet air temperature, which is why combustion is retarded. The same effect is seen for PRF 90. PRF 95 and PRF 100, two fuels with very little LTHR, show that combustion is retarded with a higher inlet air temperature i.e. combustion duration is much shorter.

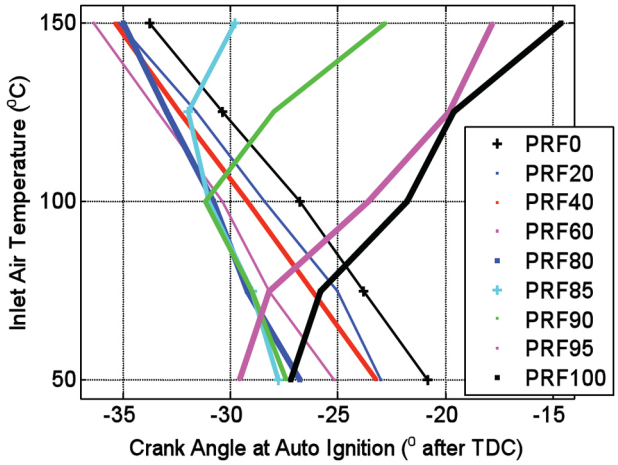

Figure 33. Start of Combustion for the PRFs (SOC with 0.2 J/CAD definition).

CORRELATION BETWEEN LTHR AND AUTO IGNITION TEMPERATURE

Figure 34 shows an almost linear correlation between amount of LTHR and auto ignition temperature. All cases with detectable LTHR (>1% and with a LTHRRmax) ignited at temperatures below 650 K.

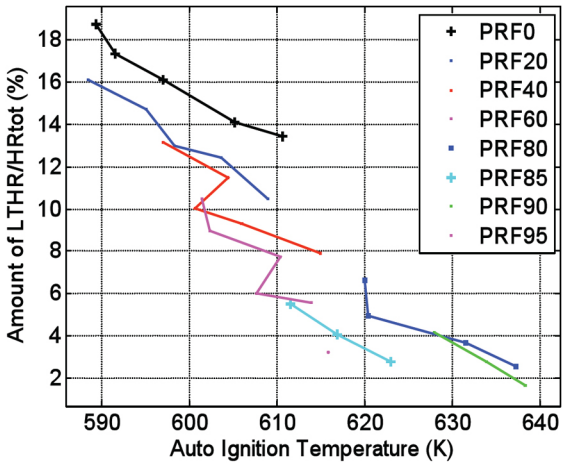

Figure 34. Amount of LTHR and Auto Ignition Temperatures (0.2 J/CAD).

In Figure 35 the cases without LTHR are also included. It can be seen that the ignition temperature quickly rises as the LTHR disappears. The definition of SOC as 0.2 J/CAD is used.

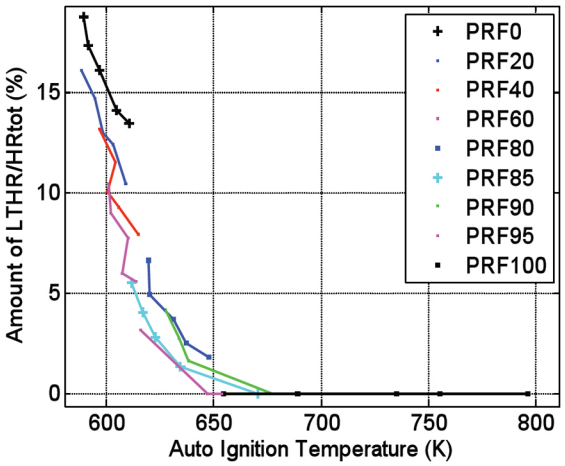

Figure 35. Amount of LTHR and Auto Ignition Temperatures (0.2 J/CAD).

RESEARCH OCTANE NUMBER

Figure 36 shows that the auto ignition temperature rises for PRFs with an octane number over 60. This is when the LTHR starts to diminish at the higher inlet air temperatures. A much larger auto ignition temperature range is seen for the higher octane number fuels. This could indicate that the AITs for these fuels are harder to predict and therefore more difficult to use for easily controlled combustion in an HCCI engine.

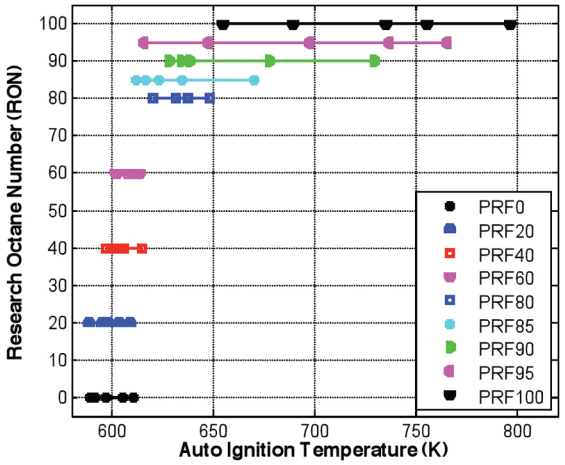

Figure 36. Auto Ignition Temperatures and RON correlation (0.2 J/CAD).

COMBUSTION PHASING

By changing the compression ratio in nine steps from 10.3 to 11.1 the combustion phasing of PRF 85 at an inlet air temperature of 150°C was changed from 0.4° before TDC to 8° after TDC, see Figure 37. The results in Figure 38 are acquired by using the definition of 0.2 J/CAD. No trend can

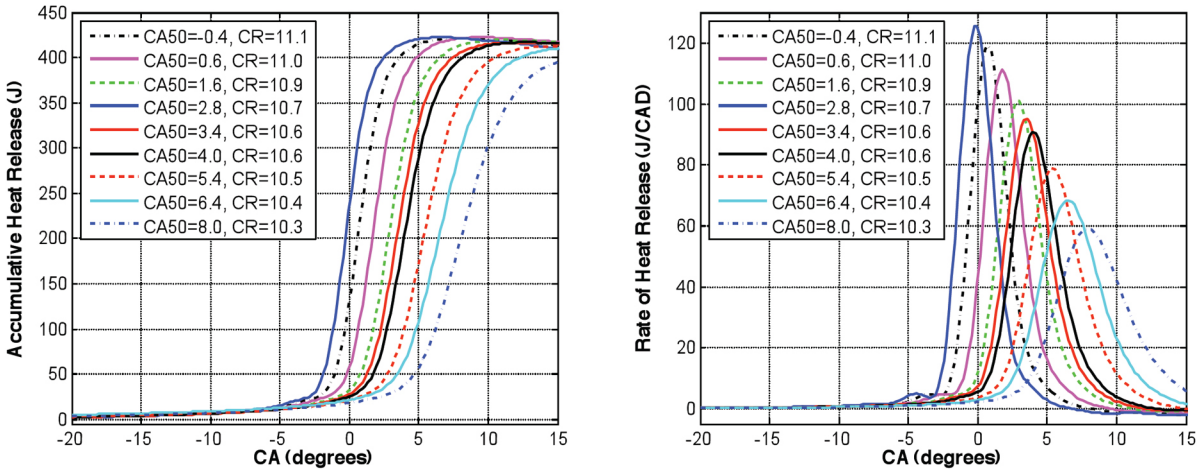

Figure 37. Accumulated heat release for different combustion phasings, PRF 85.

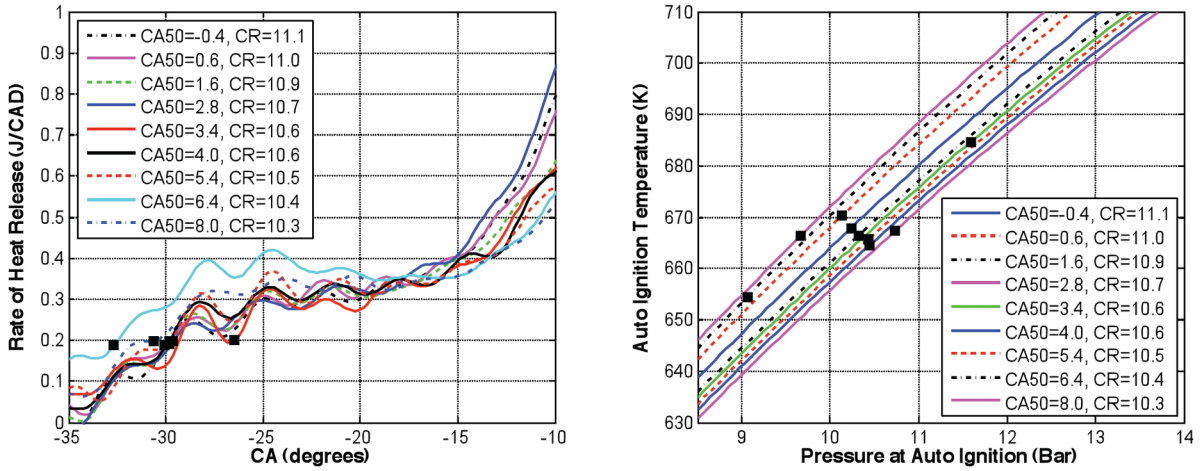

Figure 38. Auto ignition timings and temperatures for the different combustion phasings for PRF 85, 0.2 J/CAD.

be seen for auto ignition temperature at different combustion phasings.

The AIT varies 5° within the interval of combustion phasing of 3±1° after TDC as used in the previous experiments, and the pressure varies 0.3 Bar. There is no clear trend within this range and the small variations are probably a result of the random nature of the auto ignition process.

When looking at the 0.2 % burnt definition instead (Figure 39), a different result is obtained. This figure shows a trend that a later combustion phasing gives auto ignition at a lower temperature and pressure. This gives a difference of 20° between early and late combustion phasing. However there is little difference in both auto ignition temperature and pressure within the interval 3±1° after TDC used in the earlier part of the study.

ERROR ANALYSIS

HEAT RELEASE ANALYSIS

After tuning the heat release, the motored heat release was subtracted from the combustion heat release, see Figure 40 and Figure 41.

MODEL INFLUENCE

To assure that the trends seen were not dependent on the method of analysis a study was made of the results without the different models. In Figure 42 the red line represents the base case with no inlet air temperature models. The 5 points for each model represents the 5 intake temperatures with 150°C from left to 50°C on the right. The blue line shows the resulting auto ignition temperatures and pressures when the heat transfer in the inlet is added. Since the intake walls are 100°C this gives a heating effect at the lower inlet air temperatures and a cooling effect with the high inlet air temperatures. The black line shows the resulting temperatures

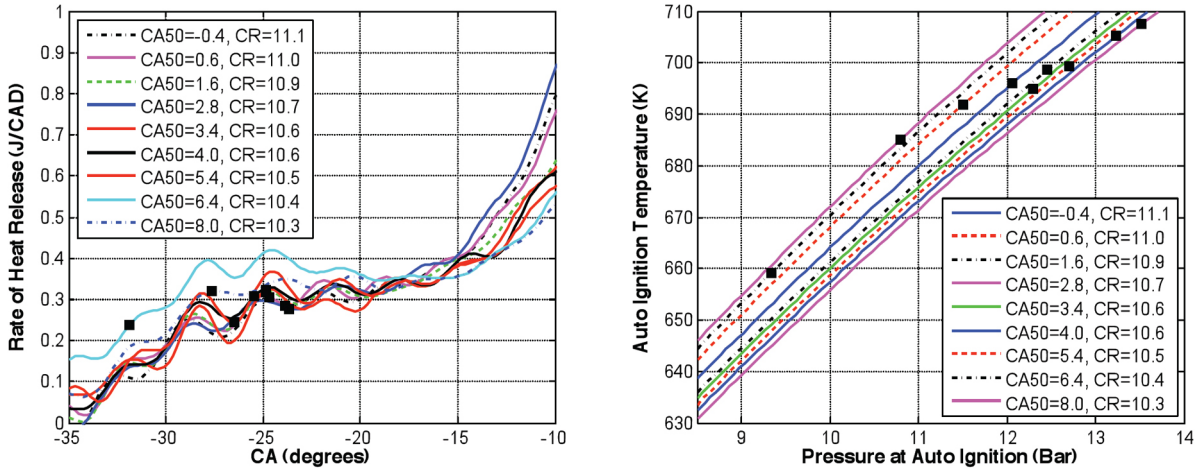

Figure 39. Auto ignition for the different combustion phasings for PRF 85, 0.2 % burnt.

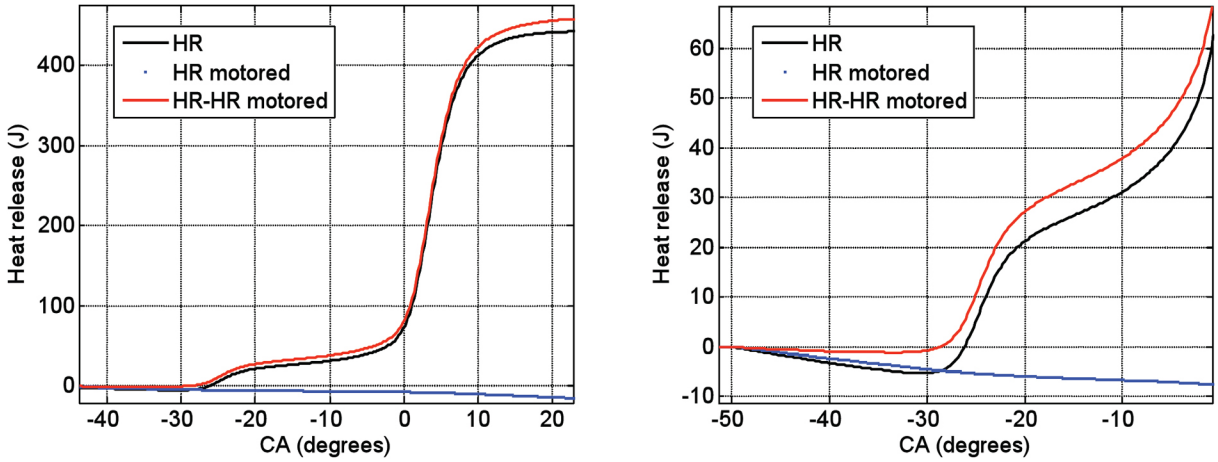

Figure 40. Heat release with and without motored heat release subtracted.

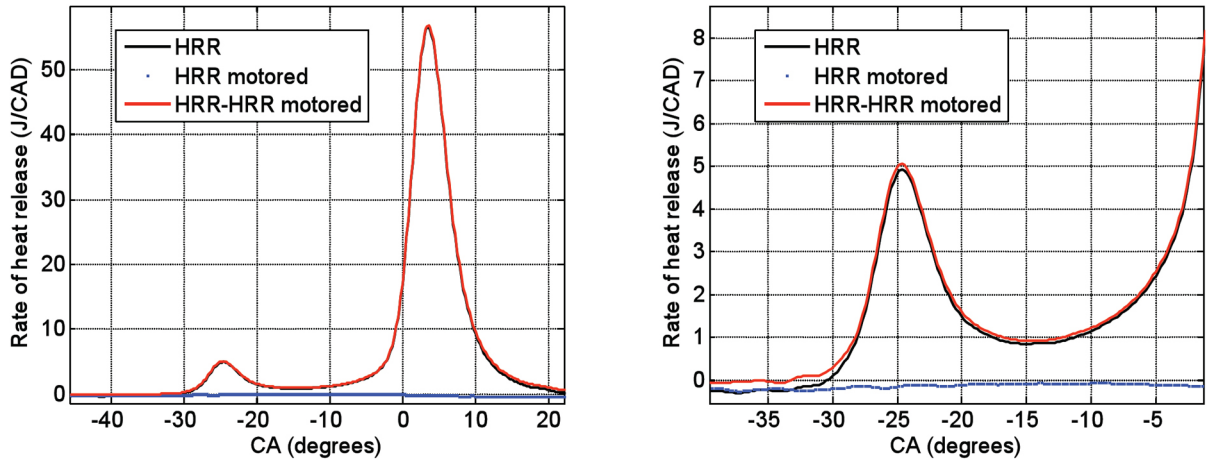

Figure 41. Heat release analysis, example of rate of heat release with and without motored heat release subtraction.

when the last model is applied, accounting for a heating of the inlet air because of mixing with residual gas. This has a more pronounced effect for the low intake temperatures due to the larger temperature difference between the intake air and the hot residuals. The conclusion is that the inlet air temperature models shows that the ignition starts at almost the same cylinder temperature, a result that is not seen without the models.

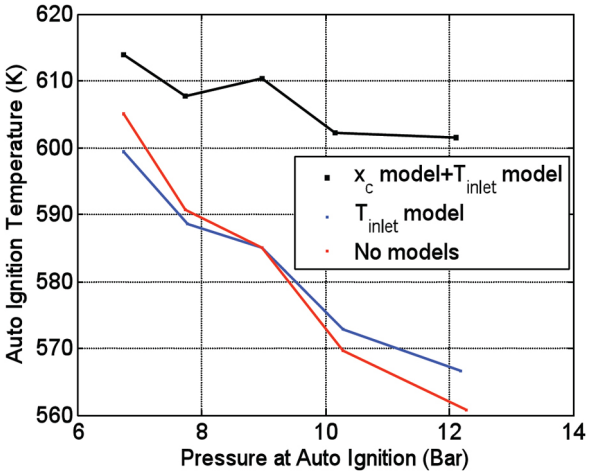

Figure 42. Sensitivity analysis, cylinder temperature and pressure at auto ignition with and without temperature models for PRF 60 (0.2 J/CAD).

REPEATABILITY

To ensure that the results were stable three independent runs were made with PRF 90 at each intake temperature. The results from the heat release analysis for all three cases are shown in Figure 43. A slight variation in CA 50 is seen, however the total heat release are the same for the different repetitions.

The auto ignition temperatures and pressures were calculated and are shown in Figure 44 (For definition see section on Start of Combustion). The 5 different clusters of points represent different intake temperatures (3 repetitions per intake temperature). The variations in auto ignition temperature for the repetition runs are small at the higher inlet air temperatures and higher at the lower inlet air temperatures. Figure 45 shows corresponding auto ignition temperatures and pressures in the rate of heat release and Figure 46 shows the cylinder pressure curves.

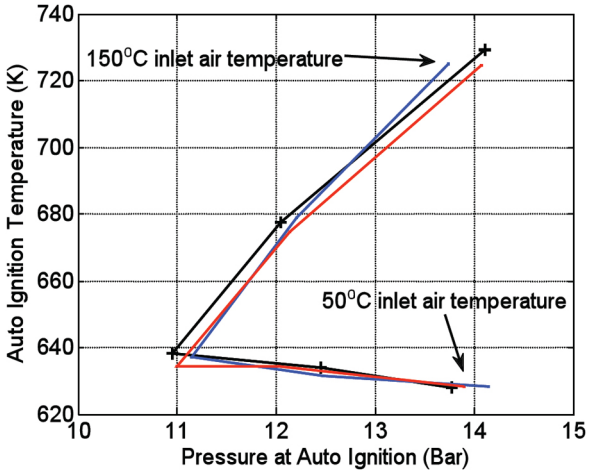

Figure 44. Cylinder temperature and pressure at auto ignition for the three PRF 90 sweeps (0.2 J/CAD).

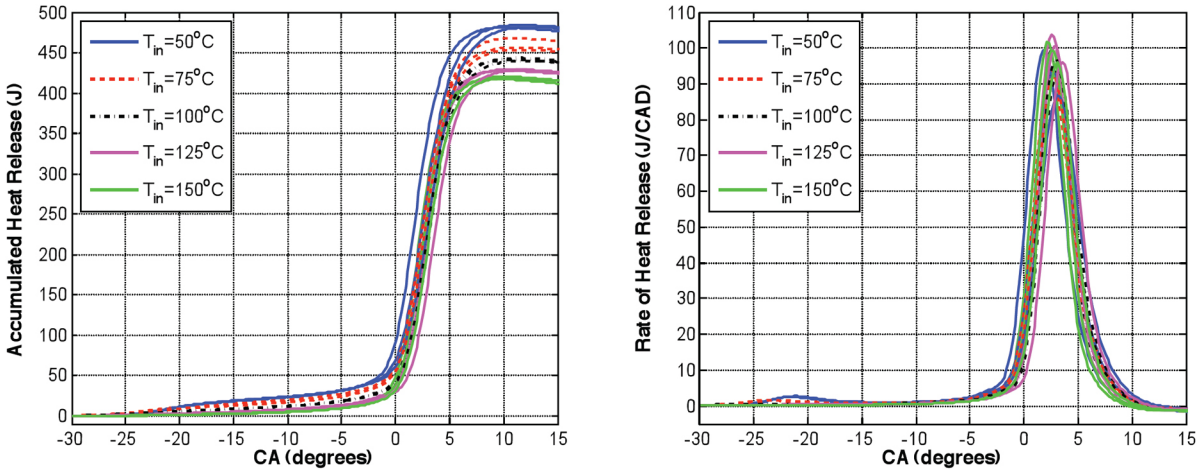

Figure 43. Accumulated heat released and rate of heat release for PRF 90, three different runs.

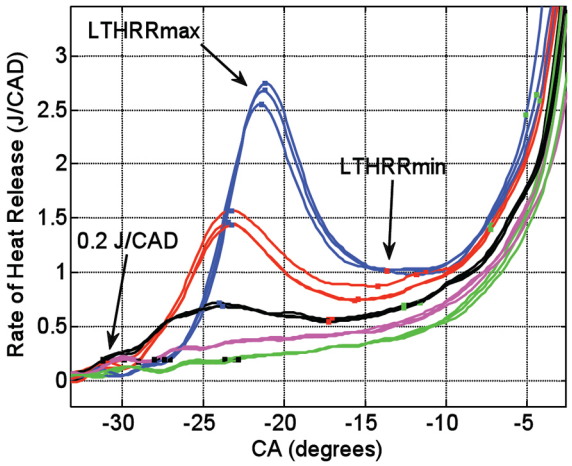

Figure 45. LTHR and Auto Ignition of PRF 90 for the three repetition runs.

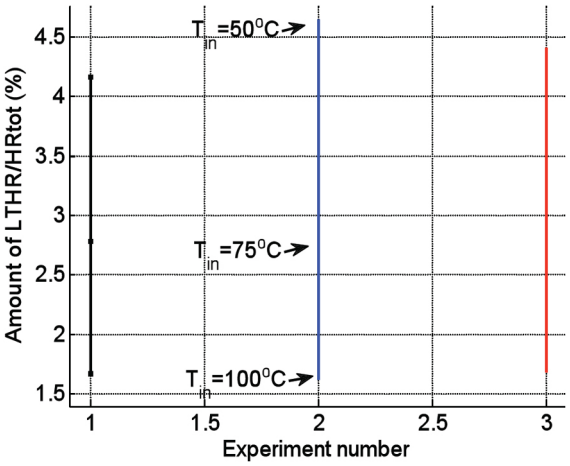

Figure 47. Amount of LTHR for the different runs of PRF 90.

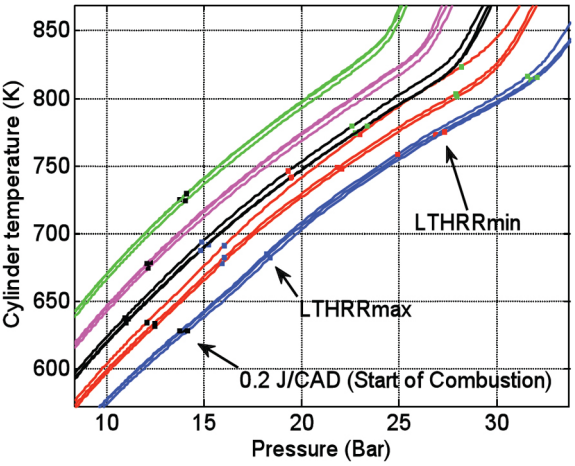

Figure 46. Auto ignition temperatures and pressures for PRF 90, three repetition runs.

Figure 47 shows the LTHR quantification for different repetition runs of PRF 90. The 3 points for each run represent 3 different intake temperatures. This demonstrates the accuracy of the LTHR quantifications.

The error analysis gives a standard variation of ±4° and ±0.4 Bar on the auto ignition temperatures and pressures. The conclusion is that the method for defining Start of Combustion is sufficient.

DISCUSSION

The main goal of the study was to develop a method to accurately determine auto ignition temperatures at different pressures for different fuels. The experiments were carried out in a modified CFR engine using Primary Reference Fuels.

A simple model for estimating the temperature at IVC was used. The effect of this on the results was evaluated. The temperature was found to change from about −5 to +30 degrees from the temperature probe to IVC. The model has to be further developed and validated for higher accuracy. The experiments were run with a combustion timing of 3±1° after TDC. The combustion phasing was found to have little or no effect on the auto ignition temperature, depending on the method of analysis. It was concluded that the combustion timing therefore could be held constant.

Different methods for defining start of combustion were discussed. In the literature a quite late start of combustion definition of 1% to 20% heat released is commonly used, but since this project focused on finding the absolute temperatures when the reaction starts, lower limits where considered. A definition of heat release rate of 0.2 J/CAD was compared to 1 % burnt. These two methods gave similar but not the same results. It is recommended that both definitions be used to more accurately describe the auto ignition event.

After determining start of combustion the amount of LTHR was calculated. The definition of LTHR used was when the amount of LTHR was more than 1%, and when there was a LTR peak before the main combustion. For some cases this is a simplification, since what appears to be LTHR can be observed, but this transcends into HTHR without a negative temperature coefficient in between. The amount of LTHR was found to be proportionate to the amount of n-heptane in the PRFs. This agrees with previous studies on PRFs.

The amount of LTHR was found to decrease with increased inlet air temperature. At a certain temperature the LTHR disappears. For example the intake temperature of 150°C suppresses LTHR for PRF 85 - PRF 100. The start of combustion advances when the inlet air temperature is increased, until the LTHR disappears. Another interpretation is that the delay from maximum rate of heat release for the LTR to the HTR increases with higher inlet air temperature, maybe because less heat is released during the LTHR. After the LTHR disappears due to the increase in intake temperature, the start of combustion is retarded with an increase in inlet air temperature. This could be explained by the lower compression ratio used at higher inlet air temperatures.

The experimental method and method of determining auto ignition temperature and auto ignition pressure was found accurate when repetitions of the experiments were made.

CONCLUSIONS

1. It was possible to determine the auto ignition temperature of different fuels using the method presented in a modified CFR engine.

2. A linear correlation between octane rating and amount of LTHR was obtained.

3. The amount of LTHR decreased with higher inlet air temperature for all PRFs.

4. A larger change in compression ratio was needed to keep CA50 constant for the PRFs with no or little LTHR (PRF 95 and PRF 100), than for the fuels with a lower octane rating.

5. The auto ignition temperatures for the PRF 0-60 were found to be almost independent of cylinder pressure. These fuels ignited at temperatures between 570 and 610 K.

6. PRF 95 and PRF 100 display a wide range of auto ignition temperatures, 620 K - 800K, depending on the temperature at inlet valve closing.

7. PRF 80-90 show an intermediate behavior with LTHR at the lower inlet air temperatures but not at the higher inlet air temperatures. The auto ignition temperatures of these fuels quickly rise when the LTHR disappears. These fuels ignite at 620 K to 730 K.

8. Main heat release was determined to start at temperatures above 730 K.

9. For the fuels with extensive LTHR (PRF 0 to PRF 80) ignition was advanced when the inlet air temperature was increased.

10. For PRF 95 and PRF 100 ignition was retarded when the inlet air temperature was increased.

ACKNOWLEDGEMENTS

The authors gratefully acknowledge Chevron for their financial support. Patrick Borgqvist is gratefully acknowledged for designing the engine control system.

REFERENCES

1. Kalghatgi, G., "Auto-Ignition Quality of Practical Fuels and Implications for Fuel Requirements of Future SI and HCCI Engines," SAE Technical Paper 2005-01-0239, 2005, doi:10.4271/2005-01-0239.
2. Shibata, G. and Urushihara, T., "Auto-Ignition Characteristics of Hydrocarbons and Development of HCCI Fuel Index," SAE Technical Paper 2007-01-0220, 2007, doi:10.4271/2007-01-0220.
3. Shibata, G., Oyama, K., Urushihara, T., and Nakano, T., "Correlation of Low Temperature Heat Release With Fuel Composition and HCCI Engine Combustion," SAE Technical Paper 2005-01-0138, 2005, doi: 10.4271/2005-01-0138.
4. Hosseini, V., Neill, W., and Chippior, W., "Influence of Engine Speed on HCCI Combustion Characteristics using Dual-Stage Autoignition Fuels," SAE Technical Paper 2009-01-1107, 2009, doi: 10.4271/2009-01-1107.
5. Sjöberg, M. and Dec, J., "EGR and Intake Boost for Managing HCCI Low-Temperature Heat Release over Wide Ranges of Engine Speed," SAE Technical Paper 2007-01-0051, 2007, doi:10.4271/2007-01-0051.
6. Tanaka, S., Ayala, F., Keck, J.C, Heywood, J.B., "Two-stage ignition in HCCI combustion and HCCI control by fuels and additives", Combustion and Flame, 132 (2003) 219-239
7. Machrafi, H., Cavadiasa, S., "An experimental and numerical analysis of the influence of the inlet temperature, equivalence ratio and compression ratio on the HCCI auto-ignition process of Primary Reference Fuels in an engine", Fuel Processing Technology, 89 (2008) 1218-1226
8. Christenssen, M., "HCCI Combustion - Engine Operation and Emission Characteristics", Doctoral Thesis, 2002
9. Silke, E., Pitz, W., Westbrook, C., Sjöberg, M. et al., "Understanding the Chemical Effects of Increased Boost Pressure under HCCI Conditions," *SAE Int. J. Fuels Lubr.* 1(1):12-25, 2009, doi: 10.4271/2008-01-0019.
10. Mehl, M., Faravelli, T., Ranzi, E., Miller, D., Cernansky, N., "Experimental and kinetic modeling study of the effect of fuel composition in HCCI engines", Proceedings of the Combustion Institute, 32 (2009) 2843-2850
11. Heywood, J. B., 1988, "Internal Combustion Engine Fundamentals", McGraw Hill, New York, 1989
12. Warnatz, J., Maas, U., Dibble, R.W., "Combustion - Physical and Chemical Fundamentals, Modeling and Simulation, Experiments, Pollutant Formation", Springer, Berlin, 2006

CONTACT

For further information please contact Ida Truedsson, ida.truedsson@energy.lth.se

DEFINITIONS AND ABBREVIATIONS

AIP
Auto Ignition Pressure
AIT
Auto Ignition Temperature
ATDC
After Top Dead Center
BTDC
Before Top Dead Center
CA 50
Crank Angle for 50 % of total Heat Release
CAD
Crank Angle Degree
CFR
Cooperative Fuel Research
EGR
Exhaust Gas Recirculation
HTR
High Temperature Reactions
HTHR
High Temperature Heat Release
IAT
Inlet Air Temperature
IVC
Inlet Valve Closes
LTR
Low Temperature Reactions
LTHR
Low Temperature Heat Release

LTHRRmax
Maximum Low Temperature Heat Release Rate
LTHRRmin
Minimum Rate of Heat Release beween LTHR and HTHR
MON
Motor Octane Number
PRF
Primary Reference Fuel
RON
Research Octane Number
SOC
Start of Combustion
TDC
Top Dead Center

Paper II

Pressure Sensitivity of HCCI Auto-Ignition Temperature for Oxygenated Reference Fuels

Ida Truedsson

Martin Tuner

Bengt Johansson

Lund University,
223 63 Lund, Sweden

William Cannella
Chevron,
Richmond, CA 94802

The current research focuses on creating a homogeneous charge compression ignition (HCCI) fuel index suitable for comparing different fuels for HCCI operation. One way to characterize a fuel is to use the auto-ignition temperature (AIT). The AIT can be extracted from the pressure trace. Another potentially interesting parameter is the amount of low temperature heat release (LTHR) that is closely connected to the ignition properties of the fuel. The purpose of this study was to map the AIT and the amount of LTHR of different oxygenated reference fuels in HCCI combustion at different cylinder pressures. Blends of n-heptane, iso-octane, and ethanol were tested in a cooperative fuels research (CFR) engine with a variable compression ratio. Five different inlet air temperatures ranging from 50 °C to 150 °C were used to achieve different cylinder pressures and the compression ratio was changed accordingly to keep a constant combustion phasing, CA50, of 3 ± 1 deg after top dead center (TDC). The experiments were carried out in lean operation with a constant equivalence ratio of 0.33 and with a constant engine speed of 600 rpm. The amount of ethanol needed to suppress the LTHR from different primary reference fuels (PRFs) was evaluated. The AIT and the amount of LTHR for different combinations of n-heptane, iso-octane, and ethanol were charted. [DOI: 10.1115/1.4023614]

Keywords: HCCI, auto-ignition temperature, LTHR, reference fuels

Introduction

The HCCI combustion mode is used to reduce emissions to the level of traditional spark ignition engines with three-way catalyst, combined with maintaining efficiency as high as for diesel combustion. The main challenge for the HCCI is to control the ignition timing and combustion rate, since they are not controlled by a spark (spark ignition (SI) combustion) or by fuel injection (compression ignition (CI) combustion) but rather are controlled by chemical kinetics.

An index to relate fuel properties to auto-ignition properties would be useful. The indices for SI engines, the research octane number (RON) and motor octane number (MON), are known to be insufficient to explain the fuel behavior in an HCCI engine [1]. Several researchers have worked with the development of an HCCI index [2–6]. One such index is the octane index (OI), which is of the form $OI = (1-K)RON + KMON$ where K depends on the pressure and temperature evolution in the unburnt gas. However, there are indications that the OI is not applicable for oxygenated fuels [1], which is why a new fuel index is needed to predict the performance of any fuel in an HCCI engine. More knowledge of the combustion process is needed to create a useful HCCI fuel index, which is why a standardized method for determining the HCCI fuel performance was desired. The idea is that the fuel auto-ignition temperature can be related to the fuel performance in an HCCI engine.

The combustion of fuel that contains a significant amount of *n*-paraffins, such as n-heptane, exhibits a characteristic bump in the rate of the heat release trace before the main heat release. This is called the low temperature reaction (LTR) or the low temperature heat release (LTHR), referring to the exothermic prereactions that occur before the main combustion event. Low temperature reactions are usually more prominent at lower temperatures but diminish as the intake air temperature increases. The reason for this is that the precursors for this chain branching (the LTR) are decomposed back to the reactants at higher temperatures [7]. The amount of LTHR also decreases with a higher engine speed because there is less time for reactions [8]. Exhaust gas recirculation (EGR) can advance the start of LTRs, probably because they contain reactive species such as H_2O_2 [9,10]. A higher cylinder pressure induced by super- or turbocharging is also known to increase the amount of LTHR [11]. This indicates that a higher compression ratio would also increase the amount of LTHR. Andrae and Head [12] shows that the fuels without a LTHR, e.g., ethanol, act as a radical scavenger and, therefore, decreases the LTHR for fuels such as *n*-heptane. When the LTHR is present the auto-ignition temperature is substantially lower [13].

Lü et al. [14] studied the effect of different inhibitors, including ethanol. One observation from kinetic modeling of an *n*-heptane and ethanol mixture was that only the *n*-heptane part of the fuel was consumed in the LTR and that the *n*-heptane was the first to be consumed by the main heat release.

A thorough summary of hydrocarbon fuel models and how two-stage combustion is affected by different parameters is presented by Floweday [15]. They describe the pressure sensitivity and comment that it is a complex behavior where the pressure affects the auto-ignition in different temperature regions in different ways.

Studies performed at a Brazilian refinery [16] concluded that gasoline contains more than 400 components, with only 20–25 components greater than 1% by mass. Because of the complexity of gasoline, surrogate fuels are often studied in order to understand the effects from the different components.

Pitz et al. [17] reviews the development of surrogate fuels, particularly for HCCI combustion, and concludes that the three necessary components of any gasoline fuel surrogate are *n*-heptane, iso-octane, and toluene. Toluene is the most common aromatic in gasoline. They rated different gasoline surrogate fuel components and placed ethanol, 1-pentene, di-isobutylene, and xylene at the second importance level.

Machado et al. [16] compared different gasoline surrogate fuels in an SI engine to find a suitable fuel to describe high ethanol (20 vol. %) gasoline. They concluded that mixtures of *n*-heptane, iso-octane, toluene, and ethanol could be used as surrogate fuels for oxygenated gasoline.

Manuscript received November 23, 2012; final manuscript received January 8, 2013; published online June 10, 2013. Editor: David Wisler.

Table 1 Specifications for the CFR engine

Displacement volume	612 cm^3
Number of cylinders	1
Bore	83 mm
Stroke	114 mm
CR	Variable (4:1 to 18:1)
Number of valves	2
Length of connecting rod	254 mm
Intake valve opens	10 deg ATDC ± 2.5 deg
Intake valve closes	146 deg BTDC ± 2.5 deg
Exhaust valve opens	140 deg ATDC ± 2.5 deg
Exhaust valve closes	15 deg ATDC ± 2.5 deg
Valve lifts	6.25 mm
Valve diameters	9.53 mm
Engine speed	600 rpm
Fuel supply	Port injection

Currently, ethanol is usually added to gasoline as a renewable fuel. Regular U.S. and Swedish gasoline both contain up to 10 vol. % ethanol and this amount is expected to increase in the future.

The main objective of this study was to determine the effect of ethanol addition on the auto-ignition temperatures and the amount of low temperature heat release at different cylinder pressures. The authors plan to continue with fuel blends of *n*-heptane, iso-octane, ethanol, and toluene in the future. These studies are in preparation for further experiments with real gasoline, providing insight into the combustion process so that the more complex behavior of real gasoline can be explained.

Experimental

A Waukesha variable compression ratio cooperative fuels research (CFR) engine was used for the experiments. The setup included an air-fuel mixture heater and a fuel injection system for port injection. A scale was used for measuring the fuel flow. The heat release was calculated from the pressure trace measured with a Kistler piezoelectric pressure transducer mounted in the cylinder. An intake air conditioner was included in the setup in order to ensure constant air humidity throughout the experiments. The engine specifications are listed in Table 1. The spark ignition was switched off.

Fuels

The test fuels were blends of *n*-heptane, iso-octane, and ethanol, according to Table 2. Fuels designated as HxEy contain *x*% *n*-heptane, *y*% ethanol, and (100-*x*-*y*)% iso-octane.

Table 2 Fuel matrix, vol. %

n-heptane	Iso-octane	Ethanol	Name
20	80	0	PRF 80
20	79	1	H20E1
20	75	5	H20E5
20	70	10	H20E10
20	60	20	H20E20
30	70	0	PRF 70
30	69	1	H30E1
30	65	5	H30E5
30	60	10	H30E10
30	50	20	H30E20
60	0	40	H60E40
55	0	45	H55E45
50	0	50	H50E50
45	0	55	H45E55
40	0	60	H40E60

Method

A fuel matrix consisting of 15 different oxygenated reference fuels was run. All fuels were analyzed with a change in the inlet air temperature (IAT) in five steps from 50 °C to 150 °C. At each temperature, a combustion phasing with CA50 at 3 ± 1 deg after TDC was held by changing the compression ratio. Motored pressure traces were extracted for all data points for validation. The engine was run naturally aspirated at 1 bar inlet air pressure. The fuel amount was adjusted for each case in order to achieve an equivalence ratio of 0.33. All experiments were run at 600 rpm. No EGR was used.

Heat Release Calculation. The Woschni heat transfer model was used and the motored heat release was subtracted from the fired heat release in order to reduce measurement and model errors. The assumptions are that the temperature when the inlet valve closes is known. This temperature is calculated from the measured temperature in the intake by applying a simple model. All figures are based on the average of 300 cycles. The heat release calculations are described in more detail in Ref. [13].

Results and Discussion

The different resistances to auto-ignition of the fuels result in different minimum compression ratios required for auto-ignition; see Fig. 1. A temperature model according to Ref. [13], accounting for heating from mixing with hot residuals and from pipes in the intake, was used to calculate T_{IVC} (shown in Fig. 1) from the inlet air temperature.

Start of Combustion. The start of combustion (SOC), which is the point of auto-ignition, was defined as when the reaction rate had reached a threshold value. This value was chosen to be 0.2 J/CAD, corresponding to a rate of heat release when early combustion can be seen [13]. This definition is preferred since it indicates the onset of the chemical reactions. A more commonly used definition of 1% burnt CA1 is also presented for comparison.

Low Temperature Heat Release and Auto-Ignition Temperatures. Here, the low temperature heat release is defined as when there is a peak before the main combustion event; see Figs. 2 and 3. The end of the LTHR is chosen as the point of the minimum value of the rate of heat release between the two peaks. The PRF70 fuel exhibited the highest amount of LTHR; see

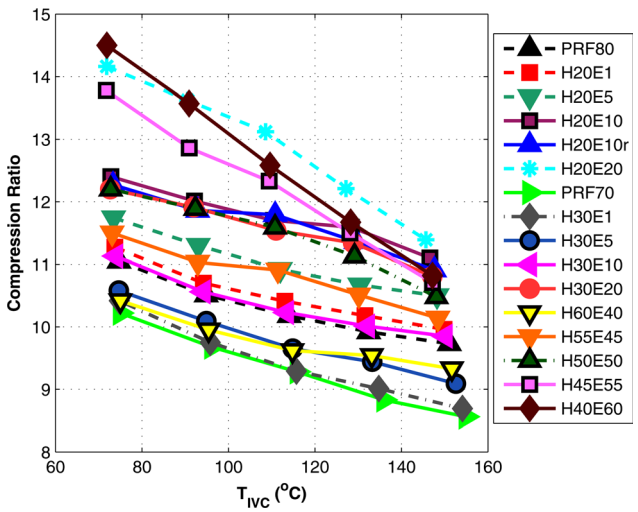

Fig. 1 Temperature at the IVC and corresponding compression ratios

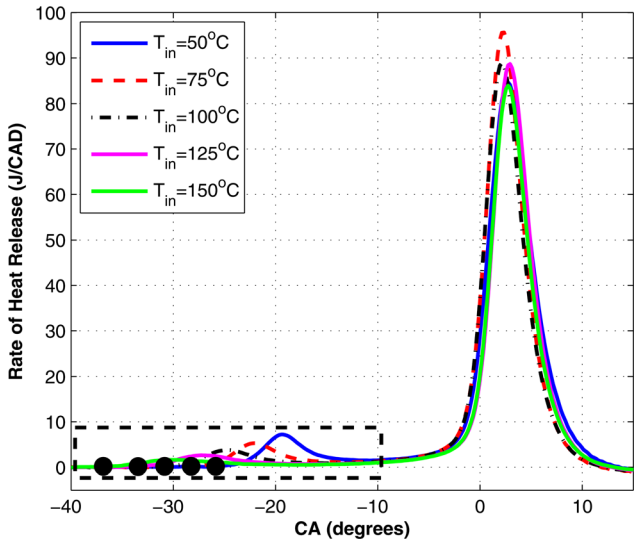

Fig. 2 Rate of heat release with the start of combustion for PRF70. The black box marks the magnified area for Fig. 3.

Figs. 2 and 3. The LTHR curves for this fuel include the points of the SOC. As expected, as the intake temperature increased, the amount of LTHR decreased.

The auto-ignition temperature is extracted from the start of combustion previously described. Corresponding auto-ignition temperatures for PRF 70 are shown by the black circles in Figs. 3 and 4. The blue squares mark the maximum rate of heat release for the LTHR and the red triangles mark the minimum rate of heat release between the LTHR and the main combustion. The auto-ignition temperatures for all of the fuels are presented in figures in Appendix A.

In contrast to PRF70, fuel H40E60 exhibited no LTHR, as shown in Fig. 5. For this fuel, the ignition occurs at a higher temperature resulting from the higher inlet air temperature and lower compression ratio; see Fig. 6. Note that ignition occurs at similar in-cylinder pressures. The low temperature heat release and auto-ignition plots for the other fuels are presented in Appendix A.

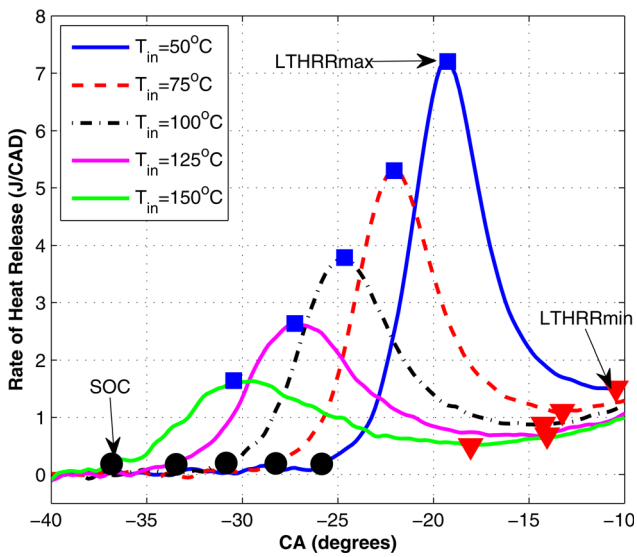

Fig. 3 The LTHR for PRF70. The black dots indicate the start of combustion as 0.2 J/CAD.

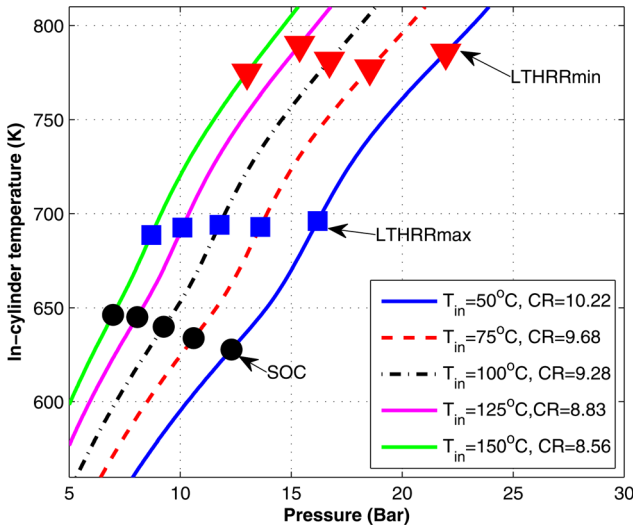

Fig. 4 Temperatures and pressures at auto-ignition for PRF 70

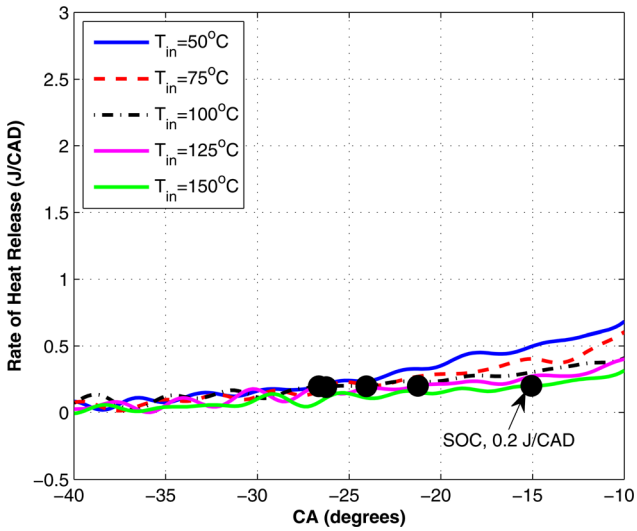

Fig. 5 The LTHR for H40E60 The five lines represent the different intake air temperatures. The black dots indicate the start of combustion as 0.2 J/CAD.

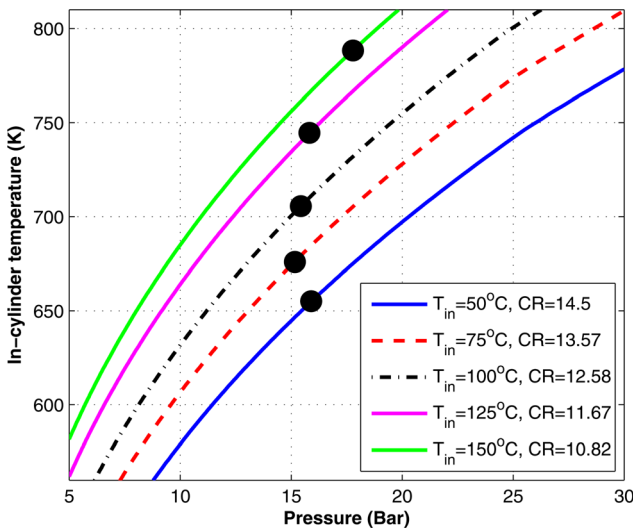

Fig. 6 Temperatures and pressures at auto-ignition for H40E60

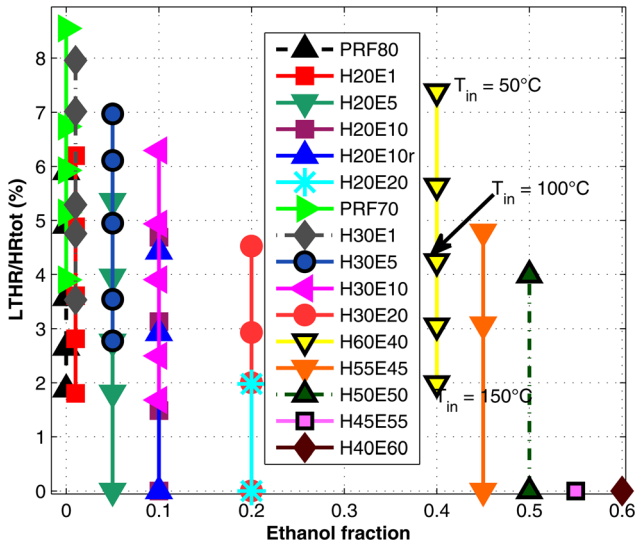

Fig. 7 Amount of the LTHR as a function of ethanol fraction. The marks for each fuel represent the different IATs, with 50 °C at the top and 150 °C at the bottom. Zero means no LTHR at one or more temperatures.

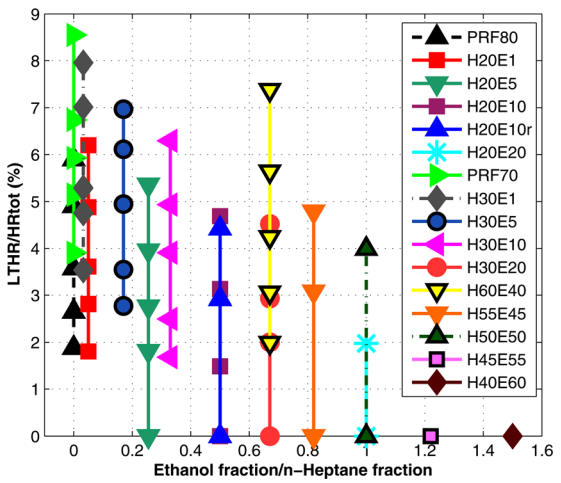

Fig. 8 The LTHR as a function of ethanol/*n*-heptane proportions. The marks for each fuel represent the different IATs, with 50 °C at the top and 150 °C at the bottom. Zero means no LTHR at one or more temperatures.

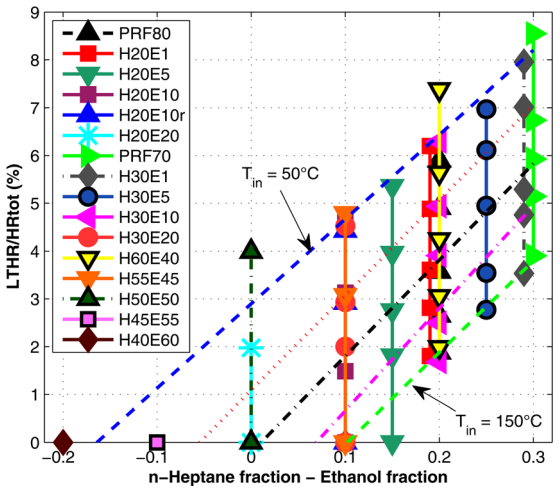

Fig. 9 The LTHR as a function of the difference between the amounts of *n*-heptane and ethanol

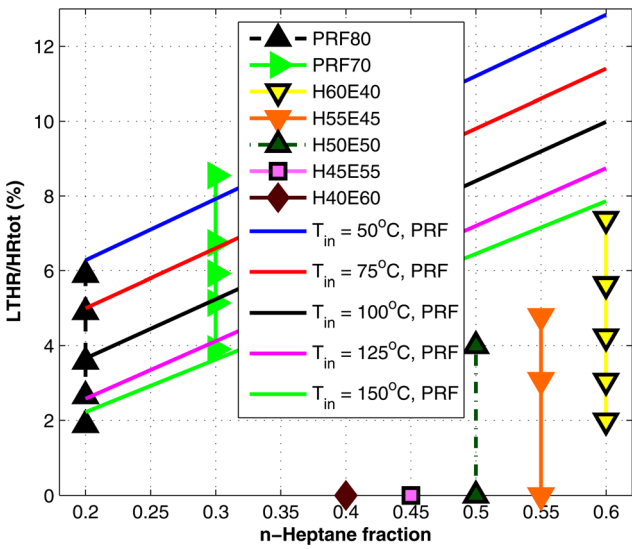

Fig. 10 When the iso-octane is replaced with ethanol the amount of LTHR is reduced

LTHR Quantification. Low inlet air temperatures lead to higher amounts of LTHR. Since high pressure is known to induce LTHR [10], one reason for this could be the higher compression ratio required to keep a constant combustion phasing. The amount of ethanol also affected the amount of LTHR. The ethanol acted as an inhibitor so that less LTHR was obtained as the ethanol concentration increased and the *n*-heptane concentration decreased. This is demonstrated in Figs. 7–9. At higher ethanol concentrations, the LTHR disappears at higher intake temperatures. For fuel H20E20, the LTHR is only observed for an intake temperature of 50 °C and is not observed at any intake temperature for fuel H40E60 or fuel H45E55.

Looking at Fig. 7 for the fuels containing iso-octane and a fixed amount of *n*-heptane (20 or 30%) the amount of LTHR decreases as the percentage of ethanol increases. However, it seems as if the amount of LTHR is not only determined by the amount of ethanol, since the two-component fuels that do not contain iso-octane (those having an ethanol content of 40% or higher) do not line up with the other fuels. Those fuels, especially H60E40, also do not line up with the others when plotted with the ratio of ethanol to *n*-heptane, as shown in Fig. 8.

A more linear behavior is seen when the percentage of the LTHR is plotted versus the difference between the fractions of *n*-heptane and ethanol, as seen in Fig. 9. The points corresponding to the same inlet air temperatures appear to fall on the same line, with a different line for each inlet air temperature. It seems that this difference describes the amount of the LTHR within the measurement errors. For fuels having equal amounts of ethanol and *n*-heptane, the LTHR is completely quenched at the inlet air temperature of 75 °C. More than 10%-units more *n*-heptane than ethanol is needed to keep the LTHR at the highest inlet air temperatures of 150 °C.

Figure 10 compares the effects of ethanol and iso-octane on the LTHR. The lines show the amount of LTHR obtained for PRFs from a previous study [13]. When the iso-octane is replaced with ethanol (e.g., when PRF 40 is compared to H60E40), the LTHR is reduced. The higher amount of LTHR for the PRF lines than the points for the ethanol fuels shows that ethanol is a stronger LTHR inhibitor than iso-octane.

Auto-Ignition Temperatures. Almost all of the fuels studied show the LTHR at some intake air temperature. As shown in

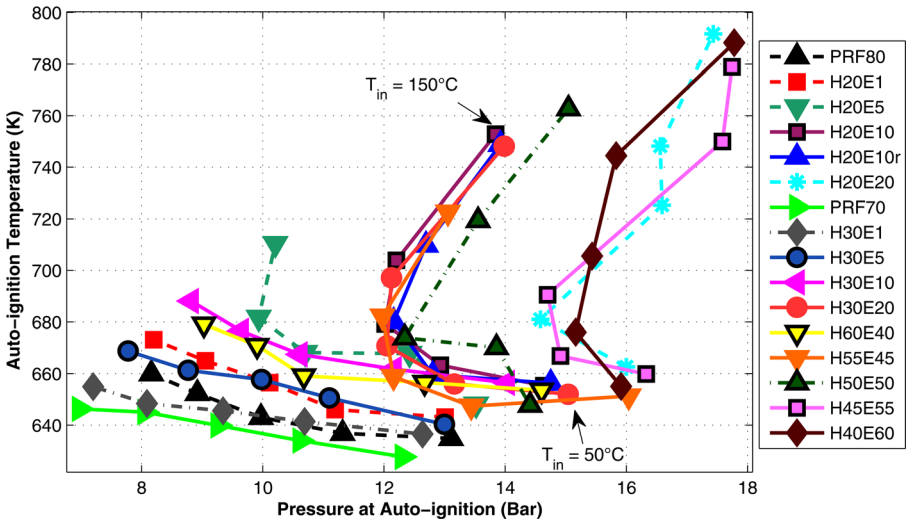

Fig. 11 Temperature and pressure at auto-ignition; 0.2 J/CAD. The five marks for each fuel correspond to the five different inlet air temperatures.

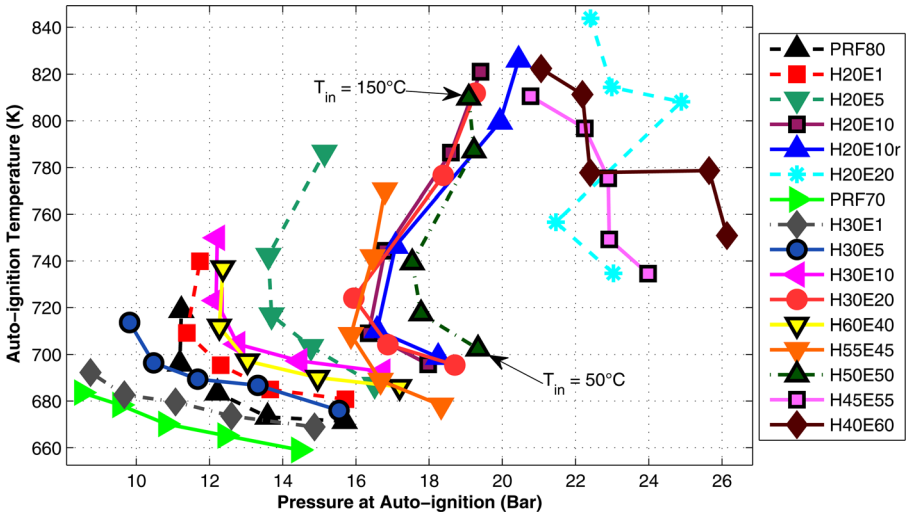

Fig. 12 Temperature and pressure at auto-ignition; 1% burnt. The five marks for each fuel correspond to the five different inlet air temperatures.

Fig. 11, for those fuels and conditions where the LTHR existed, auto-ignition temperatures were in a narrow range of around 650 ± 20 K. For a constant amount of *n*-heptane, the AIT increased with the increased ethanol content.

There is a wide range in auto-ignition temperatures for the fuels where the LTHR disappears at the higher inlet air temperatures. For the fuels with 20% *n*-heptane, at the highest inlet air temperature, the AIT increases from 635 K to almost 800 K. This increase is due to the complete quenching of the LTR by the ethanol addition. At the lowest inlet air temperature, the AIT rises from 635 K to 660 K.

Looking at 1% burnt CA1 in Fig. 12, the same trends are seen. The AIT is higher for this definition since it requires a larger heat release to detect the SOC.

Start of Combustion Crank Angle Degree (CAD). There are two different phenomena affecting the crank angle position at the SOC. At first, as the inlet air temperature is increased the LTHR starts earlier due to the higher temperature in the cylinder, as shown earlier for PRF 70 in Fig. 3. Note that the SOC appears at almost the same temperature for all inlet air temperatures for PRF 70; see Fig. 11. Second, for fuels where the LTHR disappears as the inlet air temperature is increased, the SOC is again retarded, as seen earlier for H40E60 in Fig. 5.

It was observed that the CAD at the start of combustion was fairly constant at the lowest inlet air temperatures when the LTHR is seen for all fuels; see Fig. 13. An analysis on how the varying start of combustion affects the results are shown in the section titled "Error Analysis."

RON Correlation. The octane number (ON) of the fuel blends was calculated from the pure components according to $x*0 + y*108.6 + (1 - x - y)*100 = \text{ON}$ where x, y, and z refer to the vol. % and the multipliers (0, 108.6, and 100) refer to the RON's of *n*-heptane, ethanol, and iso-octane, respectively. It seems that ethanol has a greater effect on the amount of LTHR than is expected by the octane rating of 108.6 [18]. In Fig. 14, at similar values of the ON (i.e., 70 or 80), the fuels having the greater amounts of ethanol have the lower amounts of LTHR. The auto-ignition temperature shows no correlation with this calculated ON; see Fig. 15.

However, by increasing the apparent ON of ethanol from 107 to 190, a better correlation is seen between the calculated ON and

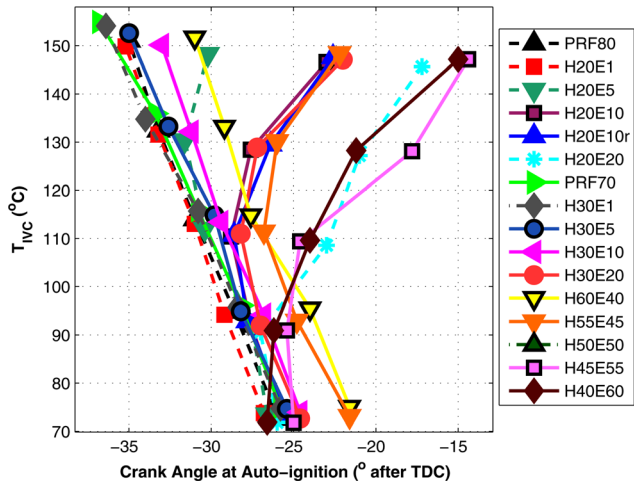

Fig. 13 Crank angle at the start of combustion

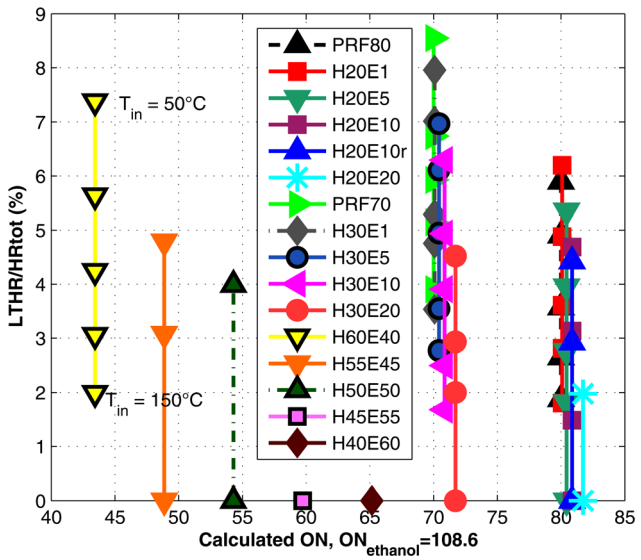

Fig. 14 Amount of the LTHR as a function of the calculated ON; $ON_0 = 108.6$

both the amount of LTHR and the auto-ignition temperature; see Figs. 16 and 17. This implies that the quenching effect of ethanol is greater in the HCCI conditions than the RON indicates. An increased apparent ON for ethanol in other combustion modes than SI has been suggested before by, for example, Ref. [19], however, this has been questioned by Yates [18].

Error Analysis

Repeatability. A repetition run of fuel H20E10 was made to ensure stable results. The results are shown in Figs. 18 and 19. Only minor variations were detected even though it was 11 days between the two experiments.

To assure that the CAD at the SOC did not affect the auto-ignition temperature, an experiment with a constant SOC was also performed. By varying the compression ratio (CR), the SOC was held constant at 30 deg before TDC. As a result, the CA50 varied from about −10 deg to 4 deg after TDC. Because of the experimental difficulties in detecting the SOC when running the experiments, the actual SOC varied within ±1.5 deg; see Fig. 20. At the lowest and highest temperatures (50 and 150 °C) the CR was increased to obtain an earlier SOC. It seems that the auto-ignition temperature and pressure are fairly similar, as shown in Fig. 21, and varies slightly more than the standard deviation that was reported in Ref. [13] with ±4 deg and ±0.4 bar.

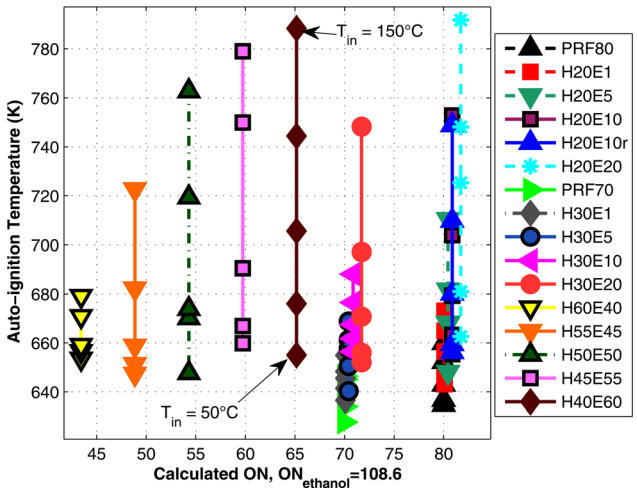

Fig. 15 Auto-ignition temperature as a function of the calculated ON; $ON_{ethanol} = 108.6$

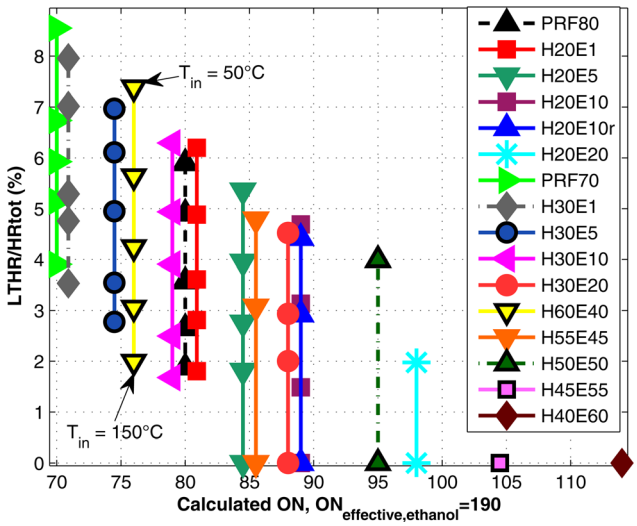

Fig. 16 Amount of the LTHR as a function of the calculated ON; $ON_{ethanol} = 190$

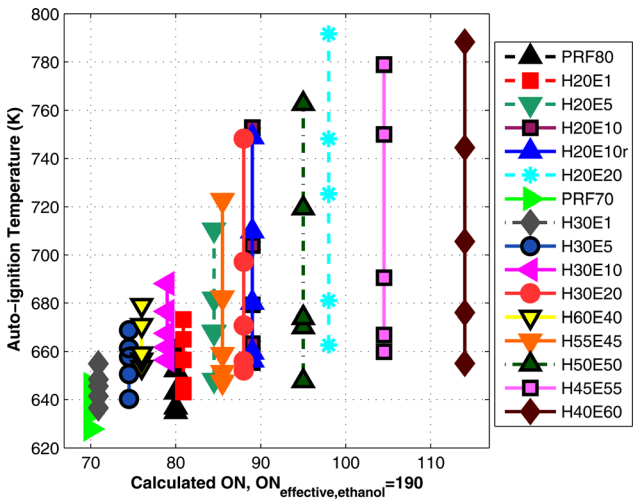

Fig. 17 Auto-ignition temperature as a function of the calculated ON; $ON_{ethanol} = 190$

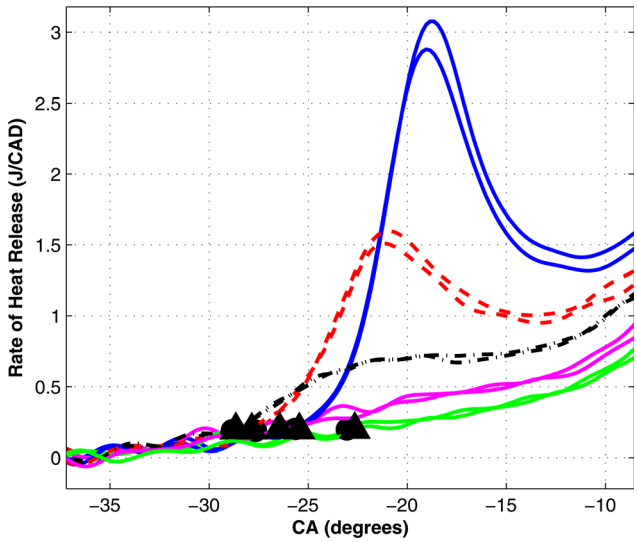

Fig. 18 The LTHR for H20E10 run and repetition

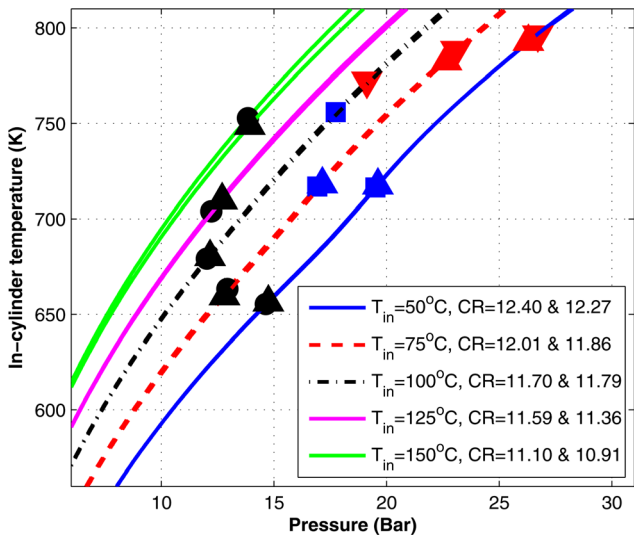

Fig. 19 Temperatures and pressures at auto-ignition for H20E10 and repetition

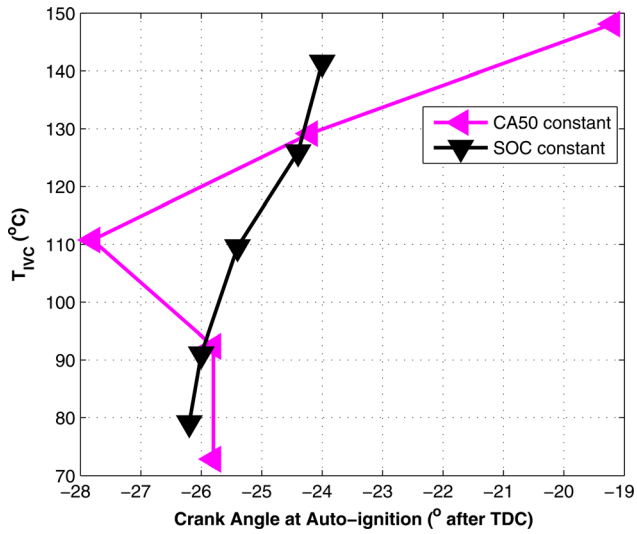

Fig. 20 The CAD at the SOC for the experiment with the constant SOC compared to the original experiment with the constant CA50

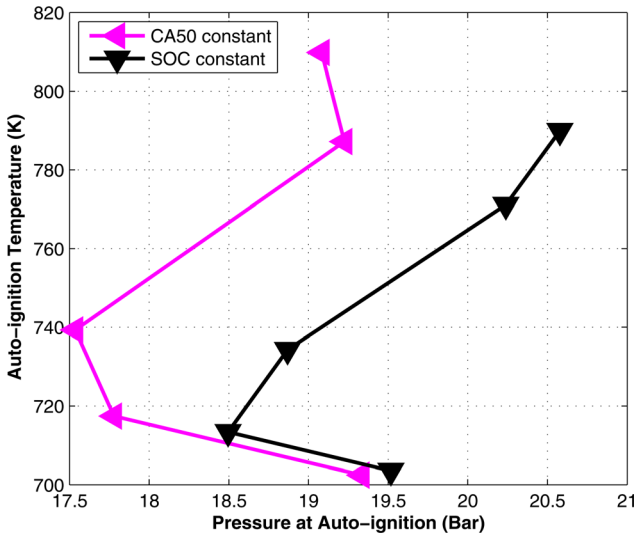

Fig. 21 Temperatures and pressures at auto-ignition (using the 0.2 J/CAD definition)

Summary and Conclusions

The main goal to map the auto-ignition temperatures of reference fuels containing different amounts of ethanol was fulfilled.

When adding ethanol to a fuel with a constant amount of *n*-heptane, the auto-ignition temperature increased and the amount of LTHR decreased.

The amount of LTHR was not linearly decreasing with increased ethanol content but rather a function of the difference between the fractions of *n*-heptane (inducing LTHR) and ethanol (inhibiting LTHR). There seemed to be an effect of the iso-octane on the amount of LTHR and on the auto-ignition temperature, however, this effect was weak compared to the effects from *n*-heptane and ethanol.

By comparing with the RON for pure ethanol, ethanol seems to have a more pronounced quenching effect on the LTR in the HCCI combustion with a much higher apparent ON.

1. Ethanol works as a low temperature heat release inhibitor even at low concentrations. It is a much stronger inhibitor than iso-octane.
2. When enough ethanol is added to quench the LTHR the auto-ignition temperature quickly rises.
3. When adding ethanol to a mixture of iso-octane and a constant amount of *n*-heptane, the amount of LTHR decreased as the amount of ethanol increased.
4. The amount of LTHR could be estimated by comparing the amounts of *n*-heptane and ethanol. This was shown to be approximately linear.
5. More ethanol was needed to quench the LTHR at lower inlet air temperatures.
6. The quenching effect of ethanol on the LTHR is stronger for the HCCI than is expected from the RON.

Acknowledgment

The authors gratefully acknowledge Chevron for their financial support. Patrick Borgqvist is gratefully acknowledged for designing the engine control system.

Nomenclature

AIP = auto-ignition pressure
AIT = auto-ignition temperature
ATDC = after top dead center
BTDC = before top dead center

CA50 = crank angle for 50% of the total HR
CAD = crank angle degree
CFR = cooperative fuels research
EGR = exhaust gas recirculation
HTR = high temperature reactions
HTHR = high temperature heat release
IAT = inlet air temperature
IVC = inlet valve closing
LTR = low temperature reactions
LTHR = low temperature heat release
$LTHRR_{max}$ = maximum low temperature HRR
$LTHRR_{min}$ = minimum rate of HR between LTHR and HTHR
MON = motor octane number
ON = octane number
PRF = primary reference fuel
RON = research octane number
SOC = start of combustion
TDC = top dead center

Appendix A

Low Temperature Heat Release. The low temperature heat release plots are shown in Figs. 22–36.

Auto-Ignition Temperatures. The auto-ignition temperature plots are shown in Figs. 37–51.

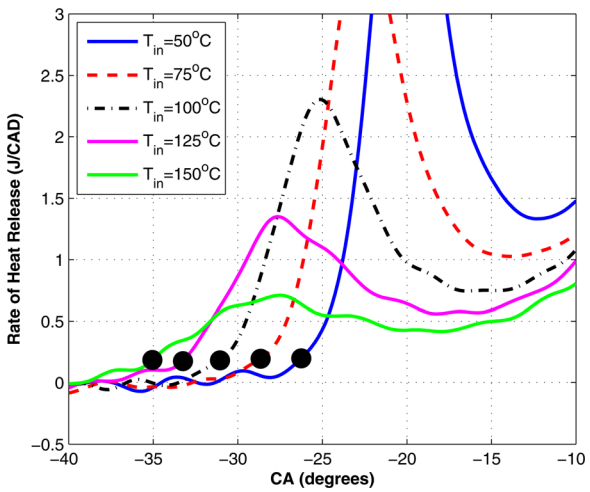

Fig. 22 The LTHR for PRF 80

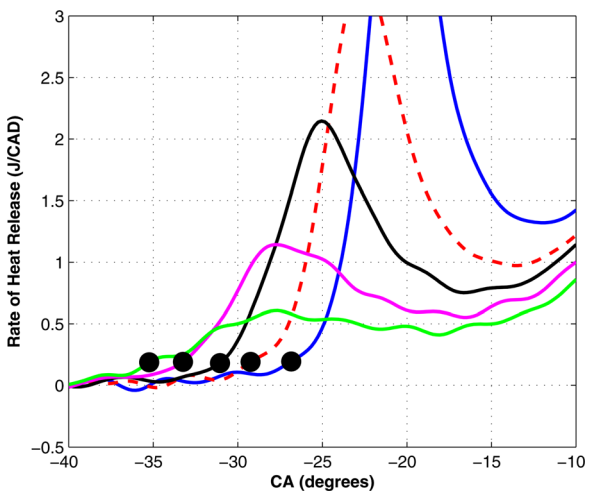

Fig. 23 The LTHR for H20E1

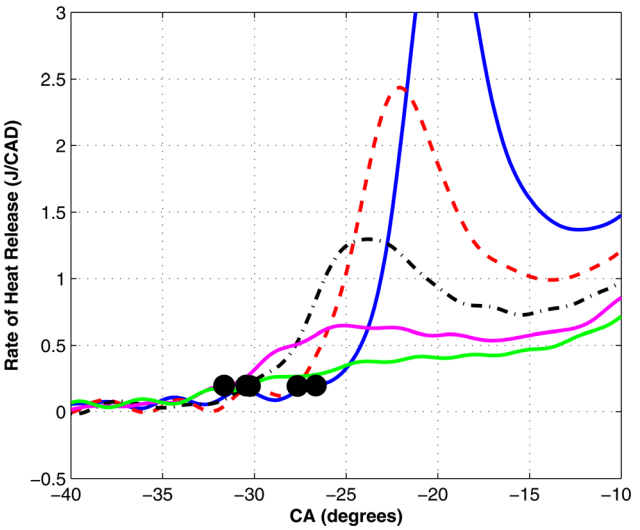

Fig. 24 The LTHR for H20E5

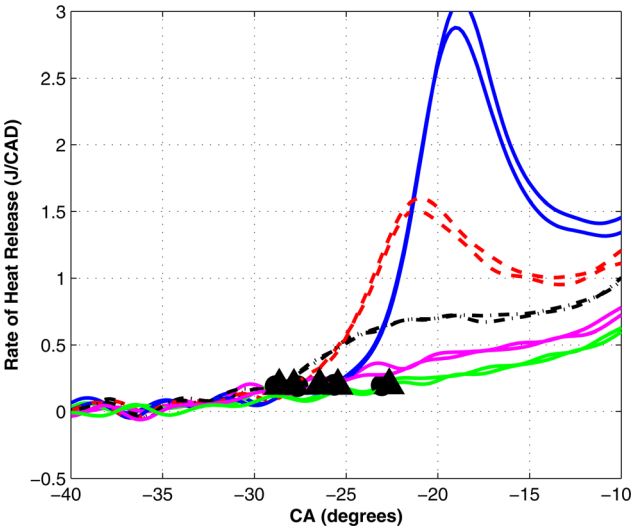

Fig. 25 The LTHR for H20E10

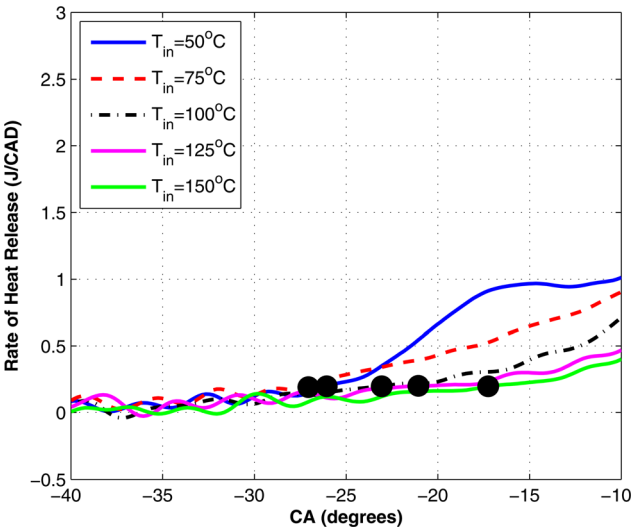

Fig. 26 The LTHR for H20E20

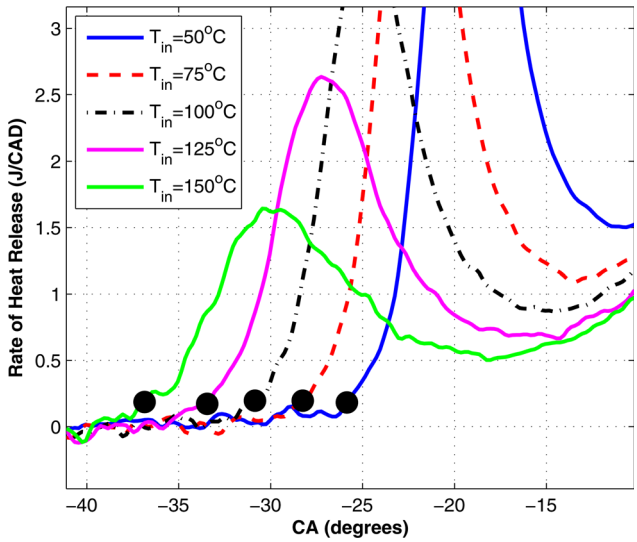

Fig. 27 The LTHR for PRF 70

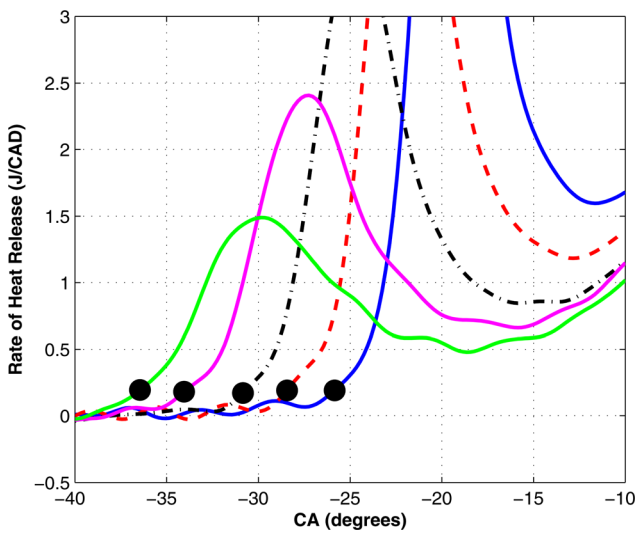

Fig. 28 The LTHR for H30E1

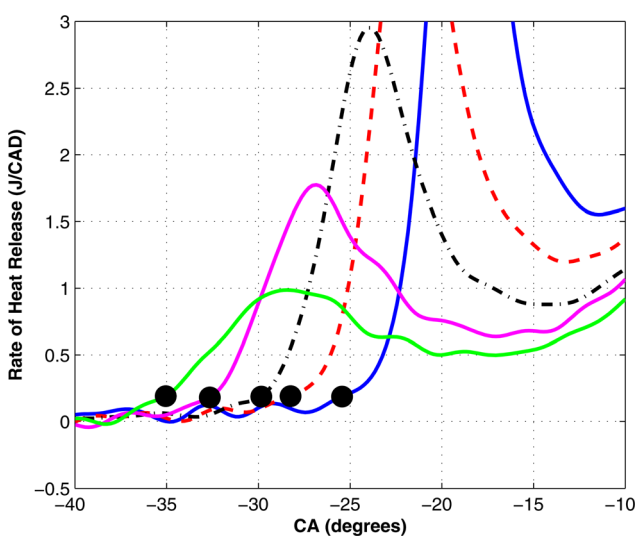

Fig. 29 The LTHR for H30E5

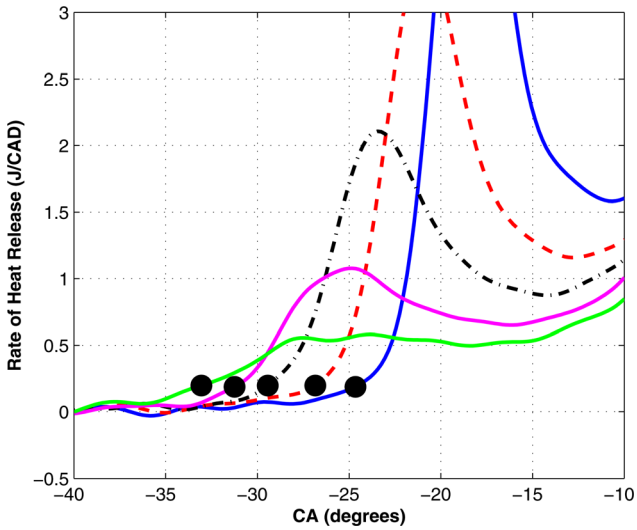

Fig. 30 The LTHR for H30E10

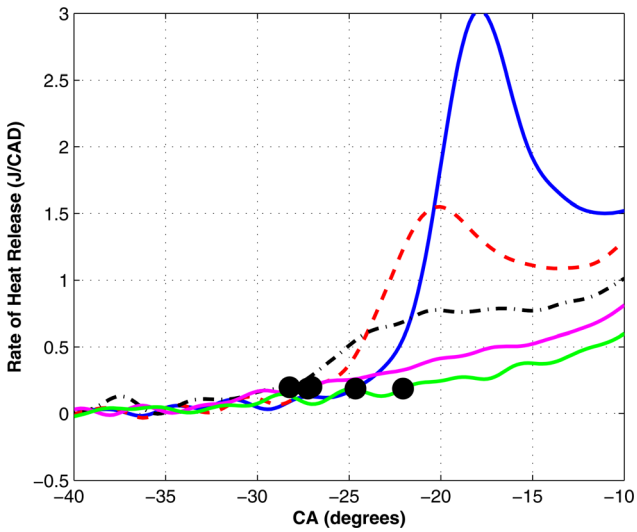

Fig. 31 The LTHR for H30E20

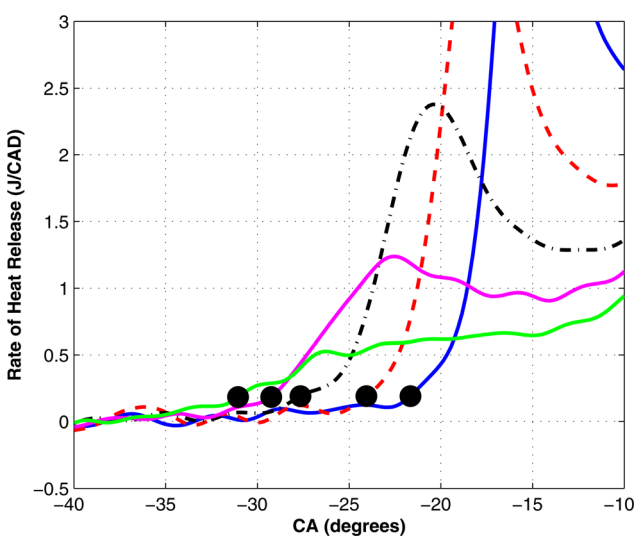

Fig. 32 The LTHR for H60E40

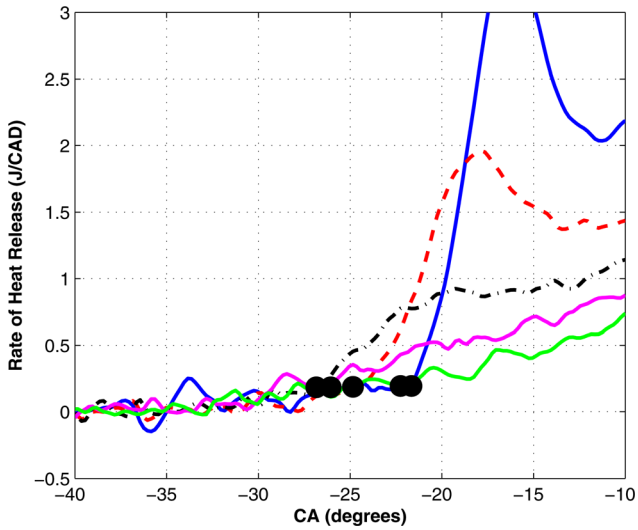

Fig. 33 The LTHR for H55E4

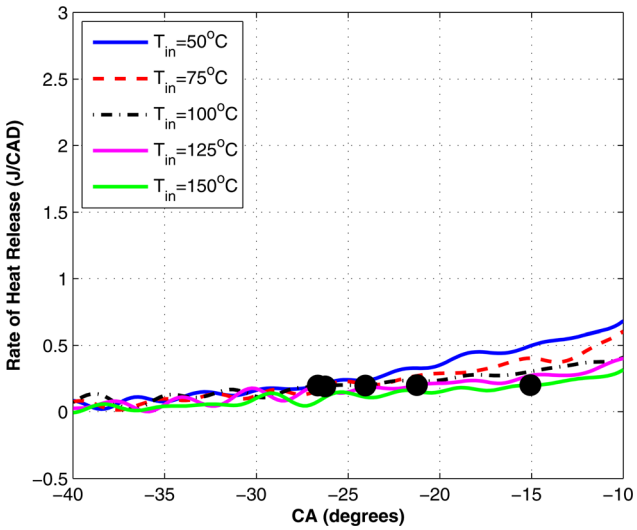

Fig. 36 The LTHR for H40E60

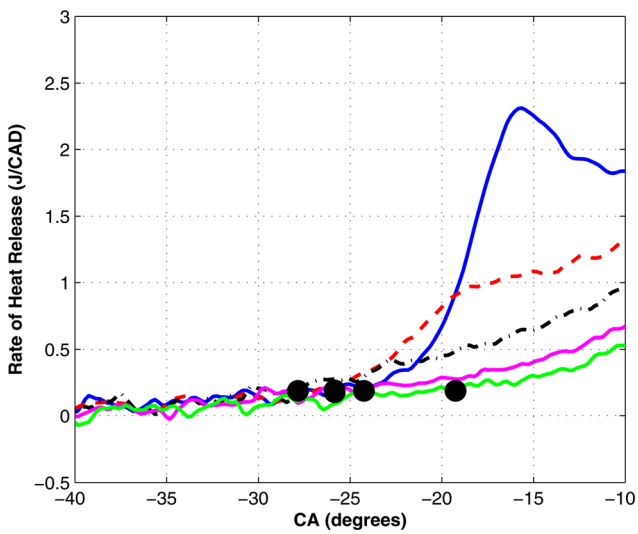

Fig. 34 The LTHR for H50E5

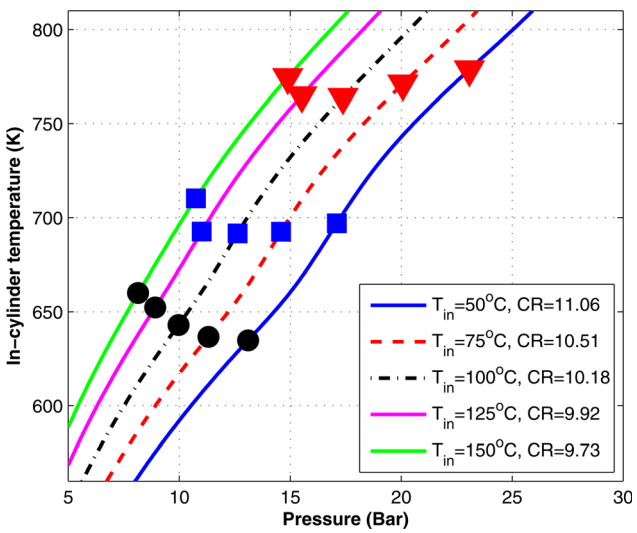

Fig. 37 Auto-ignition temperatures for PRF 80

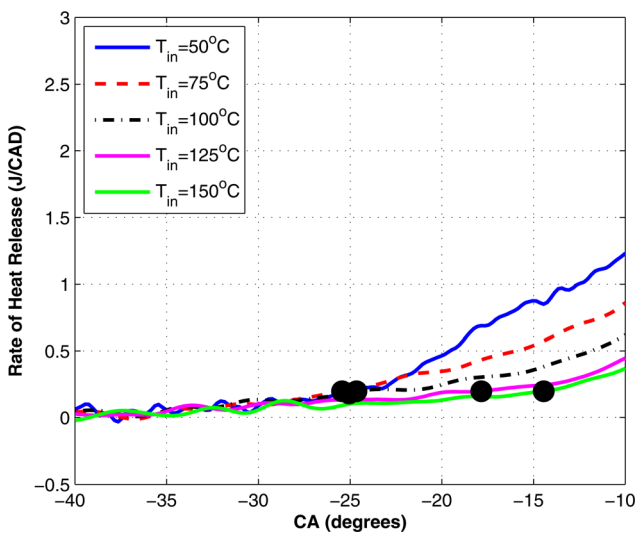

Fig. 35 The LTHR for H45E5

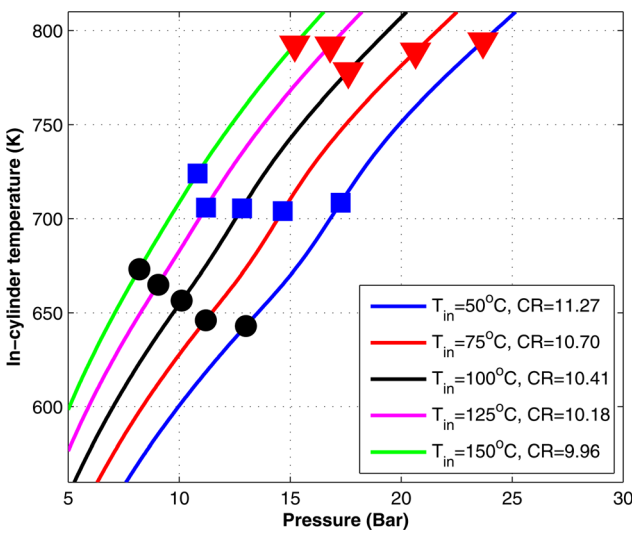

Fig. 38 Auto-ignition temperatures for H20E1

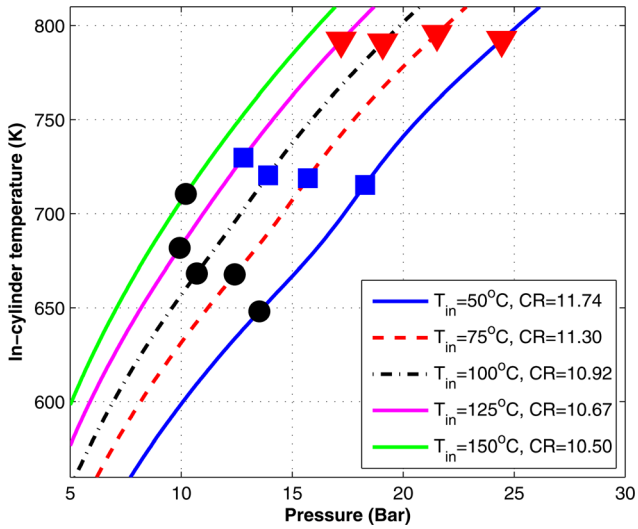

Fig. 39 Auto-ignition temperatures for H20E5

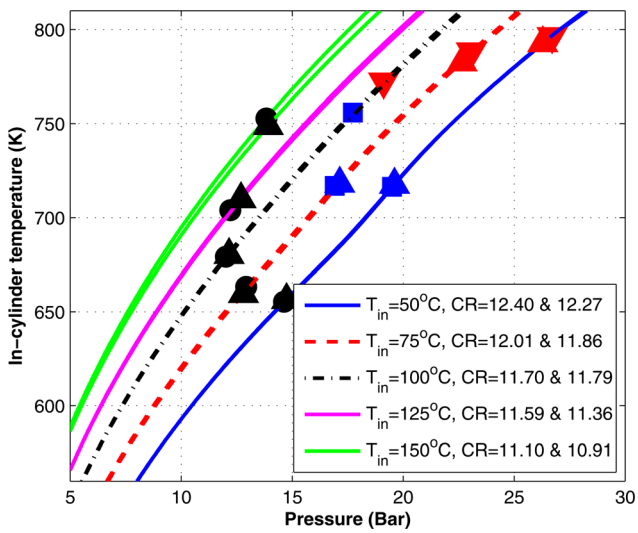

Fig. 40 Auto-ignition temperatures for H20E10

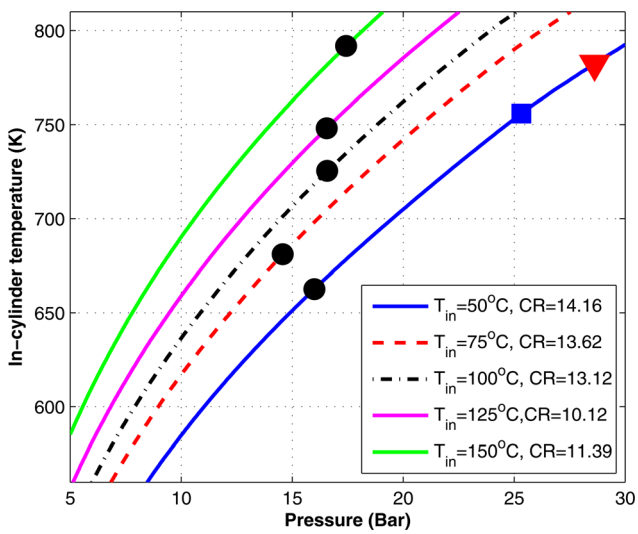

Fig. 41 Auto-ignition temperatures for H20E20

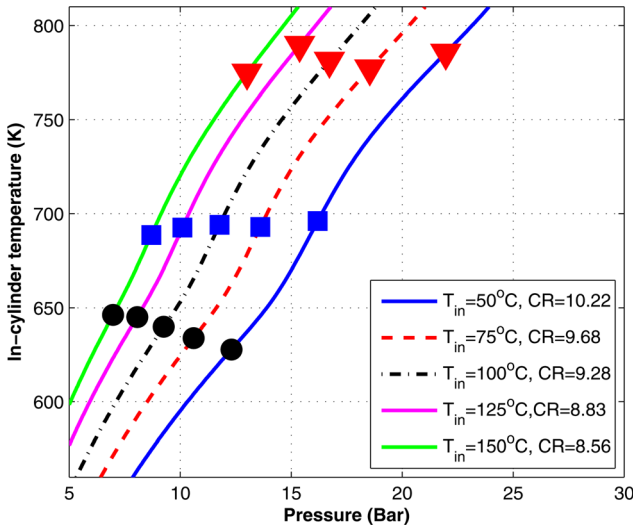

Fig. 42 Auto-ignition temperatures for PRF 70

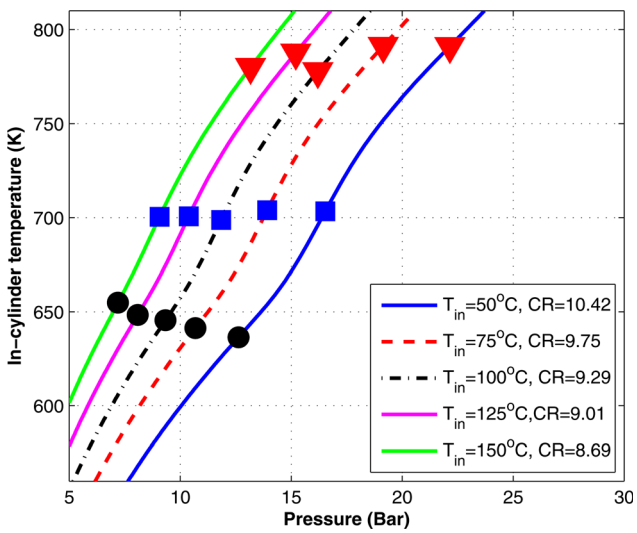

Fig. 43 Auto-ignition temperatures for H30E1

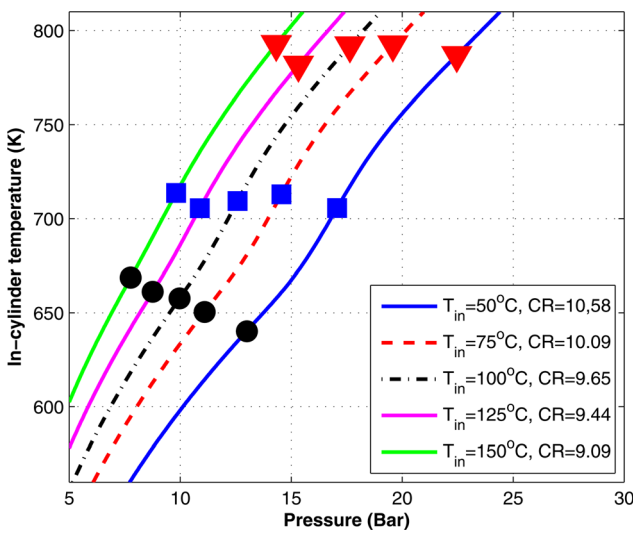

Fig. 44 Auto-ignition temperatures for H30E5

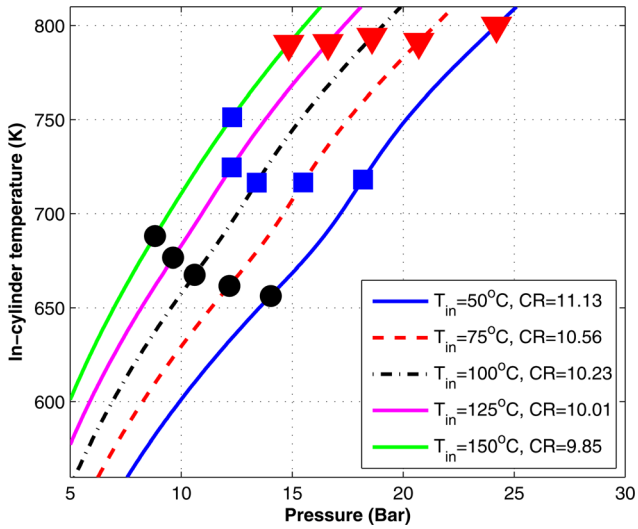

Fig. 45 Auto-ignition temperatures for H30E10

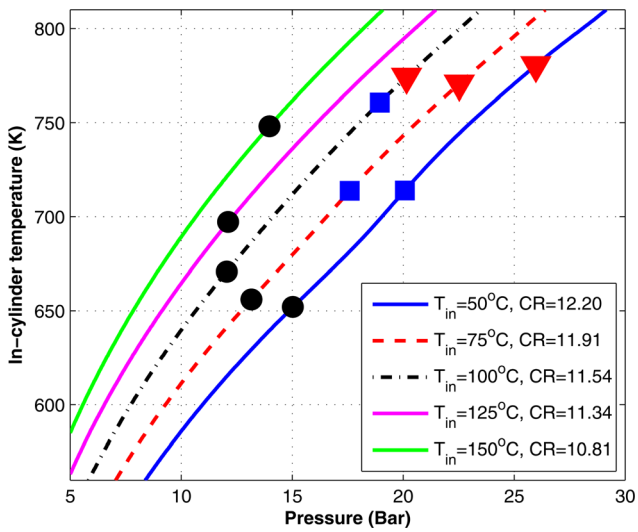

Fig. 46 Auto-ignition temperatures for H30E2

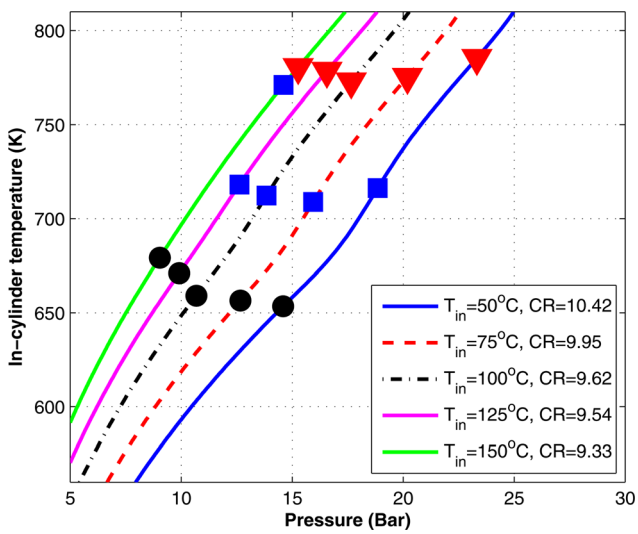

Fig. 47 Auto-ignition temperatures for H60E40

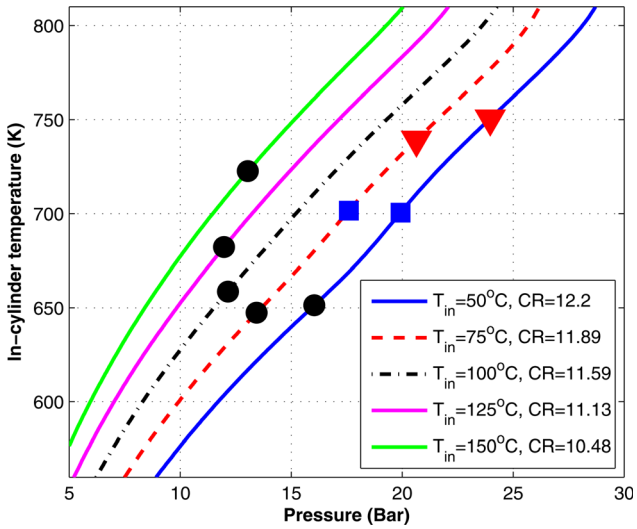

Fig. 48 Auto-ignition temperatures for H55E45

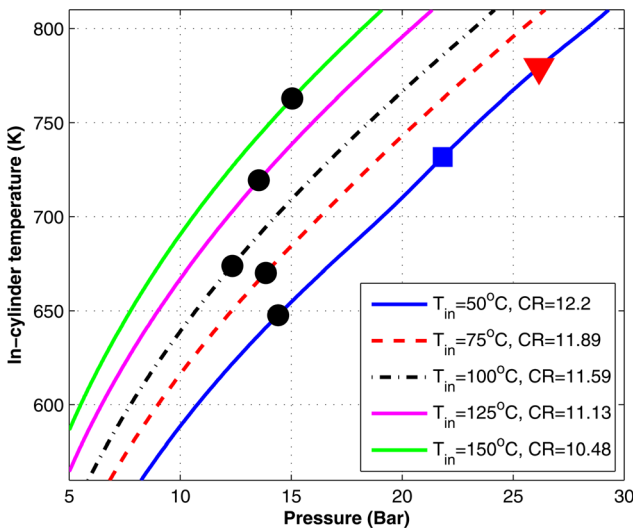

Fig. 49 Auto-ignition temperatures for H50E50

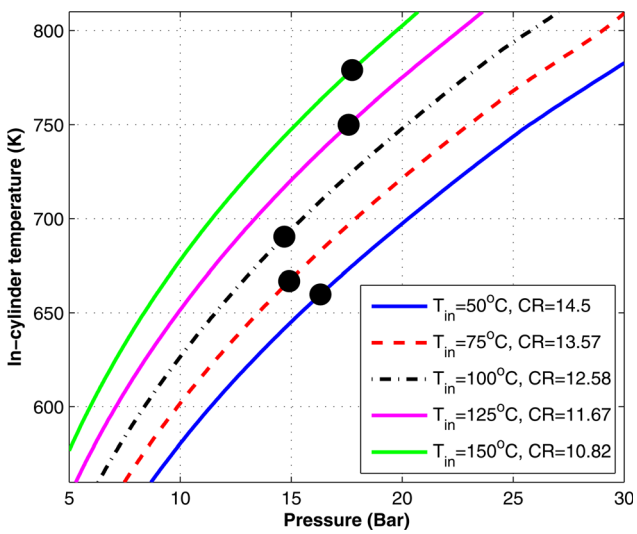

Fig. 50 Auto-ignition temperatures for H45E55

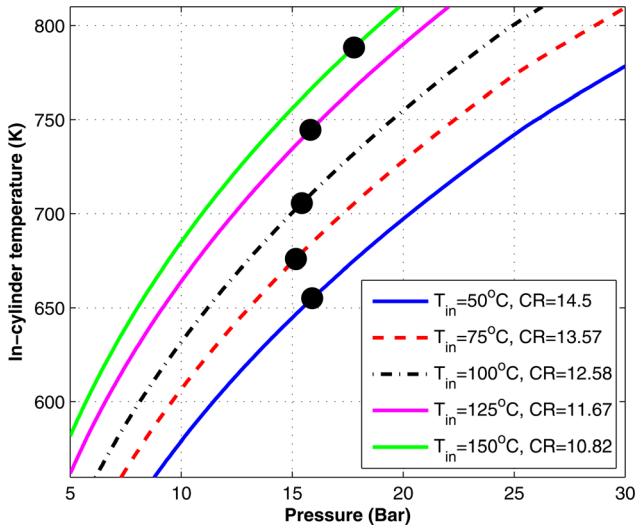

Fig. 51 Auto-ignition temperatures for H40E60

References

[1] Liu, H., Yao, M., Zhang, B., and Zheng, Z., 2009, "Influence of Fuel and Operating Conditions on Combustion Characteristics of a Homogenous Charge Compression Ignition Engine," Energy Fuels, **23**, pp. 1422–1430.

[2] Kalghatgi, G. T., 2005, "Auto-Ignition Quality of Practical Fuels and Implications for Fuel Requirements of Future SI and HCCI Engines," SAE Paper No. 2005-01-0239.

[3] Shibata, G., and Urushihara, T., 2007, "Auto-Ignition Characteristics of Hydrocarbons and Development of HCCI Fuel Index," SAE Paper No. 2007-01-0220.

[4] Shibata, G., and Oyama, K., 2005, "Correlation of Low Temperature Heat Release With Fuel Composition and HCCI Engine Combustion," SAE Paper No. 2005-01-0138.

[5] Tanaka, S., Ayala, F., Keck, J. C., and Heywood, J. B., 2003, "Two-Stage Ignition in HCCI Combustion and HCCI Control by Fuels and Additives," Combust. Flame, **132**, pp. 219–239.

[6] Aroonsriopon, T., Sohm, V., Werner, P., Foster, D. E., Morikawa, T., and Iida, M., 2002, "An Investigaton Into the Effect of Fuel Composition on HCCI Combustion Characteristics," SAE Paper No. 2002-01-2830.

[7] Warnatz, J., Maas, U., and Dibble, R. W., 2006, *Combustion Physical and Chemical Fundamentals, Modeling and Simulation, Experiments, Pollutant Formation*, Springer, Berlin.

[8] Hosseini, V., Neill, W. S., and Chippior, W. L., 2009, "Influence of Engine Speed on HCCI Combustion Characteristics Using Dual-Stage Autoignition Fuels," SAE Paper No. 2009-01-1107.

[9] Silke, E. J., Pitz, W. J., Westbrook, C. K., Sjöberg, M., and Dec, J. E., 2008, "Understanding the Chemical Effects of Increased Boost Pressure Under HCCI Conditions, SAE Paper No. 2008-01-0019.

[10] Sjöberg, M., and Dec, J. E., 2011, "Effects of EGR and Its Constituents on HCCI Autoignition of Ethanol," Proc. Combust. Inst., **33**, pp. 3031–3038.

[11] Sjöberg, M., and Dec, J. E., 2007, "EGR and Intake Boost for Managing HCCI Low-Temperature Heat Release Over Wide Ranges of Engine Speed," SAE Paper No. 2007-01-0051.

[12] Andrae, J. C. G., and Head, R. A., 2009, "HCCI Experiments With Gasoline Surrogate Fuels Modeled by a Semidetailed Chemical Kinetic Model," Combust. Flame, **156**, pp. 842–851.

[13] Truedsson, I., Tuner, M., Johansson, B., and Cannella, B., 2012, "Pressure Sensitivity of HCCI Auto-Ignition Temperature for Primary Reference Fuels," SAE Paper No. 2012-01-1128.

[14] Lü, X., Ji, L., Zu, L., Hou, Y., Huang, C., and Huang, Z., 2007, "Experimental Study and Chemical Analysis of *n*-Heptane Homogeneous Charge Compression Ignition Combustion With Port Injection of Reaction Inhibitors," Combust. Flame, **149**, pp. 261–270.

[15] Floweday, G., 2010, "A New Functional Global Auto-Ignition Model for Hydrocarbon Fuels—Part 1 of 2: An Investigation of Fuel Auto-Ignition Behaviour and Existing Global Models," SAE Paper No. 2010-01-2161.

[16] Machado, G. B., Barros, J. E. M., Braga, S. L., Braga, C. V. M., Oliviera, E. J., Silva, A. H. M. F. T., and Carvalho, L. O., 2011, "Investigation on Surrogate Fuels for High-Octane Oxygenated Gasolines," Fuel, **90**, pp. 640–646.

[17] Pitz, W. J., Cernansky, N. P., Dryer, F. L., Egolfopoulos, F. N., Farrell, J. T., Friend, D. G., and Pitsch, H., 2007, "Development of an Experimental Database and Chemical Kinetic Models for Surrogate Gasoline Fuels," SAE Paper No. 2007-01-0175.

[18] Yates, A., Bell, A., and Swarts, A., 2010, "Insights Relating to the Autoignition Characteristics of Alcohol Fuels," Fuel, **89**, pp. 83–93.

[19] SAE J1297, 2002, "Surface Vehicle Information Report, Alternative Automotive Fuels," SAE Standard No. J1297.

Paper III

SAE International

Pressure Sensitivity of HCCI Auto-Ignition Temperature for Gasoline Surrogate Fuels

2013-01-1669
Published
04/08/2013

Ida Truedsson, Martin Tuner and Bengt Johansson
Lund University

William Cannella
Chevron

doi:10.4271/2013-01-1669

ABSTRACT

An index to relate fuel properties to HCCI auto-ignition would be valuable to predict the performance of fuels in HCCI engines from their properties and composition. The indices for SI engines, the Research Octane Number (RON) and Motor Octane Number (MON) are known to be insufficient to explain the behavior of oxygenated fuels in an HCCI engine. One way to characterize a fuel is to use the Auto-Ignition Temperature (AIT). The AIT can be extracted from the pressure trace. Another potentially interesting parameter is the amount of Low Temperature Heat Release (LTHR) that is closely connected to the ignition properties of the fuel.

A systematic study of fuels consisting of gasoline surrogate components of n-heptane, iso-octane, toluene, and ethanol was made. 21 fuels were prepared with RON values ranging from 67 to 97. Five different inlet air temperatures ranging from 50°C to 150°C were used to achieve different cylinder pressures and the compression ratio was changed accordingly to keep a constant combustion phasing, CA50, of 3±1° after TDC. The experiments were carried out in lean operation with a constant equivalence ratio of 0.33 and with a constant engine speed of 600 rpm. The effect of ethanol and toluene on the LTHR was evaluated. The conclusion was that ethanol had a quenching effect, which is consistent with other studies. Toluene was found only to have a quenching effect at the lowest inlet air temperature. The AIT and the amount of LTHR for different combinations of n-heptane, iso-octane, ethanol and toluene were charted.

INTRODUCTION

The HCCI combustion mode can potentially be used to reduce emissions without using expensive and bulky aftertreatment. With HCCI, it is possible to reduce the NOx and soot emissions to the level of a traditional spark ignition engine with a TWC, while maintaining the efficiency as high as for diesel combustion. The main challenge for HCCI is to control the ignition timing and combustion rate, since they are not controlled by a spark (SI combustion) nor by fuel injection (CI combustion) but rather controlled by chemical kinetics.

An index to relate fuel properties and composition to autoignition would be useful to predict the performance of various fuels in HCCI engine operation. The indices for SI engines, the Research Octane Number (RON) and Motor Octane Number (MON) are on their own known to be insufficient to explain the fuel behavior in an HCCI engine. Several researchers have worked with HCCI fuel properties and the development of an HCCI index [2,3,4,5,6]. One such index is the Octane Index, which is on the form OI=(1-K)RON+ KMON where K is an engine and operating condition specific parameter that depends on the pressure and temperature evolution in the unburnt gas. However, there are indications that the OI is not applicable for oxygenated fuels [1], which is why a new fuel index is needed to predict the performance of any fuel in an HCCI engine. To achieve this, more knowledge of the combustion process is needed. A standardized method for determining the HCCI fuel performance was desired. The idea was that the fuel auto-ignition temperature could be related to the fuel performance in an HCCI engine.

Combustion of fuel that contains a significant amount of n-paraffins, such as n-heptane, exhibits a characteristic bump in the rate of heat release trace before the main heat release. This is referred to as Low Temperature Heat Release LTHR) which is caused by the Low Temperature Reactions (LTR) - the exothermic pre-reactions that occur before the main combustion event. LTR are usually more prominent at lower temperatures but diminish as the intake air temperature increases. The reason is that the precursors for this chain branching (the LTR) are decomposed back to the reactants at higher temperatures [7]. The amount of LTHR also decreases with higher engine speed because there is less time for the pre-reactions to occur [8]. Exhaust gas recirculation (EGR) can advance the start of LTR, probably because they contain reactive species such as H_2O_2 [9,10]. A higher cylinder pressure induced by super- or turbocharging is also known to increase the amount of LTHR [11]. This indicates that a higher compression ratio should also increase the amount of LTHR.

Andrae et al. [12] show that fuel components such as ethanol, acts as radical scavengers and therefore decrease the LTHR for fuels like n-heptane. Lü et al. [14] studied the effect of different inhibitors on LTHR, including ethanol. One observation from kinetic modeling of an n-heptane and ethanol mixture was that only the n-heptane part of the fuel was consumed in the LTR, and that the n-heptane was the first to be consumed by the main heat release.

A thorough summary of hydrocarbon fuel models and how two-stage combustion is affected by different parameters is presented by Floweday [15]. They describe the pressure sensitivity and comment that it is a complex behavior where the pressure affects auto-ignition in the different temperature regions in different ways.

Studies performed at a Brazilian refinery [16] concluded that gasoline contain more than 400 components, with only 20-25 components greater than 1 % by mass. Because of the complexity of gasoline, surrogate fuels are often studied to understand the effects from different components. Pitz et al. [17] reviews the development of surrogate fuels particularly for HCCI combustion and concludes that the three necessary components of any gasoline fuel surrogate are n-heptane, isooctane and toluene. Toluene is typically the most common aromatic in gasoline. They rated different gasoline surrogate fuel components and placed ethanol, 1-pentene, di-isobutylene and xylene at the second importance level. Machado et al. [16] compared different gasoline surrogate fuels in an SI engine to find a suitable fuel to describe high ethanol (20 vol.%) gasoline. They concluded that mixtures of n-heptane, isooctane, toluene and ethanol could be used as surrogate fuels for oxygenated gasoline. Currently, ethanol is usually added to gasoline as a renewable fuel. US and Swedish gasoline both contain up to 10 vol.% ethanol, and this amount is expected to increase in the future.

In studies of gasoline surrogate fuels, Shibata et al. conclude that toluene inhibits LTHR and thus increases ignition delay [4]. Sakai et al. [18] on the other hand, found that the ignition delay in iso-octane decreased with the addition of up to 50% toluene.

The main objective of the current study was to determine the effect of ethanol and toluene addition in blends with nheptane and iso-octane on the auto-ignition temperatures and amount of low temperature heat release at different cylinder pressures in HCCI combustion. These studies prepare for further experiments with real gasoline, providing insight into the combustion process so that the more complex behavior of real gasoline can be explained.

EXPERIMENTAL SETUP

A Waukesha variable compression ratio Cooperative Fuels Research (CFR) engine was used for the experiments. The setup included an air-fuel mixture heater mounted after the fuel port injection. A scale was used for measuring the fuel flow. The heat release was calculated from the pressure trace measured with a Kistler piezoelectric pressure transducer mounted in the cylinder. An intake air refrigerator was included in the setup to ensure constant air humidity throughout the experiments. Temperature of the fuel air mixture was measured by a thermocouple placed in the inlet, close to the inlet valve. The spark ignition was switched off. The engine specifications are listed in Table 1.

Table 1. Specifications for CFR engine.

Displacement volume	612 cm^3
Number of cylinders	1
Bore	83 mm
Stroke	114 mm
CR	Variable (4:1 to 18:1)
Number of valves	2
Length of connecting rod	254 mm
Intake valve opens	10°ATDC±2.5°
Intake valve closes	146°BTDC±2.5°
Exhaust valve opens	140°ATDC±2.5°
Exhaust valve closes	15°ATDC±2.5°
Valve lifts	6.25 mm
Valve diameters	9.53 mm
Engine speed	600 rpm
Fuel supply	Port injection

FUELS

Two fuel matrices were used in this study. The first set of test fuels consisted of blends of n-heptane, iso-octane and toluene listed in Table 2. Fuels designated as HxTy contain x vol.% nheptane, y vol.% toluene, and (100-x-y) vol.% iso-octane. N-heptane content was kept constant at 20% while the toluene content was varied from 10% to 60%. These fuels

were tested to study the effects of toluene addition to blends of n-heptane and iso-octane.

Table 2. First fuel matrix, vol.%.

Fuel	N-heptane (vol.%)	Toluene (vol.%)	Iso-octane (vol.%)
H20T10	20	10	70
H20T20	20	20	60
H20T40	20	40	40
H20T60	20	60	20

The second test matrix consisted of blends of n-heptane, isooctane, toluene and ethanol according to Table 3. This matrix was designed to be able to separate the effects of pressure from the fuel effects on the amounts of LTHR. This is possible since the octane rating is not only dependent on one parameter. For example the amount of toluene can be varied while the ON is kept constant by adding ethanol. It is also possible to see co-effects between toluene and ethanol. We refer to these fuels as TERF's (Toluene-Ethanol Reference Fuels). RON's and MON's were measured for these fuels and the results are presented in Table 3. They were not measured for fuel #17, but rather assumed to be the same as for fuels #7 and #11, which had the same fuel composition. The sensitivity of the fuel, given by the difference between the fuels RON and MON (S=RON-MON), is also given in Table 3.

Table 3. Second fuel matrix, vol.%.

Fuel	n-Hept	Toluene	Ethanol	iso-Oct	MON	RON	S
T1	40	10	5	45	63,7	67,1	3,4
T2	20	10	20	50	88,5	94,7	6,2
T3	20	30	20	30	87,6	97	9,4
T4	40	30	20	10	73	80,8	7,8
T5	30	20	5	45	74,5	79,6	5,1
T6	30	30	12,5	27,5	78,6	85,3	6,7
T7	30	20	12,5	37,5	78,1	83,8	5,7
T8	40	30	5	25	65,8	71,8	6
T9	30	10	12,5	47,5	77,9	81,6	3,7
T10	20	30	5	45	84,1	90,2	6,1
T11	30	20	12,5	37,5	78,2	83,8	5,6
T12	40	10	20	30	74,3	78,3	4
T13	20	10	5	65	83,6	86,1	2,5
T14	40	20	12,5	27,5	68,9	74,8	5,9
T15	20	20	12,5	47,5	86,4	92,3	5,9
T16	30	20	20	30	81,4	87,9	6,5
T17	30	20	12,5	37,5	-	-	-

METHOD

All fuels were analyzed with a change in inlet air temperature (T_{in}) in five steps from 50° to 150°C. At each temperature a combustion phasing with CA50 at 3±1° after TDC was held by changing the compression ratio. A constant CA50 was used to ensure stable combustion in all cases and to represent a realistic operating condition. This also simplifies when comparing emissions. Motored pressure traces were extracted for all data points for validation. The engine was run naturally aspirated. The fuel amount was adjusted for each case to achieve an equivalence ratio of 0.33. This was chosen since a diluted charge is needed in HCCI combustion to keep pressure rise rates at an acceptable level. The auto-ignition temperatures are assumed to be insensitive to small changes of equivalence ratio in this range. All experiments were run at 600 rpm. No EGR was used.

Heat Release Calculations

The Woschni heat transfer model was used, and the motored heat release was subtracted from the fired heat release to reduce measurement and model errors. The assumptions were that the temperature when the inlet valve closes was known. This temperature was calculated from the measured temperature in the intake by applying a simple model for the temperature change due to mixing with hot internal residuals, and also heating from the intake walls between the temperature probe mounted just before the intake, and the cylinder. All figures are based on the average of 300 cycles. The heat release calculations are described in more detail in [13]. Start of combustion was defined as when the rate of heat release had reached 0.2 J/CAD, and this was compared with 1 % burnt, see Figure 1,2,3. This low value was chosen to be able to detect very small amounts of heat released. A discussion about how this affects the results is included in previous papers by the authors [13]. The auto-ignition temperature was extracted from the start of combustion described above. Corresponding auto-ignition temperatures for fuel T1 are shown by black circles in Figure 2 and Figure 3. The blue squares mark the maximum rate of heat release for the LTHR and the red triangles mark the minimum rate of heat release between LTHR and the main combustion.

Amount of LTHR is calculated as the area under the curve as shown in Figure 4. End of LTHR is chosen as the minimum value between the two peaks. The amount of low temperature heat release is then divided with the total amount of heat released to account for the different fuel amounts at the different inlet air temperatures.

Fuel T2 in Figure 5 shows no LTHR. However it can be noted that there might be some pre-reactions at the low inlet air temperature case, even if there are no rate maximum and therefore not detected as such.

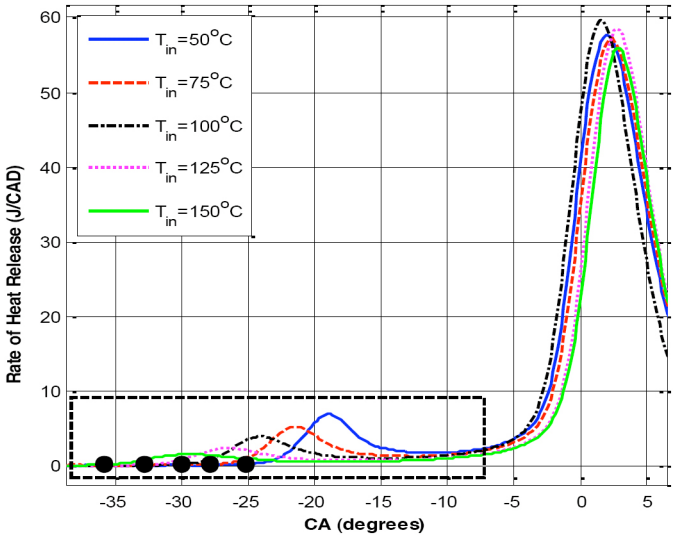

Figure 1. Rate of heat release with start of combustion for fuel T1. The black box marks the zoom area for Figure 2.

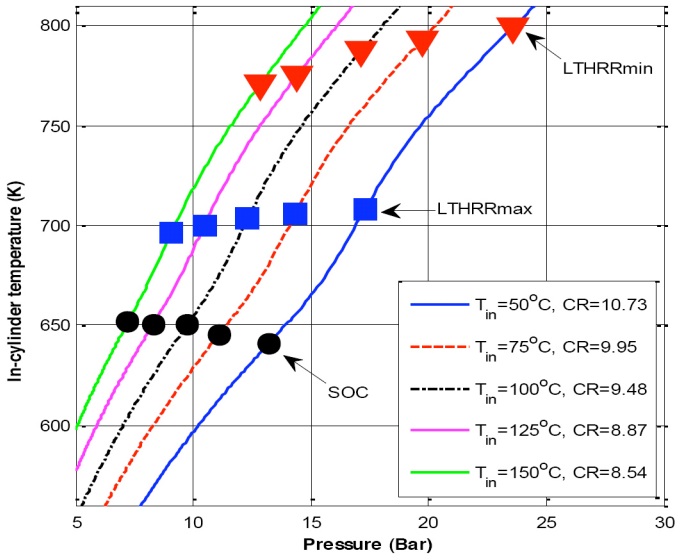

Figure 3. Temperatures and pressures at auto-ignition for fuel T1.

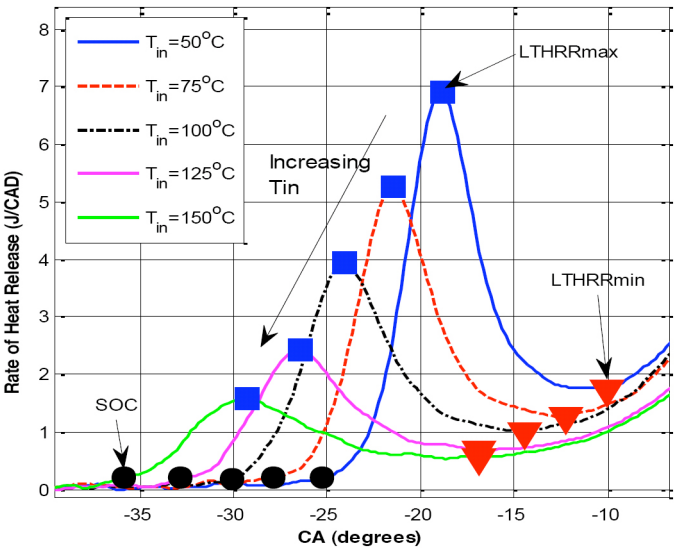

Figure 2. LTHR for fuel T1. Start of combustion (black dots), maximum rate of heat release for low temperature reactions (LTHRRmax, blue squares) and minimum rate of heat release for low temperature reactions (LTHRRmin, red triangles).

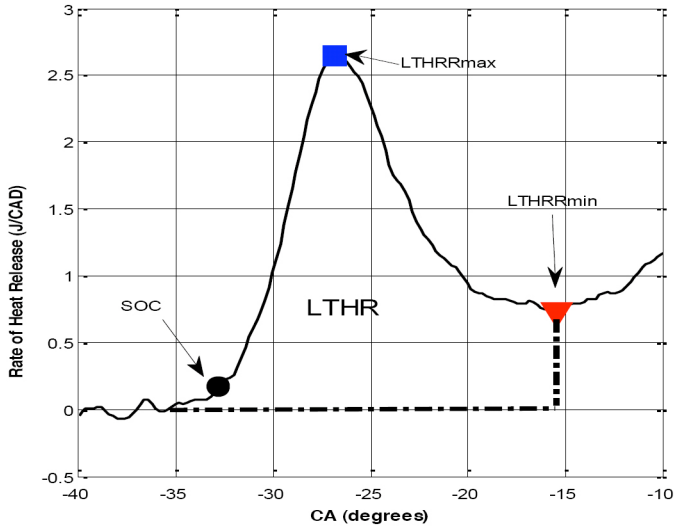

Figure 4. Area for calculating amount of LTHR.

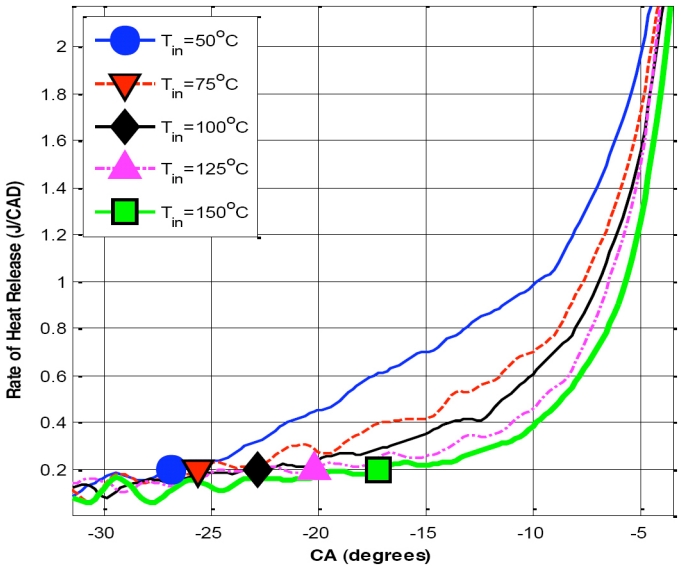

Figure 5. Start of combustion for fuel T2. SOC is retarded as inlet air temperature is increased.

RESULTS AND DISCUSSION

Toluene Reference Fuels (TRF)

The first fuel matrix was designed to study the effects on autoignition temperatures and amount of LTHR when toluene was added to PRFs. The temperatures and pressures at which autoignition occurred for each fuel are presented in Figure 6 where start of auto-ignition is defined as the release of 0.2 J/CAD heat and in Figure 7 where it is defined as the point of 1% of total heat release. For each fuel, there are 5 points corresponding to the 5 different inlet air temperatures (T_{in}). In general, as T_{in} is increased, the auto-ignition temperature (AIT) increased, although to a different extent for different fuels and different T_{in}. The shapes of the curves are similar to those we previously reported for PRF mixtures [13] and blends of ethanol with PRF's [19]. For both fuel sets, toluene addition was found to increase the auto-ignition temperature. This is evidenced by a shift of the curves upward and to the right as the toluene content increased. This increase is mostly seen at higher inlet air temperature, and the auto-ignition temperature differs only slightly at the lowest inlet air temperature.

Figure 8 shows the % of LTHR relative to total heat release as a function of toluene content for the 5 different T_{in}. The normalization with the total heat release is to account for differences in the supplied fuel energy at different inlet air temperatures. For a given fuel, as T_{in} increases, the amount of LTHR decreases. For some fuels the LTHR reaches 0% before the T_{in} reaches 150°C (that's why there are less than 5 points for some fuels). These effects are similar to what we previously reported for PRF's [13] and mixtures of ethanol with PRF's [19]. Figure 8 indicates that the amount of LTHR decreases as the amount of toluene increases. This shows that toluene inhibits LTHR.

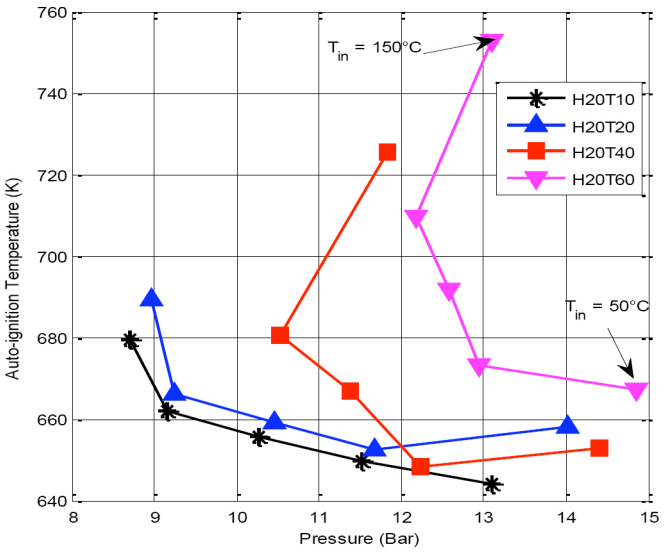

Figure 6. Auto-ignition temperatures, 0.2 J/CAD. The five marks for each fuel correspond to the five different inlet air temperatures.

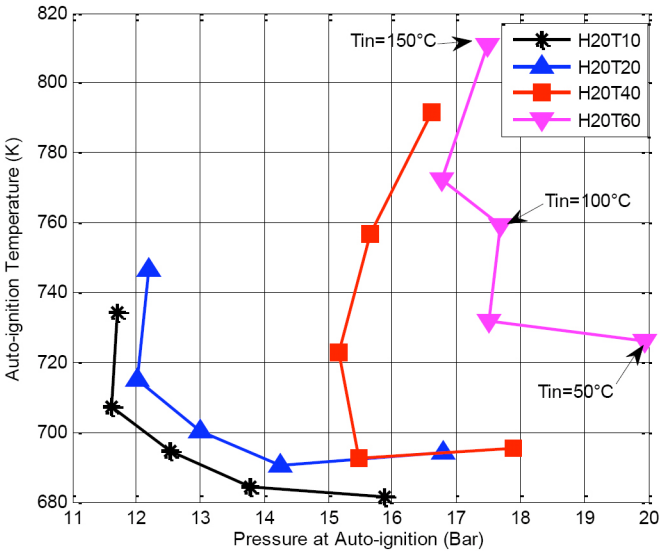

Figure 7. Auto-ignition temperatures, 1 % burnt. The five marks for each fuel correspond to the five different inlet air temperatures.

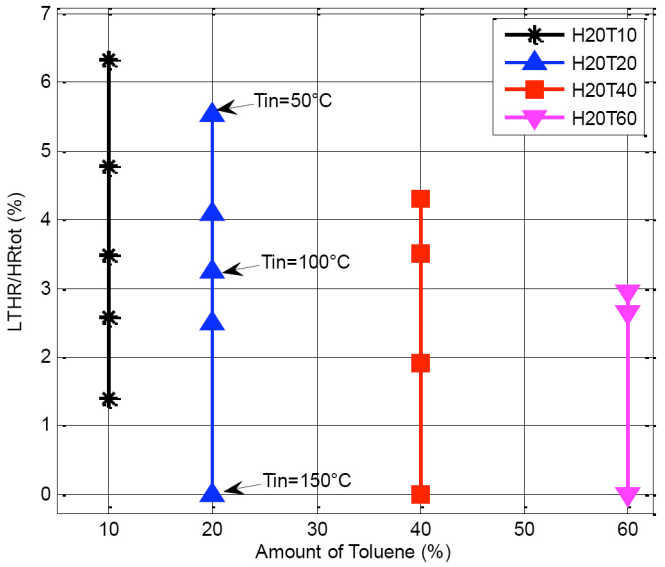

Figure 8. Amount of LTHR for TRFs. The marks for each fuel represent the different T_{in}, with 50°C at the top and 150°C at the bottom. Zero means no LTHR at one or more temperatures.

Morgan et al. [20] have developed a response surface model to estimate the RON for blends of n-heptane, iso-octane and toluene when measurements are not available. They showed that their model was more accurate than the "linear-by-volume" method often used. These calculated RON are shown in Figure 9. The amount of LTHR seen is comparable to that of the PRFs.

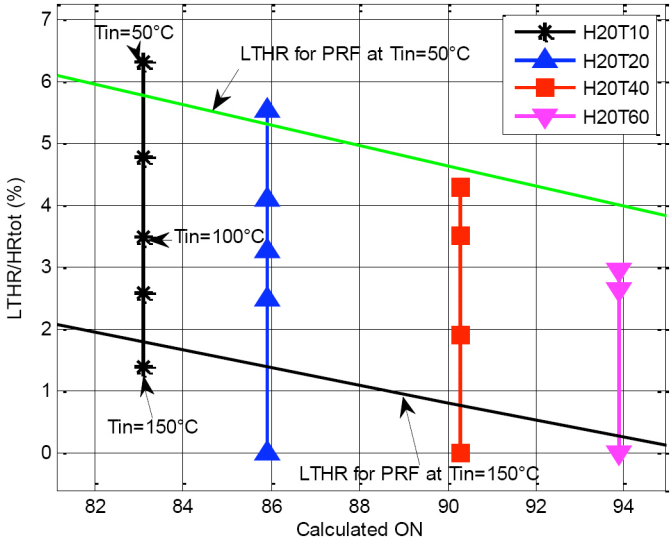

Figure 9. Amount of LTHR. The marks for each fuel represent the different T_{in}, with 50°C at the top and 150°C at the bottom. Zero means no LTHR at one or more temperatures.

Toluene Reference Fuel Conclusions

Toluene addition was found to quench the low temperature reactions and to increase the auto-ignition temperature. When comparing the calculated ON of the TRFs, the amount of LTHR was comparable to that of the PRFs of the same octane number.

Toluene Ethanol Reference Fuels (TERF)

The second fuel matrix was designed to be able to separate the effects of pressure from the fuel effects on the amounts of LTHR. Co-effects between ethanol and toluene were also studied.

Auto-Ignition Temperatures

Figures 10 and 11 show the auto-ignition temperatures of the TERFs. The auto-ignition temperatures are within the same range as the PRFs containing ethanol (ERFs) studied earlier by the authors [19]. The fuels showing LTHR at all 5 inlet air temperatures (fuel 1, 5, 8, and 14) auto-ignite at an almost constant temperature, and the fuels having very little or no LTHR (e.g. fuel 15 and 16) exhibit a different behavior with very different auto-ignition temperatures depending on the temperature-pressure history.

Additional DoE analysis was applied using the statistical software MODDE. The DoE analysis showed that ethanol increased the AIT, the n-heptane decreased the AIT and toluene addition had no effect on this. The same effects were seen on the pressures at auto-ignition. These effects can also be seen in Figures 10 and 11.

LTHR Quantifications and RON Correlation

The DoE-analysis showed that n-heptane had the largest effect on amount of LTHR and was, as expected, shown to increase this. Ethanol was seen to reduce the amount of LTHR. Toluene was found to have a small quenching effect on the LTHR at the lowest inlet air temperature, but this effect disappeared at the higher inlet air temperatures.

The weak quenching effect of toluene addition to fuels with a low amount of ethanol (5 vol.%) is seen in Figure 12, based on the DoE model. When adding toluene to a fuel with high amounts of ethanol (20 vol.%) no effect is seen on the amount of LTHR at the lowest inlet air temperature, see Figure 13. Since there are only a few fuels showing LTHR at the 125° and 150°C inlet air temperatures, the effect on LTHR in this temperature range could not be accurately modeled.

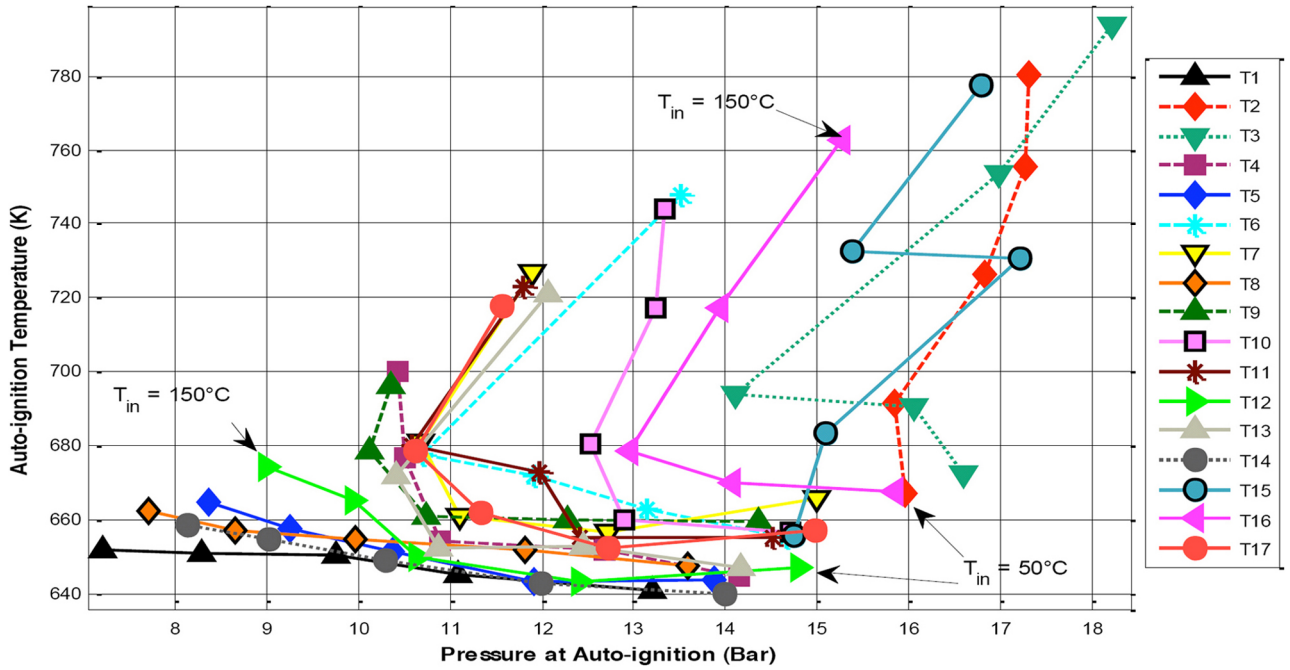

Figure 10. Auto-ignition temperatures, 0.2 J/CAD. The five marks for each fuel correspond to the five different inlet air temperatures.

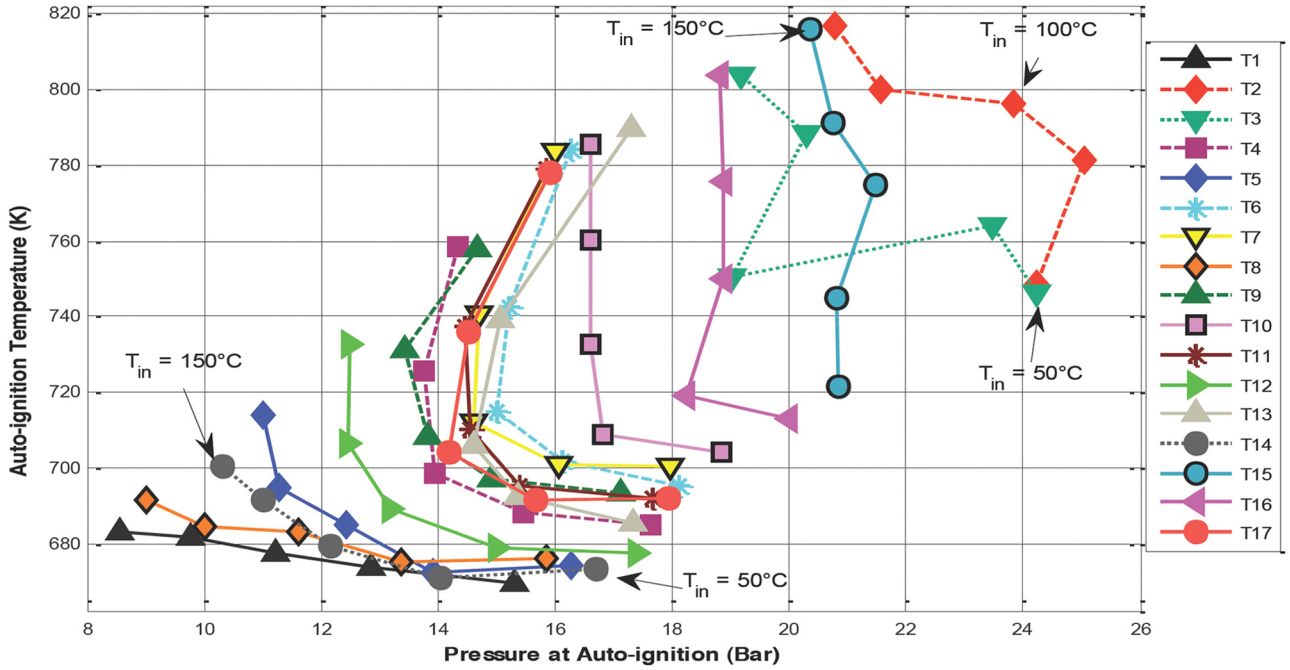

Figure 11. Auto-ignition temperatures, 1 % burnt. The five marks for each fuel correspond to the five different inlet air temperatures.

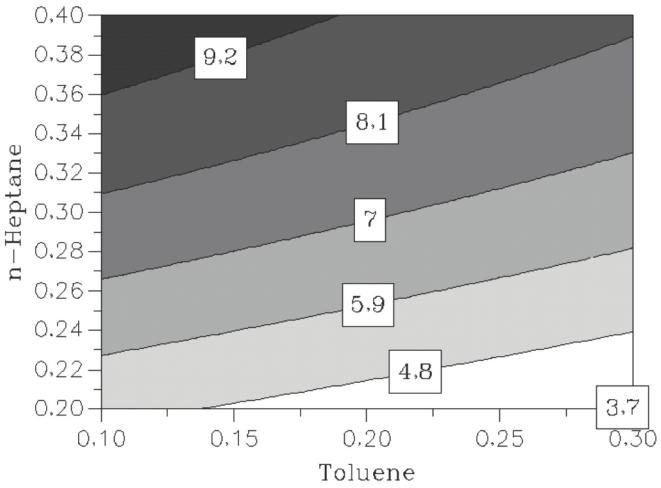

Figure 12. Effect on amount of LTHR of toluene addition to fuels with a constant low level of ethanol (5 vol.%). This is for T_{in}=50°C from the DoE model.

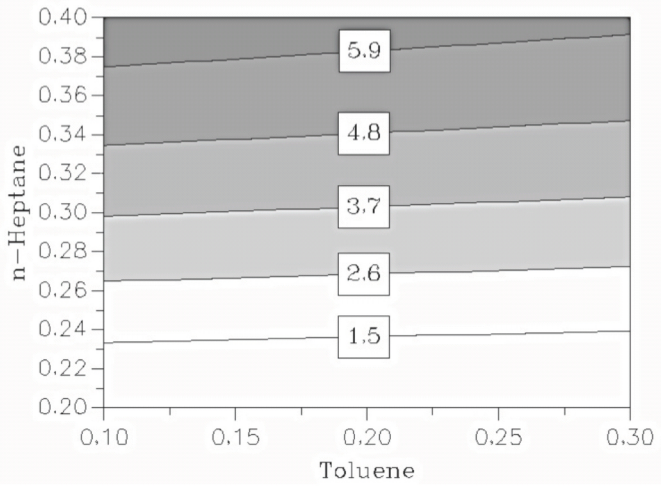

Figure 13. Effect on amount of LTHR from toluene addition to fuels at high levels of ethanol (20 vol.%). This is for T_{in}=50°C from the DoE model.

As an example of the LTHR quenching, three fuels with the same concentrations of n-heptane (30 vol.%) and toluene (20 vol.%) but varying concentrations of ethanol (5 vol.%, 12.5 vol.%, and 20 vol.%) are shown in Figure 14.

The amount of LTHR for the TERFs is compared to that of the PRFs previously studied [13]. Figure 15 shows the lowest inlet air temperature of 50°C and Figure 16 shows the highest inlet air temperature of 150 °C. The green and black lines in both figures are the results for the PRF's. A higher octane rating clearly decreases the amount of LTHR.

The LTHR percentage can be described by a separate linear correlation at each inlet air temperature, similar to that of the PRFs but more sensitive to an increased ON, see the blue line in Figure 15. It can however be noted that also the PRFs show less LTHR than the linear approximation suggests at RONs over 85, since this is adapted for the whole octane span from PRF 0-95 [13].

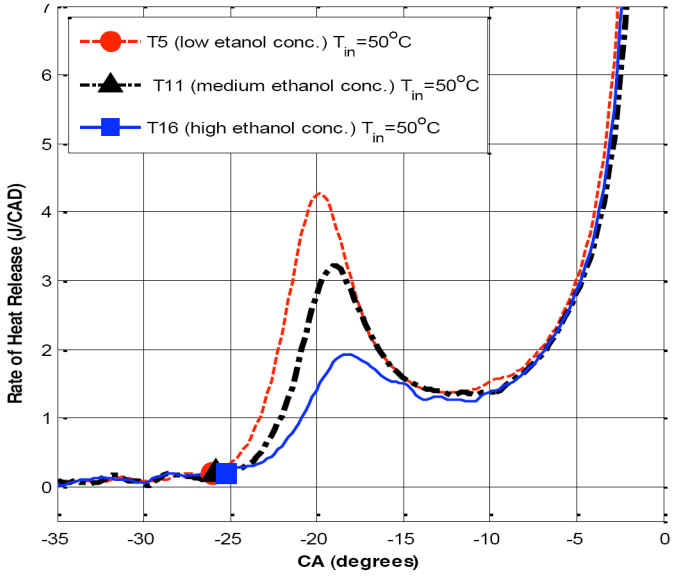

Figure 14. Effect of ethanol addition on amount of LTHR.

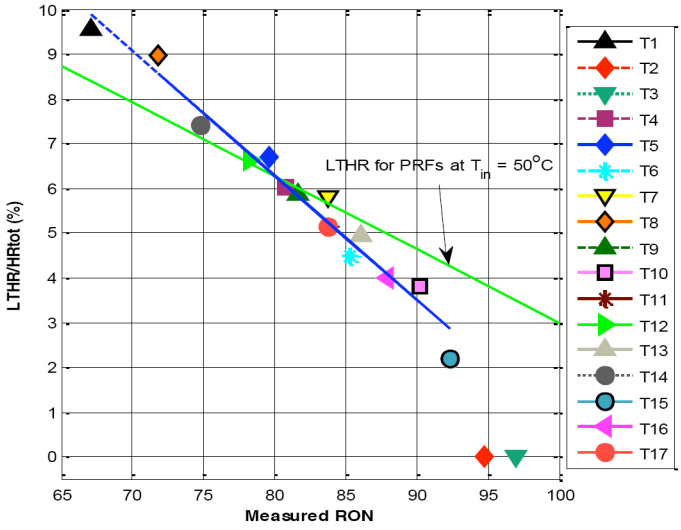

Figure 15. LTHR at Tin=50°C. The blue line is a best fit and does not include fuel 2 and 3.

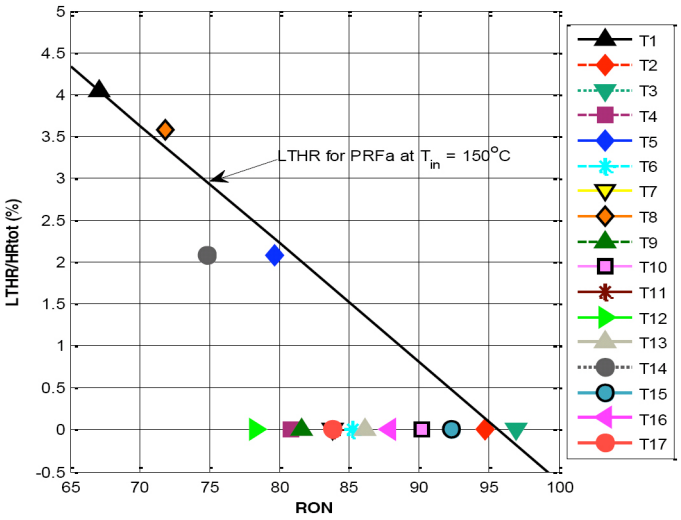

Figure 16. LTHR at Tin=150°C. Zero means no LTHR for that fuel at shown temperature.

Auto-Ignition Temperatures and RON

The correlation between RON and auto-ignition temperature (AIT) is shown in Figures 17 and 18. The blue lines in Figure 17 and 18 are best fits for the T_{in}=50°C case. The scatter in the data in Figure 17 indicates that fuels having similar RON values can have somewhat different AIT's, suggesting that RON is not sufficient for characterizing the fuel AIT behavior, at least at T_{in}=50°C. In Figure 18, the four fuels having some LTHR at the T_{in}=150°C (Fuels 1, 5, 8, and 14) exhibit a different behavior than the other fuels. The black line in Figure 18 is for the fuels showing some LTHR at T_{in}=150°C. The red line is the best fit for fuels not having any LTHR at this inlet air temperature. There seems to be an offset at different inlet air temperatures but a similar trend for fuels having LTHR.

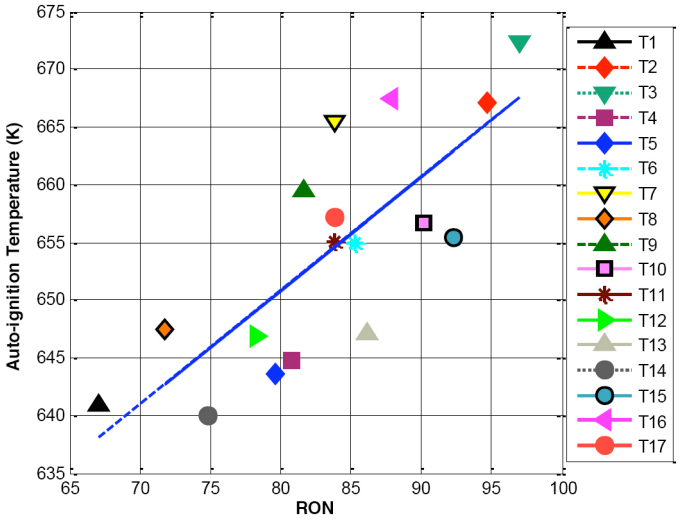

Figure 17. Auto ignition temperature and RON at T_{in}=50°C. The blue line is a best fit for all fuels.

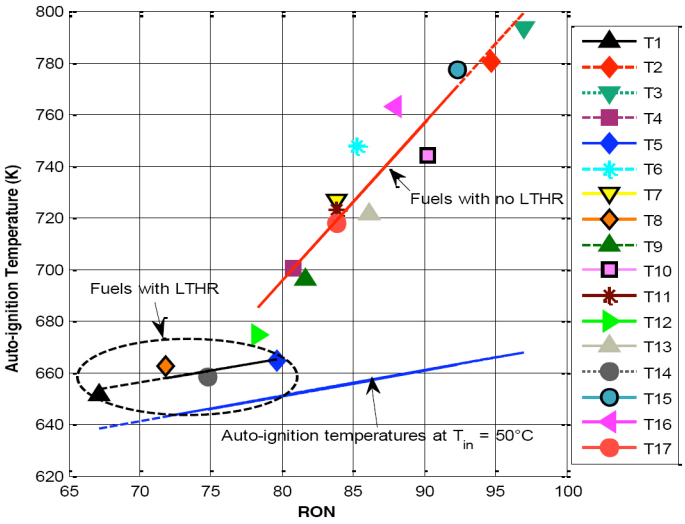

Figure 18. The red line is a best fit for the fuels with no LTHR at 150°C (1, 5, 8, and 14 are not included). The black line is for the fuels with LTHR at this inlet air temperature. The blue line is the best fit at T_{in}=50°C, same as in Figure 17.

Pressure Sensitivity

The different resistances to auto-ignition of the fuels result in different compression ratios required for auto-ignition at a constant CA50, as shown in Figure 19. A temperature model according to [13] accounting for heating from mixing with hot residuals and from heating in the intake was used to calculate T_{IVC} (shown in Figure 19) from the inlet air temperature.

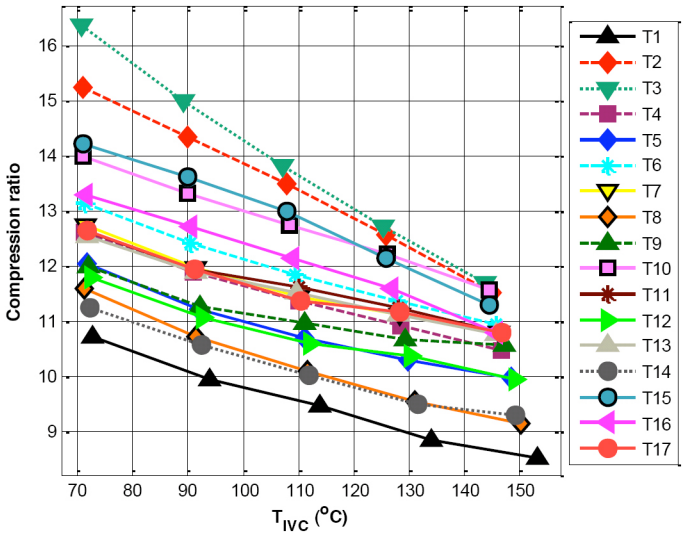

Figure 19. Temperature in cylinder at IVC with corresponding compression ratios for keeping CA50 constant. The five marks for each fuel correspond to the five different inlet air temperatures.

Figure 20 and 21 shows the compression ratio required to keep a constant CA50 at the different inlet air temperatures and the measured RON and MONs for the fuels, respectively. The five data points for each fuel represent the different inlet air temperatures, where a lower inlet air temperature requires a higher compression ratio. It can be noted that the fuels with the highest amount of toluene tested (from left; 8, 4, 6, 10, 3) differ from the rest of the fuels by requiring a slightly higher compression ratio than is indicated by the measured RON. This effect is even more pronounced for the plots of CR vs. MON in Figure 21, see the dashed arrows.

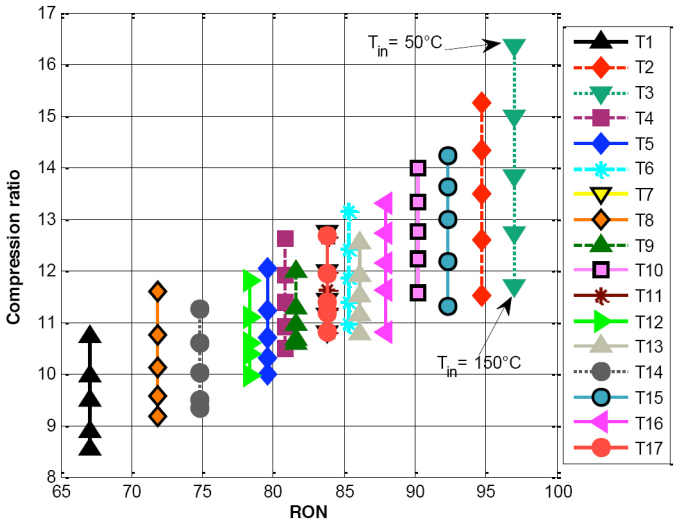

Figure 20. Measured RON and corresponding compression ratios. The five marks for each fuel correspond to the five different inlet air temperatures.

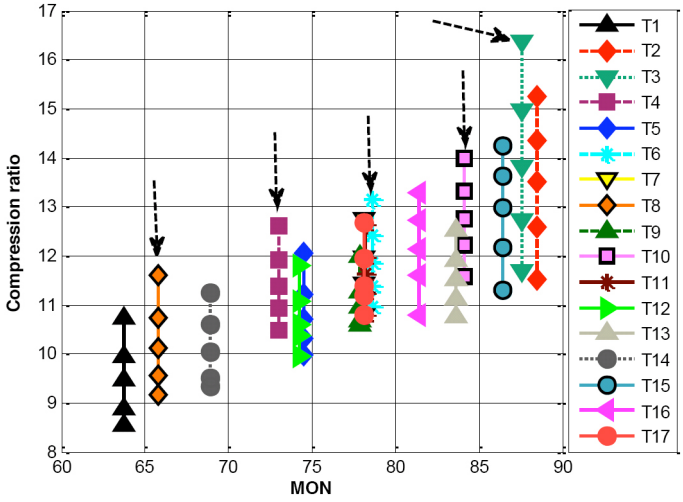

Figure 21. Measured MON and corresponding compression ratios. The five marks for each fuel correspond to the five different inlet air temperatures. Arrows mark the fuels with the highest concentration of toluene.

The sensitivity of the fuel, given by the difference between the fuels RON and MON, has been said to correlate with the engine performance. This however is not observed in the current results, shown as the scatter in Figure 22. For example at a S value of 6 there is a wide range in both the compression ratio and the compression ratio difference. A slight tendency that a higher S requires a greater change in compression ratio is indicated.

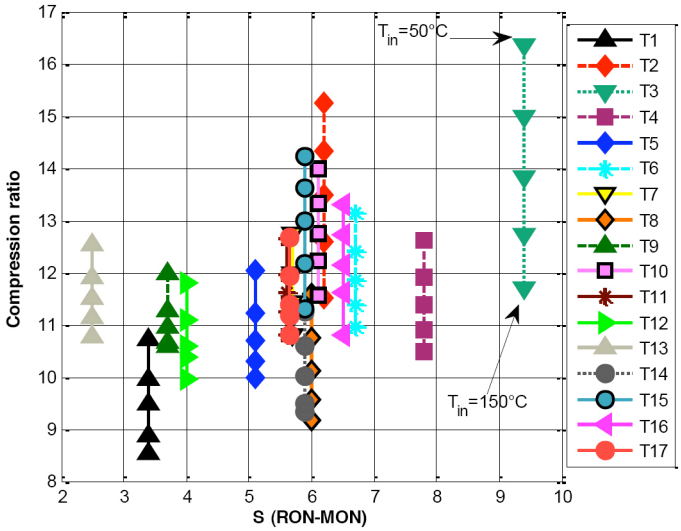

Figure 22. Compression ratio compared with sensitivity (RON-MON). The five marks for each fuel correspond to the five different inlet air temperatures.

The sensitivity of the fuel was connected to high amounts of ethanol. The four fuels with the highest sensitivity all have the maximum amount of ethanol. The same response can be seen for the fuels with low ethanol concentrations, which have low sensitivity.

Blending Octane Number

The measured octane number was compared to a calculated octane number based on the volume fractions of the different components. The ON of the fuel blends was calculated from the pure components according to x*0+y*108.6+z*120+(1-xy-z)*100=ON where x, y, and z refer to the volume% and the multipliers (0,108.6, 120, and 100) refer to the RON's of pure n-heptane, ethanol, toluene, and iso-octane, respectively. Results are represented in Figure 23 by the triangles. The match isn't very good as evidenced by the distance of the triangles from the 45° line. The calculated RONs are all lower than the measured RONs. For gasoline blends, it is known that components such as ethanol can increase the octane number of the blend more than expected based on the octane number of the pure component. This is the basis of "blending octane numbers". By assuming a linear decrease in amount of LTHR with octane rating as have been seen for PRFs, an ON of 190 for ethanol was found [19]. Using this value as the "blending octane" RON for ethanol in the TERFs, calculated octane values shown by the squares in

Figure 23 are obtained. These values appear to be fit by a straight line that is very close to the 45° line.

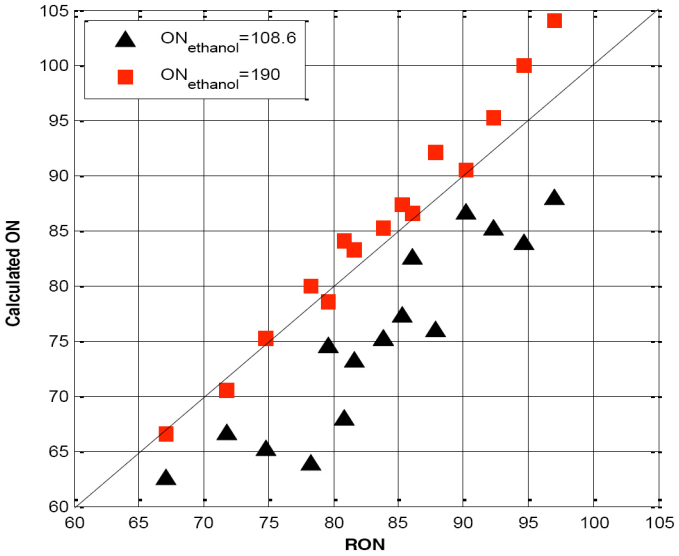

Figure 23. Comparison between measured RON and calculated ON.

Start of Combustion CAD

CAD at start of ignition is shown in Figure 24 as a function of inlet valve closing temperature (T_{IVC}, which is related to inlet air temperature). As an effect of the constant CA50, this is related to the combustion duration, where an earlier start of combustion indicates a longer duration of LTHR. Fuels having LTHR at all inlet air temperatures appear to be fit straight lines, with CAD at auto-ignition advancing as T_{in} and T_{IVC}, increase (see Figure 2). When LTHR disappears, the CAD at auto-ignition retards and the curves shift to the right at the temperatures increase, see example for fuel T2 in Figure 5.

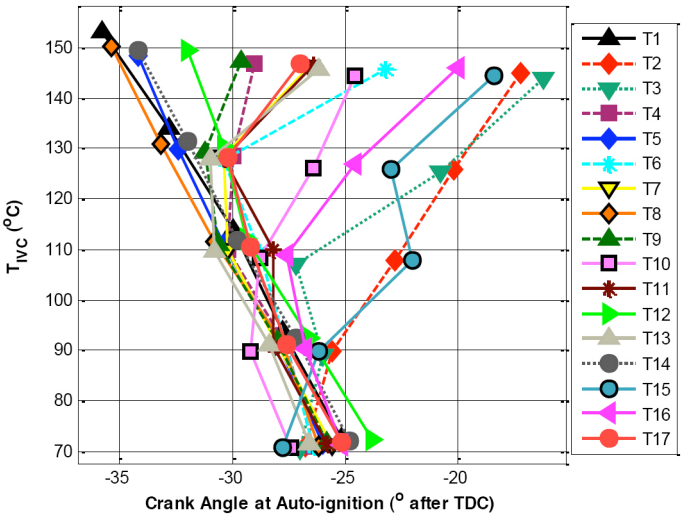

Figure 24. CAD at start of combustion.

ERROR ANALYSIS

Repeatability

The error analysis is made to see the errors originating from the fuel blending, the experimental and measurement uncertainties, and the analysis. The center point was repeated three times (Fuel T7=T11=T17). The LTHR percentages are shown in Figure 25, and the agreement is good. The autoignition temperatures in Figures 26 and 27 show only slight variations.

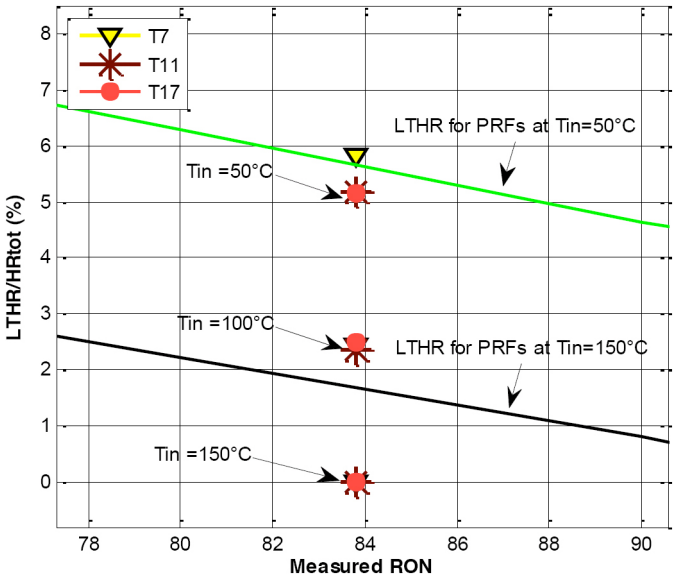

Figure 25. Amount of LTHR for the repetitions. Zero means no LTHR at shown temperature.

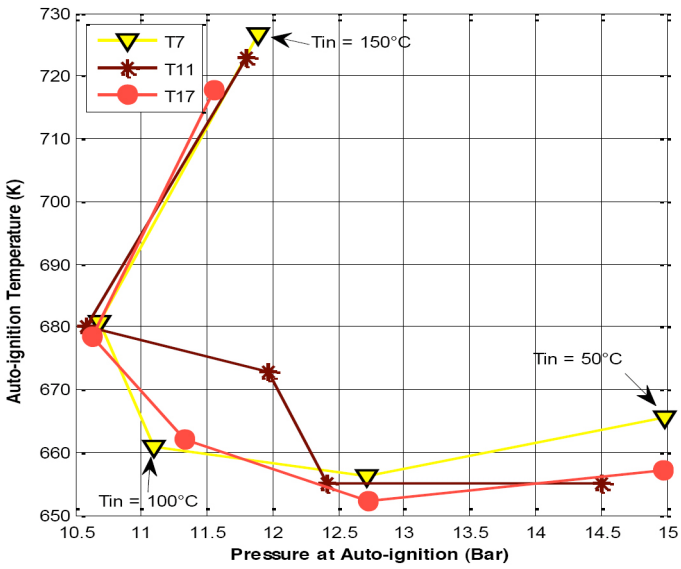

Figure 26. Auto-ignition temperatures and pressures for the repetitions, SOC defined as 0.2 J/CAD.

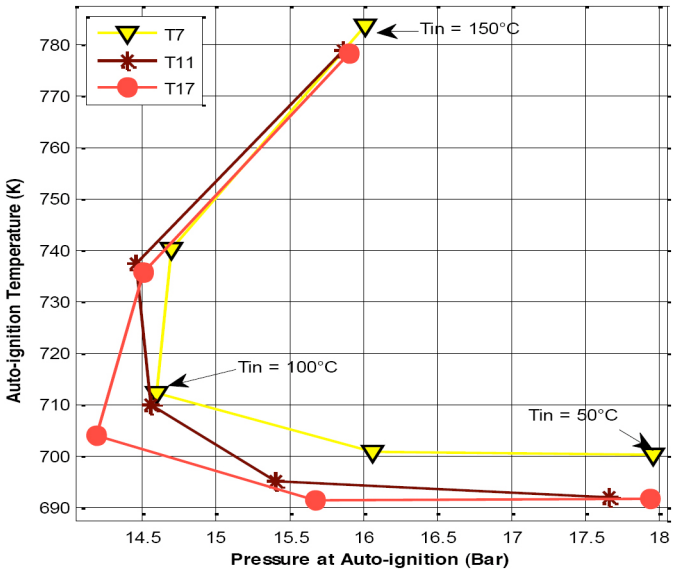

Figure 27. Auto-ignition temperatures and pressures for the repetitions, SOC defined as 1 % burnt.

SUMMARY AND CONCLUSIONS

Gasoline surrogate blends consisting of n-heptane, isooctane, toluene, and ethanol (TERFs) was studied in HCCI combustion. The inlet air temperature (T_{in}) was varied to achieve different cylinder pressures. The effects of fuel properties on auto-ignition temperatures (AIT) and amount of low temperature heat release (LTHR) were studied. The experiments were run in a CFR engine at an engine speed of 600 rpm.

Ethanol was found to increase the AIT while n-heptane was shown to decrease the AIT. Toluene was not found to affect the temperature and pressure at auto-ignition when ethanol was present. Toluene was however found to increase the auto-ignition temperature for TRFs (blends of n-heptane, iso-octane, and toluene).

In the TRF blends toluene acted as a LTHR inhibitor. A weak LTHR quenching effect of toluene was seen in the blends containing the lowest concentration of ethanol, but no quenching effect from toluene was seen on fuels with high concentrations of ethanol. Ethanol was shown to quench LTHR in the TERFs.

The higher blending RON of ethanol found in a previous publication by the authors was found to correlate well with the measured RON values of the TERFs. The amount of LTHR could be described by a linear function of the measured RON, a separate line at each inlet air temperature, with less LTHR at a higher inlet air temperature.

Ethanol addition was found to increase the fuel sensitivity (RON-MON).

Required compression ratio was found to increase with RON and MON, but not linearly. The fuels containing the highest concentrations of toluene required a higher compression ratio than expected from the MON, compared to the other fuels. No clear connection was seen between RON, MON, or S and the compression ratio change needed to keep constant combustion phasing.

REFERENCES

1. Liu, H., Yao, M., Zhang, B., Zheng, Z., 2009, "Influence of Fuel and Operating Conditions on Combustion Characteristics of a Homogenous Charge Compression Ignition Engine", Energy & Fuels, 23, pp. 1422-1430

2. Kalghatgi, G., "Auto-Ignition Quality of Practical Fuels and Implications for Fuel Requirements of Future SI and HCCI Engines," SAE Technical Paper 2005-01-0239, 2005, doi: 10.4271/2005-01-0239.

3. Shibata, G. and Urushihara, T., "Auto-Ignition Characteristics of Hydrocarbons and Development of HCCI Fuel Index," SAE Technical Paper 2007-01-0220, 2007, doi: 10.4271/2007-01-0220.

4. Shibata, G., Oyama, K., Urushihara, T., and Nakano, T., "Correlation of Low Temperature Heat Release With Fuel Composition and HCCI Engine Combustion," SAE Technical Paper 2005-01-0138, 2005, doi: 10.4271/2005-01-0138.

5. Tanaka, S., Ayala, F., Keck, J.C., Heywood, J.B., 2003, "Two-stage ignition in HCCI combustion and HCCI control by fuels and additives", Combustion and Flame, 132, pp. 219-239

6. Aroonsrisopon, T., Sohm, V., Werner, P., Foster, D. et al., "An Investigation Into the Effect of Fuel Composition on HCCI Combustion Characteristics," SAE Technical Paper 2002-01-2830, 2002, doi: 10.4271/2002-01-2830.

7. Warnatz, J., Maas, U., Dibble, R.W., 2006, "Combustion Physical and Chemical Fundamentals, Modeling and Simulation, Experiments, Pollutant Formation", Springer, Berlin

8. Hosseini, V., Neill, W., and Chippior, W., "Influence of Engine Speed on HCCI Combustion Characteristics using Dual-Stage Autoignition Fuels," SAE Technical Paper 2009-01-1107, 2009, doi: 10.4271/2009-01-1107.

9. Silke, E., Pitz, W., Westbrook, C., Sjöberg, M. et al., "Understanding the Chemical Effects of Increased Boost Pressure under HCCI Conditions," *SAE Int. J. Fuels Lubr.* 1(1):12-25, 2009, doi: 10.4271/2008-01-0019.

10. Sjöberg, M., Dec, J.E., 2011, "Effects of EGR and its constituents on HCCI autoignition of ethanol", Proceedings of the Combustion Institute 33, pp. 3031-3038

11. Sjöberg, M. and Dec, J., "EGR and Intake Boost for Managing HCCI Low-Temperature Heat Release over Wide

Ranges of Engine Speed," SAE Technical Paper 2007-01-0051, 2007, doi: 10.4271/2007-01-0051.

12. Andrae, J.C.G., Head, R.A., 2009, "HCCI experiments with gasoline surrogate fuels modeled by a semidetailed chemical kinetic model", Combustion and Flame, 156, pp. 842-851

13. Truedsson, I., Tuner, M., Johansson, B., and Cannella, W., "Pressure Sensitivity of HCCI Auto-Ignition Temperature for Primary Reference Fuels," *SAE Int. J. Engines* 5(3):1089-1108, 2012, doi: 10.4271/2012-01-1128.

14. Lü, X., Ji, L., Zu, L., Hou, Y., Huang, C., Huang, Z., 2007, "Experimental study and chemical analysis of n-heptane homogeneous charge compression ignition combustion with port injection of reaction inhibitors", Combustion and Flame, 149, pp. 261-270

15. Floweday, G., "A New Functional Global Autoignition Model for Hydrocarbon Fuels - Part 1 of 2: An Investigation of Fuel Auto-Ignition Behaviour and Existing Global Models," *SAE Int. J. Fuels Lubr.* 3(2):710-724, 2010, doi: 10.4271/2010-01-2161.

16. Machado, G.B., Barros, J.E.M., Braga, S.L., Braga, C.V.M., Oliviera, E.J., Silva, A.H.M.F.T., Carvalho, L.O., 2011, "Investigation on surrogate fuels for high-octane oxygenated gasolines", Fuel, 90, pp. 640-646

17. Pitz, W., Cernansky, N., Dryer, F., Egolfopoulos, F. et al., "Development of an Experimental Database and Chemical Kinetic Models for Surrogate Gasoline Fuels," SAE Technical Paper 2007-01-0175, 2007, doi: 10.4271/2007-01-0175.

18. Sakai, Y., Ozawa, H., Ogura, T., Miyoshi, A. et al., "Effects of Toluene Addition to Primary Reference Fuel at High Temperature," SAE Technical Paper 2007-01-4104, 2007, doi: 10.4271/2007-01-4104.

19. Truedsson, I., Johansson, B., Tuner, M., Cannella, B., 2012, "Pressure sensitivity of HCCI auto-ignition temperatures for oxygenated reference fuels", ASME ICEF 2012-92074

20. Morgan, N., Smallbone, A., Bhave, A., Kraft, M., Cracknell, R., Kalghatgi, G., 2010, "Mapping surrogate gasoline compositions into RON/MON space", Combustion and Flame, 157, pp.1122-1131

CONTACT INFORMATION

Corresponding author,

ida.truedsson@energy.lth.se

ACKNOWLEDGMENTS

The authors gratefully acknowledge Chevron for their financial support. Patrick Borgqvist is acknowledged for designing the engine control system.

DEFINITIONS/ABBREVIATIONS

AIP - auto-ignition pressure

AIT - auto-ignition temperature

ATDC - after top dead center

BTDC - before top dead center

CA 50 - crank angle for 50 % of total heat release

CAD - crank angle degree

CFR - cooperative fuel research

EGR - exhaust gas recirculation

HTR - high temperature reactions

HTHR - high temperature heat release

IVC - inlet valve closing

LTR - low temperature reactions

LTHR - low temperature heat release

$LTHRR_{max}$ - maximum low temperature heat release rate

$LTHRR_{min}$ - minimum rate of heat release between LTHR and HTHR

MON - motor octane number

ON - octane number

PRF - primary reference fuel

RON - research octane number

S - fuel sensitivity, S = RON-MON

SOC - start of combustion

TDC - top dead center

T_{in} - inlet air temperature, measured

T_{IVC} - temperature in the cylinder at inlet valve closing, calculated from T_{in}

TWC - three way catalyst

The Engineering Meetings Board has approved this paper for publication. It has successfully completed SAE's peer review process under the supervision of the session organizer. This process requires a minimum of three (3) reviews by industry experts.

ISSN 0148-7191

SAE Customer Service:
Tel: 877-606-7323 (inside USA and Canada)
Tel: 724-776-4970 (outside USA)
Fax: 724-776-0790
Email: CustomerService@sae.org
SAE Web Address: http://www.sae.org
Printed in USA

Paper IV

Emission Formation Study of HCCI Combustion with Gasoline Surrogate Fuels

2013-01-2626

Published
10/14/2013

Ida Truedsson, Martin Tuner, and Bengt Johansson
Lund University

William Cannella
Chevron

doi:10.4271/2013-01-2626

ABSTRACT

HCCI combustion can be enabled by many types of liquid and gaseous fuels. When considering what fuels will be most suitable, the emissions also have to be taken into account. This study focuses on the emissions formation originating from different fuel components.

A systematic study of over 40 different gasoline surrogate fuels was made. All fuels were studied in a CFR engine running in HCCI operation. Many of the fuels were blended to achieve similar RON's and MON's as gasoline fuels, and the components (n-heptane, iso-octane, toluene, and ethanol) were chosen to represent the most important in gasoline; nparaffins, iso-paraffins, aromatics and oxygenates. The inlet air temperature was varied from 50°C to 150°C to study the effects on the emissions. The compression ratio was adjusted for each operating point to achieve combustion 3 degrees after TDC. The engine was run at an engine speed of 600 rpm, with ambient intake air pressure and with an equivalence ratio of 0.33.

NO_x emissions were low for all operating points, and ethanol and toluene addition was found to decrease NO_x emissions for higher octane fuels. CO emissions were related to in-cylinder temperature by formation from HC and oxidation to CO_2. HC emissions were found to be mainly dependent on the compression ratio used in each case. Ethanol addition was shown to reduce HC emissions for combustion at a given compression ratio. Toluene addition was found to increase HC emissions at a given CR when high concentrations (40-60 vol.%) were added. Low concentrations of toluene showed a small decrease of or no effect on HC emissions.

INTRODUCTION

Since gasoline fuel contains hundreds of different components, surrogate fuels are often used to be able to pinpoint the effect of different fuel components of a well specified fuel. Pitz et al. [1] reviews the development of surrogate fuels particularly for HCCI combustion and concludes that the three necessary components of any gasoline fuel surrogate are n-heptane, isooctane and toluene. Toluene is typically the most common aromatic in gasoline. They rated different gasoline surrogate fuel components and placed ethanol, 1-pentene, di-isobutylene and xylene at the secondary importance level. Currently, ethanol is usually added to gasoline as a renewable fuel. US and Swedish gasoline both contain up to 10 vol.% ethanol, and this amount is expected to increase in the future. Machado et al. [2] compared different gasoline surrogate fuels in an SI engine to find a suitable fuel to represent high ethanol (20 vol.%) gasoline. They concluded that mixtures of n-heptane, iso-octane, toluene and ethanol could be used as surrogate fuels for oxygenated gasoline.

Research on HCCI combustion started in the 1970's and much work has been performed on emissions formation. Nitrogen oxides, NO and NO_2, (here combined to NO_x) are mainly formed at temperatures above 1800 K where the formation can be described by the Zeldovich mechanism for thermal NO_x. There are other paths leading to NO_x formation such as fuel NO_x, prompt NO_x and formation via nitrous oxide, where the latter is more likely at lean premixed conditions [3].

Unburned hydrocarbons (HC) and carbon monoxide (CO) result from incomplete combustion in crevices and in the bulk gas [4,5,6]. In reference [7], unreacted fuel was found to be the

most dominant component in HC emissions. High dilution is thermodynamically favorable, but very diluted charges leads to incomplete combustion, which is further studied in [7]. Limiting HC and CO emissions in-cylinder is important since the low exhaust temperatures from HCCI combustion are a challenge for conventional oxidation catalysts.

For carbon monoxide, the required temperature for oxidation to CO_2 is from 1400 to 1500 K. This temperature has been found to be independent of fuel type and auto-ignition characteristics [8]. In reference [9] different ways to decrease HC and CO emissions of a HCCI engine were studied, and it was reported that an early combustion phasing was needed and that this could be combined with the use of EGR. They also reported that N_2O emissions were higher than NO_x in lean operations at equivalence ratios under 0.30.

The goal of the current study is to further understand emissions formation in HCCI combustion, to see if the different components of gasoline fuel can be associated with certain emissions, and to try to separate physical effects related to compression ratio from kinetic effects. This knowledge could be useful when proposing a suitable fuel for HCCI engines. Since emissions formation is a result of the in-cylinder conditions, a heat release analysis was done to help explain the emissions.

In this paper, NO_x, HC, and CO emission behavior are first studied separately based on the in-cylinder conditions. Then the effect on emissions from different fuel components and fuel octane rating is studied. The combustion efficiency combining HC and CO emissions are discussed, and last a few fuels showing different emission compromises are shown.

EXPERIMENTAL SETUP

A Waukesha variable compression ratio Cooperative Fuel Research (CFR) engine was used for the experiments. This type of engine is typically used for measuring the RON and MON of gasoline. The setup included an air-fuel mixture heater mounted downstreams from the port fuel injector. A scale was used for measuring the fuel flow. The heat release was calculated from the pressure trace measured with a Kistler piezoelectric pressure transducer mounted in the cylinder. An intake air refrigerator was included in the setup to ensure constant air humidity throughout the experiments. Temperature of the air-fuel mixture (T_{in}) was measured by a thermocouple placed in the inlet, close to the inlet valve. The spark ignition was switched off. The engine specifications are listed in Table 1. HC, CO, CO_2, and NO_x emissions were measured with a Horiba Mexa 7500 analyzer system. Equivalence ratio was calculated from the measured emissions.

Table 1. Specifications for CFR engine.

Displacement volume	612 cm^3
Number of cylinders	1
Bore	83 mm
Stroke	114 mm
CR	Variable (4:1 to 18:1)
Number of valves	2
Length of connecting rod	254 mm
Intake valve opens	10°ATDC±2,5°
Intake valve closes	146°BTDC±2,5°
Exhaust valve opens	140°ATDC±2,5°
Exhaust valve closes	15°ATDC±2,5°
Valve lifts	6,25 mm
Valve diameters	9,53 mm
Engine speed	600 rpm
Fuel supply	Port injection

FUELS

The fuel matrices listed in Tables 2, 3, 4 were used in the experiments. The matrices consisted of blends of iso-octane, n-heptane, toluene, and/or ethanol. A fuel matrix consisting of primary reference fuel (PRF), blends of n-heptane and isooctane (PRF 0, 20, 40, 60, 80, 85, 90, 95, and 100) was also studied, but not shown in the tables since the vol.% iso-octane and both RON and MON are well known and given by the number of the PRF. Blends of n-heptane, toluene, and isooctane are referred to as toluene reference fuels, TRF. Blends of n-heptane, iso-octane, and ethanol are referred to as ethanol reference fuels, ERF. Blends of n-heptane, iso-octane, toluene, and ethanol are referred to as toluene ethanol reference fuels, TERF.

The sensitivity of the fuels, calculated by the difference between the RON and MON (S=RON-MON), is given in Tables 2 and 4. Stoichiometric air-fuel ratios (AFR_s) are given in Table 5 in Appendix.

Table 2. Toluene reference fuel matrix (TRF). *RON and MON calculated from correlation by Morgan et al. [10].

Fuel	n-Heptane (vol.%)	Toluene (vol.%)	iso-Octane (vol.%)	RON*	MON*	S
H20T10	20	10	70	83,1	81,1	2,0
H20T20	20	20	60	85,9	81,9	4,0
H20T40	20	40	40	90,3	83,0	7,3
H20T60	20	60	20	93,9	84,1	9,8

Table 3. Ethanol reference fuel matrix (ERF).

Fuel	n-Heptane (vol.%)	iso-Octane (vol.%)	Ethanol (vol.%)
PRF80	20	80	0
H20E1	20	79	1
H20E5	20	75	5
H20E10	20	70	10
H20E20	20	60	20
PRF70	30	70	0
H30E1	30	69	1
H30E5	30	65	5
H30E10	30	60	10
H30E20	30	50	20
H60E40	60	0	40
H55E45	55	0	45
H50E50	50	0	50
H45E55	45	0	55
H40E60	40	0	60

Table 4. Toluene ethanol fuel matrix (TERF).

Fuel	n-Hept (vol.%)	Toluene (vol.%)	Ethanol (vol.%)	iso-Oct (vol.%)	RON	MON	S
T1	40	10	5	45	67,1	63,7	3,4
T2	20	10	20	50	94,7	88,5	6,2
T3	20	30	20	30	97	87,6	9,4
T4	40	30	20	10	80,8	73	7,8
T5	30	20	5	45	79,6	74,5	5,1
T6	30	30	12,5	27,5	85,3	78,6	6,7
T7	30	20	12,5	37,5	83,8	78,1	5,7
T8	40	30	5	25	71,8	65,8	6
T9	30	10	12,5	47,5	81,6	77,9	3,7
T10	20	30	5	45	90,2	84,1	6,1
T11	30	20	12,5	37,5	83,8	78,2	5,6
T12	40	10	20	30	78,3	74,3	4
T13	20	10	5	65	86,1	83,6	2,5
T14	40	20	12,5	27,5	74,8	68,9	5,9
T15	20	20	12,5	47,5	92,3	86,4	5,9
T16	30	20	20	30	87,9	81,4	6,5
T17	30	20	12,5	37,5	-	-	-

METHOD

The CFR engine is ideal for fuel emission studies, in the sense that conditions such as compression ratio can be varied to maintain a constant, acceptable combustion phasing for all fuels. Emissions formation is very dependent on in-cylinder temperature, and therefore also combustion timing. To get more useful information from the emission analysis the emissions were related to the cylinder temperature. The CFR engine might give more HC emissions from the crevice losses due to the variable compression ratio (VCR) mechanism and design. It is not designed for low HC emissions but it is a standardized engine.

Each fuel was tested at five different inlet air temperature levels from 50° to 150°C (323 to 423 K), a total of 85 operating points. At each temperature a combustion phasing with CA50 at 3±1° after TDC was established by changing the compression ratio. Motored pressure traces were extracted for all data points for validation. The engine was run naturally aspirated. The fuel amount was adjusted for each operating condition to achieve an equivalence ratio of 0.33. This was chosen since a diluted charge is needed in HCCI combustion to keep the pressure rise rate at an acceptable level. All experiments were run at a constant engine speed of 600 rpm. No exhaust gas recirculation (EGR) was used.

Heat Release Calculations

The Woschni heat transfer model [11] was used, and the motored heat release was subtracted from the fired heat release to reduce measurement and model errors. This model requires the in-cylinder temperature at the inlet valve closing. This temperature was calculated from the measured temperature in the intake by applying a model for the temperature change due to mixing with hot internal residuals, and also heating from the intake walls between the temperature probe mounted just before the intake, and the cylinder. All heat release figures are based on the average of 300 cycles. All emission numbers are based on 50 subsequent measurement points with an interval of about a second between each. The heat release calculations are described in more detail in [12,13].

ERROR ANALYSIS

Equivalence Ratio

By using fuel properties and the measured emissions the equivalence ratio could be calculated for all operating points. The set value was an equivalence ratio of 0.33 for all operating points, but the calculated equivalence ratio after post processing was observed to be slightly higher for the ERFs (0.33-0.35). No correction factor was used when measuring the HC emissions for fuels containing ethanol, which may introduce an uncertainty. The two TRF fuels containing the highest amounts of toluene (H20T40 and H20T60) also showed a larger scatter in equivalence ratios, for the former fuel an equivalence ratio of around 0.32, and for the latter an equivalence ratio of 0.37. Two measurement points for fuel T8 in the TERF matrix was found to have a higher equivalence ratio of around 0.35, and were therefore shown in the results with a dashed line.

Repeatability

Emissions from repetitions of a toluene ethanol reference fuel are shown in Figure 1 (tests T7, T11, T17). The wide spread in HC and CO emissions for an inlet air temperature of 100°C in Figure 1a indicates a measurement error in one of the experiments. The wider spread at lower inlet air temperatures indicates larger cycle-to-cycle variations at these operating conditions, and more stable combustion at the higher inlet air temperatures. NO_x emissions and used compression ratio values in Figure 1b show good repeatability, even at 100°C.

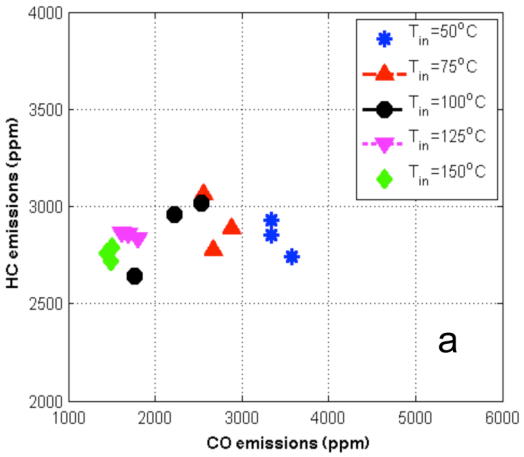

Figure 1. a) Repeatability of HC and CO emissions. b) Repeatability of NO_x emissions and compression ratio. Toluene ethanol reference fuel tests T7, T11, and T17, all with the same composition.

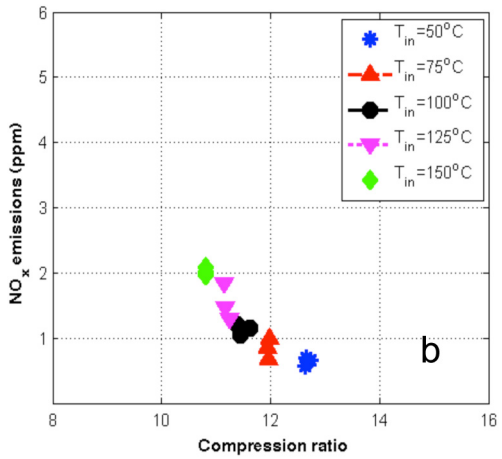

Figure 1. (cont.) a) Repeatability of HC and CO emissions. b) Repeatability of NO_x emissions and compression ratio. Toluene ethanol reference fuel tests T7, T11, and T17, all with the same composition.

RESULTS AND DISCUSSION

NO_x Emissions

NO_x emissions for the PRFs are shown in Figure 2a. No operating point reaches a temperature of 1800 K or above, where the thermic NO_x formation speeds up due to the Arrhenius behavior of the rate limiting reaction, which has a high activation energy. Therefore the NO_x formation should be described either by the prompt NO_x reaction paths, or, since these experiments were performed in lean premixed combustion, by NO_x generated via nitrous oxides (N_2O) [3].

It should be noted that the presented temperature is a global in-cylinder temperature calculated from the pressure trace, and there might be a temperature gradient in the cylinder, and therefore the maximum temperature can be underpredicted in the global temperature calculation.

High octane number fuel PRF 100 shows higher NO_x emissions than PRF 0, which might be connected to higher maximum temperatures for higher octane rated fuels. NO_x emissions for all toluene ethanol reference fuels (TERF) are shown in Figure 2b, and these fuels show lower NO_x emissions than the PRFs with an octane rating over 80, indicating that toluene and/or ethanol addition lowers NO_x emissions. Despite the variation, NO_x emissions were low for all fuels, especially at the lower inlet air temperature conditions. In Figure 2b, for any given intake air temperature, a higher cylinder temperature appears to result in higher NO_x emissions.

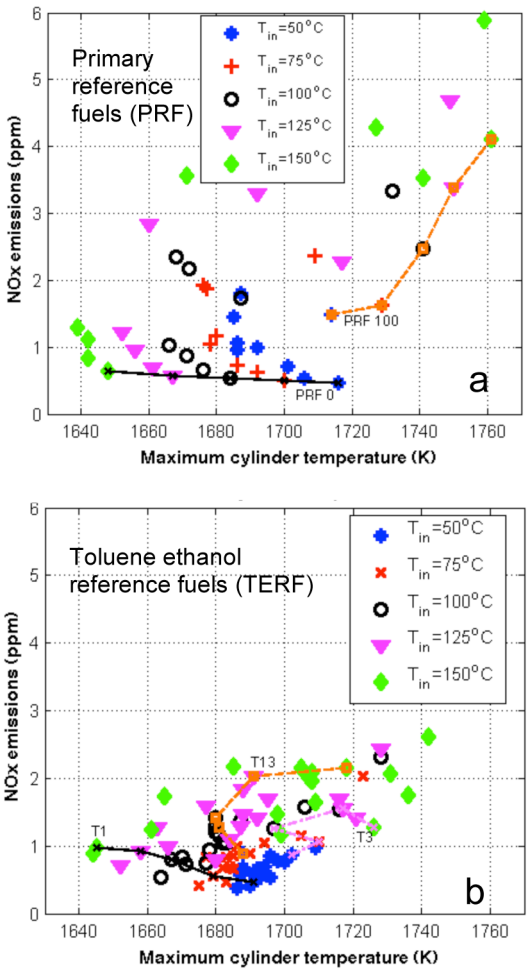

Figure 2. $T_{cyl,max}$ and NO_x emissions.

HC Emissions

HC emissions for the PRFs and TERFs as a function of the maximum cylinder temperature are plotted in Figure 3. HC emissions might be expected to decrease with increased cylinder temperature, as is the case for the 50°C inlet air temperature operating points. This trend seems to be true for all inlet air temperatures for the lower octane PRFs (PRF 0 to PRF 60), but not for the high octane PRFs as seen for PRF 100 in Figure 3a, showing high HC emissions even though the calculated maximum cylinder temperature is relatively high. The high octane number fuels require a higher compression ratio, which might be the reason for the HC emissions. The TERFs in Figure 3b indicates that a higher maximum cylinder temperature gives higher HC emissions, which again indicates that the global maximum temperature is not the main effect for HC oxidation, since a higher temperature should oxidize and decrease HC emissions.

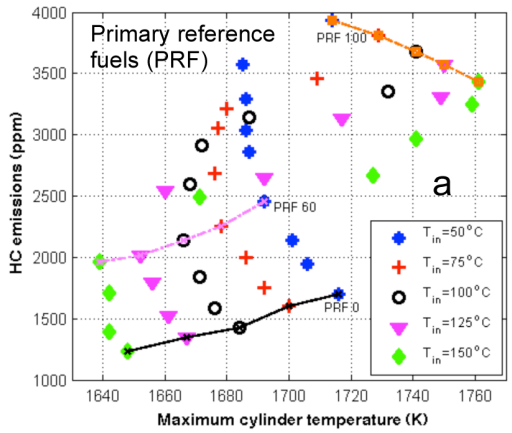

Figure 3. $T_{cyl,max}$ and HC emissions for various inlet air temperatures.

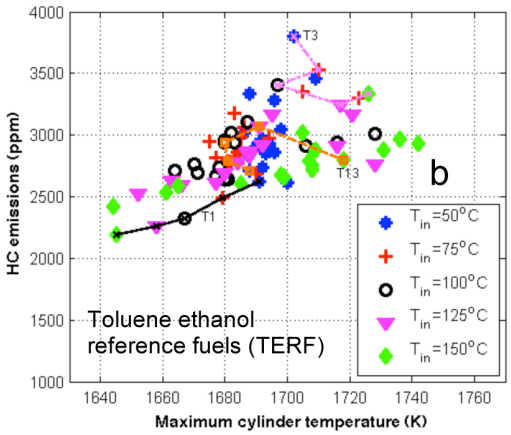

Figure 3. (cont.) $T_{cyl,max}$ and HC emissions for various inlet air temperatures.

The HC emissions from the PRFs, TRFs, ERFs, and TERFs are plotted vs. compression ratio in Figures 4 a, b, c, d, respectively. In addition, plots of all of the fuels are overlayed in Figure 5. As seen in Figure 4a, HC emissions for the PRFs are proportional to the compression ratio. This is expected due to the relative importance of the crevice volumes. At a higher compression ratio a larger portion of the air and fuel mixture will be found in the crevices during the combustion event, where the temperature is not high enough for oxidation. The HC emissions can be described by a separate linear correlation at each inlet air temperature. Deviations from this line could be expected to have other causes, e.g. fuel effects.

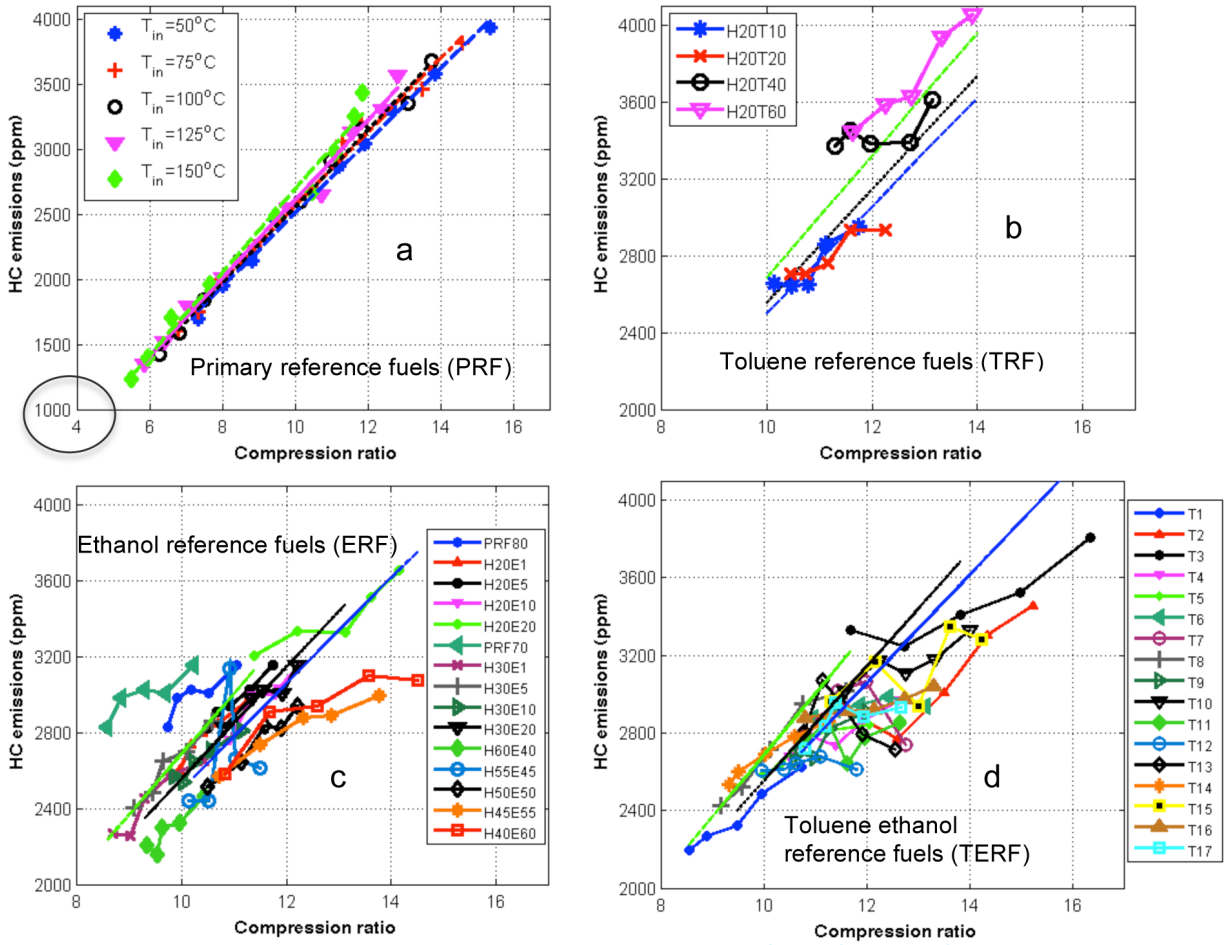

Figure 4. Blue, black and green linear approximations are for primary reference fuels at 50°C, 100°C and 150°C inlet air temperatures respectively, as seen in a Figure 4a.

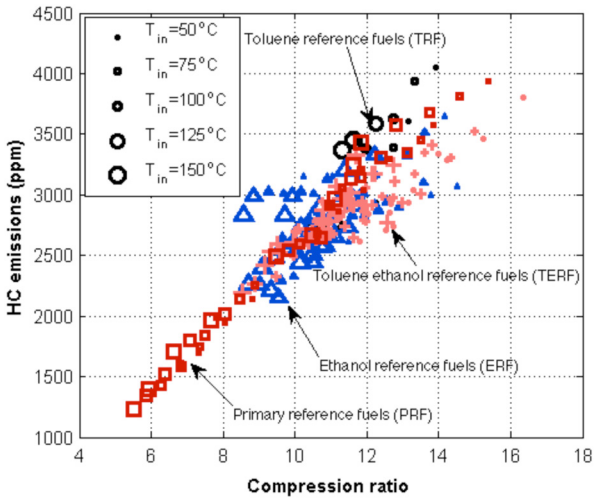

Figure 5. A smaller marker shows a lower inlet air temperature. Four different data sets are included, data for PRF (square), ERF(triangle), TRF (circle), and TERF (cross).

A fuel effect on HC emissions is seen in Figure 5. The PRFs seem to show a narrower span of HC emissions, where HC emissions are based mainly on the compression ratio.

The TRFs containing high amounts of toluene (40 and 60 vol% respectively), show higher amounts of HC emissions at a given compression ratio, see details in Figure 4b. The TRFs containing lower amounts of toluene, however, show similar to or slightly lower HC emissions than a PRF used at the same compression ratio. The TERFs, all containing lower amounts of toluene (10 - 30 vol%), and also containing ethanol, show similar to or lower HC emissions than the PRFs. This would indicate that ethanol and/or addition of low concentrations of toluene leads to a decrease in HC emissions. The decrease from ethanol addition might be due to the oxygen content in the ethanol.

The larger range in HC emissions at a certain compression ratio for TERF compared to PRF indicates a fuel effect from ethanol or toluene. In Figure 4d it can be seen that the fuels below and right to the PRF lines are fuels with high ethanol content and a high octane rating (e.g. fuels T2, T3, T15), whereas the fuels overlapping with the PRF line on the left (e.g. fuels T1, T8, and T14) are low ethanol and low octane number fuels.

The offset between the PRF fuels in the ERF matrix (see Figure 4c, these are repetitions of PRF 70 and PRF 80) can be explained by the slightly higher equivalence ratio for this matrix, as discussed in the error analysis. It can be seen that the two component fuels not containing iso-octane but instead higher amounts of ethanol (e.g. fuels H60E40 to H40E60), show less HC emissions than predicted from the compression ratio alone.

CO Emissions

CO emissions as a function of maximum cylinder temperature for PRF, ERF, TRF, and TERF are plotted in Figures 6, 7, 8. The maximum in-cylinder temperature can be seen to only vary about 100 K between the highest and lowest temperature. The maximum cylinder temperature is relatively low for all operating points, resulting in high levels of CO. For the operating points with an inlet air temperature of 50°C the span between highest and lowest cylinder temperature is even smaller, about 40 K. We should keep in mind that the calculated cylinder temperature assumes an even temperature distribution throughout the combustion chamber, which is a simplification since there will be a slight temperature gradient by the colder cylinder walls, or if the fuel-air mixture is not homogenous. It has been shown that a temperature of 1500 K is needed to oxidize CO into CO_2 [8]. The CO peak at a maximum temperature of about 1700 K indicates a temperature gradient, where some parts of the cylinder have not reached the sufficient temperature for CO oxidation. This inhomogeneity seems to be similar for the different fuel matrices. CO emissions will be a balance of the conversion of HC to CO and the subsequent conversion of CO to CO_2.

On the left side of the CO peak in Figures 6 and 7, the amount of CO decreases with decreased cylinder temperature since the temperature is too low to convert HC into CO, see schematic in Figure 6. For example fuel T1 and T8 (in Figure 8) have low CO emissions at the higher inlet air temperatures, but for these two fuels the HC emissions are instead higher. Because of the low cylinder temperature, these two fuels also show low combustion efficiency as will be shown later. On the right hand side of the CO peak the CO emissions decrease with increasing cylinder temperature since larger fractions of the cylinder will reach a temperature sufficiently high for CO oxidation.

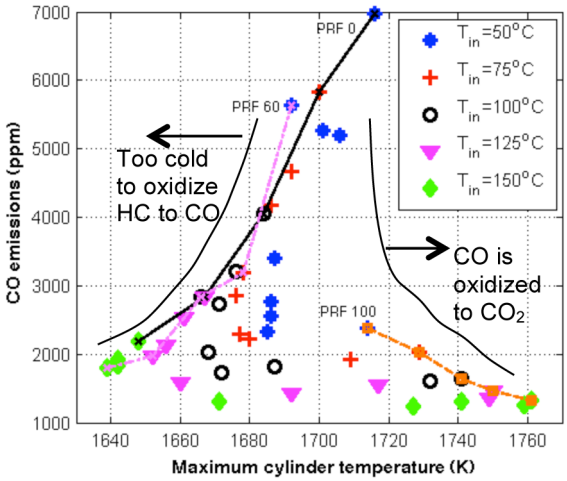

Figure 6. CO emissions and maximum cylinder temperature for primary reference fuels.

The lower CO emissions at a higher inlet air temperature compared to a lower inlet air temperature can be a result of a more uniform temperature distribution in the cylinder, less cooler zones where the temperature is too low for CO oxidation.

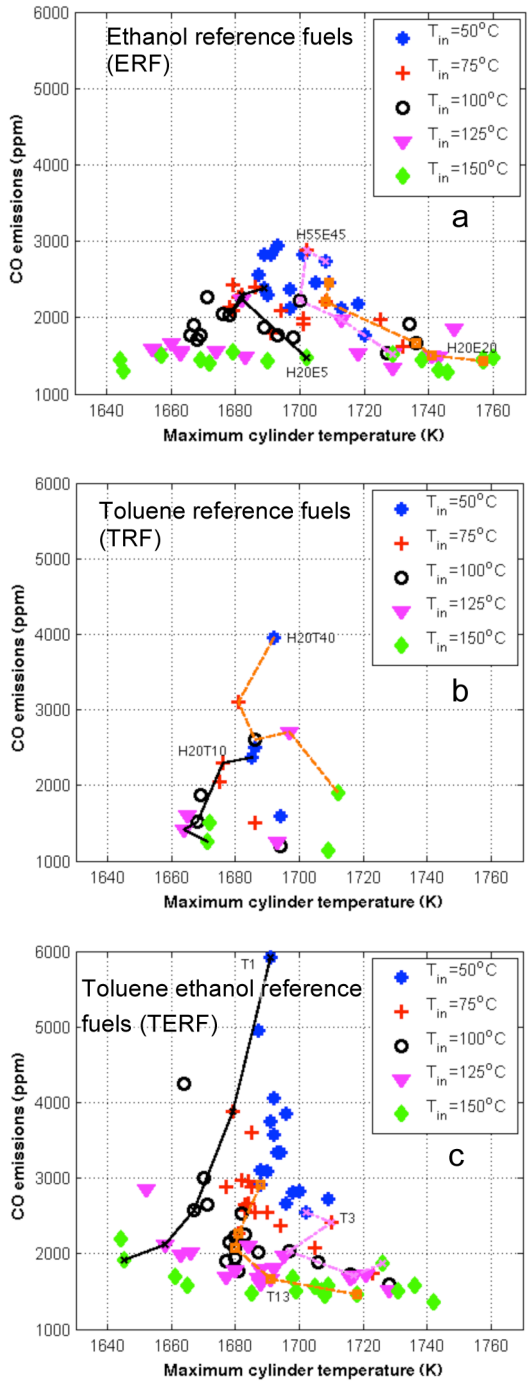

Figure 7. $T_{cyl,max}$ and CO emissions for various inlet air temperatures

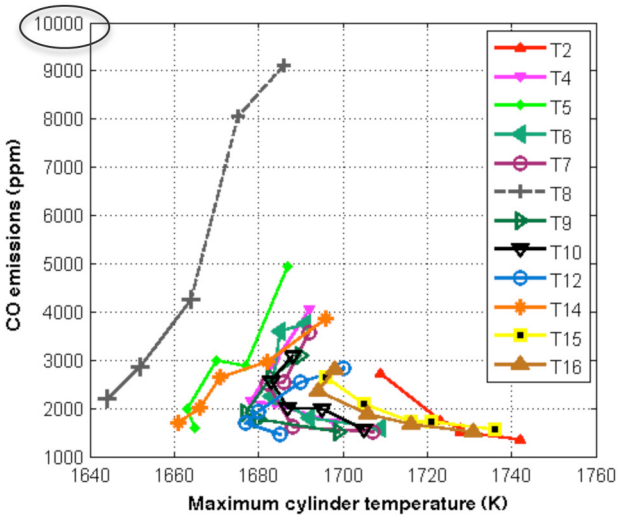

Figure 8. $T_{cyl,max}$ and CO emissions, TERFs. The dashed line connects the two operating points for fuel T8 running at a too high equivalence

Fuel Composition Effects

Ethanol Addition Effect on Emissions

Earlier it was noted that ethanol addition seemed to decrease the HC emissions at a given compression ratio. In Figure 9 the HC emissions for all of the TERF fuels for three different inlet air temperatures (50, 100 and 150°C) are shown. At the three different levels of ethanol shown (5 vol.%, 12.5 vol.%, and 20 vol.% respectively) the amount of the other components varies. The HC emissions seem to be slightly increased for fuels with higher concentrations of ethanol. The scatter indicates that the ethanol addition is not the main source of HC emissions. Since ethanol has a higher RON than many of the other fuel components, it could be the compression ratio increase associated with a higher RON fuel leading to the increased HC emissions. In Figure 10 the trend lines indicates that ethanol addition decreases CO emissions, since the fuels showing the highest amounts of CO are fuels with the lowest amount of ethanol. Ethanol addition shows no particular effect on NO_x emissions, however it can again be noted that the NO_x emissions are low for all fuels.

Toluene Addition Effect on Emissions

From Figures 11 and 12 it was seen that higher concentrations of toluene increased HC emissions. This could, as with the ethanol addition, be explained by the higher compression ratio required for a fuel containing toluene, since toluene has a higher ignition resistance than both n-heptane and iso-octane. There were no clear effects from toluene on either CO or NO_x emissions.

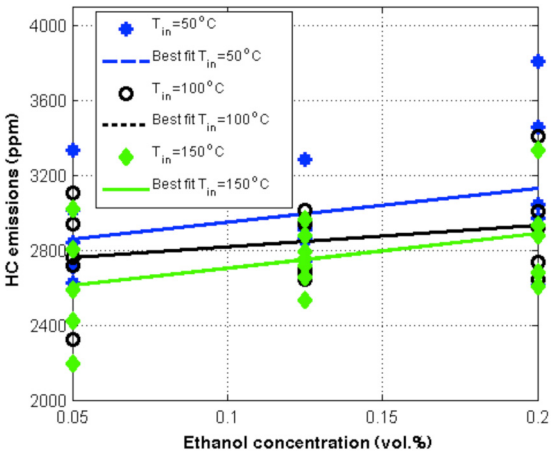

Figure 9. Ethanol effect on HC emissions for TERFs at various inlet air temperatures.

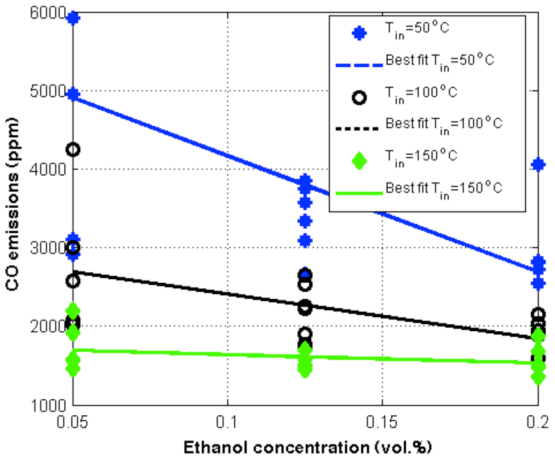

Figure 10. Ethanol effect on CO for TERFs at various inlet air temperatures.

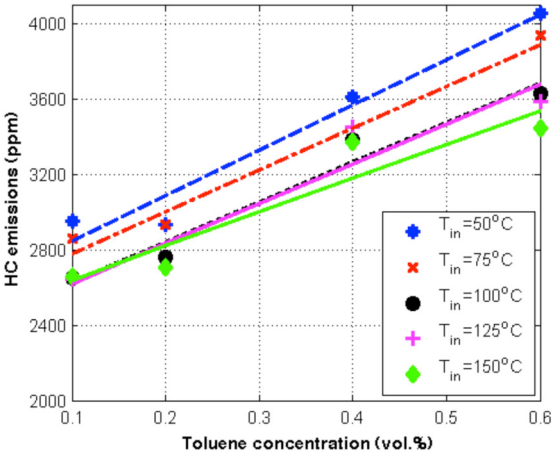

Figure 11. Toluene effect on HC emissions for the TRFs at various inlet air temperatures.

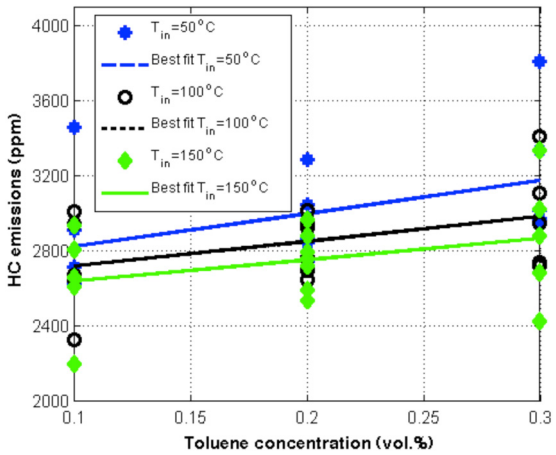

Figure 12. Toluene effect on HC emissions for TERFs at various inlet air temperatures.

Fuel Octane Rating Effects

Fuel octane rating, describing the fuels resistance to autoignition, appears to be correlated to the amount of hydrocarbon emissions, see Figure 13 and 14. From these plots it appears that a higher octane rating of a fuel leads to higher HC emissions. This should be a result from a higher compression ratio giving higher HC emissions as mentioned earlier. Since the octane rating of a PRF directly follows the compression ratio, so do the HC emissions. For the surrogate fuels in Figure 14 there is an overall trend that a higher RON gives higher HC emissions. A few fuels show more variation from this trend, for example RON 72 and RON 95 fuels T8 and T2, respectively. TRF and ERF are not shown since RON's were not measured for these fuels.

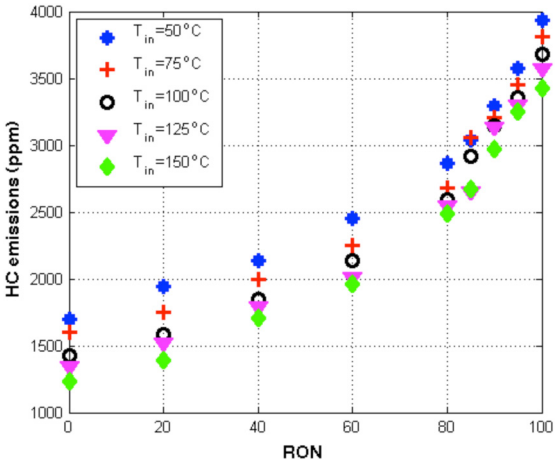

Figure 13. Hydrocarbon emissions as a function of fuel octane rating, PRFs at various inlet air temperatures

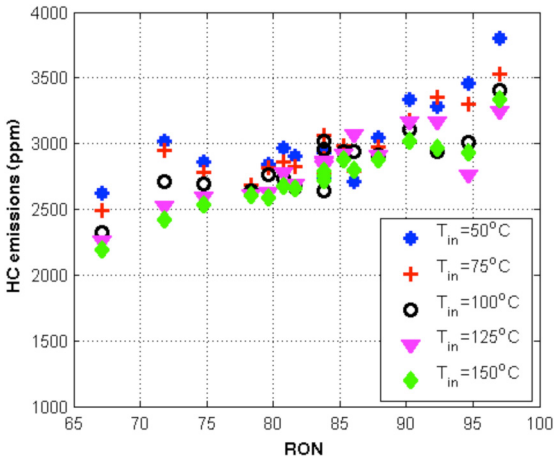

Figure 14. HC emissions increases with higher RON. TERFs for various inlet air temperatures.

For CO emissions, shown in Figures 15 and 16, there seems to be a peak at a RON of about 70. This should be a engine specific number, corresponding to the cylinder temperature that is in turn coupled with CO formation and oxidation. The CO emissions shows the opposite trend to the HC emissions, that lower octane number fuels shows increasing amounts of CO. All fuels show lower amounts of CO at the higher inlet air temperature.

NO_x emissions are plotted vs. RON in Figure 17 for the PRFs and TERFs. For NO_x emissions from the PRFs, NO_x production started to rise sharply for RONs between 60 and 80, especially for the highest inlet air temperatures. The rise of NO_x emissions for the TERFs was much less.

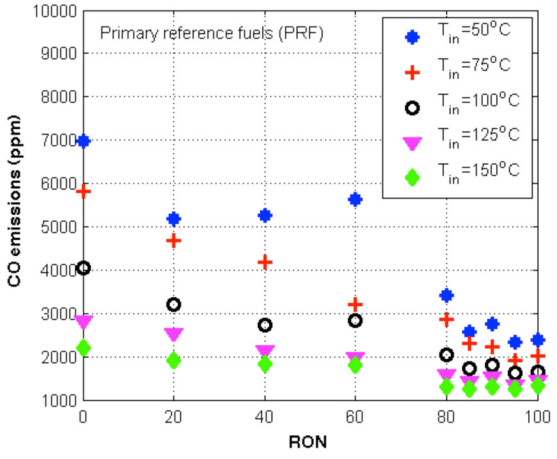

Figure 15. CO emissions as a function of RON, for primary reference fuels (PRF), at various inlet air temperatures.

The maximum cylinder temperature and the emissions are believed to correlate with the burn duration, and therefore also the maximum rate of heat release, shown with the fuel octane rating in Figure 18. A correlation is seen between RON and the maximum rate of heat release at the lowest inlet air temperature of 50°C, and this can be explained by slow combustion and higher amounts of LTHR for the low octane fuel. At higher inlet air temperatures as 150°C the burn rate however decreases for the highest octane number fuels. A reason for this could be the absence of LTHR at higher inlet air temperature, especially for the higher octane number fuels, which in turn makes the start of the main combustion slower.

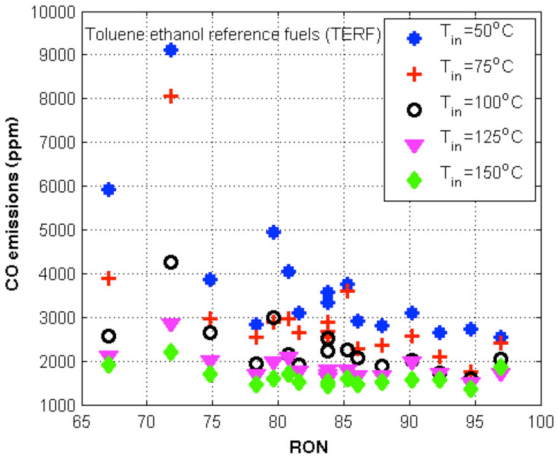

Figure 16. CO emissions decreases with increasing RON for the toluene ethanol reference fuels.

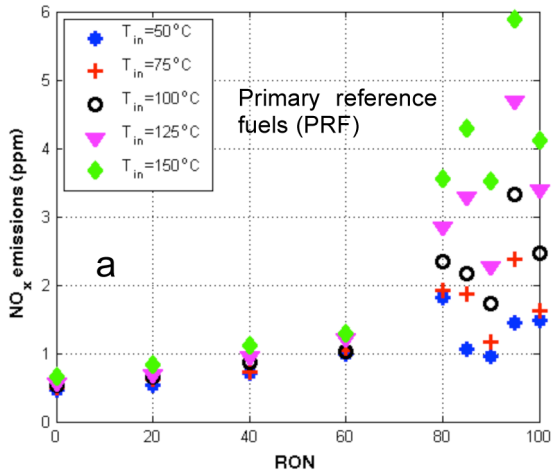

Figure 17. NOx emissions for different RON values.

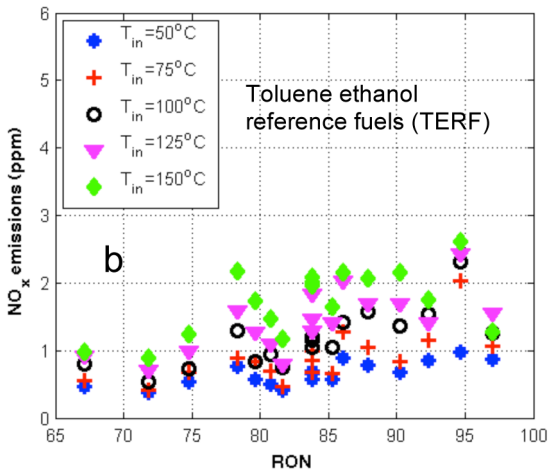

Figure 17. (cont.) NOx emissions for different RON values.

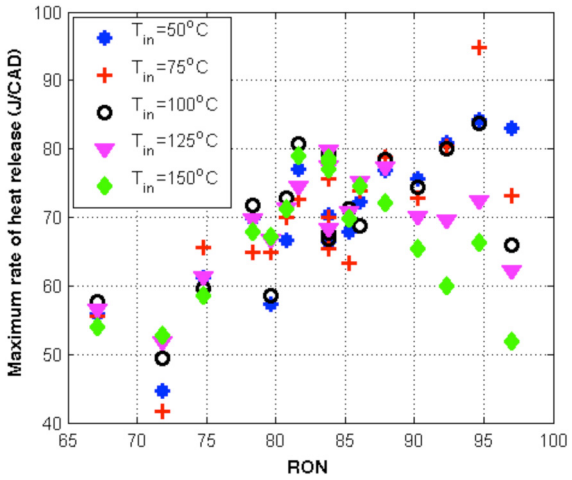

Figure 18. Correlation between RON and maximum rate of heat release for TERFs at various inlet air temperatures.

Combustion Efficiency

Combustion efficiency is calculated from the measured emissions. Results from primary reference fuels in Figure 19a indicate that for a specific fuel, combustion efficiency decreases as CR increases (corresponding to a lower inlet air temperature). For a given compression ratio, a higher octane number fuel, containing more iso-octane and less n-heptane, has higher combustion efficiency than a fuel of a lower octane rating.

The effects of ethanol addition are shown in Figures 19 c, d, e for thirteen of the ethanol reference fuels (ERFs). The series of fuels in Figure 19c all contain 20% n-heptane, 0-20% ethanol, and iso-octane for the balance. The series of fuels in Figure 19e all contain 30 % n-heptane, 0-20 % ethanol, and isooctane for the balance. The series of fuels in Figure 19 d only contain n-heptane and ethanol. For all fuels in all three plots, it appears that combustion efficiency decreases as compression ratio increases, although there is a leveling out effect for the nheptane/ethanol fuels in Figure 19d at the highest compression ratios. No direct correlation is seen by ethanol addition for these series of fuels. It should be noted that a higher compression ratio also corresponds to a lower inlet air temperature, something that could affect vaporization of the fuels.

In Figure 19b for the TRFs, the general trend is that a higher toluene concentration, corresponding to a higher octane rating, lead to higher combustion efficiencies even though a higher compression ratio is used.

Combustion efficiencies for TERFs are shown in Figure 19f. Fuel T1 and T8, the two fuels having the lowest RON's, have lower combustion efficiency than the other fuels when plotted vs. CR. In this plot, the three fuels having the highest RONs (T2, T3, and T15) appear to have the highest combustion efficiencies at a given CR.

The trend of higher combustion efficiency with higher RON appears to be mostly valid, as shown in Figure 20, although the T8 and T2 fuels appear to be slightly lower and slightly higher, respectively, than surrounding fuels. Earlier we showed that a higher RON gives higher HC emissions. Counteracting this, a lower RON gives higher CO emissions. These components (HC and CO) account for most of the combustion losses, which seem to be fairly constant with fuel octane rating.

Fuel Comparison

The five different inlet air temperatures can be seen as different loads, since less air enters the cylinder at a higher inlet air temperature, and therefore also less fuel to keep a certain equivalence ratio. The load behavior can therefor be studied by comparing these five cases. Four different fuels (T1, T3, T8, and T13) were chosen for comparison, see Figure 21. Rate of heat release plots for the other toluene ethanol reference fuels are shown in Figures 24, 25, 26, 27, 28, 29, 30, 31, 32, 33, 34, 35, 36, 37, 38, 39 in Appendix. For fuel T1 in Figure 21a, the main combustion shown by the second peak looks practically the same for the different inlet air temperatures and compression ratios, with the same rate of heat release peak. However for this fuel there is a large difference in amount of low temperature reactions, seen as the pre-reactions beginning at around 30 crank angle degrees before TDC.

Low ethanol and low RON fuels T1 and T8 show similar emissions in Figures 22 and 23 even though they exhibit different RoHR in Figures 21a and 21c. These fuels, exhibiting the highest amounts of LTHR for the chosen fuels, have lower HC but higher CO emissions (see Figure 22). This occurs because the cylinder temperature is not high enough to oxidize HC to CO. The low maximum temperature also lead to the lowest NO_x emissions, see Figure 23. Fuel T8 was earlier shown to have been operated at too high equivalence ratios at the 50 and 75 °C inlet air temperatures, which could be the reason for the high CO emissions.

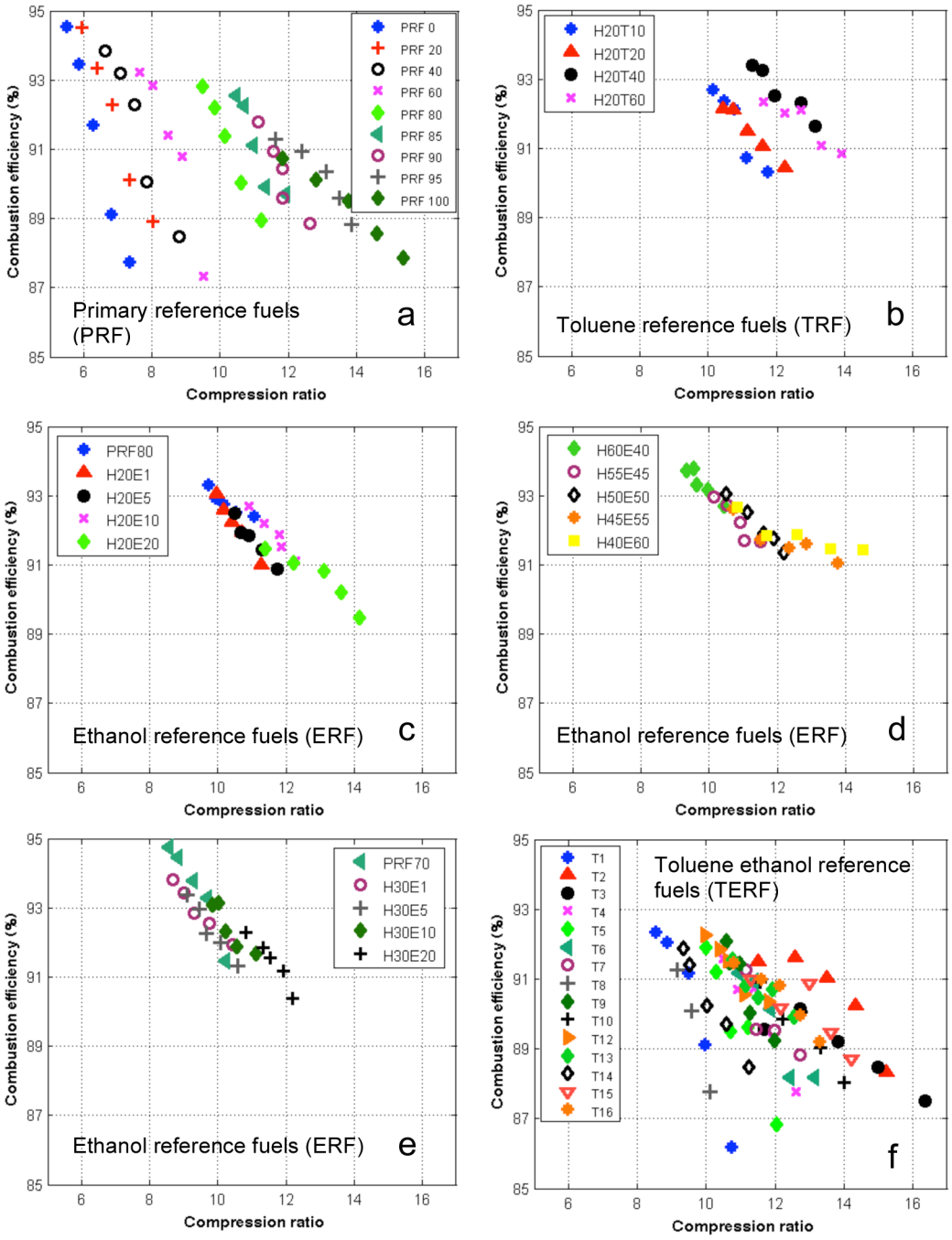

Figure 19. Combustion efficiency decreases with increased compression ratio for all fuels. The two operating points for fuel T8, operating at a slightly higher equivalence ratio, resulting in lower combustion efficiencies of 82 and 83 % respectively, are not shown in this figure.

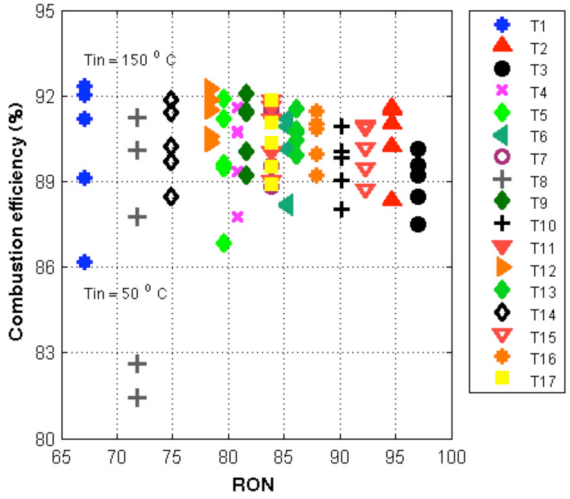

Figure 20. Combustion efficiencies as a function of RON for the toluene ethanol reference fuels. The combustion efficiency is slightly decreased with a higher octane rating at the higher inlet air temperatures, which is shown by the uppermost mark for each fuel.

Fuels T12 and T13, see Figure 37 in appendix and Figure 21d, show similar emissions even though these two fuels have very different compositions, one with low ethanol and low nheptane (T13), and one with high ethanol and high n-heptane (T12), resulting in similar RON's (78.3 and 86.1, respectively). The very high RON (97) and sensitivity (RON-MON=9.4) fuel T3, Figure 21b, shows high HC emissions and high maximum cylinder temperatures.

Most fuels show a correlation between HC and CO emissions, as for fuels T1 and T8, with higher HC and CO emissions at a lower inlet air temperature and a higher compression ratio.

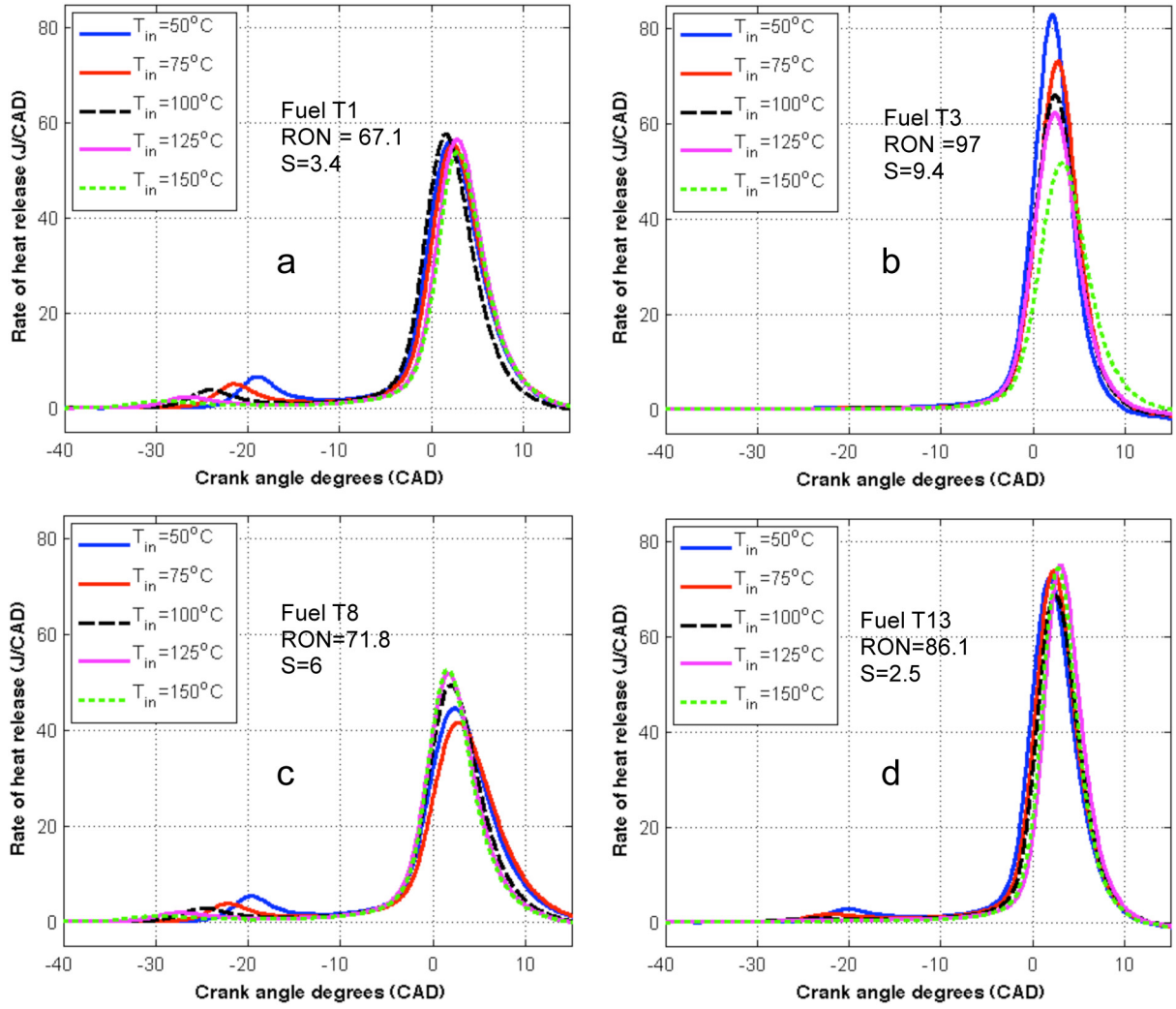

Figure 21. Rate of heat release for toluene ethanol reference fuels T1, T3, T8, and T13

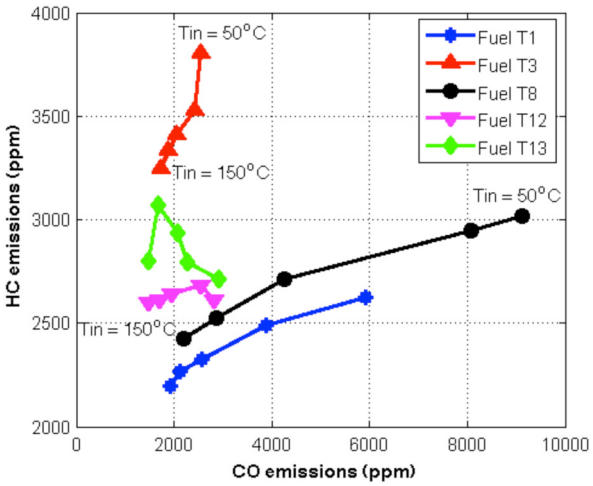

Figure 22. HC and CO for fuels T1, T3, T8, T12 and T13.

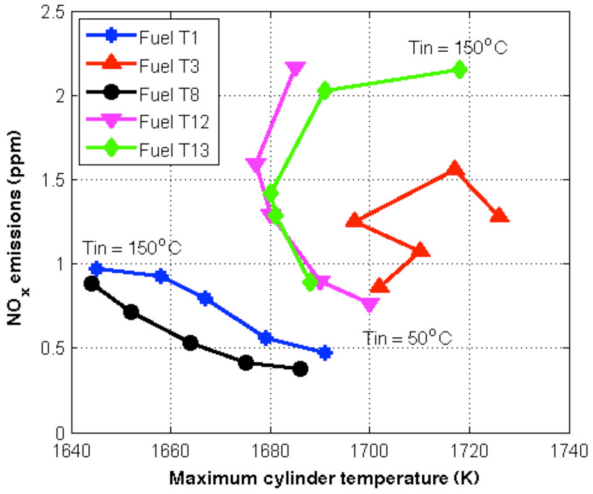

Figure 23. NOx emissions and corresponding maximum cylinder temperatures for fuels T1, T3, T8, T12 and T13.

SUMMARY AND CONCLUSIONS

A systematic study of over 40 gasoline surrogate fuels was performed. Intake air temperature was varied to see the effect on emissions for each fuel.

NO_x emissions were low (below 5 ppm) for all operating points. For the primary reference fuels (PRF) a fuel with a higher RON gave higher NO_x emissions. The toluene ethanol reference fuels (TERF) showed lower NO_x emissions than the PRFs with an octane rating over 80, indicating that ethanol and/or toluene addition can decrease NO_x emissions for fuels with a higher octane rating. For the TERFs, at a certain inlet air temperature, a higher maximum cylinder temperature gave more NO_x.

The main factor leading to hydrocarbon (HC) emissions was believed to be fuel trapped in the crevices during the combustion event, since HC emissions were found to be proportional to compression ratio. HC emissions for the PRFs could be described by a linearly increasing function of compression ratio (CR) and an exponentially increasing function for RON. A slightly different behavior was seen for the fuels containing toluene and ethanol. The fuel effect found was that toluene, representing aromatics in this study, was shown to increase HC emissions if added in high concentrations (40 - 60 vol.%). At low concentration addition of toluene, a weak decreasing effect on HC emission was seen. Ethanol addition was found to decrease HC emissions for combustion at a constant CR. Ethanol addition at low concentrations might therefore be useful to lower HC emissions by increase in oxidization of HC.

Carbon monoxide (CO) emissions were found to have a maximum for fuels with an octane rating of about 70. This was believed to be an engine specific number correlating with a compromise between CO formation and oxidation. The CO emissions could be related to temperature inhomogeneity in the engine, since the CO to CO_2 oxidization temperature of 1500 K likely had not been reached in parts of the combustion chamber at some operating points, showing large amounts of CO as a result.

PRF and TERF fuels with a higher octane rating had better combustion efficiency when comparing at a given CR. When HC emissions increased with RON because of the higher compression ratio needed and therefore higher losses in crevice volumes, combustion temperature was higher for higher octane number fuels leading to less CO emissions. These two effects combined lead to roughly constant combustion efficiency for fuels throughout the range of RON.

REFERENCES

1. Pitz, W., Cernansky, N., Dryer, F., Egolfopoulos, F. et al., "Development of an Experimental Database and Chemical Kinetic Models for Surrogate Gasoline Fuels," SAE Technical Paper 2007-01-0175, 2007, doi:10.4271/2007-01-0175.

2. Machado, G.B., Barros, J.E.M., Braga, S.L., Braga, C.V.M., Oliviera, E.J., Silva, A.H.M.F.T., Carvalho, L.O., "Investigation on surrogate fuels for high-octane oxygenated gasolines", Fuel, 90:640-646, 2011.

3. Warnatz, J., Maas, U., Dibble, R.W., 2006, "Combustion Physical and Chemical Fundamentals, Modeling and Simulation, Experiments, Pollutant Formation", Springer, Berlin.

4. Christensen, M., Johansson, B., and Hultqvist, A., "The Effect of Piston Topland Geometry on Emissions of Unburned Hydrocarbons from a Homogeneous Charge Compression Ignition (HCCI) Engine," SAE Technical Paper 2001-01-1893, 2001, doi:10.4271/2001-01-1893.

5. Aceves, S., Flowers, D., Espinosa-Loza, F., Martinez-Frias, J. et al., "Spatial Analysis of Emissions Sources for HCCI Combustion at Low Loads Using a Multi-Zone Model," SAE Technical Paper 2004-01-1910, 2004, doi:10.4271/2004-01-1910.

6. Dec, J., "A Computational Study of the Effects of Low Fuel Loading and EGR on Heat Release Rates and Combustion Limits in HCCI Engines," SAE Technical Paper 2002-01-1309, 2002, doi:10.4271/2002-01-1309.

7. Dec, J., Sjöberg, M., Hwang, W., Davisson, M. et al., "Detailed HCCI Exhaust Speciation and the Sources of Hydrocarbon and Oxygenated Hydrocarbon Emissions," *SAE Int. J. Fuels Lubr.* 1(1):50-67, 2008, doi:10.4271/2008-01-0053.

8. Sjöberg, M. and Dec, J.E., "An Investigation into Lowest Acceptable Combustion Temperatures for Hydrocarbon Fuels in HCCI Engine", Proceedings of the Combustion Institute, Vol. 30: 2719-2726, 2005.

9. Li, H., Neill, W., Chippior, W., Graham, L. et al., "An Experimental Investigation on the Emission Characteristics of HCCI Engine Operation Using N-Heptane," SAE Technical Paper 2007-01-1854, 2007, doi:10.4271/2007-01-1854.

10. Morgan, N., Smallbone, A., Bhave, A., Kraft, M., Cracknell, R., Kalghatgi, G., "Mapping surrogate gasoline compositions into RON/MON space", Combustion and Flame, 157, 1122-1131, 2010.

11. Heywood, J. B., 1988, "Internal Combustion Engine Fundamentals", McGraw-Hill, New York.

12. Truedsson, I., Tuner, M., Johansson, B., and Cannella, W., "Pressure Sensitivity of HCCI Auto- Ignition Temperature for Gasoline Surrogate Fuels," SAE Technical Paper 2013-01-1669, 2013, doi:10.4271/2013-01-1669.

13. Truedsson, I., Tuner, M., Johansson, B., and Cannella, W., "Pressure Sensitivity of HCCI Auto- Ignition Temperature for Primary Reference Fuels," *SAE Int. J. Engines* 5(3):1089-1108, 2012, doi:10.4271/2012-01-1128.

CONTACT INFORMATION

Corresponding author
ida.truedsson@energy.lth.se

ACKNOWLEDGMENTS

The authors gratefully acknowledge Chevron for their financial support. Patrick Borgqvist is acknowledged for designing the engine control system.

DEFINITIONS/ABBREVIATIONS

AFR - air fuel ratio
ATDC - after top dead center
BTDC - before top dead center
CA 50 - crank angle for 50 % of total heat release
CAD - crank angle degree
CFR - cooperative fuel research
CO - carbon monoxide
CR - compression ratio
EGR - exhaust gas recirculation
ERF - ethanol reference fuel (n-heptane, iso-octane, and ethanol)
HC - hydrocarbons
HCCI - homogenous charge compression ignition
IVC - inlet valve closing
LTHR - low temperature heat release
MON - motor octane number
NO_x - NO (nitric oxide) and NO_2 (nitrogen dioxide) combined
ON - octane number
PRF - primary reference fuel (n-heptane and iso-octane)
RON - research octane number
S - fuel sensitivity, S = RON-MON
SI - spark ignition
TDC - top dead center
T_{in} - inlet air temperature, measured
TERF - toluene ethanol reference fuel (n-heptane, iso-octane, toluene, and ethanol)
TRF - toluene reference fuel (n-heptane, isooctane, and toluene)
VCR - variable compression ratio

APPENDIX

Rate of heat release plots for toluene ethanol reference fuels (TERF) are shown in Figures 29, 30, 31, 32, 33, 34, 35, 36, 37, 38, 39 to 44.

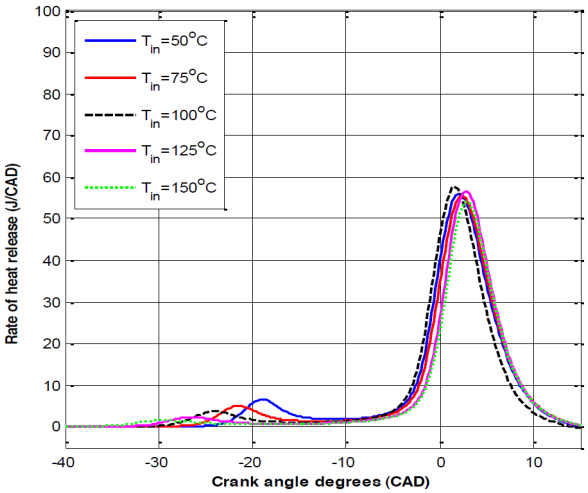

Figure 24. Rate of heat release for fuel T1

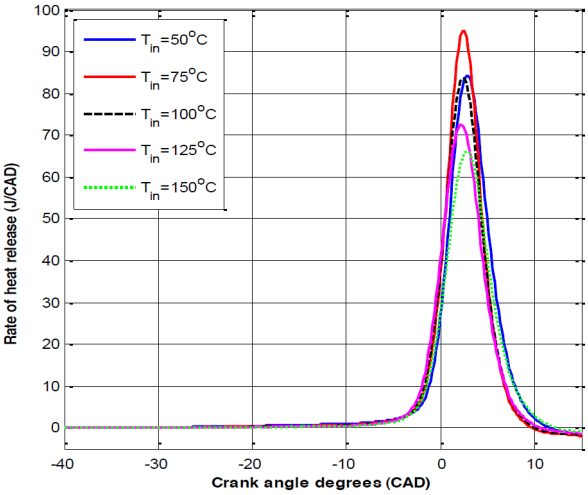

Figure 25. Rate of heat release for fuel T2

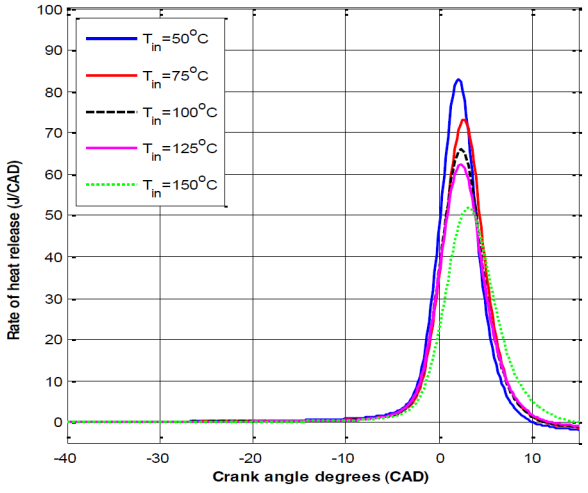

Figure 26. Rate of heat release for fuel T3

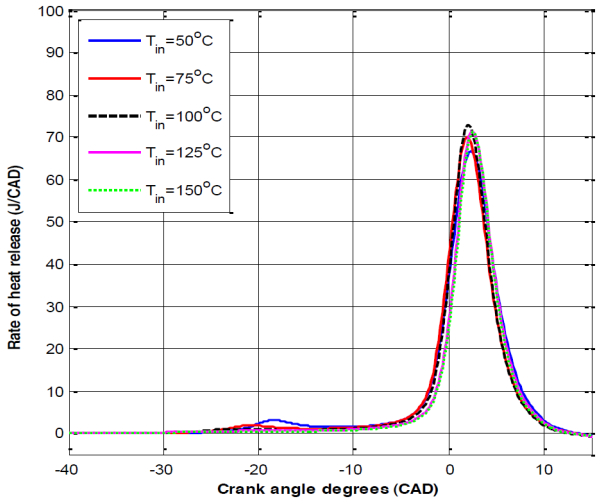

Figure 27. Rate of heat release for fuel T4

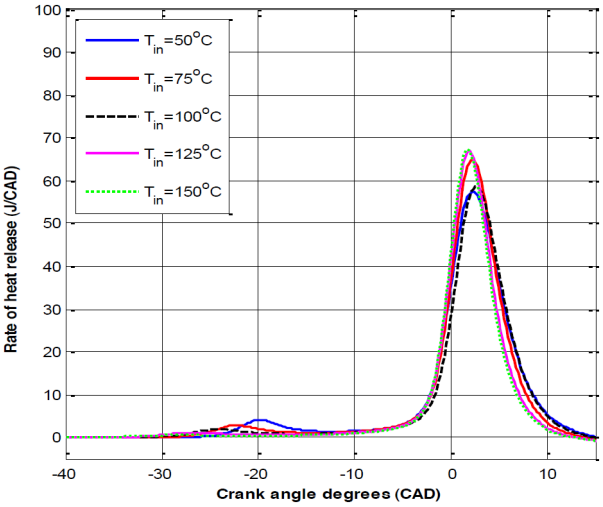

Figure 28. Rate of heat release for fuel T5

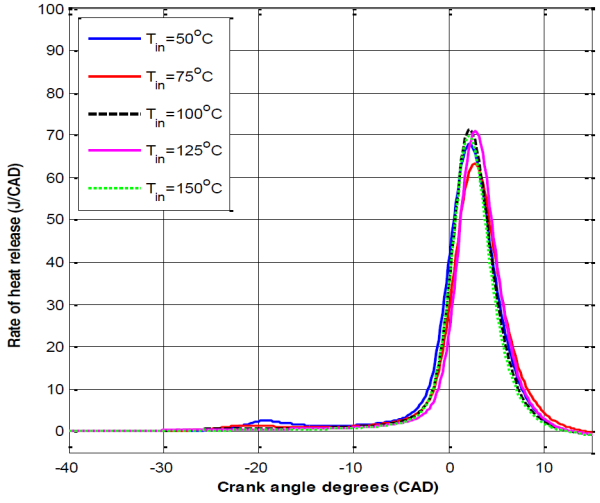

Figure 29. Rate of heat release for fuel T6

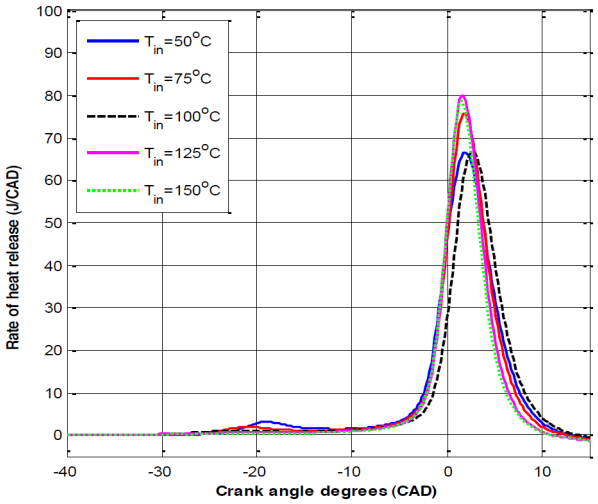

Figure 30. Rate of heat release for fuel T7

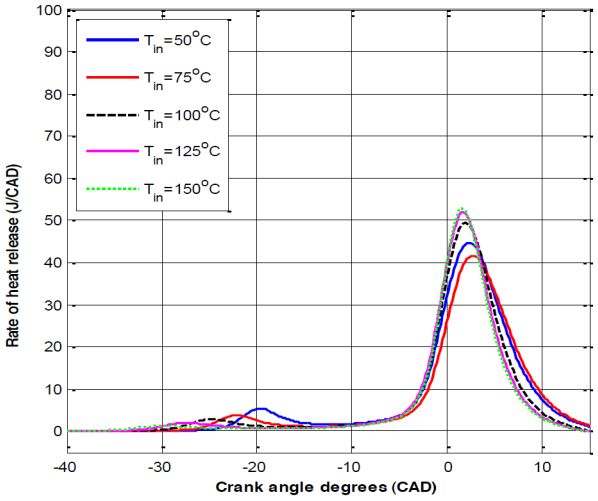

Figure 31. Rate of heat release for fuel T8

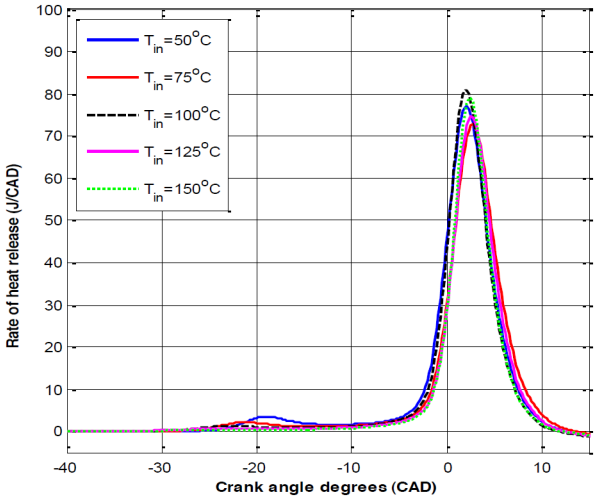

Figure 32. Rate of heat release for fuel T9

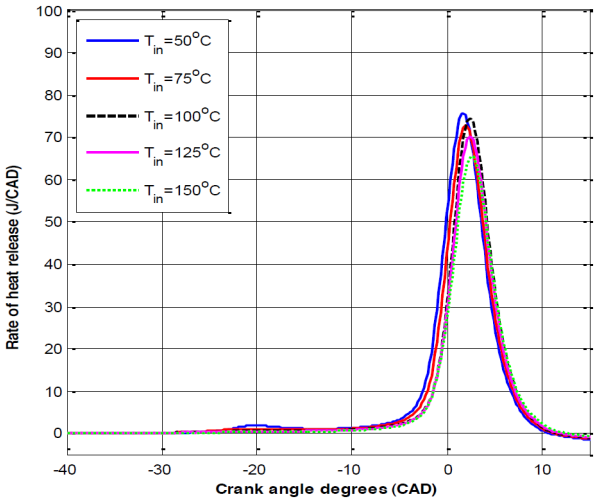

Figure 33. Rate of heat release for fuel T10.

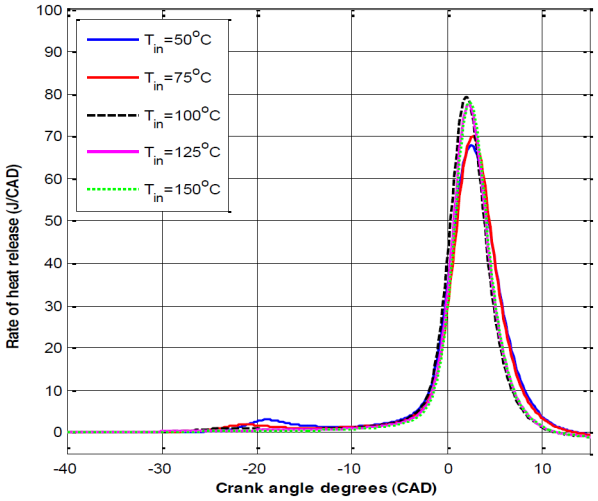

Figure 34. Rate of heat release for fuel T11

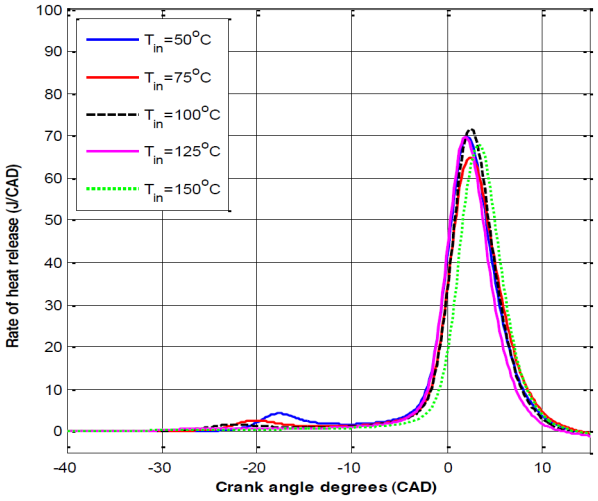

Figure 35. Rate of heat release for fuel T12.

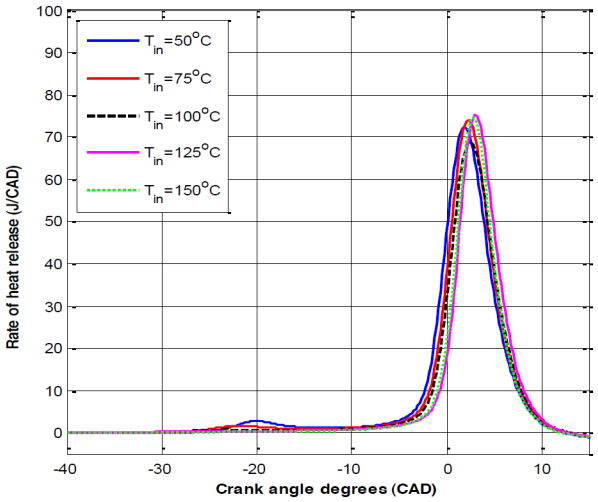

Figure 36. Rate of heat release for fuel T13.

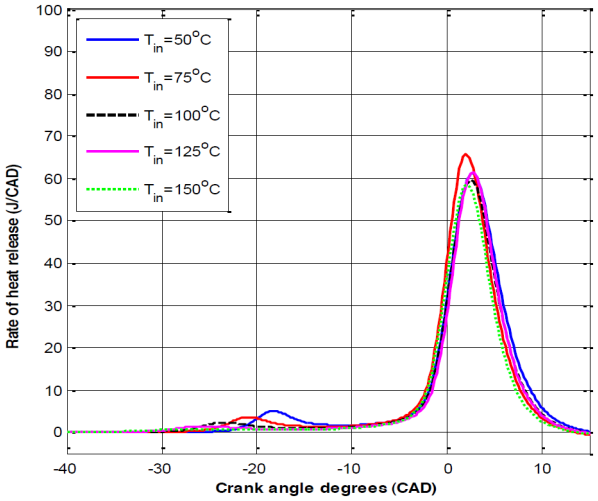

Figure 37. Rate of heat release for fuel T14.

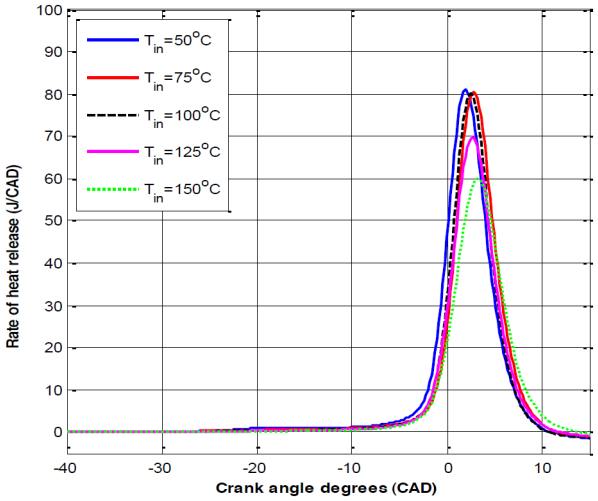

Figure 38. Rate of heat release for fuel T15.

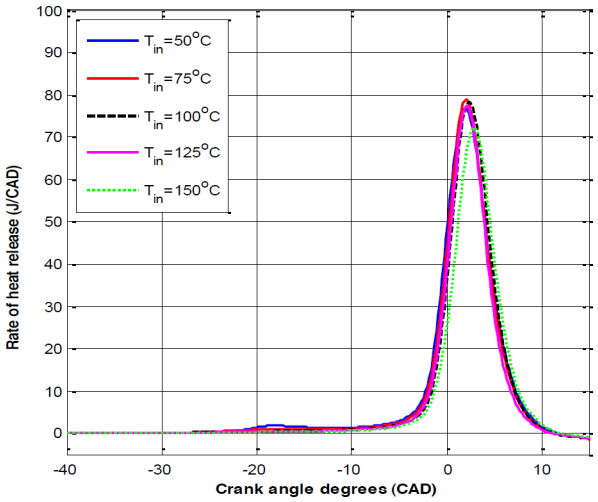

Figure 39. Rate of heat release for fuel T16.

Table 5. Stoichiometric air fuel ratios, AFRs

TERF		ERF		TRF	
Fuel	AFR	Fuel	AFR_s	Fuel	AFR_s
T1	14,4	PRF80	15,0	H20T10	14,7
T2	13,5	H20E1	15,0	H20T20	14,3
T3	12,8	H20E5	14,7	H20T40	13,6
T4	12,8	H20E10	14,4	H20T60	12,9
T5	14,0	H20E20	13,8		
T6	13,2	PRF70	15,0		
T7	13,6	H30E1	15,0		
T8	13,7	H30E5	14,7		
T9	13,9	H30E10	14,4		
T10	13,7	H30E20	13,8		
T11	13,6	H60E40	12,6		
T12	13,5	H55E45	12,3		
T13	14,4	H50E50	12,0		
T14	13,6	H45E55	11,7		
T15	13,6	H40E60	11,4		
T16	13,1				
T17	13,6				

The Engineering Meetings Board has approved this paper for publication. It has successfully completed SAE's peer review process under the supervision of the session organizer. This process requires a minimum of three (3) reviews by industry experts.

ISSN 0148-7191

SAE Customer Service:
Tel: 877-606-7323 (inside USA and Canada)
Tel: 724-776-4970 (outside USA)
Fax: 724-776-0790
Email: CustomerService@sae.org
SAE Web Address: http://www.sae.org
Printed in USA

Paper V

Engine Speed Effect on Auto-Ignition Temperature and Low Temperature Reactions in HCCI Combustion

Ida Truedsson, Martin Tuner, Bengt Johansson
Lund University

William Cannella
Chevron

Abstract

HCCI is a promising concept to reduce NO_x and soot emissions. To be able to accurately control the combustion, more information is needed about the auto-ignition. Many fuels, often containing n-paraffins, exhibit pre-reactions before the main heat release event, originating from reactions that are terminated when the temperature in the cylinder reaches a certain temperature. These pre-reactions are called low temperature heat release (LTHR), and are known to be affected by engine speed. This paper goes through engine speed effects on auto-ignition temperatures and LTHR for both reference fuels and real gasolines, a total of 9 fuels.

Earlier studies show effects on both quantity and timing of the low temperature heat release when engine speed is varied. In this study, these effects are further explained by looking at the auto-ignition temperatures and the pressure and temperature evolution in the cylinder.

Primary reference fuels (PRF), blends of n-heptane and iso-octane, but also real gasoline fuels, were chosen to study the effects from different fuel components and octane rating. All fuels were tested in a CFR engine with variable compression ratio, running in HCCI operation. Engine speed was varied from 600 to 1500 rpm. An equivalence ratio of 0.33 was used, and a constant combustion phasing of 3 degrees after TDC was held by changing the compression ratio for each operating point. Different pressure and temperature evolutions were achieved by varying the inlet air temperature from 50 ^{o}C to 150 ^{o}C.

At higher engine speeds the amount of LTHR decreased or disappeared for different fuels, due to the shorter delay time before start of ignition. Auto-ignition temperature change with engine speed was charted for the different fuels. The speed effect on the auto-ignition behavior was also related to the fuel octane ratings, RON and MON, and the combination thereof, the octane sensitivity S (S=RON-MON).

Introduction

Homogenous charge compression ignition (HCCI) combustion is a concept used to reduce engine out soot and NO_x emissions, with engine efficiency as high as with diesel engines, therefore also reducing emissions of CO_2. The limitations of the HCCI engine is relatively low maximum loads and a need for complex control strategies, since start of combustion is controlled by chemical kinetics. This paper aims at extending the knowledge of auto ignition behavior as the engine speed is changed.

Among other things, engine speeds effects the available time for the low temperature heat release. This is demonstrated in [9], where they also concluded that toluene addition changed the speed sensitivity of a fuel.

In [10] a CFR engine has been used to investigate the load range for engine speeds from 600 to 2000 rpm, with intake temperatures from 300 to 400 K with four different fuels. Three of these fuels had the same octane rating of 91.8, but showed different HCCI operating ranges. They observed that, for a certain inlet air temperature, the low temperature reactions started at the same crank angle position (about -25 degrees before TDC) as the engine speed increased.

In (1) a CFR engine is used to test engine speed effects on combustion of different diesel fuels, but also n-heptane and iso-octane. Engine speed and increased inlet air temperature to keep a constant combustion timing is shown to decrease LTHR.

Auto ignition in an HCCI engine is governed by the pressure-temperature history of the fuel-air charge.

It is believed that different fuels show a unique response in change of auto-ignition temperature for different cylinder pressures. This paper aims at explaining yet another part of the auto ignition process by looking at the effect from engine speed.

Experimental setup

A Waukesha variable compression ratio Cooperative Fuel Research (CFR) engine was used for the experiments. This type of engine is typically used for measuring the RON and MON of gasoline. The setup included an air-fuel mixture heater mounted downstreams from the port fuel injector. A scale was used for measuring the fuel flow. The heat release was calculated from the pressure trace measured with a Kistler piezoelectric pressure transducer mounted in the cylinder. An intake air refrigerator unit model 8042E was included in the setup to ensure constant air quality throughout the experiments. Temperature of the air-fuel mixture (T_{in}) was measured by a thermocouple placed in the inlet, close to the intake valve. The spark ignition was switched off. The engine specifications are listed in Table 1. HC, CO, CO_2, and NO_x emissions were measured with a Horiba Mexa 7500 analyzer system. Equivalence ratio was calculated from the measured emissions.

Table 1. Specifications for CFR engine.

Displacement volume	612 cm^3
Number of cylinders	1
Bore	83 mm
Stroke	114 mm
CR	Variable (4:1 to 18:1)
Number of valves	2
Length of connecting rod	254 mm
Intake valve opens	10°ATDC±2,5°
Intake valve closes	146°BTDC±2,5°
Exhaust valve opens	140°ATDC±2,5°
Exhaust valve closes	15°ATDC±2,5°
Valve lifts	6.25 mm
Engine speed	600 rpm
Fuel supply	Port injection

Fuels

10 different fuels, including both reference fuels and real gasoline, were run. Four primary reference fuels (PRF) where used, and 6 gasoline fuels in the same octane range were tested. All fuels are shown in Table 2.

Table 2. Fuel specifications.

Fuel	RON	MON	n-Heptane	iso-Octane
			vol.%	vol.%
PRF 70	70	70	30	70
PRF 80	80	80	20	80
PRF 90	90	90	10	90
PRF 100	100	100	0	100

Method

The fuels were thoroughly studied by varying engine speeds from 600 to 1200 rpm (600, 800, 900, 1000, and 1200 rpm) at each inlet air temperature (50, 100, and 150 °C), a total of 15 operating points for each fuel.

Heat release analysis and definitions

In this paper, two methods were used for determining the amount of pre-reactions. The first method was used for low temperature heat release (LTHR), which is shown in Figure 1. The period of LTHR is defined as the time between the start of combustion and the minimum value between the LTHR and high temperature heat release (HTHR, main combustion) peak.

The second method to quantify pre-reactions included both LTHR and what is also called intermediate temperature heat release. Since the rate of heat release for the main peak has a curve often resembling a normal distribution, a gaussian curve was fit to the main heat release. The area before this was called early heat release (eHR), see Figure 2. Sometimes ITHR pre-reactions are present even when LTHR is not. With this method, fuels showing the least low temperature reactivity (here represented by PRF 100), at conditions having a high inlet air temperature and high engine speed (known to reduce LTHR), show some early heat release by this definition, see Figure 8. For both methods, pre-reactions were normalized by dividing with the total amount of heat released to account for the different fuel amounts at the different inlet air temperatures, giving a LTHR or eHR fraction.

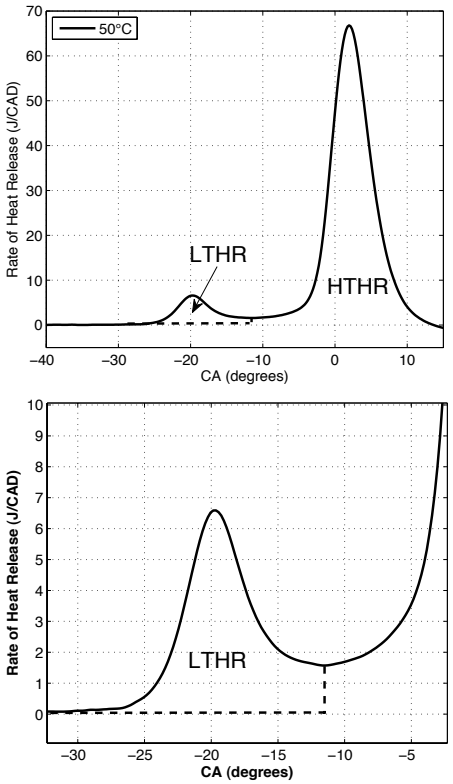

Figure 1. Definition of low temperature heat release (LTHR).

T_{in} is the measured temperature of the air and fuel flow in the intake, measured close to the intake. To calculate the temperature in the cylinder when the intake valve closes, the temperature is then corrected with a temperature model, explained in detail in reference [7], accounting for heating from intake walls and from mixing with hot residuals.

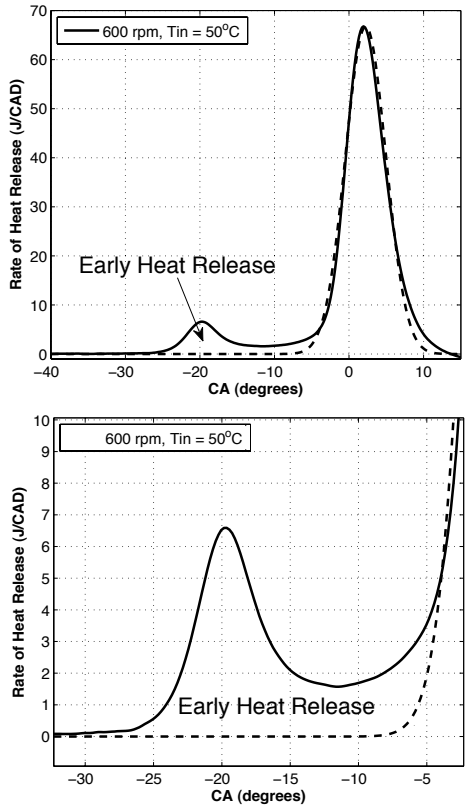

Figure 2. Definition of early heat release (eHR).

Gas exchange

The CFR engine is designed to run at 600 rpm for RON measurements and 900 rpm at MON measurements. The engine has two valves, and the gas exchange will therefore be limited at higher engine speeds. In the original engine setup, where a carburetor is used, an orifice (diameter of 14 mm, mounted about 500 mm upstream from the intake port just before the fuel injectors) was mounted in the intake. This was kept in the experiments, and this was believed to be the main reason for the pressure drop at higher engine speeds. This study was chosen to still operate with atmospheric pressure, and the cylinder charge was therefore decreased as less air entered the cylinder at higher engine speeds. To study the effect of this, one fuel (PRF 80) was run with constant fuel flow (and therefore closer to the same load) at a higher engine speed. Only a small effect was seen on the auto-ignition temperature.

Results

Auto-ignition temperatures

Part of the linearity of the primary reference fuels can be explained by the low temperature heat release, which makes start of combustion easier to detect.

The reference fuels behave more likes gasoline at higher engine speeds – at 1200 rpm. At the higher inlet air temperatures of 100 and 150°C, a large difference is seen for the lower engine speeds between reference fuels and real gasolines, where the reference fuels shows a lower auto-ignition temperature.

In analogue with previous work by the authors [5,6,7], auto-ignition temperature was studied when changing the engine speed. It was found that the auto-ignition temperature increased with higher engine speed. This expected due to the decreased residence time before combustion.

Another observation is that for the full distillation fuels (not PRF), the pressure at auto ignition was decreased substantially when the engine speed reached 1200 rpm.

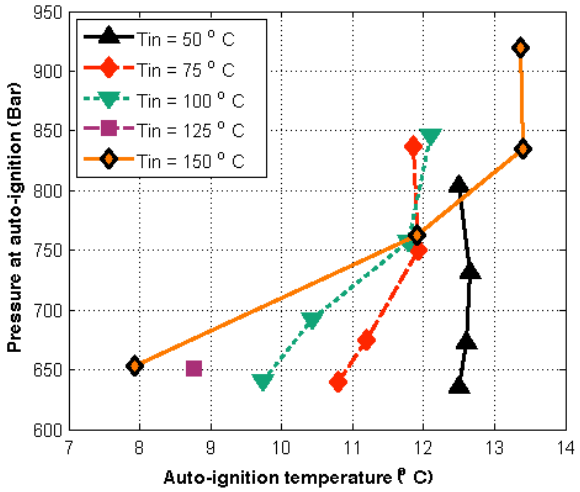

Figure 3. Auto-ignition temperatures for PRF80 at different engine speeds.

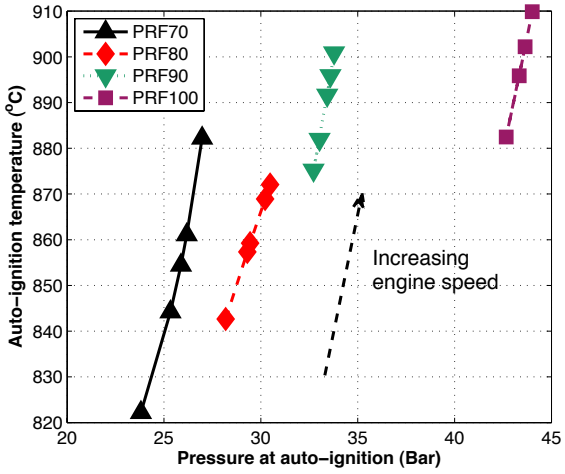

Figure 4. Auto-ignition temperatures, calculated by the use of CA10 as start of combustion.

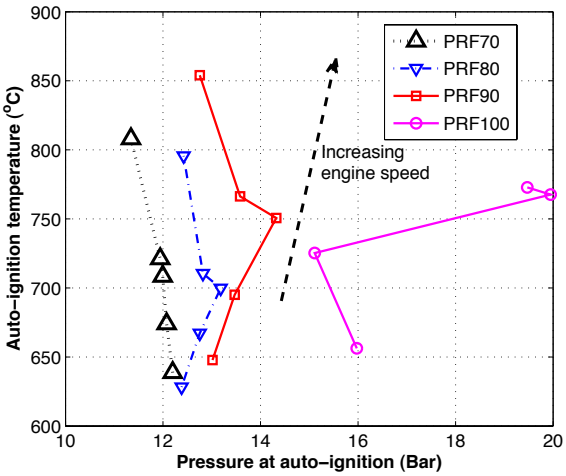

Figure 5. Auto-ignition temperatures for Tin=50°C. Start of combustion of 0.2 J/CAD used.

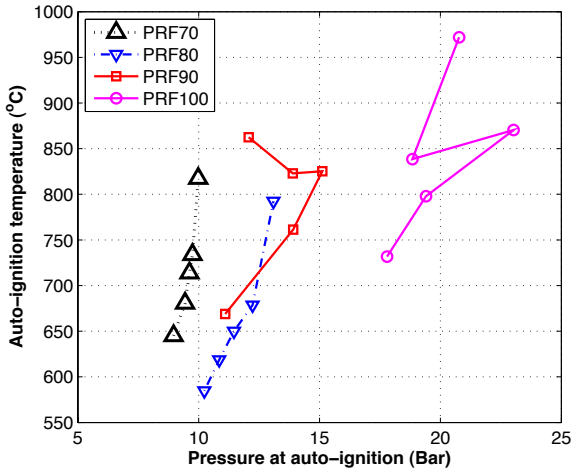

Figure 6. Auto-ignition temperatures for Tin=100°C. Start of combustion of 0.2 J/CAD used.

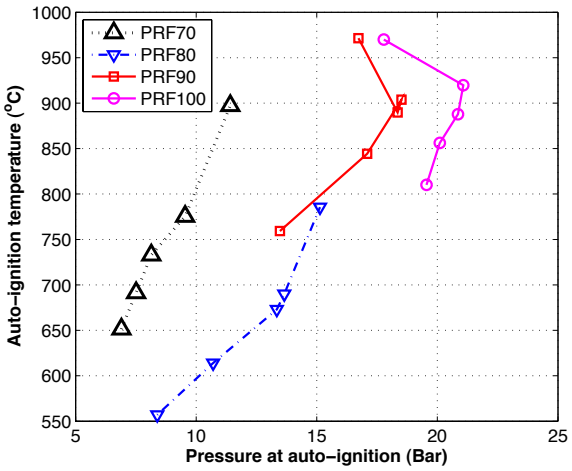

Figure 7. Auto-ignition temperatures for Tin=150°C. Start of combustion of 0.2 J/CAD used.

When looking at CA10, see Figure 5, a general trend seems to be that a higher engine speed leads to a higher auto-ignition temperature.

Compression ratio

The compression ratio had to be increased at higher engine speeds, to keep a constant combustion phasing. This could be explained both by the shorter residence time in the cylinder, why the charge will require a higher temperature and pressure to auto-ignite at the same moment. The increased need of compression ratio could also be a product of the reduced air-fuel charge, why heat transfer to the walls will play a more dominant role.

At lower inlet air temperatures the compression ratio seems to be connected to the RON of the fuels. However at higher inlet air temperatures PRF80 shows the highest required compression ratio. For PRF 100 with Tin=50°C, the engine maximum compression ratio was reached at 1000 rpm, why no stable operating point could be achieved at 1200 rpm.

Rate of heat release and start of low temperature reactions

In some cases the combustion timing was slightly retarded to avoid knock, as is seen in Figures 2 and 4 at the highest engine speed of 1200 rpm.

Looking at Figures 2 to 4, the low temperature reactions start at the same crank angle independent of engine speed. This is not consistent with results obtained in (1), where engine speed was seen to move the low temperature reactions earlier for n-heptane and diesel fuels. However, in that study the intake air temperature was changed to keep a constant combustion phasing. The authors have previously shown [5,6,7] that increased intake air temperature moves the low temperature reactions earlier.

The observation that the low temperature reactions start at a constant crank angle degree if the speed is changed (10) is

illustrated in Figures. At a certain inlet air temperature, the amount of low temperature is decreased with increased engine speed, but it appears at the same crank angle degree. Even if a different CA50 and compressions ratios are used in this study, the same observation is seen for an intake temperature of 50°C (320 K), that low temperature combustion starts about 25 degrees before TDC.

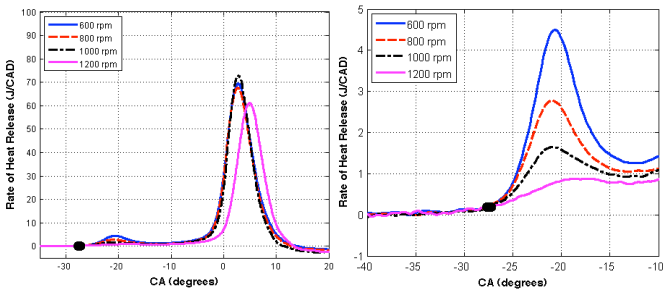

Figure 8. ROHR at Tin=50°C for different engine speeds.

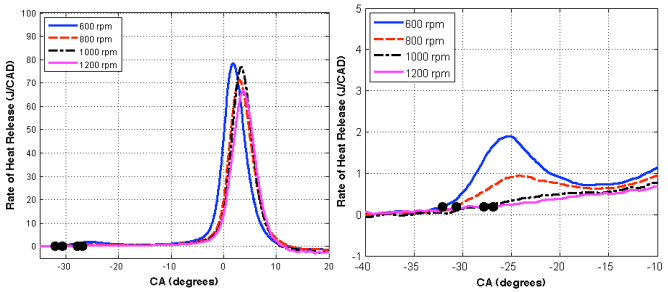

Figure 9. ROHR at Tin=100°C for different engine speeds.

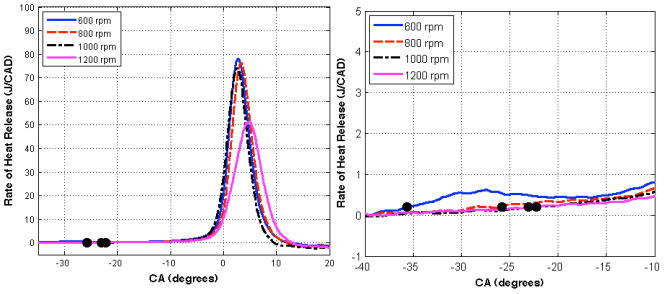

Figure 10. ROHR at Tin=150°C for different engine speeds.

Increasing inlet air temperature, decreasing inlet air pressure, and increasing engine speed, are all shown to give a more pronounced NTC region [14], as shown in Figure 27 for PRF 70, where the NTC zone is the duration between the squares and triangles in this figure. All these changes are performed together when changing from RON to MON conditions, and are connected with the effect on autoignition temperatures. Leppard [14] concludes that NTC behavior is more prominent at MON conditions (higher speed and intake temperature) than at RON conditions.

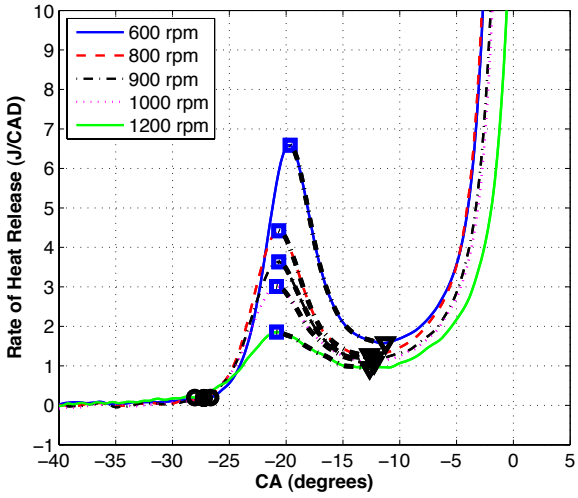

Figure 11. Area of negative temperature coefficient marked for low temperature heat release, PRF70.

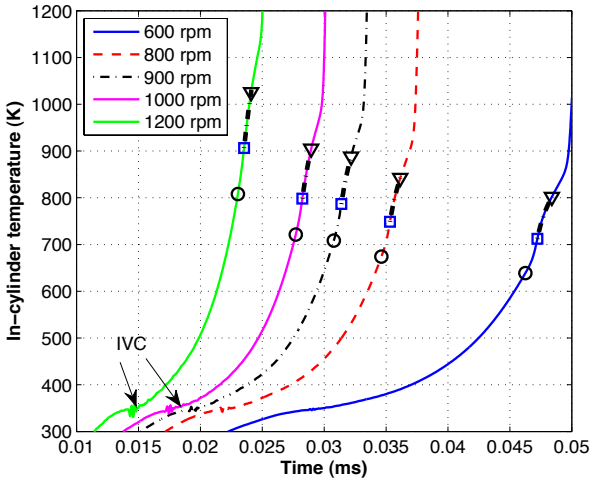

Figure 12. Speed effect on temperature history, PRF70.

Pre-reactions - low and intermediate temperature heat release quantification

The amount of early heat release decreased as engine speed increased, as shown in Figure 16 for gasoline fuel G3. Among other things, engine speed effects the available time for the low temperature heat release, which is explained in [11]. Higher engine speeds leads to less time available for the LTHR reactions to develop before the HTHR reactions occur. Using the LTHR definition, many of the fuels did not show any LTHR. By instead using the definition of early heat release, see Section 3.3.1, pre-reactions could still be studied.

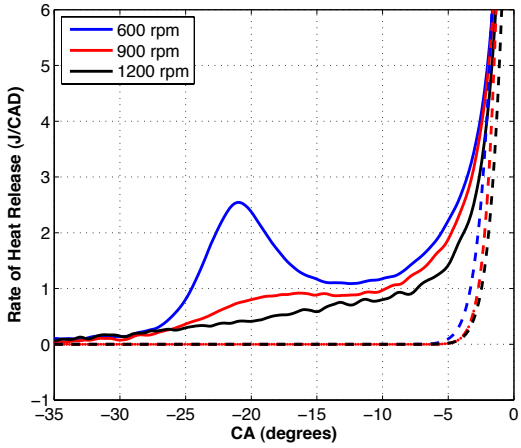

Figure 13. Early heat release for PRF90.

The results of the early heat release are shown in Figures 14-16. The apparent increase of eHR at the highest engine speeds is a result of the scaling. Less total energy is released at higher engine speed (due to less efficient gas exchange), why a constant amount of eHR at higher engine speed will be seen as increasing if the total released energy is decreased. As discussed previously, this definition will also include pre-reactions at higher temperatures than what is usually defined as LTHR, one term used for this is intermediate temperature heat release. The intermediate temperature heat release as a concept was introduced when discussing auto ignition and pre-reactions, when pre-reactions could be seen, but no peak of LTHR and no negative temperature coefficient. ITHR is first described in [12,13] and explained further in [11], where it is seen for fuels with no apparent LTHR. Optical experiments [11] showed that this phase was dominated by formaldehyde chemiluminescence, just as for the LTHR phase for a fuel exhibiting this, even though the temperature was higher than for LTHR.

The difference between LTHR and ITHR may be a little arbitrary, but some numbers used are for example that temperatures from 850 to 1000 K can be considered ITHR (29), temperatures where the low temperature processes should no longer be dominant. In [31], methods of quantifying ITHR are discussed. It is concluded that the temperature definition of 850 to 1000 K is a good indicator for ITHR, but that it is not possible to use to precisely determine the amount of ITHR. The shift in the 850-1000 K temperature range with an increase in engine speed is shown in Figure below, showing fuel PRF70. The dotted bold lines for each engine speed highlight the temperature range of 850 to 1000 K for different engine speeds. At the lowest engine speed, the ITHR is well within the HTHR phase, and at the highest engine speed the temperature range has shifted earlier, now coinciding with the LTHR and the negative temperature coefficient.

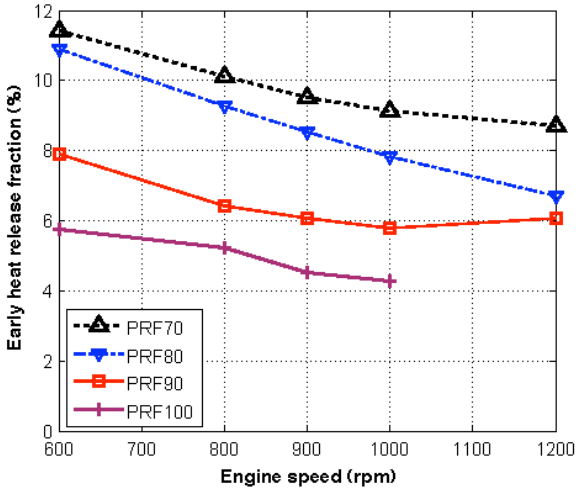

Figure 14. Early heat release as a function of engine speed for Tin=50°C

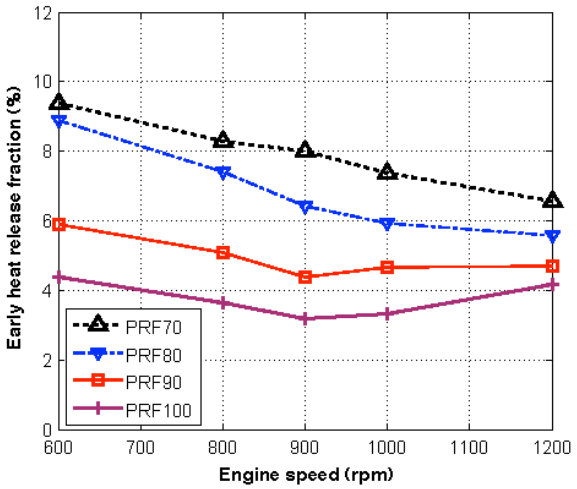

Figure 15. Early heat release as a function of engine speed for Tin=100°C

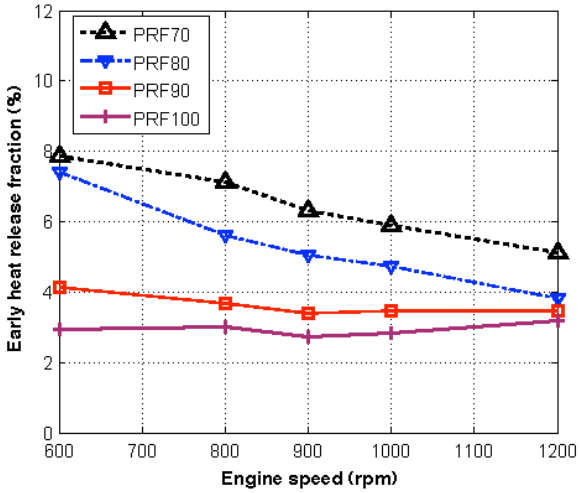

Figure 16. Early heat release as a function of engine speed for Tin=150°C

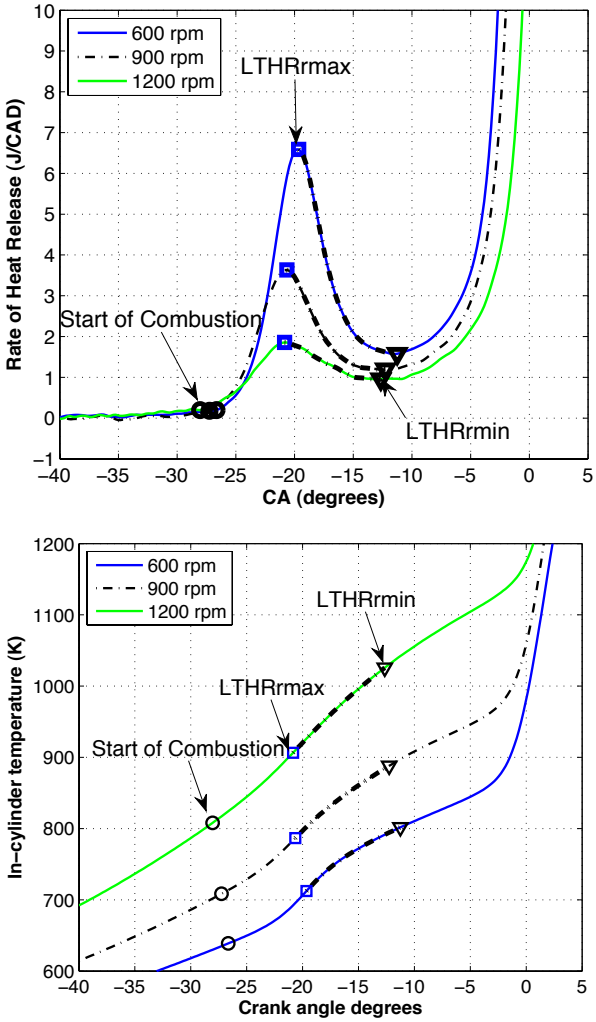

Figure 17. Low temperature heat release for PRF 70 and corresponding temperature evolution during speed sweep with Tin = 50°C.

Even though it appears at the same crank angle, the temperature range of the negative temperature coefficient zone is changed when increasing the engine speed, see Figure 17. The temperature range is from 700-800 K at the lowest engine speed, up to 900-1000 K at the highest engine speed. This shift is also seen in Figure 18, when the temperature range of 850-1000 K, sometimes referred to as the intermediate temperature area, are shown to shift with higher engine speeds. This therefore shows that this temperatur interval does not always correlate with intermediate temperature heat release.

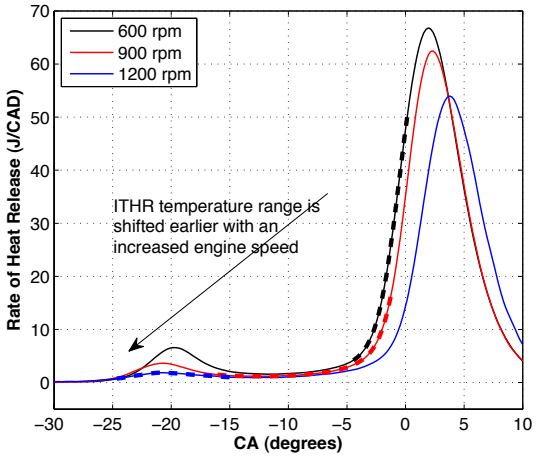

Figure 18. Shift of ITHR temperature regime (dashed lines), here defined as 850 to 1000 K, with increased engine speed. Fuel PRF 70 is shown at Tin=50°C.

Summary/Conclusions

The auto-ignition temperature was found to increase with increased engine speed.

Low temperature heat release was found to decrease with engine speed.

A second definition of pre-reactions, called early heat release, was used in this study. This was defined as heat release above a gaussian fit made for the main heat release, and was believed to include intermediate temperature heat release. This early heat release was shown to decrease at higher engine speed.

The temperature range of low temperature reactions were found to shift with engine speed. At higher engine speeds, the low temperature heat release was found at higher in-cylinder temperatures. This could be a co-effect with the residence time for the fuel charge, limiting available time for reactions to occur.

References

1. Hosseini, V., Neill, W., and Chippior, W., "Influence of Engine Speed on HCCI Combustion Characteristics using Dual-Stage Autoignition Fuels," SAE Technical Paper 2009-01-1107, 2009, doi:10.4271/2009-01-1107

2. Swarts, A., Yates, A., Viljoen, C., and Coetzer, R., "A Further Study of Inconsistencies between Autoignition and Knock Intensity in the CFR Octane Rating Engine", SAE Technical Paper 2005-01-2081, 2005, doi:10.4271/2005-01-2081.

3. Pitz, W., Cernansky, N., Dryer, F., Egolfopoulos, F. et al., "Development of an Experimental Database and Chemical Kinetic Models for Surrogate Gasoline Fuels," SAE Technical Paper 2007-01-0175, 2007, doi:10.4271/2007-01-0175

4. Heywood, J. B., 1988, "Internal Combustion Engine Fundamentals", McGraw-Hill, New York.

5. Truedsson, I., Tuner, M., Johansson, B., Cannella, W., "Pressure Sensitivity of HCCI Auto-Ignition Temperature for Gasoline Surrogate Fuels", SAE Technical Paper 2013-01-1669, 2013, doi:10.4271/2013-01-1669.

6. Truedsson, I., Johansson, B., Tuner, M., Cannella, B., 2012, "Pressure sensitivity of HCCI auto-ignition temperatures for oxygenated reference fuels", ASME ICEF 2012-92074

7. Truedsson, I., Tuner, M., Johansson, B., Cannella, W., 2012, "Pressure sensitivity of HCCI auto ignition temperatures for primary reference fuels", *SAE Int. J. Engines* 5(3):1089-1108, 2012, doi:10.4271/2012-01-1128.

8. Liu, H., Yao, M., Zhang, B., Zheng, Z., 2009, "Influence of Fuel and Operating Conditions on Combustion Characteristics of a Homogenous Charge Compression Ignition Engine", Energy & Fuels, 23, pp. 1422-1430

9. Sjöberg, M., Dec, J.E., 2007, "EGR and Intake Boost for Managing HCCI Low-Temperature Heat Release over Wide Ranges of Engine Speed", SAE 2007-01-0051

10. Aroonsrisopon, T., Foster, D., Morikawa, T., and Iida, M., "Comparison of HCCI Operating Ranges for Combinations of Intake Temperature, Engine Speed and Fuel Composition," SAE Technical Paper 2002-01-1924, 2002, doi:10.4271/2002-01-1924
11. Zheng, J., Yang, W., Miller, D., and Cernansky, N., "Prediction of Pre-ignition Reactivity and Ignition Delay for HCCI Using a Reduced Chemical Kinetic Model", SAE Technical Paper 2001-01-1025, 2001, doi:10.4271/2001-01-1025
12. Chen J.-S., Litzinger, T.A, Curran H.J, "The Lean Oxidation of Iso-Octane in the Intermediate Temperature Regime at Elevated Pressures", Combustion Science and Technology, 156:1, 49-79, (2000) DOI:10.1080/00102200008947296
13. W. Hwang, Dec. J., Sjöberg, M., " Spectroscopic and chemical-kinetic analysis of the phases of HCCI autoignition and combustion for single- and two-stage ignition fuels", Combustion and Flame 154 (2008) 387–409, doi:10.1016/j.combustflame.2008.03.019
14. Leppard, W., "The Chemical Origin of Fuel Octane Sensitivity", SAE Technical Paper 902137, 1990, doi:10.4271/902137

Contact Information

Ida.truedsson@energy.lth.se

Acknowledgments

The authors gratefully acknowledge Chevron for their financial support.

Definitions/Abbreviations

AFR	air fuel ratio
ATDC	after top dead center
BTDC	before top dead center
CA 50	crank angle for 50 % of total heat release
CAD	crank angle degree
CFR	cooperative fuel research
CO	carbon monoxide
CR	compression ratio
EGR	exhaust gas recirculation
ERF	ethanol reference fuel (n-heptane, iso-octane, and ethanol)
HC	hydrocarbons
HCCI	homogenous charge compression ignition
IVC	inlet valve closing
LTHR	low temperature heat release
MON	motor octane number
NO_x	NO (nitric oxide) and NO_2 (nitrogen dioxide) combined
ON	octane number
PRF	primary reference fuel (n-heptane and iso-octane)
RON	research octane number
S	fuel sensitivity, S = RON-MON
SI	spark ignition
TDC	top dead center
T_{in}	inlet air temperature, measured
TERF	toluene ethanol reference fuel (n-heptane, iso-octane, toluene, and ethanol)
TRF	toluene reference fuel (n-heptane, iso-octane, and toluene)
VCR	variable compression ratio

Paper VI

Development of new test method for evaluating HCCI fuel performance

Ida Truedsson, Martin Tuner, Bengt Johansson
Lund University

William Cannella
Chevron

Abstract

This study examines auto-ignitability and shows a method for determining HCCI fuel performance by engine experiments.

Previous methods for measuring HCCI fuel performance were found not to be able to predict required CR for HCCI auto-ignition. The Lund-Chevron HCCI number was instead proposed, using fuel testing in a CFR engine just as for the indices for spark ignition (research octane number and motor octane number, RON and MON) and compression ignition (cetane number, CN). By running the engine in HCCI mode, the required compression ratio for achieving a combustion phasing of CA50 3^{o} after TDC was noted for each fuel, and this value was compared to a primary reference fuel at the same operating condition.

The basis of the presented HCCI number was experiments of primary reference fuels (PRF), from PRF 60 to PRF 100. To evaluate the number, gasoline surrogate fuels consisting of n-heptane, iso-octane, toluene, and ethanol was made. 21 surrogate fuels were prepared with RON values ranging from 67 to 97. In addition, 21 different full distillate gasoline fuels were prepared from refinery feedstocks, some with addition of single components. Five different inlet air temperatures ranging from 50°C to 150°C were used to achieve different pressure-temperature combinations in the engine, and the compression ratio was changed accordingly to keep a constant combustion phasing, CA50, of 3±1° after TDC. The experiments were carried out in lean operation with a constant equivalence ratio of 0.33 and with an engine speed of 600 rpm, and an additional set of experiments with higher engine speeds, up to 1200 rpm.

Auto-ignitability was described by relating to the applied compression ratio, and an HCCI number was created. The HCCI number was seen to be related to the pre-reactions for the gasoline fuels.

Introduction

With HCCI combustion, it is possible to reduce the engine-out NO_x and soot emissions to the tailpipe-out level of a traditional spark ignition engine equipped with a three way catalyst (TWC), while maintaining the engine efficiency as high as for diesel combustion. The main challenge for HCCI is to control the ignition timing and combustion rate, since they are not controlled by a spark (SI combustion) nor by fuel injection (CI combustion) but rather controlled by chemical kinetics.

For spark ignited (SI) engines, gasoline ignition quality is described by the research octane number (RON) and motor octane number (MON), which is measured in a CFR engine by adjusting compression ratio to achieve a certain knock intensity. The required compression ratio is then compared to compression ratios for primary reference fuels (PRF, binary reference fuel blends of n-heptane and iso-octane) and the tested fuel receives the octane rating of the corresponding PRF. RON operating conditions are performed at an air temperature of 52^{o}C and an engine speed of 600 rpm. MON operating conditions are an engine speed of 900 rpm, and a temperature of 149^{o}C, measured after the fuel injection. The different temperature definitions for RON and MON also include the heat of vaporization in the differences between the two numbers. For compression ignition engines the fuel auto-ignition properties are measured by ignition delay, using the cetane number (CN). This is tested in a CFR engine with direct injection of the fuel.

Several researchers have previously proposed various indices to characterize the performance of fuels under HCCI conditions. The octane index (OI) was originally proposed by Kalghatgi for characterizing fuel anti-knock quality in spark ignition engines [21], and was subsequently extended for HCCI combustion [2,22,23]. It is defined as: OI=(1-K)RON+ KMON where K is an engine and operating condition specific parameter that depends on the pressure and temperature evolution in the unburnt gas. However, there are indications that the OI is not applicable for oxygenated fuels in HCCI combustion [1], which is an issue since many countries require the addition of oxygenates to gasoline. In addition, Shibata et al. [3,4] felt that RON and MON were not sufficient to adequately characterize fuel performance in HCCI and that additional fuel parameters were needed. They developed an HCCI index based on MON and fuel composition terms. Their

initial studies were conducted with blends of pure components in the gasoline range.

The applicability of the Kalghatgi and Shibata-Urushihara indices was assessed and an improved method for characterizing the HCCI performance of gasoline-type fuels was developed and presented.

Method

A Waukesha variable compression ratio Cooperative Fuels Research (CFR) engine was used for the experiments, the same kind of engine that is used for RON and MON testing. The engine specifications are listed in Table 1.

The engine setup was modified to fit HCCI experiments. A faster air-fuel mixture heater was mounted upstreams from the intake valve. The original carburetor was replaced with port injection. A scale was used for measuring the fuel flow. The heat release was calculated from the pressure trace measured with a Kistler piezoelectric pressure transducer mounted in the cylinder. An intake air refrigerator was included in the setup to ensure a constant water content of 0.0036 to 0.0072 kg H_2O/kg dry air throughout the experiments, fulfilling the standards in the ASTM methods for RON and MON testing. Temperature of the fuel air mixture (T_{in}) was measured by a thermocouple placed in the inlet, close to the inlet valve. The spark ignition was switched off to enable HCCI operation. An orifice plate was mounted in the intake in the original carburetor, and this was kept in the new setup, placed 50 cm upstream from the inlet valve, just before the fuel injectors. This caused a pressure drop at higher engine speeds, and is further discussed in the error analysis chapter. The original convectively driven water-cooling system of the CFR engine was kept. It keeps a water temperature of 100°C, relying on a condenser condensing the produced steam.

Table 1. – Specifications for CFR engine.

Displacement volume	612 cm^3
Number of cylinders	1
Bore	83 mm
Stroke	114 mm
CR	Variable (4:1 to 18:1)
Number of valves	2
Length of connecting rod	254 mm
Intake valve opens	10°ATDC±2.5°
Intake valve closes	146°BTDC±2.5°
Exhaust valve opens	140°ATDC±2.5°
Exhaust valve closes	15°ATDC±2.5°
Valve lifts	6.25 mm
Engine speed	600 rpm
Fuel supply	Port injection

Fuels

The surrogate fuels sets tested included Primary Reference Fuels (PRFs – blends of n-heptane and iso-octane) and Toluene-Ethanol Reference Fuels (TERFs - blends of n-heptane, iso-octane, toluene and ethanol) The compositions and some properties of the TERFs are listed in Table 2. The sensitivity of the fuels, S, are calculated by the difference between the RON and MON (S=RON-MON). The compositions and the properties of the PRFs tested (PRF 0, 20, 40, 60, 80, 85, 90, 95, and 100) are not shown in the table since the vol.% iso-octane and both RON and MON are by the number of the PRF.

In addition to the surrogate fuels, 21 different gasoline fuels prepared from blends of refinery streams were provided by Chevron. The, RON, MON, and S for these fuels are shown in Table 6.

Table 2. Fuel properties.

Pure component	RON	MON	S	Boiling point
n-Heptane	0	0	0	*98 to 99 °C*
iso-Octane	100	100	0	*99 to 100 °C*
Ethanol	109	90	19	77.8 °C
Toluene	120	109	11	111 °C

Table 3. Toluene reference fuels (TRF).

Fuel	n-Heptane (vol.%)	Toluene (vol.%)	iso-Octane (vol.%)	RON	MON	S
H20T10	20	10	70	82.8	80.7	2.1
H20T20	20	20	60	84.9	81.8	3.1
H20T40	20	40	40	89.8	82.9	6.9
H20T60	20	60	20	93.9	83.9	10

Table 4. Ethanol reference fuels (ERF).

Fuel	n-Heptane (vol.%)	iso-Octane (vol.%)	Ethanol (vol.%)	RON	MON	S
PRF80	20	80	0	80	80	0
H20E1	20	79	1	80.5	80.4	0.1
H20E5	20	75	5	84.4	83.2	1.2
H20E10	20	70	10	87.9	85.6	2.3
H20E20	20	60	20	94.1	88.2	5.9
PRF70	30	70	0	70	70	0
H30E1	30	69	1	70.6	70.2	0.4
H30E5	30	65	5	73.2	73.1	0.1
H30E10	30	60	10	78.7	76.7	2
H30E20	30	50	20	85.1	81.2	3.9
H60E40	60	0	40	71.4	65	6.4
H55E45	55	0	45	78	71.6	6.4
H50E50	50	0	50	84.7	76.8	7.9
H45E55	45	0	55	89.7	80.4	9.3
H40E60	40	0	60	94.4	82.8	11.6

Table 5. Toluene ethanol reference fuel matrix, vol.%.

Fuel	n-Hept	Toluene	EtOH	iso-Oct	MON	RON	S
T1	40	10	5	45	63,7	67,1	3,4
T2	20	10	20	50	88,5	94,7	6,2
T3	20	30	20	30	87,6	97	9,4
T4	40	30	20	10	73	80,8	7,8
T5	30	20	5	45	74,5	79,6	5,1
T6	30	30	12,5	27,5	78,6	85,3	6,7
T7	30	20	12,5	37,5	78,1	83,8	5,7
T8	40	30	5	25	65,8	71,8	6
T9	30	10	12,5	47,5	77,9	81,6	3,7
T10	20	30	5	45	84,1	90,2	6,1
T11	30	20	12,5	37,5	78,2	83,8	5,6
T12	40	10	20	30	74,3	78,3	4
T13	20	10	5	65	83,6	86,1	2,5
T14	40	20	12,5	27,5	68,9	74,8	5,9
T15	20	20	12,5	47,5	86,4	92,3	5,9
T16	30	20	20	30	81,4	87,9	6,5
T17	30	20	12,5	37,5	-	-	-

Table 6. RON, MON, and S (S=RON-MON) for the gasoline fuels.

Fuel	RON	MON	S
G82	83,5	79,9	3,6
G83	91,4	83,9	7,5
G84	87,7	80,9	6,8
G85	86,7	79,7	7
G86	91,6	84,0	7,6
G87	90,1	83,4	6,7
G88	92,5	83,5	9
G89	92,4	84,5	7,9
G90	88,6	81,4	7,2
G91	89,9	82,2	7,7
G92	86,2	79,4	6,8
G93	91,6	82,2	9,4
G0	87,1	80,5	6,6
G1	92,9	84,7	8,2
G2	97,7	87,5	10,2
G3	78,2	73,4	4,8
G4	69,4	66,1	3,3
G5	99	96,9	2,1
G6	70,3	65,9	4,4
G7	96,5	86,1	10,4
G8	88,6	79,5	9,1

Method

All fuels were tested with a change in inlet air temperature (T_{in}) in five steps from 50° to 150°C. At each temperature a combustion phasing with CA50 at 3±1° after TDC was held constant by changing the compression ratio. A constant CA50 was used to ensure stable combustion in all cases and to represent a more realistic operating condition. Motored pressure traces were extracted for all data points for validation. The engine was run naturally aspirated. The fuel amount was adjusted for each case to achieve an equivalence ratio of 0.33. This value was chosen since a diluted charge is needed in HCCI combustion to keep pressure rise rates at an acceptable level. All fuels were run at 600 rpm. Additional experiments for 4 primary reference fuels and five gasolines were run at higher engine speeds from 600 to 1200 rpm. No EGR was used.

Heat release calculations

The Woschni heat transfer model was used, and the motored heat release was subtracted from the fired heat release to reduce measurement and model errors. The assumptions were that the gas temperature in the cylinder when the inlet valve closes was known. This temperature was calculated from the measured temperature in the intake by applying a simple model for the temperature change due to mixing with hot internal residuals, and also heating from the intake walls between the temperature probe mounted just before the intake, and the cylinder. All values were based on the average of 300 cycles. The heat release calculations are described in more detail in [13]. For some fuels at some operating conditions, two peaks were observed in the rate of heat release vs engine crank angle (CA) curves, as shown in Figure 1. The large peak is associated with the heat release from the main combustion reactions. The smaller peak (when present) is associated with early heat release from precombustion reactions that form free radicals. Sometimes this early heat releases is divided into low temperature heat release (LTHR) and intermediate heat release (ITHR). ITHR has been analysed with detailed chemical kinetics [24] and for reference fuel experiments [25].

For simplicity in this paper we refer to total heat release before the main heat release peak (LTHR + ITHR) as LTHR. To calculate the amount of LTHR, first a Gaussian curve was fit to the main heat release peak. As depicted in Figure 2, the amount of LTHR was then calculated as the area between the total heat release curve (solid curve) and the front part of the Gaussian curve (dashed curve) from the starting point of combustion (defined in this study as the point where the rate of heat release reaches 0.2 J/CAD). The amount of low temperature heat release was then normalized by dividing by the total amount of heat released to account for the different fuel amounts at the different inlet air temperatures.

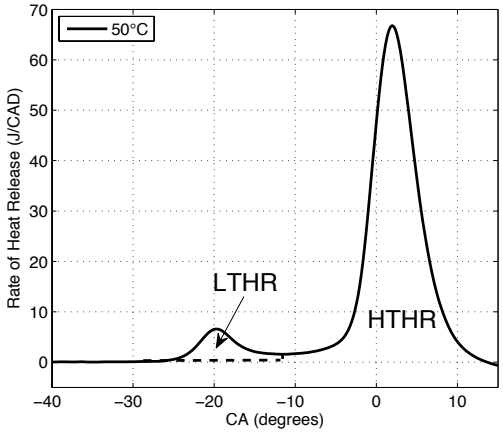

Figure 1. Definition of low temperature heat release.

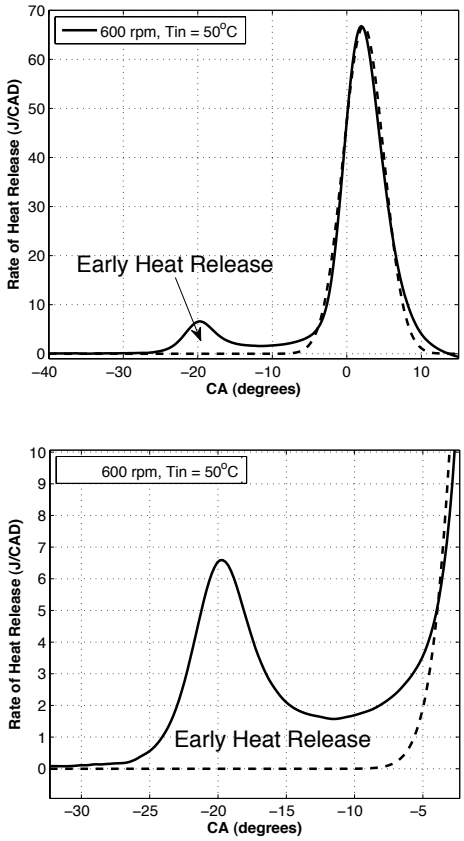

Figure 2. Definition of early heat release.

Results and Discussion

Figure 3 shows that fuels having the same RON number can have very different heat release rates and combustion performance in HCCI. This has lead to several research groups proposing different indices to characterize a fuels HCCI performance. The applicability of two of these indices to the current combustion data is discussed below.

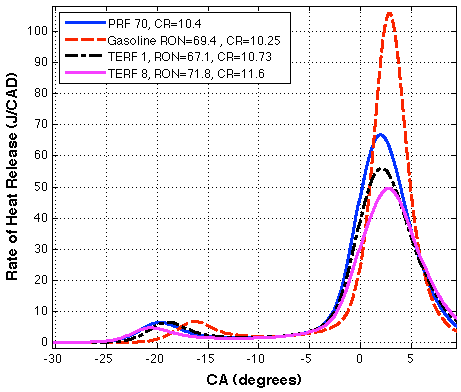

Figure 3. Comparison of reference fuels with gasoline. Fuels with similar RON will behave differently in an HCCI engine, here requiring different compression ratios for a constant combustion phasing.

Previous indices and numbers

RON and MON

The most common way of describing auto ignition qualities of a fuel is by the use of the standards RON and MON. Plots of the compression ratios required for the constant combustion phasing used in this study at 50 and 150°C inlet air temperature, and RON and MON, respectively, are shown in Figure 4,5,6, and 7 for all reference and gasoline fuels. There is a fairly wide range of RON and MON values that give the same CR. Thus they confirm that RON and MON are not sufficient to predict fuel behavior in HCCI combustion.

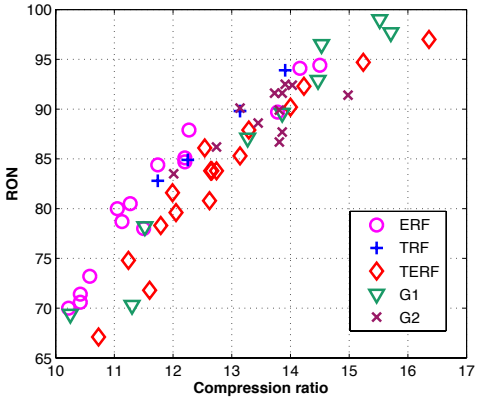

Figure 4. Correlation between compression ratio and RON compared with compression ratio at Tin=50oC, 600 rpm

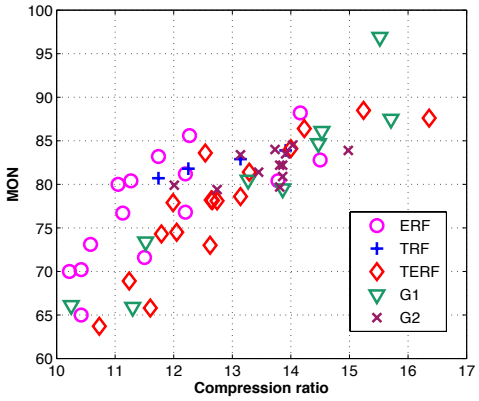

Figure 5. Correlation between compression ratio and MON compared with compression ratio at Tin=50°C, 600 rpm.

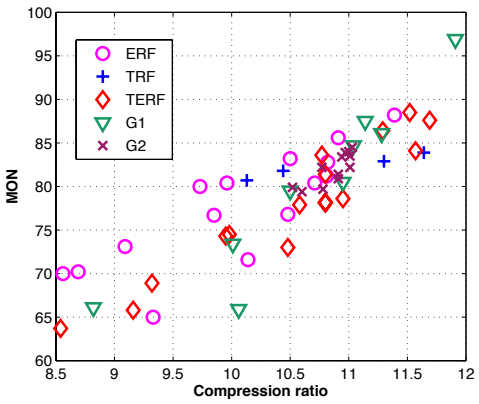

Figure 6. MON and CR at Tin=150°C.

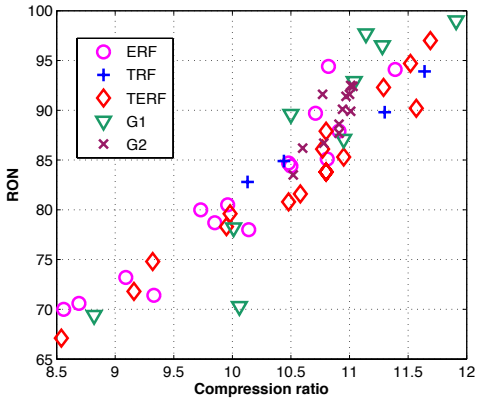

Figure 7. How well MON corresponds with required compression ratio at Tin=150°C.

Kalghatgi octane index

As mentioned in the introduction, Kalghatgi has proposed an octane index for HCCI that is dependent only on the fuel parameters RON and MON (or S=RON-MON) and an engine parameter K:

$$OI=(1-K)*RON + K*MON = RON - K*S \quad (1)$$

Combustion phasing (CA50) is proposed to be a linear function of OI:

$$CA50 = c + (a+b)*OI = c + (a+b)*(RON-K*S) \quad (2)$$

At each operating condition, the CA50 values for fuels having various RON and MON values are measured and the value of K is determined through regression analysis by finding the value that provides the best linear fit in the plot of CA50 vs. OI. K is not a constant, but is dependent on the specific engine and engine operating conditions such as: in cylinder temperature c inlet air temperature, boost pressure and compression ratio, but in theory independent of fuel properties. In this thesis study, CA50 was held constant for all fuels and conditions while the compression ratio for a combustion timing 3° after TDC (50% of the total heat released, CA50) auto-ignition (CR_{AI}) was measured. So direct use of Kalghatgi's correlation was not possible. Instead the applicability of the following equation was tested:

$$CR_{AI} = c' + (a'+b')*OI' = c' + (a'+b')*(RON - K'*S) \quad (3)$$

For each fuel set, the values of K' at each T_{in} were determined by finding the values that gave the best linear fit to the plot of CR vs OI' (=RON-K*S).

Plots of the compression ratio and octane index data at Tin=50˚C are shown in Figures 8, 9, 10, and 11 for the all reference fuels, TERFs, ERFs, and gasolines, respectively. The K' values for all fuel sets at the 5 Tin's are listed in Table 18. The very different values of K' for each fuel set suggest that the linear OI approach does not apply here. The K-value calculated from regression analysis was found to differ significantly from the empiric correlations in Equations 4 and 5.

$$K=0.0426(T_{comp,15})-35.2 \text{ if } T_{comp,15} \text{ is above 825 K} \quad (4a)$$

or

$$K=0.0056(T_{comp,15})-4.68 \text{ if } T_{comp,15} \text{ is below 825 K} \quad (4b)$$

Or with lambda dependence;

$$K=0.00497*T_{comp,15}-0.135*\lambda-3.67 \quad (5)$$

For both fuel sets, the K values increased as T_{intake} increased. Thus at least in this study, the K values are dependent on both fuel properties as well as engine parameters, making it more complicated to use the OI equation.

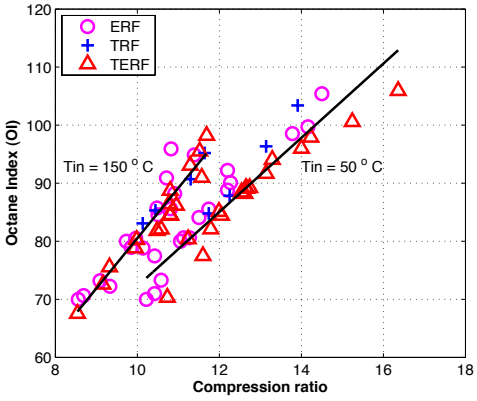

Figure 8. Agreement between the octane index (OI) and compression ratio for all reference fuels.

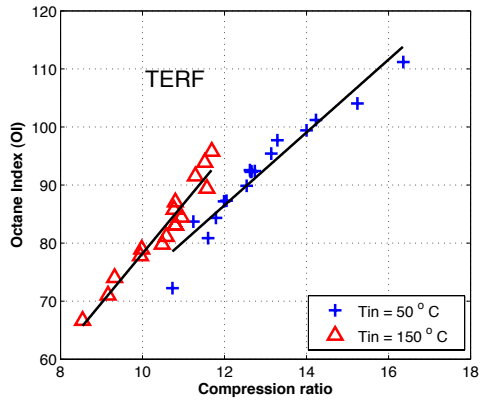

Figure 9. Agreement between the octane index (OI) and compression ratio for TERFs.

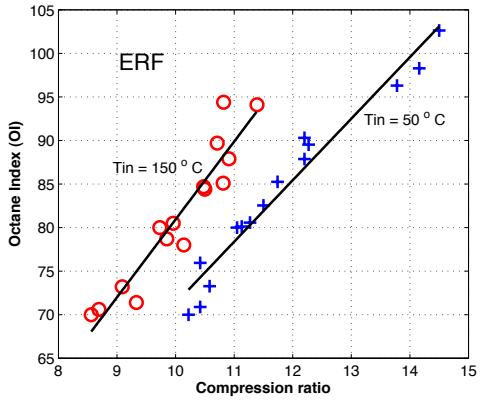

Figure 10. Agreement between the octane index (OI) and compression ERFs.

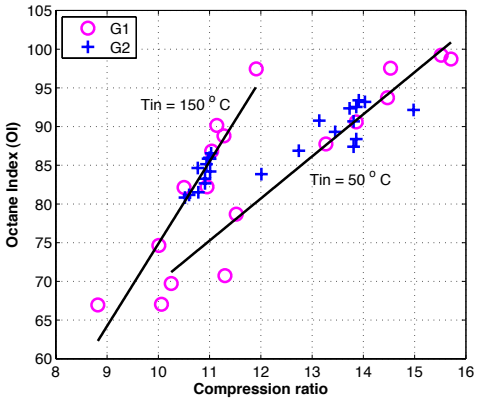

Figure 11. Agreement between the octane index (OI) and compression ratio for gasoline fuels.

Table 7. K values from linear regression at the different inlet air temperatures. R^2 value in parenthesis.

K-values (R^2)		
Tin	ERF	TERF
50 °C	-0.71 (0.96)	-1.51 (0.93)
75 °C	-0.58 (0.97)	-1.13 (0.94)
100 °C	-0.43 (0.96)	-0.65 (0.97)
125 °C	-0.29 (0.94)	-0.24 (0.98)
150 °C	0 (0.90)	0.13 (0.94)
Tin	All reference fuels	Gasolines
50 °C	-0.95 (0.89)	-0.1 (0.89)
75 °C	-0.76 (0.94)	0.09 (0.92)
100 °C	-0.54 (0.95)	0.25 (0.91)
125 °C	-0.34 (0.95)	0.41 (0.88)
150 °C	-0.13 (0.91)	0.74 (0.86)

Shibata Urushihara Index

The Shibata Urushihara index (3) is based on the fuel composition and MON or RON. The fuel components are divided into 5 groups based on hydrocarbon classes: n-paraffin (n-P), iso-paraffin (i-P), olefin (O), aromatic (A), and oxygenates (OX). One form of their index is based on the vol.% of each of these hydrocarbon classes and MON as shown in Equation 6. Coefficients can be found in [3].

$$\text{S-U HCCI Index (abs)} = mMON + a(n\text{-}P) + b(i\text{-}P) + c(O) + d(A) + e(OX) + Y \quad (6)$$

The coefficients (m, a, b, c, d, e, and Y) are temperature dependent parameters whose values are reported in reference [3]. In addition, the values of coefficient e depends upon the specific oxygenate in the fuel formulation. In their study, the S-U HCCI index corresponded to the crank angle timing for 20% completion of the HTHR. Values of the calculated S- U indices vs compression ratio required for auto-ignition for the reference fuels (PRF, TRF, ERF, and TERF) at a T_{in} of 50˚C are shown in Figures 12. Linear fits for these fuel sets are poor. In addition, the different fuel sets don't align with each other. Thus the need exists for an HCCI index that better correlates with auto-igniton compression ratio.

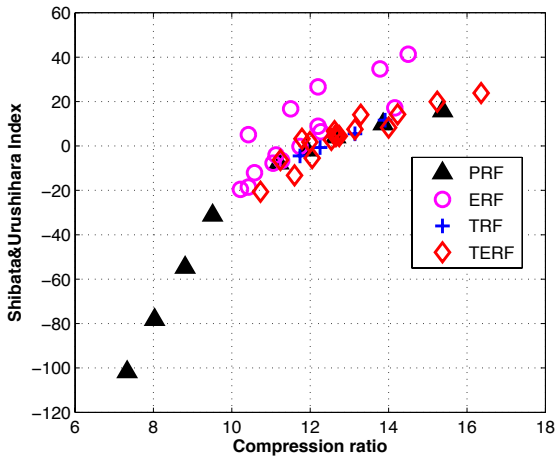

Figure 12. Shibata HCCI index calculated for all reference fuels at operating conditions with Tin=50°C.

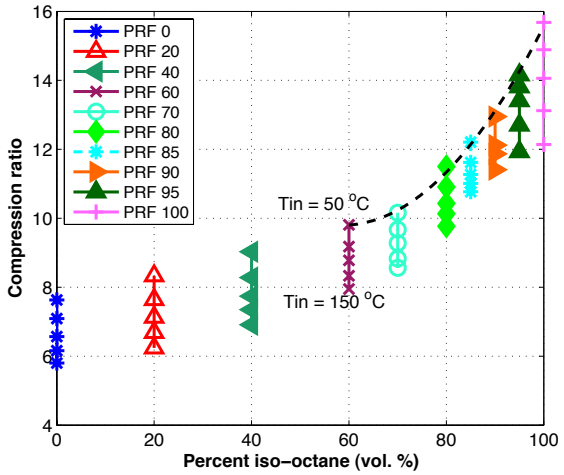

Figure 13. Plots of autoigntion compression ratios vs. octane number for the PRFs at 5 T_{in}. Equation is quadratic polynomial fit for T_{in}=50°C, 600 rpm, data.

Lund-Chevron HCCI number

The results discussed above indicate that a need exists for an HCCI number analogous to that of RON and MON for SI engines. For this purpose the Lund-Chevron HCCI number was developed.

The first step for determining the Lund-Chevron HCCI number of a fuel consists of establishing a set of reference curves of the compression ratio for auto-ignition with a CA50 of 3˚ after TDC for the PRFs at the five different intake temperatures from 50-150˚C. By fitting a quadratic equation to the PRF data in the gasoline range (PRF 60 to 100 was chosen), a function of compression ratios vs. octane number was obtained, see Figure 8, with the quadratic equations listed in Table 4. For each fuel and condition of interest, the autoignition CR was plotted vs. RON, along with the reference quadratic curve for the PRFs at the same conditions (T_{in}, combustion phasing and speed). The HCCI number for each fuel was then set equal to the RON of the PRF that had the same CR. This is shown in Figure 9 for the TERFs at T_{in}=50˚C and 600 rpm. For example fuel T1, has an autoignition compression ratio of about 10.8 and is assigned a HCCI number of 78 at this operating condition (Tin=50°C, 600 rpm). In this manner, HCCI numbers can be established for each fuel at each condition of interest.

For example, as shown in Figure 9, for fuel T1, the compression ratio is 10.8, which is the same value as for PRF 75, and so the HCCI number is set equal to 75. The HCCI numbers are then all a function of the fuel's compression ratio required for auto-ignition, 10.

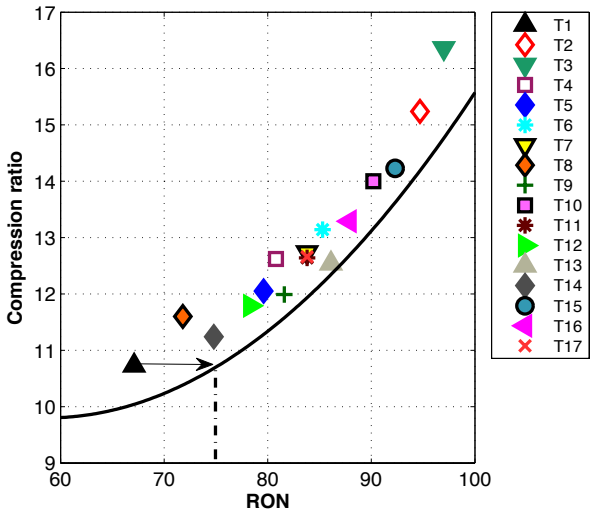

Figure 14. Compression ratio/RON comparison with TERFs, PRF correlation shown with the black line at Tin=50°C. As an example, fuel T1, having a RON of 67, will have a HCCI number of 75.

Temperature effect

To see the temperature effect on the HCCI behavior for each fuel, five operating points with different inlet air temperatures were studied. A constant engine speed of 600 rpm was used, and the equivalence ratio was kept at 0.33. For each temperature, a separate quadratic function between % iso-octane and CR for the primary reference fuels was developed, and used as baselines for the other fuels. The quadratic equations for the PRFs at the 5 Tin are listed in Table 5 in the Appendix. Once again, the HCCI number of a fuel is assigned by finding the RON of the PRF that has the same auto-ignition CR of the fuel at the same conditions. If a fuel behaves just like the PRFs throughout the entire temperature range, it will therefore have a constant HCCI number at all operating points. The temperature effect on HCCI number for the toluene

ethanol reference fuels (TERFs) are shown in Figure 10. Some fuels (T6, T9, T10) show practically the same HCCI number over the whole temperature range, behaving like the primary reference fuels. In contrast, other fuels (e.g. T1 and T8) show a larger change in HCCI number with temperature. The HCCI number values for the TERFs at the 5 T_{in} are listed in Table 5. The effects of temperature on the HCCI numbers for the gasolines are plotted in Figure 11.

Table 8. Parameters for the equation; $CR_{AI} = a*x^2+b*x+c$, where x is the % iso-octane for PRFs.

	Inlet air temperature				
	50°C	75°C	100°C	125°C	150°C
a	0.00338	0.00309	0.00243	0.00123	0.00017
b	-0.3962	-0.35513	-0.25126	-0.06908	0.08698
c	21.4205	19.4396	15.0801	7.9613	2.0135

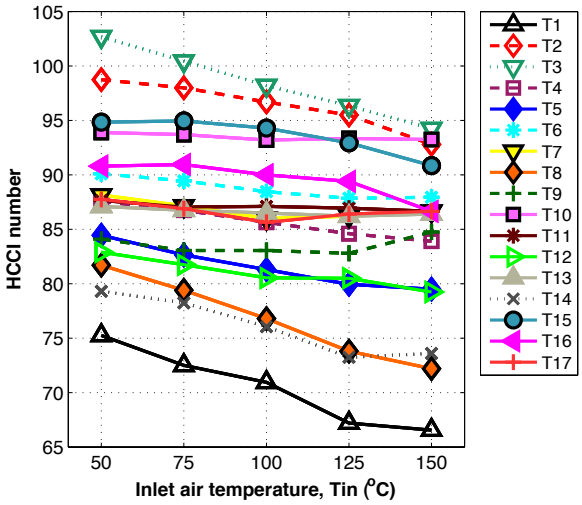

Figure 15. Inlet air temperature effect on the HCCI number for toluene ethanol reference fuels (TERF). The fuel composition and measured RON and MON can be found in Table 2.

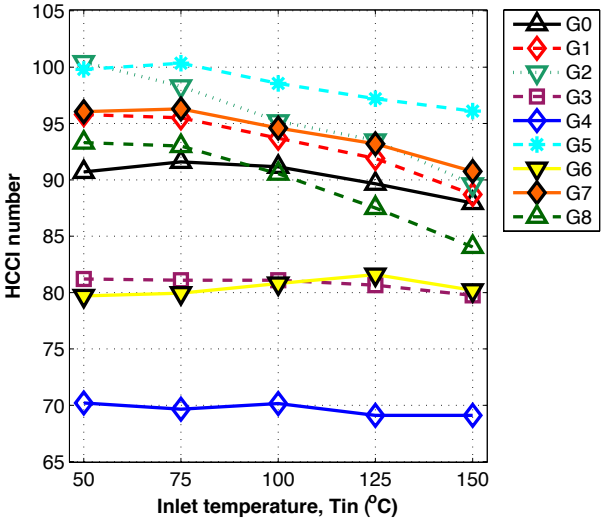

Figure 16. Inlet air temperature effect on the HCCI number for the gasoline fuels.

Speed effect

To see the speed effect on the HCCI number, four primary reference fuels (PRF 70, 80, 90, 100) were run at five engine speeds from 600 to 1200 rpm. At each engine speed, three inlet air temperatures (50°C, 100°C, and 150°C) were used. The results are shown in Figures 12, 13, and 14. The quadratic equations for the PRFs at each condition are summarized in Table 5 in the Appendix. At all speeds at 50˚C, the CRs increase more than linearly as the octane number increases. In contrast, at all speeds at 150˚C, the CRs increase less than linearly. At the intermediate temperature of 100˚C, the curve at the lowest speed increases more than linearly, while the curves for the highest speeds increase less than linearly.

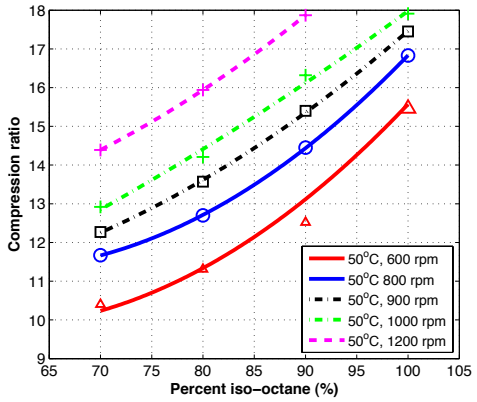

Figure 17. Speed effect on compression ratio for PRFs at Tin=150°C.

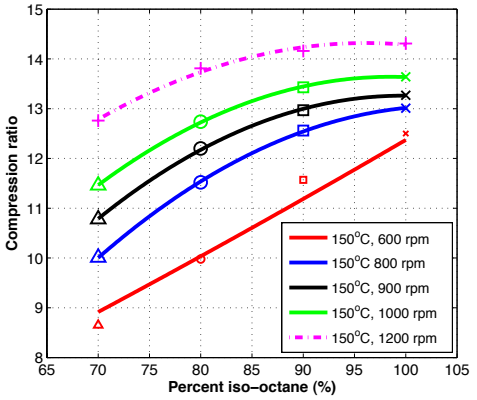

Figure 18. Speed effect on compression ratio for PRFs at Tin=150°C.

Table 9. Speed effect on HCCI number,

	Engine speed (rpm)				
	600	800	900	1000	1200
Tin = 50°C, CR_{AI} = $a*x^2+b*x+c$					
a	0.00338	0.00337	0.00187	0.00075	0.0019
b	-0.3962	-0.40145	-0.14505	0.0433	-0.13
c	21.42054	23.2295	13.2205	6.147	14.18
Tin = 100°C, CR_{AI} = $a*x^2+b*x+c$					
a	0.00243	$5.00*10^{-5}$	-0.0006	-0.00178	-0.00265
b	-0.25126	0.1367	0.234	0.42065	0.5387
c	15.08017	0.698	-2.08	-8.6165	-10.952
Tin = 150°C, CR_{AI} = $a*x^2+b*x+c$					
a	0.00017	-0.00265	-0.0028	-0.00267	-0.00225
b	0.08698	0.5509	0.5584	0.52705	0.4325
c	2.01356	-15.574	-14.579	-12.3205	-6.465

Pre-reactions

Early heat release (eHR) was determined as discussed in Section 3.3.1. Plots of early heat release vs. RON and the Lund-Chevron HCCI number are presented in Figures 19 and 20. for the refinery gasoline blends. For these refinery fuels, the HCCI number is more closely correlated than RON to the amount of early heat release (R^2 for HCCI number vs. eHR = 0.93, R^2 for RON vs. eHR = 0.77). The same is seen for correlation between early heat release vs. MON and the HCCI number at Tin = 150°C, see Figures 21 and 22.

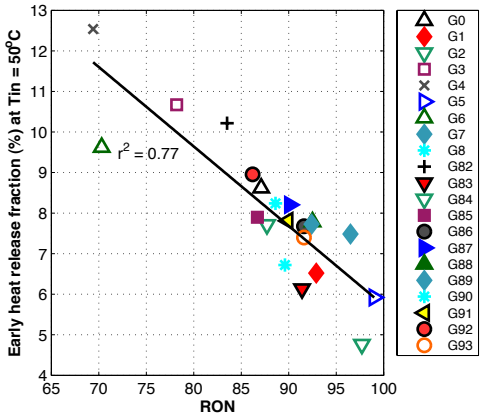

Figure 19. Correlation between early heat release and RON.

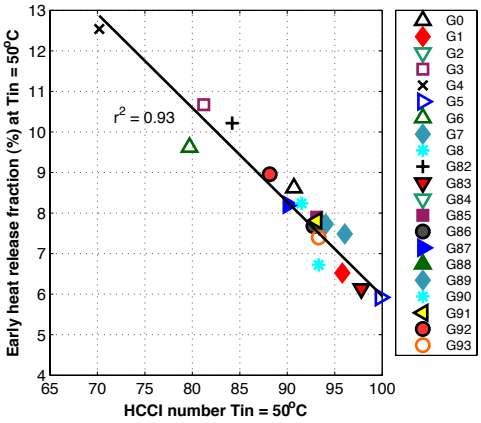

Figure 20. Correlation between early heat release and HCCI number. HCCI number at 600 rpm an Tin= 50°C are used.

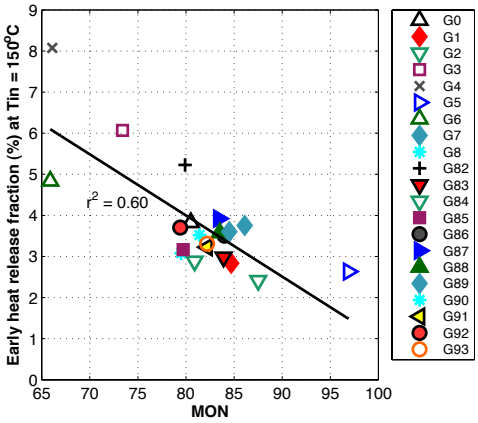

Figure 21. Correlation between early heat release for gasoline fuels vs MON. HCCI number at 600 rpm and Tin= 150°C are used.

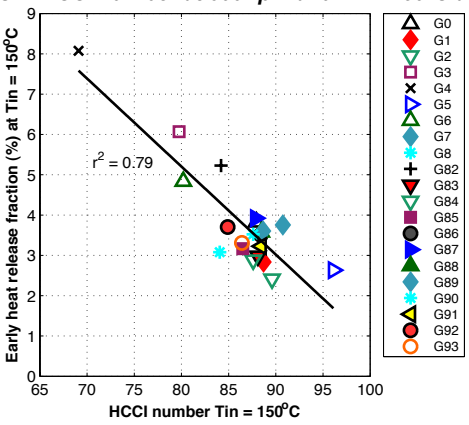

Figure 22. Correlation between early heat release for gasoline fuels vs. HCCI number. HCCI number at 600 rpm and Tin= 150°C are used.

Correlation Between HCCI Number and RON and MON

The HCCI number is compared to RON and MON in Figures 23 and 24. It is shown that the ethanol reference fuels, for example, receives similar values at RON and HCCI number at low inlet air temperature conditions, but that many of these fuels show a greater difference between MON and HCCI number at high inlet air temperatures. The toluene ethanol reference fuels shows an offset, and show higher HCCI numbers than their RONs and MONs at both high and low inlet air temperatures. Most fuels have a higher HCCI number that RON and MON, which means that they require a higher compression ratio in HCCI operation, than the PRF correlating to their RON.

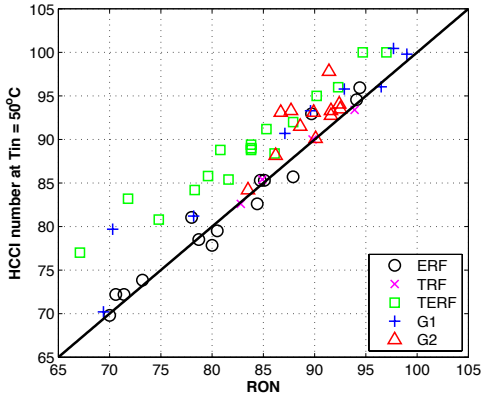

Figure 23. Correlation between HCCI number at low inlet air temperatures and RON. The black line is 1:1 correlation, and G1 and G2 are gasoline fuel datasets #1 and #2.

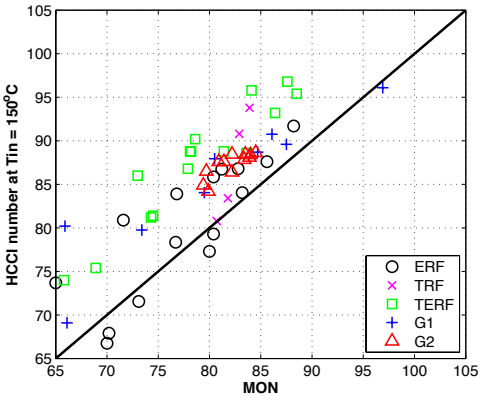

Figure 24. Correlation between HCCI number at high inlet air temperatures and MON. The black line is 1:1 correlation, and G1 and G2 are gasoline fuel datasets #1 and #2.

Summary and conclusions

Previous methods for measuring HCCI fuel performance were found not to be able to predict required CR for HCCI auto-ignition. The Lund-Chevron HCCI number was instead proposed, using fuel testing in a CFR engine just as for the indices for spark ignition (research octane number and motor octane number, RON and MON) and compression ignition (cetane number, CN). By running the engine in HCCI mode, the required compression ratio for achieving a combustion phasing of CA50 3° after TDC was noted for each fuel, and this value was compared to a primary reference fuel at the same operating condition.

The Lund-Chevron HCCI number was seen to be closely coupled with the amount of low temperature reactions.

Previous indices by Kalghatgi and Shibata-Urushihara were tested for agreement with the data of required compression ratio for auto-ignition with a CA50 3° after TDC. Both indices showed variations from this data, however the K-value was not correctly calculated due to lack of data with a spread in CA50.

References

1. Liu, H., Yao, M., Zhang, B., Zheng, Z., 2009, “Influence of Fuel and Operating Conditions on Combustion Characteristics of a Homogenous Charge Compression Ignition Engine”, Energy & Fuels, 23, pp. 1422-1430
2. Kalghatgi, G.T., 2005, ”Auto-Ignition Quality of Practical Fuels and Implications for Fuel Requirements of Future SI and HCCI Engines”, SAE 2005-01-0239
3. Shibata, G., Urushihara, T., 2007, ”Auto-Ignition Characteristics of Hydrocarbons and Development of HCCI Fuel Index”, SAE 2007-01-0220
4. Shibata, G., Oyama, K., 2005, ”Correlation of Low Temperature Heat Release With Fuel Composition and HCCI Engine Combustion”, SAE 2005-01-0138
5. Tanaka, S., Ayala, F., Keck, J.C, Heywood, J.B., 2003, ”Two-stage ignition in HCCI combustion and HCCI control by fuels and additives”, Combustion and Flame, 132, pp. 219-239
6. Aroonsrisopon, T., Sohm, V., Werner, P., Foster, D.E., Morikawa, T., Iida, M., 2002, “An Investigaton Into the Effect of Fuel Composition on HCCI Combustion Characteristics”, SAE 2002-01-2830
7. Warnatz, J., Maas, U., Dibble, R.W., 2006, “Combustion Physical and Chemical Fundamentals, Modeling and Simulation, Experiments, Pollutant Formation”, Springer, Berlin
13. Truedsson, I., Johansson, B., Tuner, M., Cannella, B., 2012, “Pressure sensitivity of HCCI auto ignition temperatures for primary reference fuels”, SAE Int. J. Engines 5 (3): doi:10.4271/2012-01-1128
16. Machado, G.B., Barros, J.E.M., Braga, S.L., Braga, C.V.M., Oliviera, E.J., Silva, A.H.M.F.T., Carvalho, L.O., 2011, “Investigation on surrogate fuels for high-octane oxygenated gasolines”, Fuel, 90, pp. 640-646
17. Pitz, W.J., Cernansky, N.P., Dryer, F.L., Egolfopoulos, F.N., Farrell, J.T., Friend, D.G., Pitsch, H., 2007,

"Development of an experimental Database and Chemical Kinetic Models for Surrogate Gasoline Fuels", SAE 2007-01-0175

18. Sakai, Y., Ozawa, H., Ogura, T., Miyoshi, A., Koshi, M., Pitz, W.J., , 2007, "Effects of Toluene Addition to Primary Reference Fuel at High Temperature ", SAE 2007-01-4104
19. Truedsson, I., Johansson, B., Tuner, M., Cannella, B., 2012, "Pressure sensitivity of HCCI auto-ignition temperatures for oxygenated reference fuels", J. Eng. Gas Turbines Power 135(7), doi:10.1115/1.4023614
20. Morgan, N., Smallbone, A., Bhave, A., Kraft, M., Cracknell, R., Kalghatgi, G., 2010, "Mapping surrogate gasoline compositions into RON/MON space", Combustion and Flame, 157, pp.1122-1131
21. Kalghatgi, G., "Fuel Anti-Knock Quality - Part I. Engine Studies," SAE Technical Paper 2001-01-3584, 2001, doi:10.4271/2001-01-3584.
22. Risberg, P., Kalghatgi, G., and Ångstrom, H., "Auto-ignition Quality of Gasoline-Like Fuels in HCCI Engines", SAE Technical Paper 2003-01-3215, 2003, doi:10.4271/2003-01-3215.
23. Kalghatgi, G. and Head, R., "The Available and Required Autoignition Quality of Gasoline - Like Fuels in HCCI Engines at High Temperatures," SAE Technical Paper 2004-01-1969, 2004, doi:10.4271/2004-01-1969.
24. Mehl, M., Pitz, W., Sarathy, M., Yang, Y. et al., "Detailed Kinetic Modeling of Conventional Gasoline at Highly Boosted Conditions and the Associated Intermediate Temperature Heat Release," SAE Technical Paper 2012-01-1109, 2012, doi:10.4271/2012-01-1109.
25. Vuilleumier, D., Selim, H., Dibble, R., and Sarathy, M., "Exploration of Heat Release in a Homogeneous Charge Compression Ignition Engine with Primary Reference Fuels," SAE Technical Paper 2013-01-2622, 2013, doi:10.4271/2013-01-2622.

Contact Information

Corresponding author, email ida.truedsson@energy.lth.se

Acknowledgments

The authors gratefully acknowledge Chevron for their financial support.

Definitions/Abbreviations

ATDC	after top dead center
BTDC	before top dead center
CA 50	crank angle for 50 % of total heat release
CAD	crank angle degree
CFR	cooperative fuel research
EGR	exhaust gas recirculation
IVC	inlet valve closing
LTR	low temperature reactions
LTHR	low temperature heat release
MON	motor octane number
OI	octane index, developed by G. Kalghatgi
ON	octane number
PRF	primary reference fuel
RON	research octane number
S	fuel sensitivity, S = RON-MON
TDC	top dead center
T_{in}	temperature of fuel air mixture, measured
T_{IVC}	temperature in the cylinder at inlet valve closing, calculated from T_{in}

Appendix

Table 10. HCCI numbers for five different inlet air temperatures for toluene reference fuels (TRF) and ethanol reference fuels (ERF) with compositions presented in Table -. All for an engine speed of 600 rpm and an equivalence ratio of 0.33.

Fuel	Tin=50°C	Tin=75°C	Tin=100°C	Tin=125°C	Tin=150°C
H20T10	83	82	82	81	81
H20T20	85	85	84	83	83
H20T40	90	91	89	89	91
H20T60	93	94	93	93	94
H20E1	80	79	79	79	79
H20E5	83	83	83	83	84
H20E10	86	86	88	88	88
H20E20	95	95	95	93	92
H30E1	72	70	69	69	68
H30E5	74	74	73	73	72
H30E10	79	78	78	78	78
H30E20	85	87	87	88	87
H60E40	72	73	72	74	74
H55E45	81	81	83	82	81
H50E50	85	87	87	86	84
H45E55	93	92	91	89	86
H40E60	96	95	92	90	87

Table 11. HCCI numbers for five different inlet air temperatures for toluene ethanol reference fuels (TERF) with composition shown in Table 5. All for an engine speed of 600 rpm and an equivalence ratio of 0.33.

Fuel	Tin=50oC	Tin=75oC	Tin=100 oC	Tin=125 oC	Tin=150 oC
T1	75	72	71	67	66
T2	99	98	97	95	93
T3	103	100	98	96	94
T4	87	87	86	85	84
T5	84	83	81	80	79
T6	90	89	88	88	88
T7	88	87	86	86	87
T8	82	79	77	74	72
T9	84	83	83	83	85
T10	94	94	93	93	93
T11	88	87	87	87	87
T12	83	82	80	80	79
T13	87	87	86	86	86
T14	79	78	76	73	74
T15	95	95	94	93	91
T16	91	91	90	89	87
T17	88	87	86	86	87

Table 12. HCCI numbers for five different inlet air temperatures for gasoline fuels. All for an engine speed of 600 rpm and an equivalence ratio of 0.33.

Fuel	Tin=50°C	Tin=75°C	Tin=100 °C	Tin=125 °C	Tin=150 °C
G82	84	85	86	85	84
G83	98	96	94	91	88
G84	93	94	92	91	88
G85	93	94	92	90	87
G86	93	93	93	91	88
G87	90	91	90	90	88
G88	94	94	93	91	88
G89	94	95	93	91	89
G90	92	92	92	90	88
G91	93	94	92	90	88
G92	88	89	89	87	85
G93	93	93	92	89	86
G0	91	92	91	90	88
G1	96	96	94	92	89
G2	100	98	95	94	90
G3	81	81	81	81	80
G4	70	70	70	69	69
G5	100	100	99	97	96
G6	80	80	81	82	80
G7	96	96	95	93	91
G8	93	93	91	88	84